ANIONS AND ELECTRON-DEFICIENT AROMATIC RINGS

by

ORION BOYD BERRYMAN

A DISSERTATION

Presented to the Department of Chemistry
and the Graduate School of the University of Oregon
in partial fulfillment of the requirements
for the degree of
Doctor of Philosophy

June 2008

University of Oregon Graduate School

Confirmation of Approval and Acceptance of Dissertation prepared by:

Orion Berryman

Title:

"Anions and Electron-Deficient Aromatic Rings"

This dissertation has been accepted and approved in partial fulfillment of the requirements for the Doctor of Philosophy degree in the Department of Chemistry by:

James Hutchison, Chairperson, Chemistry
Darren Johnson, Advisor, Chemistry
Michael Haley, Member, Chemistry
Kenneth Doxsee, Member, Chemistry
David Schmidt, Outside Member, Geological Sciences

and Richard Linton, Vice President for Research and Graduate Studies/Dean of the Graduate School for the University of Oregon.

June 14, 2008

Original approval signatures are on file with the Graduate School and the University of Oregon Libraries.

An Abstract of the Dissertation of

Orion Boyd Berryman for the degree of Doctor of Philosophy

in the Department of Chemistry to be taken June 2008

Title: ANIONS AND ELECTRON-DEFICIENT AROMATIC RINGS

Approved: _____
Darren W. Johnson

More than two-thirds of all enzyme substrates and cofactors are anionic, emphasizing the essential role that anions play in biological processes. Moreover, anions can have detrimental effects on the environment by causing ground water contamination when anions such as perchlorate, phosphate and nitrate develop in intolerable levels. Owing to the prevalent nature of anions, traditional strategies employed to target anions—including hydrogen bonding, metal ion coordination and electrostatic interactions—have been extensively studied. An alternative approach to anion binding would complement the powerful array of existing techniques. Recently, in the supramolecular chemistry community, new insight has been cast on how anions attractively interact with electron-deficient arenes, suggesting that aromatic rings are a viable anion binding strategy to balance existing methods.

Chapter I provides a historical perspective of anions interacting with electron-deficient arenes. This outlook has its origins in the late 1800s with the discovery of

colored charge-transfer complexes between donor and acceptor molecules and continues with the progression of the field leading up to the recent supramolecular fascination. Chapter II represents our initial efforts at measuring anion/arene interactions in solution. In particular, sulfonamide based hydrogen bonding receptors were developed with pendant aromatic rings to test the strength of anion/arene interactions in solution. Complementary computational chemistry and crystallography were utilized to supplement the solution studies. Chapter III describes our quantum calculations and crystallographic efforts at using only electron-deficient arenes to bind halides. A Cambridge Structure Database survey supports our emphasis of understanding multiple anion/arene interactions. Chapter IV illustrates how tripodal anion receptors can be developed to bind anions using only electron-deficient aromatic rings. Furthermore, subtle changes in anion binding geometries are observed with isomeric receptors and corroborated with Density Functional Theory calculations. Chapter V is dedicated to the preparation of electron-deficient anion receptors that are conformationally stabilized by hydrogen bonds. Chapter VI is committed to using our knowledge of anion binding to study a series of ethynyl-pyridine sulfonamides capable of hydrogen bonding to small molecules and anions. In conclusion, Chapter VII is a summary and future prospective for the field of anion/arene interactions.

This dissertation includes previously published and co-authored material.

CURRICULUM VITAE

NAME OF AUTHOR: Orion B. Berryman

PLACE OF BIRTH: Homer, Alaska

DATE OF BIRTH: August, 4th 1981

GRADUATE AND UNDERGRADUATE SCHOOLS ATTENDED:

University of Oregon, Eugene, Oregon
University of New Hampshire, Durham, New Hampshire

DEGREES AWARDED:

Doctor of Philosophy, 2008, University of Oregon
Bachelor of Arts, Chemistry, Minor, Music, 2003, University of New Hampshire

AREAS OF SPECIAL INTEREST:

Supramolecular Chemisty
Single Crystal X-ray Diffraction
Organic Chemistry

PROFESSIONAL EXPERIENCE:

Research Assistant, Summer Internship, University of New Hampshire 2001-2003

Teaching Assistant, University of Oregon, 2003

GRANTS, AWARDS AND HONORS:

IGERT fellowship, University of Oregon, 2005-2008

Travel Grant, ISMSC, University of Pavia, Italy, 2007

Magna Cum Laude, University of New Hampshire, 1999-2003

PUBLICATIONS:

Berryman, O. B.; Johnson, C. A.; Zakharov, L. N.; Haley, M. M.; Johnson, D. W. *"Water and hydrogen halides serve the same structural role in a series of 2+2 hydrogen-bonded dimers based on 2,6-bis(2-anilinoethynyl)pyridine sulfonamide receptors."* *Angewandte Chemie International Edition,* **2007**, *46*, 117-120.

Berryman, O. B.; Bryantsev, V. S.; Stay, D. P.; Johnson, D. W.; Hay, B. P. *"Structural criteria for the design of anion receptors: the interaction of halides with electron-deficient arenes."* *Journal of the American Chemical Society*, **2007**, *129*, 48-58 (highlighted in UO Press release – December **2006).**

Meisner, J. S.; Berryman, O. B.; Zakharov, L. N.; Johnson, D. W. *"Methyl 4-bromo-3,5-dinitrobenzoate."* *Acta Crystallographica Section E,* **2007**, *63*, o2466.

Cangelosi, V. A.; Sather, A. C.; Zakharov, L. N.; Berryman, O. B.; Johnson, D. W. *"Diastereoselectivity in the self-assembly of $As_2L_2Cl_2$ macrocycles is directed by the As-π interaction."* *Inorganic Chemistry,* **2007**, *46,* 9278-9284.

Rather Healey, E.; Vickaryous, W. J.; Berryamn, O. B.; Johnson, D. W. *"In BOTTOM-UP NANOFABRICATION: Supramolecules, Self-Assemblies, and Organized Films;"* *Ariga, K., Nalwa, H. S., Eds.; American Scientific Publishers: Stevenson Ranch,* **2007**.

Berryman, O. B. ; Hof, F.; Hynes, M. J.; Johnson, D. W. *"Anion-π interaction augments halide binding in solution."* *Chemical Communications,* **2006**, 506-508.

Johnson, C. A.; Baker, B. A.; Berryman, O. B.; Zakharov, L.; O'Connor, M. J.; Haley, M. M. *"Synthesis and characterization of pyridine- and thiophene-based platinacyclyne topologies."* *Journal of Organometallic Chemistry,* **2006**, *691*, 413-421.

Vickaryous, W. J.; Healey, E. R.; Berryman, O. B.; Johnson, D. W. *"Synthesis and characterization of two isomeric, self-assembled arsenic-thiolate macrocycles."* *Inorganic Chemistry,* **2005**. *44*, 9247-9252.

ACKNOWLEDGMENTS

I must first express my sincere gratitude to my research advisor Darren W. Johnson for his continued direction and support throughout my doctoral tenure. My educational journey would have been wrought with difficulty without Dr. Johnson's continued zeal for chemistry. Additionally, I would like to thank my committee chair Prof. Jim Hutchison and members Profs Mike Haley, Ken Doxsee and David Schmidt for their insight and guidance.

My doctoral research has profited from access to the UO single crystal X-ray diffractometer and I must express my sincere appreciation to the individuals that taught me the intricacies of single crystal X-ray diffraction. Namely, Darren W. Johnson, Elizabeth Rather-Healey and Lev N. Zakharov have been instrumental in this regard.

The collaborative aspect of this dissertation has been possible through a number of excellent professional relationships that I would like to acknowledge. In particular, I would like to thank Dr. Benjamin P. Hay for an internship at the Northwest National Laboratory as well as a number of extended, yet insightful conversations. Additionally, Profs Fraser Hof and Michael J. Hynes have beneficially influenced my education.

I have had the privilege of mentoring a number of beginning chemists but above all Aaron C. Sather has expressed excellence and hard work in the laboratory. I must acknowledge my coworkers for their continued entertainment and support.

This investigation was sustained by funding from a National Science Foundation IGERT fellowship.

This body of work is dedicated to a few special people that have touched my heart, mind and soul. I must express my sincere gratitude to my loving parents Jon Martin Berryman and Julia Rene Berryman who have chiseled and worked this rough stone throughout the years. My grandmother Betty L. Snow and Trumpet teacher Howard Hedges who showed me inspiration through music and the written word. Finally, my loving wife Erin Jane Berryman who's eternal patience wears away stone.

TABLE OF CONTENTS

LIST OF FIGURES

Figure Page

Figure Page

CHAPTER VII

LIST OF TABLES

LIST OF SCHEMES

CHAPTER I

HISTORICAL PERSPECTIVE OF ANIONS INTERACTING WITH ELECTRON-DEFICIENT AROMATIC RINGS

INTRODUCTION

The underpinnings of this body of research focus on stabilizing anion complexes through the use of reversible non-covalent interactions. In particular, special attention has been afforded to the interactions exhibited between anions and electron-deficient aromatic rings, as well as the development of highly conjugated scaffolds for hydrogen bonding anion receptors. The 85 references found in Chapter I are quite impressive considering the nascent state of the field when we first started this project in 2004. While the interaction of anions with electron-deficient aromatic rings has recently garnered much attention, this by no means is a recent phenomenon. Chapter I of this dissertation begins with a succinct explanation of nomenclature and focuses on a historical perspective of anions interacting with electron-deficient aromatic rings. An introduction to recent (and not so recent) computational investigations concerning anions and electron-deficient aromatic rings as well as a structural survey of crystalline examples of this interaction is provided. Finally, the relatively few solution based observations of anions interacting with electron-deficient aromatic rings are provided

to introduce the research objectives of the current dissertation within the scope of the field. Chapters II-IV and VI include coauthored previously published work.

NOMENCLATURE AND HISTORICAL PERSPECTIVE

Anions are liberally defined as mono- or polyatomic ions bearing a negative charge. Because of the negative charge residing on the anion, an attraction to the π-system of aromatic rings (also known as arenes) or heterocycles has recently been thought to be counter-intuitive. Despite initial skepticism, a large number of computational studies and single crystal X-ray structures have definitively established the existence of this interaction when electron-deficient aromatic rings are employed.

Due to the recent burgeoning examples and the lack of historical perspective of reversible anion/arene attractions, it is easy to assume that this is a modern discovery.[1,2] However, it is important not to overlook the origins of attraction between anions and electron-deficient aromatic rings. A recent review by Hay, *et al.* also highlights this perspective.[3] Initial reports from Jackson, *et al.* in the late 1800s of highly colored complexes formed when electron-deficient picryl ethers were mixed with potassium alkoxides[4, 5] eventually led to isolation of the covalent Jackson-Meisenheimer complexes, which are considered to be isolable intermediates on the nucleophilic aromatic substitution pathway (Figure 1.1).[6]

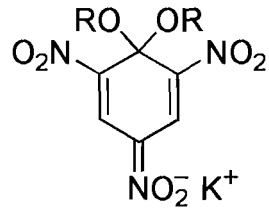

R = Alkyl

Figure 1.1 General structure of Jackson-Meisenheimer complexes formed when a picryl ether is mixed with potassium alkoxide.

The isolation and characterization of Jackson-Meisenheimer complexes was initially complicated by a number of both reversible and non-reversible interactions between the anion (or nucleophile in this case) and the π –system. The various interaction types are characterized by the degree of participation of the donor (anion) atom's electron pair.[7] For instance, π-complexes (also known as donor-acceptor or charge-transfer complexes) can form as a result of partial transfer of electron density from an electron rich donor (or anion) through the LUMO orbital of an electron-deficient aromatic ring (Figure 1.2, **1**).[8] Additionally, σ-complexes (Jackson-Meisenheimer complexes) arise as a result of the donor atom forming a covalent bond with an atom of the electron-deficient aromatic ring (Figure 1.2, **2**). Other complicating interactions include proton transfer from the electron-deficient aromatic ring to the donor atom (Figure 1.2, **4** and **5**), as well as substitution of aromatic substituents or complete transfer of an electron from the donor to the electron-deficient aromatic ring (Figure 1.2, **2**). This variety of interactions has been well understood since at least 1968 with a number of reviews having been written on the subject.[7, 9-14]

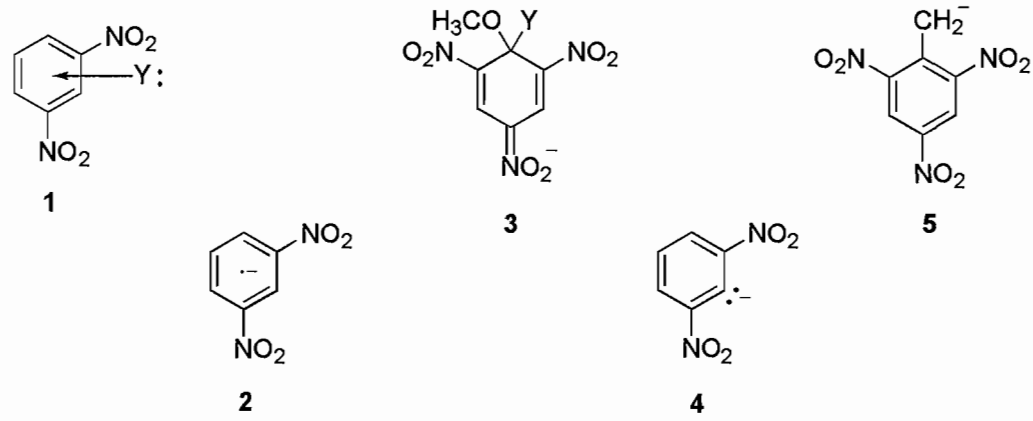

Figure 1.2 The interaction of aromatic nitro compounds with electron donors (Y).[7]

EARLY ANION/ARENE COMPUTATIONS AND MASS SPECTROMETRY

The assortment of possible anion/arene interactions suggests a continuum of possible attractions that depend on both the nucleophilicity of the anion and the degree of electron-deficiency of the aromatic ring. This multitude of binding geometries was later theoretically and experimentally established from molecular orbital calculations and binding affinities measured from gas-phase ion-molecule equilibrium measurements with pulsed electron high ion source pressure mass spectrometers.[15-26] Interestingly, gas phase techniques have resurfaced as a popular method to study anion/arene interactions.[27, 28]

RENAISSANCE OF ANION/ARENE COMPUTATIONS

The recent publication of higher level computations quantifying the interaction of anions with electron-deficient aromatic rings has regenerated interest in the

supramolecular chemistry community.[29-31] As a result, a renaissance in computational studies has emerged looking at a variety of anions. The most studied anions to date are the simple monoatomic ions,[32-51] but recent studies have progressed to more complicated polyatomic anions with an assortment of geometries.[29-31, 52-59] As for the electron-deficient aromatic ring, the most popular targets for study are fluorinated aromatic rings like hexafluorobenzene or heterocyclic rings such as triazine.[29-33, 36, 38-48, 50, 51, 53, 55, 57, 59] However, the focus of these publications has been toward symmetric non-covalent interactions (Figure 1.3, **A**). Other forms of attractive interactions between anions and electron-deficient aromatic rings have been largely overlooked. In fact, in our introduction to this field of research we were also unaware of the alternative binding modes for anions and arenes. This misconception was propagated in our first generation of receptors[60]—it was not until our following crystallographic and computational study that we came to understand that there are a number of attractive interactions with electron-deficient aromatic rings. These include: a centered electrostatic interaction (**A**), an off-centered weak σ interaction (**B** and **C**), and when available, aryl C-H hydrogen bonds (**D**, Figure 1.3). Our crystallographic and computational studies have helped refine the nature of possible interactions that were introduced in the early 1900s between anions and arenes and reminded the supramolecular community of their importance.

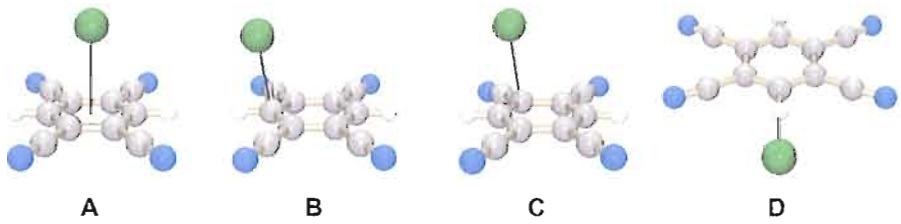

Figure 1.3 MP2/aug-cc-pVDZ optimized geometries for Cl^- interactions with 1,2,4,5-tetracyanobenzene include an unstable anion-π complex (**A**), weak σ complexes (**B** and **C**), and an aryl C-H hydrogen bond complex (**D**).

A FLOURISH OF ANION/ARENE CRYSTAL STRUCTURES

Recent computational interest has spurred the report of a number of illustrative crystal structures with anions positioned appropriately close to electron-deficient aromatic rings. This section of Chapter I focuses on relevant crystallographic examples of anions interacting with the π-systems of aromatic rings. Aryl C-H hydrogen bonds have generally been omitted; a number of excellent examples can be found in a review by Hay, *et al.*[3] In addition to attractive anion/arene interactions the vast majority of these examples exhibit accompanying stabilizing forces in the solid state. For instance, in many cases the electronic character of an aromatic ring is perturbed by direct coordination of a metal cation.[58, 61-73] The anion is often present to balance charge or fill porous networks formed from metal organic frameworks.

A representative example of a counter anion that interacts with the pyridine moieties of an octadentate copper(II) coordinated pyridine ligand is shown in Figure 1.4. In the solid state, two of the chlorides each exhibit four short contacts with adjacent copper coordinated pyridine moieties.

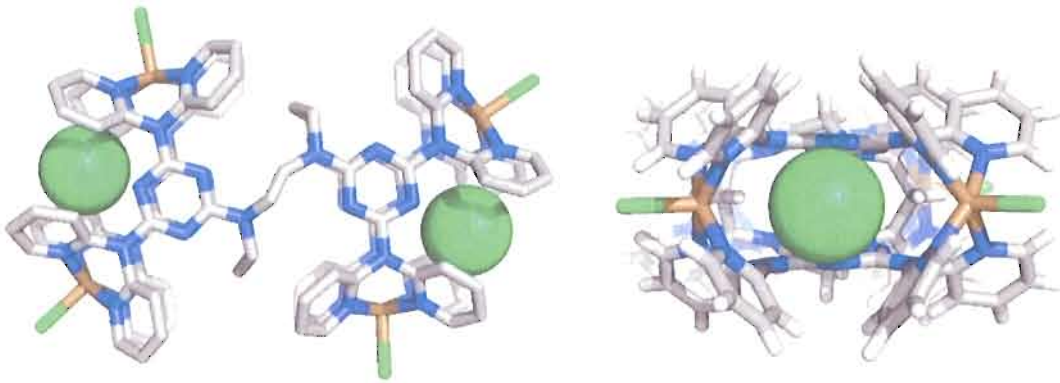

Figure 1.4 Single crystal X-ray structure from Reedijk and coworkers illustrating chloride/pyridine contacts in a copper (II) coordinated octadentate pyridine ligand. Hydrogen atoms and additional chloride counter anions have been omitted for clarity.[67] Chlorides are represented as spheres and ligands represented as sticks.

The next largest number of examples comes from crystal structures where both anion/arene interactions and ion pairing are employed to attract anions.[36, 74, 75] One illustrative solid state example of tandem ion pairing and anion/arene interactions comes from the laboratories of Frontera and coworkers where cyanuric acid derivatives adorned with ammonium substituents were shown to crystallize with the halide counter

anions Cl^-, Br^- and I^- (Figure 1.5).[36] The anions in this example are located slightly off-center from the aromatic ring centroid and are stabilized by hydrogen bonds with the positively charged ammonium substituent and contacts with the electron-deficient cyanuric acid derivatives.

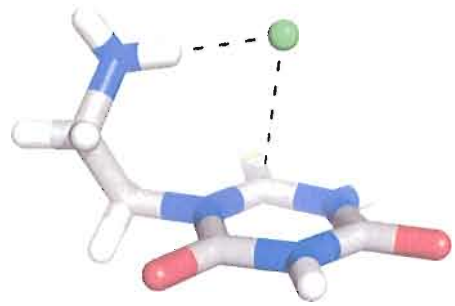

Figure 1.5 Single crystal X-ray structure of ethylammonium substituted thiocyanuric acid, illustrating both ion pairing and anion/arene interactions with chloride.[36]

Not surprisingly, a handful of examples utilize multiple interactions in addition to electron-deficient arenes to stabilize anion complexes, including hydrogen bonding, ion pairing and anion/arene interactions.[44, 45, 76-78] The very nature of crystal structures makes isolating anion/arene interactions a difficult endeavor. Exceptionally rare are the examples that utilize only anion/arene interactions to position anions near electron-deficient aromatic rings.[79, 80] For example, Rosohka, *et al.* co-crystallized electron-deficient π-systems with Br^- and I^-. The solid state structures of electron-deficient arenes such as tetracyanopyrazine with Br^- reveal multiple close contacts in the solid state depending on the ratio of starting materials (Figure 1.6). In addition to the recent

solid state highlights of anion/arene interactions, numerous structures have been located from the Cambridge Structure Database and presented as evidence for anion/arene interactions. These examples are not presented here, but can be found within the references to this chapter. Through a survey of the Cambridge Structure Database, we have shown that in the absence of additional interactions, anions are preferentially located above the edge of electron-deficient aromatic rings.[61]

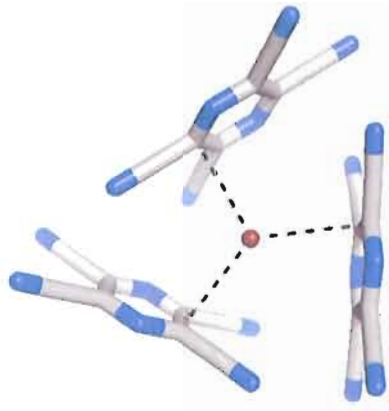

Figure 1.6 A portion of the tetracyanopyrazine/Br^- single crystal X-ray structure. Halides exhibit multiple off-center contacts in the solid state with the number of electron-deficient aromatic rings depending on the starting ratio.[80]

A RELATIVE DEARTH OF ANION/ARENE SOLUTION STUDIES

While there is a large body of research on covalent anion/arene (Jackson-Meisenheimer) complexes, we are interested in designing anion receptors that

incorporate electron-deficient aromatic rings to bind anions reversibly in solution. This section of Chapter I will focus on noncovalent or weakly covalent, reversible anion/arene interactions. Given the relatively weak nature of anion/arene interactions, only a handful of attempts have been made to measure these interactions in solution. Indeed, only two such examples existed at the outset of our research. *Furthermore, at this point no designed receptors had been shown to exhibit anion/arene interactions in solution.* In 1991, Schneider measured associations between sulfonate substituted aromatic rings and charge neutral aromatic rings in solution.[81] These insightful measurements likely represent both π-stacking and anion/arene interactions that are occurring in solution and provide an early observance of anion/arene interactions. More recently, Rosokah, *et al.* utilized Uv-vis spectroscopy to measure association constants between halides and commercially available electron-deficient π-systems.[80] Association constants of alkyl ammonium salts of Br^- and I^- with 1,2,4,5-tetracyanobenzene, 1,3,5-trinitrobenzene and tetracyanopyrazine were found to range from 0.8-9 M^{-1} in acetonitrile/dichloromethane solutions. Our initial study aimed to address the deficiency of designed receptors utilizing electron-deficient aromatic rings to bind anions. This receptor class is explained in detail in Chapter II. More recently, elegant receptor molecules illustrate or have been designed to illustrate anion/arene interactions. However, the large number of competing interactions in solution often requires the use of additional attractive forces to measure the relatively weak anion/arene interactions. Hydrogen bonds have been employed in receptors most often to assist in attracting anions to electron-deficient aromatic rings.[60, 82-85] Ballester's

group in Spain has designed calix[4]pyrrole receptors that contain electron-deficient aromatic rings to assist in halide binding. An enhancement of anion binding is observed over a similar control receptor even when only modestly electron-deficient nitrobenzene substituents are attached to the receptor core. A single crystal X-ray structure illustrates the position of the chloride within the receptor cavity (Figure 1.7).

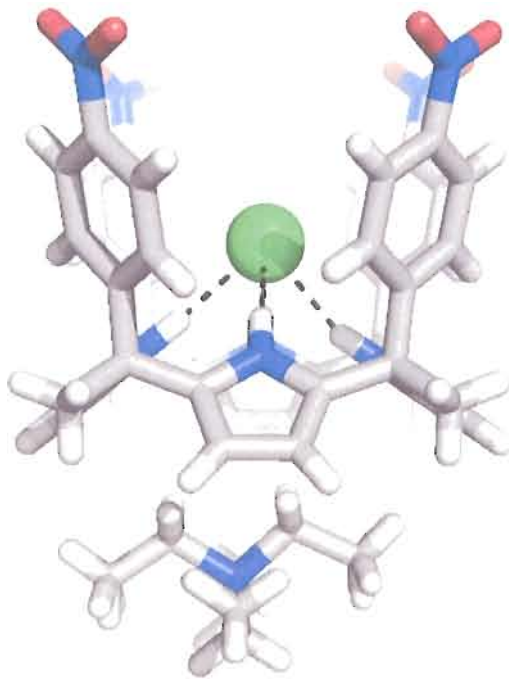

Figure 1.7 Single crystal X-ray structure of a neutral calix[4]pyrrole anion receptor hydrogen bonding to Cl^- and forming four Cl^-/nitrobenzene contacts.[83]

Other supporting attractive interactions that have been employed include ion pairing and metal coordination.[69] For instance, Ghosh and coworkers developed tripodal anion receptors containing electron-deficient aromatic rings built from tris(2-

ethylamino)amine. When protonated, these receptors bind halides in solution and X-ray crystal structures reveal close anion/arene contacts (Figure 1.8).[75]

Figure 1.8 X-ray crystal structure of a tripodal receptor/Cl^- complex. Receptor contains ion pairing and pendant electron-deficient aromatic rings to assist anion binding.[75] The tripodal receptor molecule is represented as sticks and the Cl^- as a sphere.

Metal coordination has also been employed to assist anion binding in solution. Holman and coworkers were the first to highlight a fully ruthenium metallated cryptophane that binds anions within its cavity.[86] ^1H NMR spectroscopy unequivocally showed in solution the encapsulation of anions such as $CF_3SO_3^-$, SbF_6^- and PF_6^- in the metalated molecular container. $CF_3SO_3^-$ or SbF_6^- are also contained within the cavity in the solid state and a representative crystal structure is shown in Figure 1.9.

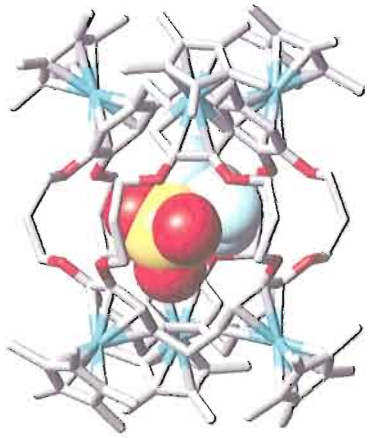

Figure 1.9 Single crystal X-ray structure of a ruthenium permetallated cryptophane that encapsulates $CF_3SO_3^-$ aided by six anion/arene interactions. Hydrogen atoms have been removed for clarity and the enclosed $CF_3SO_3^-$ is represented as spheres.[69]

SUMMARY AND BRIDGE TO CHAPTER II

Interactions between electron rich molecules or anions with electron-deficient aromatic rings have been recognized for over a century. These highly colored complexes were initially touted as intermediates to nucleophilic aromatic substitution reactions. More recently, the interactions of anions with electron-deficient aromatic rings have undergone much scrutiny leading to a better understanding of anion/arene interactions. A large number of computational studies have surfaced examining anion/arene interactions; these are supported by numerous single crystal X-ray structures and a handful of solution studies. Our contributions to this field will be presented in this dissertation with a particular focus toward the development of new binding motifs for anion receptors.

Chapter II focuses on our initial effort to probe anion/arene interactions, in which we designed and synthesized anion receptors to measure anion/arene interactions in solution. Based on the existing computational studies at the time, we felt it was necessary to incorporate an electron-deficient aromatic ring *and* a complementary hydrogen bond donor into our receptor design. This two-point recognition motif was compared to a control receptor lacking the electron-deficient aromatic ring. Complementary computational studies also supported our hypothesis that electron-deficient aromatic rings enhance halide binding in this system.

CHAPTER II

ANION-π INTERACTION AUGMENTS HALIDE BINDING IN SOLUTION

INTRODUCTION

This chapter was co-authored with Professors Fraser Hof, Michael J. Hynes and Darren W. Johnson. Professor Hof performed Hartree-Fock calculations that were used in the manuscript while Prof. Hynes assisted in calculating association constants for this system. Darren W. Johnson conceptualized the project and provided editorial assistance while Orion Berryman wrote this chapter and completed the CAChe computer modeling, synthesis, characterization, single crystal X-ray diffraction studies, literature searches, pKa measurements and titration experiments. This chapter includes work that was published in *Chemical Communications* (**2006**, 506-508, © 2006 The Royal Society of Chemistry). At the time of publication the authors of this work did not fully appreciate the distinction between different types of anion/arene interactions. Therefore, the liberal use of the term "anion-π" interaction should alert the reader to consider alternative binding modes. A detailed review of this concept is presented in Chapter III.

Molecular receptors designed to target anions utilize a variety of interactions to accomplish their goal. Some of the more common reversible bonds employed include hydrogen bonding, electrostatic interactions, hydrophobic effects, and coordination to a metal ion.[1-4] A promising binding strategy to target anions that has recently garnered much attention in the literature is the anion-π interaction. Currently, numerous computational studies[5-9] and single crystal X-ray structures[6, 10-14] support the viability of using this noncovalent interaction as a design strategy to target anions. Several of these reports compare the anion-π interaction to the familiar cation-π interaction[5, 15] where a positively charged ion attractively interacts with an electron-rich aromatic ring.[16] The anion-π interaction is similarly proposed to arise from a *negatively charged* species having a coulombic attraction to an area of low electron density in an *electron-deficient* aromatic ring. Despite the numerous solid state examples and theoretical treatments, surprisingly few solution phase examples recognize the anion-π interaction.[13]

RECEPTOR DESIGN

In an attempt to probe the efficacy of the anion-π interaction to bind anions in solution, two receptor molecules were prepared (**1** and **2**, Scheme 2.1). Design of receptor **1** focused on a two point recognition motif utilizing both a hydrogen bond and an electron-deficient aromatic ring.[17] In contrast to **1**, control receptor **2** lacked the electron-deficient aromatic substituent required for the anion-π interaction. Any

enhanced association for anions that receptor **1** exhibits over receptor **2** should be a result of the favorable anion-π interaction present in the **1**•anion complex. To the best of our knowledge, a receptor molecule *designed* to incorporate the anion-π interaction to bind anions in solution is unknown. Herein we report solution data illustrating the enhanced association for anions that designed receptor **1** shows over control receptor **2**.

RECEPTOR SYNTHESIS, X-RAY DIFFRACTION AND ELECTROSTATIC POTENTIAL SURFACE

Receptor **1** was synthesized by converting *o*-iodoaniline to the corresponding *p*-toluenesulfonamide[18] **3** followed by a palladium-mediated Ullmann coupling (Scheme **2.1**).[19, 20] ^{1}H NMR spectroscopy and single crystal X-ray diffraction confirmed the structure of receptor **1** (see Appendix A). A similar procedure provides **2** in 87% yield starting from 2-aminobiphenyl.

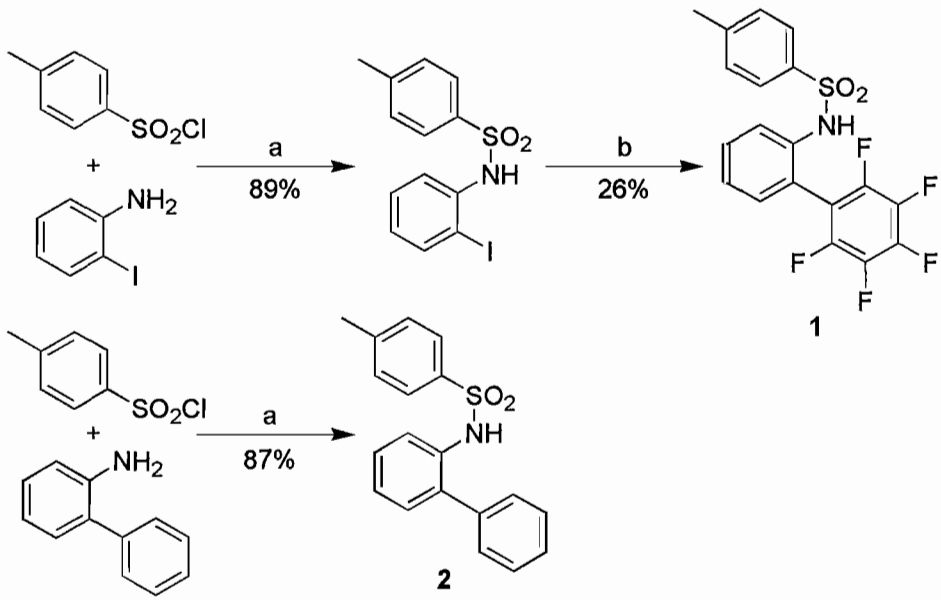

Scheme 2.1 *Reagents and conditions*: (a) dry pyridine, rt, 4h. (b) C_6BrF_5, dry DMSO, $Pd(PPh_3)_4$, Cu^0, 105 °C, 5.5 h.

Single crystals of **1** suitable for X-ray diffraction were grown by diffusing pentane into a chloroform solution of the receptor (see summary of crystallographic data). Receptor **1** crystallizes as a hydrogen bonded dimer in spacegroup *P*-1 with two molecules of **1** per unit cell. It is interesting to note that one sulfonamide oxygen from each receptor molecule is located 3.1 Å from the electron-deficient aromatic ring of an adjacent molecule.[21, 22] In the crystalline state **1** is preorganized in the optimal conformation to interact with an anion through *both* a hydrogen bond *and* an anion-π interaction.

Electrostatic potential surfaces (EPS) of molecules have been used to illustrate areas of low electron density that can interact with electron-rich anions.[7, 15] To highlight both the pre-organization of receptor **1** for binding anions and the predictive power that electrostatic potential surfaces have for the anion-π interaction, the crystal structure of **1** is shown alongside a minimized (CAChe 5.0, EHT) electrostatic potential surface plot of receptor **1** in the optimal conformation for complexing an anion (Figure 2.1).[23] The center of the electron-deficient aromatic ring of receptor **1** (Figure 2.1) exhibits a surface of low electron density (white) that is optimal for interacting with an anion.

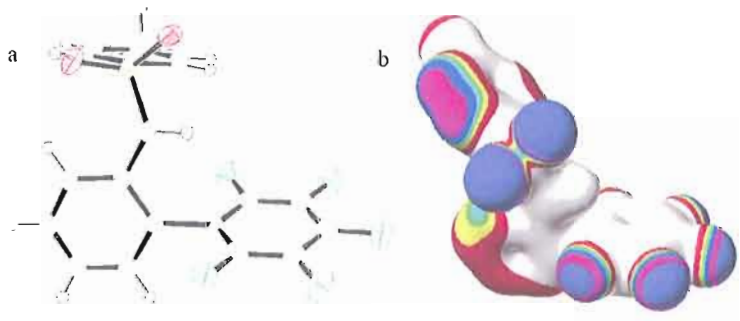

Figure 2.1 (a) ORTEP representation of the single crystal X-ray structure of **1**. Ellipsoids are at the 50% probability level with sulfur yellow, oxygen red, carbon gray, nitrogen blue, fluorine green and hydrogen light gray. (b) Calculated EPS plot of receptor **1**, scaling areas of highest electron density (blue) to lowest (white).

SOLUTION STUDIES – ANION BINDING

Following the synthesis of receptors **1** and **2**, ^{1}H NMR spectroscopic titration experiments were performed for each receptor with the tetra-*n*-butylammonium salts of chloride, bromide and iodide. The downfield shift of the N-H resonances of **1** and **2** were monitored as aliquots from a stock solution of the corresponding salt in $CDCl_3$ were added to the receptors in $CDCl_3$. WinEQNMR[24] was used to fit the raw data to a 1:1 association model (see Appendix A). Iterative calculations using WinEQNMR yielded the stability constants of the receptors with each anion[25] (Table 2.1); each reported K_a for **1** represents the average of three titrations.

Table 2.1 K_a (M^{-1}) for receptors **1** and **2** with selected halides.[a]

	Receptor **1**[b]	Receptor **2**[b]
Cl^-	30 ± 3	<1[c]
Br^-	20 ± 2	<1[c]
I^-	34 ± 6	<1[c]

[a]The NEt_4^+ salts of each hailide were used. [b]Initial receptor concentrations fall in the range of 9-25 mM; full details of the titration experiments are contained in the ESI. [c]Association constants for receptor **2** were too small to be determined by ^{1}H NMR titration experiments.

The titration experiments depict a stark contrast between the association constants of receptors **1** and **2** with a given halide. Receptor **1** binds all the halides screened (iodide, bromide and chloride) with a measurable, albeit modest association constant. However, in the case of receptor **2**—where an electron-deficient aromatic ring is not

present—there is no measurable association with any of the halides tested. Comparison of the association constants for the nearly isosteric receptors **1** and **2** allows for an initial assessment of the anion-π interaction in solution. The association constants measured for receptor **1** and the series of halides iodide, bromide and chloride fall in the range of 20-34 M^{-1}. The measured association constants are similar in magnitude with reported anion-π binding constants.[13] Receptor **2** on the other hand shows a significantly weaker binding to the same halides. The change in chemical shift from the titration experiments was so small for receptor **2** that no association constant could be determined. The association constants for receptors **1** and **2** provide strong support demonstrating the anion-π interaction in solution, highlighting the possibility of utilizing the anion-π interaction to bind anions by design.

The trend in association constant strength for receptor **1** and the halides chloride, bromide and iodide cannot solely be explained by the strength of the hydrogen bond with each anion. In a similar system containing only a sulfonamide substituent (but no adjacent aromatic ring), it was observed that chloride forms the strongest association by an order of magnitude whereas bromide and iodide are significantly weaker and equal to each other.[26] However, receptor **1**, which contains an electron-deficient aromatic ring designed to interact with anions, shows a deviation from this trend with the most polarizable anion (iodide) exhibiting a comparable association to that of the more basic chloride ion. One plausible explanation for this enhanced binding observed with iodide could be that the more polarizable iodide anion provides a stronger

interaction with the electron-deficient aromatic ring, which supplements the weaker hydrogen bond.[16, 27]

RECEPTOR pK_a MEASUREMENTS AND ANALYSIS

An alternative explanation for the differences in measured K_a values between receptors **1** and **2** could be their variation in sulfonamide N-H acidities. It is apparent that the electronic differences between receptors **1** and **2** result in sulfonamide N-H protons with different pK_a values. Abraham *et al.*[28] have shown by comparing a family of receptors, the change in association constant based on hydrogen bonding acidity is only a fraction of the pK_a difference between the H-bond donors.[29] Receptors **1** and **2** exhibit at least a two order of magnitude difference in anion binding affinity, while the pK_a values are only 2.5 log units different (see Appendix A). Therefore, the pK_a of the sulfonamide N-H cannot alone explain the difference in association constants for anions. The difference in pK_a values is an issue with any receptor that utilizes both a hydrogen bond and an anion-π interaction, therefore new receptors are being synthesized without this feature to investigate the anion-π interaction further.

ANION-RECEPTOR CO-CRYSTAL AND COMPUTATIONAL ANALYSIS

While a crystal structure of a **1**•anion complex in the proper orientation remains elusive — presumably a result of the low association constant of **1** with anions — Figure 2.2 illustrates the only solid state structure of receptor **1** and an anion observed to date (see summary of crystallographic data). In this structure the sulfonamide N-H is drastically rotated out of conjugation with the adjacent phenyl ring in order to form a very weak hydrogen bond with a bromide ion (avg. Br-H-N angle = 129.7°). This conformation precludes formation of an anion-π interaction and is adopted to allow for a polymeric ion pair between tetra-*n*-butylammonium counterions and the bromide anion to form in the crystal state (Figure 2.2, inset).

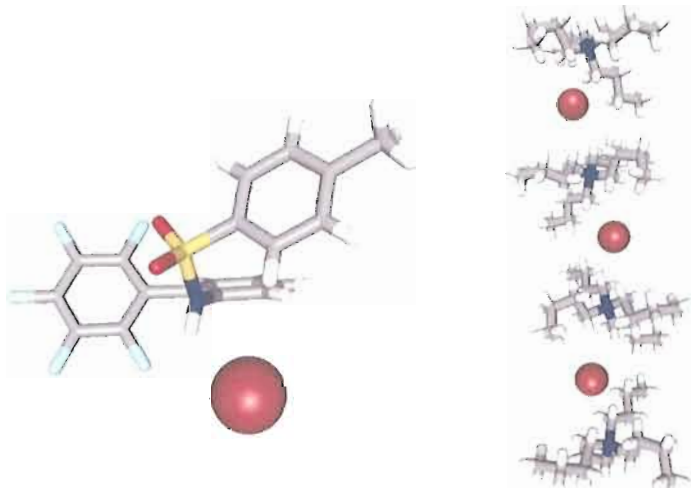

Figure 2.2 Stick representation of the X-ray crystal structure of receptor **1** and tetra-*n*-butylammonium bromide where the ion pairing in the solid state is forcing the sulfonamide N-H away from the preferred conformation. The inset shows the polymeric ion pair formed in the solid state.

This solid state structure likely does not represent the solution structure of **1** when bound to an anion: first, Hartree-Fock (6-31+G*) geometry optimizations for the complex of each receptor **1** and **2** with chloride showed two different energy minima for both receptors. Receptor **1** exhibited one minimum with the chloride over the face of the electron-deficient aromatic ring (Figure 2.3a) and one minimum with the chloride positioned to the side of the electron-deficient aromatic ring. Receptor **2** on the other hand showed no reasonable structure positioning the halide over the face of the aromatic ring (Figure 2.3b). These calculations suggest that the chloride anion is repulsed by the aromatic ring in receptor **2** while being attracted to the electron-deficient aromatic ring of receptor **1**.

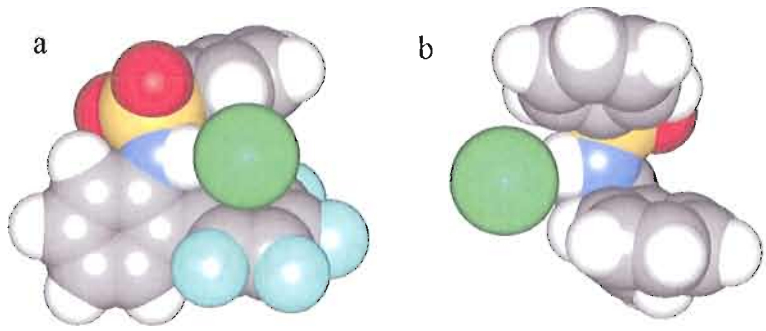

Figure 2.3 HF geometry minimizations of receptors **1** and **2** with chloride using a 6-31+G* basis set. (a) Energy minimization of receptor **1** with chloride (green) showing the halide over the face of the electron-deficient aromatic ring. (b) One of the representative minimizations of receptor **2** with chloride (green) not positioned over the face of the aromatic ring.

Secondly, the polymeric ion pair observed in the crystalline state is clearly not maintained in $CDCl_3$ solutions. Furthermore, this ion pair forming in solution would not explain the ^1H NMR chemical shift dependence of the N-H resonance of **1** on anion concentration (Table 2.1). Additionally, since receptors **1** and **2** are nearly isosteric, **2** could equally-well adopt this twisted conformation to bind anions in solution. If this were the case, **1** and **2** would have very similar binding constants for anions, which they do not. Despite this perplexing structure, the solution data are best corroborated by invoking an attractive anion-π interaction when **1** binds anions.

CONCLUSION

The solution data presented herein underscore the hypothesis that electron-deficient aromatics can be used as a component of a design strategy to target anions in solution. A pair of receptors that differ only by the substituents on their aromatic rings were designed and synthesized. Analysis of the association constants of each receptor with an array of halides has demonstrated the enhanced affinity for anions that receptor **1** shows in solution over a control receptor lacking an electron-deficient aromatic ring. The enhanced binding that receptor **1** displays results from an attractive anion-π interaction. These experiments support the use of the anion-π interaction as an emerging nonconvalent interaction for the selective targeting of anions in solution.

SUMMARY OF CRYSTALLOGRAPHIC DATA

1: $C_{19}H_{12}F_5NO_2S$, $M = 413.36$, triclinic, P-1, $a = 9.0547(11)$, $b = 10.2933(12)$, $c = 10.4106(13)$ Å, $\alpha = 97.125(2)°$, $\beta = 112.783(2)°$, $\gamma = 101.424(2)°$, $V = 854.95(18)$ Å^3, $Z = 2$, μ(Mo-Kα) = 0.257 mm^{-1}. Final residuals (242 parameters) $R1 = 0.0818$ for 3444 reflections with $I > 2\sigma(I)$, and $R1 = 0.1570$, $wR2 = 0.2413$, GooF = 1.030 for all 6901 data. CCDC #261862.

1•(n-Bu_4N•Cl): $C_{35}H_{47}BrF_5N_2O_{2.5}S$, $M = 742.72$, triclinic, P-1, $a = 10.863(4)$, $b = 16.807(6)$, $c = 21.000(7)$ Å, $\alpha = 74.118(6)°$, $\beta = 83.011(6)°$, $\gamma = 89.974(6)°$, $V = 3658(2)$ Å^3, $Z = 4$, μ(Mo-Kα) = 1.240 mm^{-1}. Final residuals (498 parameters) $R1 = 0.0916$ for 4148 reflections with $I > 2\sigma(I)$, and $R1 = 0.1400$, $wR2 = 0.2477$, GooF = 1.013 for all 6598 data. CCDC #286064.

BRIDGE TO CHAPTER III

We were pleased with our initial success of designing a system to measure anion/arene interactions in solution. However, we were somewhat frustrated with the ambiguity that surfaced from incorporating two different interaction types into one receptor. We provided evidence supporting our statement that the differences in pK_a values do not solely represent the drastically different K_a values measured for this system. Nevertheless, we felt the next logical step was to remove additional supporting interactions and focus directly on anion/arene interactions. Chapter III focuses on the interaction of anions with *only* electron-deficient aromatic rings and provides solid state and computational scrutiny that redirects the focus of anion/arene interactions from centered electrostatic interactions to off-center weakly covalent σ complexes.

CHAPTER III

STRUCTURAL CRITERIA FOR THE DESIGN OF ANION RECEPTORS: THE INTERACTION OF HALIDES WITH ELECTRON-DEFICIENT ARENES

INTRODUCTION

This chapter was co-authored with Dr. Vyacheslav S. Bryantsev, David P. Stay, Prof. Darren W. Johnson and Chief Scientist Dr. Benjamin P. Hay. David Stay isolated single crystals of the structures presented in this study. Dr. Bryantsev completed all the quantum calculations found within. Dr. Hay aided with the literature and Cambridge Structure Database searches. Both Dr. Hay and Prof. Johnson assisted in conceiving this project and provided editorial assistance. Orion B. Berryman prepared the chapter, assisted in literature searches, solved the single crystal X-ray structure and assisted in the Cambridge Structure Database searches and data compilation. This chapter includes work that was published in *Journal of the American Chemical Society* (**2007**, *129*, 48-58, © 2007 American Chemical Society)

BACKGROUND AND SIGNIFICANCE. Anion complexation by synthetic host molecules is an important theme in supramolecular chemistry.[1] One of the key challenges is the design of hosts that recognize specific anions. A variety of reversible and/or noncovalent interactions have been used to overcome these challenges, including hydrogen bonding, electrostatic interactions, hydrophobic effects and coordination to metal ions. A relatively new anion binding motif—the anion-π interaction—has attracted substantial attention in the recent literature. In this interaction, a negatively charged species is attracted to the center of a *charge neutral* electron-deficient aromatic ring as shown in Figure 3.1.[2-5] Although much of the evidence for the anion-π interaction has come from theoretical studies,[2-13] there is mounting experimental support for an attractive interaction between anions and electron-deficient arenes from both X-ray structures[14-16] and solution data.[14,17-19] Recently we,[18] along with others,[11,12,19] have begun to investigate the utility of the anion-π interaction by deliberately incorporating electron-deficient arenes as binding sites within receptors designed to target anions.

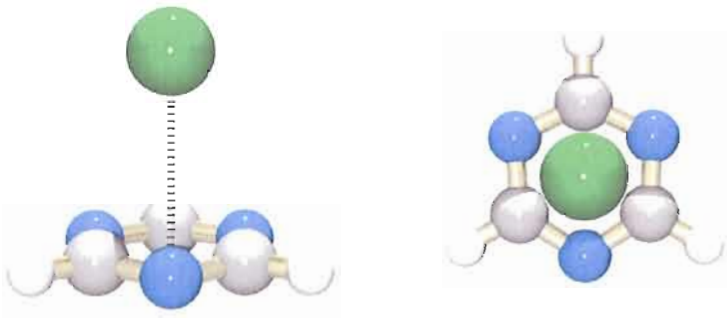

Figure 3.1 Initial theoretical observation of anion-π complexes occurred in a study of the interaction between Cl^- and triazine.[2]

Anion-π complexes involving halides have been the most widely modeled and calculated structures have been reported for a variety of arenes (Figure 3.2).[2-12] In these structures, the halide is located directly over the center of the arene ring. It has been established that this interaction is predominantly a non-covalent one, dominated by two components – (i) attraction between the negative charge of the anion and the electric field of the arene and (ii) anion-induced polarization. Despite the fact that calculations have found the strength of the anion-π interaction to be significant, typically ranging from 10 to 20 kcal mol^{-1}, there are surprisingly few reports of crystal structures that illustrate this interaction for free halides,[12,14,15] and there are no examples of halide complexes with any of the unsubstituted arenes that have been studied *in silico* (Figure 3.2).

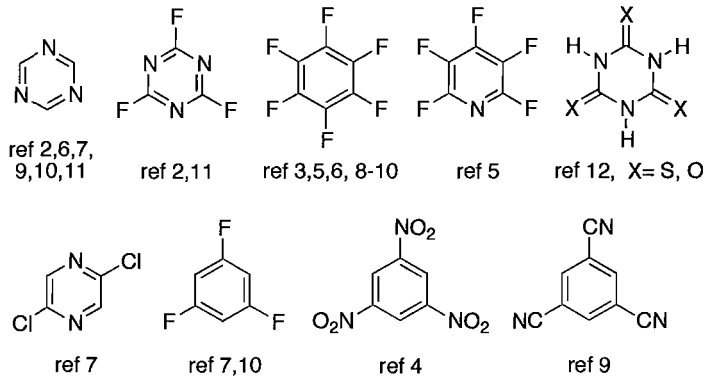

Figure 3.2 Electronic structure calculations have established that non-covalent anion-π complexes form between halide anions and these electron-deficient arenes.

Although theoretical studies have focused primarily on the non-covalent anion-π interaction, an experimental study on the solution behavior of halide complexes with highly electron-deficient arenes (Figure 3.3) suggests that a different binding motif may be operating in these systems.[14] Intense color changes were observed upon addition of halide salts to acetonitrile/dichloromethane solutions containing these arenes. Analysis of the visible spectral data revealed that the halide salts form classic electron donor-acceptor charge-transfer (CT) complexes with the organic π acceptors. This behavior is not consistent with a non-covalent anion-π interaction in which, by definition, there would be negligible CT. Moreover, crystal structures of alkylammonium halide salts with TCP and o-CA revealed the anions to be positioned over the periphery of the arene rings rather than over the center of the rings as anticipated for bonding arising primarily from electrostatic and polarization interactions.

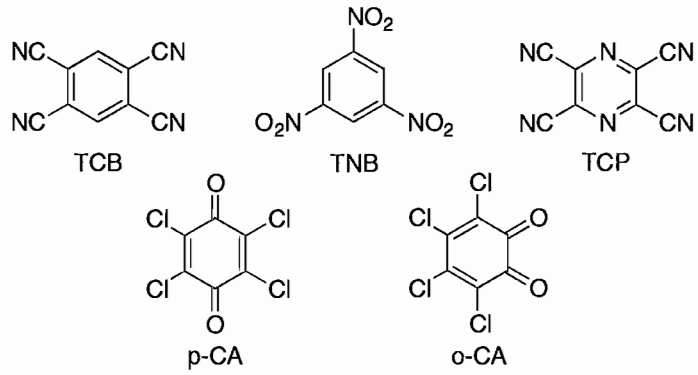

Figure 3.3 Solution and solid-state studies of these highly electron-deficient arenes yield data inconsistent with a non-covalent anion-π interaction.[14]

This discrepancy between theory and experiment, coupled with the general paucity of structural data for anion-π interactions with arenes such as those depicted in Figure 3.2 and 3.3, prompted us to undertake further investigations. To obtain additional structural information, alkali halide salts have been crystallized from solutions containing 1,2,4,5-tetracyanobenzene (TCB) and 18-crown-6. As described herein, the off-center geometries of the halide-arene complexes observed in these structures suggest an alternate interaction motif to the centered non-covalent anion-π interaction widely promulgated in the literature. Electronic structure calculations on halide complexes with TCB and other electron-deficient arenes confirm the presence of alternate binding geometries in which the halide is positioned over the periphery of the ring and there is substantial CT from the halide donor to the π acceptor. Analysis of the Cambridge Structural Database reveals that when halides interact with electron-deficient π systems, they are more likely to reside over the periphery of the ring than

over the center, suggesting that the CT binding motif is more common than the non-covalent one. The results indicate that molecular design strategies for incorporating electron-deficient π systems within host architectures should consider the differing geometries attendant with CT versus non-covalent binding motifs.

METHODS

GENERAL. 1,2,4,5-tetracyanobenzene was obtained from TCI. Acetonitrile and dichloromethane were obtained from Aldrich and stored over 3 Å molecular sieves. 18-crown-6 as well as the potassium and sodium salts were obtained from commercial suppliers without the need for further purification.

SINGLE CRYSTAL GROWTH. Single crystals suitable for X-ray diffraction were grown by slow evaporation of acetonitrile/dichloromethane solutions at room temperature. TCB (0.030 g, 0.168 mmol), 18-crown-6 (0.100 g, 0.378 mmol) and KI or NaI (0.972 mmol) were added to acetonitrile (1 ml). The resulting suspension was sonicated and heated to reflux. The remaining dark red solution was evaporated at room temperature to yield dark purple crystals of the form $[K(18\text{-crown-}6)(TCB)_2]^+I^-$ or $[Na(18\text{-crown-}6)(TCB)_2]^+I^-$. The corresponding KBr structure, $[K(18\text{-crown-}6)(TCB)_2]^+Br^-$ was obtained in an analogous manner substituting KBr (0.116 g, 0.972 mmol) and a 9:1 dichloromethane:acetonitrile solution as the solvent. Evaporation at room temperature resulted in orange single crystals of the KBr complex.

X-RAY DIFFRACTION. Single-crystal X-ray diffraction data for the [K(18-crown-6)$(TCB)_2]^+Br^-$, [K(18-crown-6)$(TCB)_2]^+I^-$ and [Na(18-crown-6)$(TCB)_2]^+I^-$ compounds were collected on a Bruker-AXS SMART APEX/CCD diffractometer using $Mo_{K\alpha}$ radiation (λ = 0.7107 Å) at 152 K. Diffracted data have been corrected for Lorentz and polarization effects, and for absorption using SADABS.[20] The structures were solved by direct methods and the structure solution and refinement was based on $|F|^2$. All non-hydrogen atoms were refined with anisotropic displacement parameters whereas all hydrogen atoms were located and given isotropic U values 1.2 times that of the atom to which they are bonded. All crystallographic calculations were conducted with SHELXTL.[21] Crystallographic data (excluding structure factors) have been deposited with the Cambridge Crystallographic Data Centre as supplementary publication numbers 606748, 606749, and 606750. Copies of the data can be obtained free of charge on application to The Director, CCDC, 12 Union Road, Cambridge CB21EZ, UK (fax: international code + (1223)336-033; email: deposit@chemcrys.cam.ac.uk).

ELECTRONIC STRUCTURE CALCULATIONS. Electronic structure calculations were carried out with the NWChem program[22] using second order Möller-Plesset perturbation theory (MP2).[23] Geometries were optimized using the augmented correlation consistent double-ζ basis set (aug-cc-pVDZ)[24] and frozen core approximation in the correlation treatment. Tight geometry optimization cutoffs were employed since standard optimization criteria may results in spurious negative frequencies. Frequency calculations were performed at the same level of theory to

characterize each stationary point as a minimum or a transition state. The electrostatic potential fit charges[22] and NPA natural charges[25] were calculated using HF/aug-cc-pVDZ electron densities.

CAMBRIDGE STRUCTURAL DATABASE SEARCHES. The Cambridge Structural Database[26] was searched for examples in which a halide anion was located within 4.0 Å of the centroid of any six-membered ring in which all ring atoms were connected to exactly three other atoms. A total of 591 hits were obtained when the search was subject to the following general constraints: (i) R-factor less than 0.10, (ii) no disorder, and (iii) error free. Visual inspection revealed that the majority of the π-systems were either positively charged or bound to a positively charged atom. A much smaller subset of this data was retained after applying the additional constraints that either the molecule containing the π-system is charge-neutral or when the π-system occurred in a positively charged molecule, the positive charge is at least two bonds removed from the π-system. This yielded 30 examples most representative of the neutral electron-deficient arenes that have been studied theoretically.[2-12] To examine the behavior when the π-system is in contact with a positive charge, we extracted a larger subset of the data, 138 fragments, in which the halide interacts with an arene ring containing a single nitrogen atom bound to a metal cation (Figures 3.13 and 3.14 in Results and Discussion).

A second search was performed to investigate the assertion that there is a preference for neutral electronegative atoms to be located over the center of

perfluoroarenes.[3] A hit was counted if (i) an electronegative atom F, Cl, Br, I, O, S, or N was within 4.0 Å of the centroid of any pentafluoroarene (ii) the contact was intramolecular or intermolecular, (iii) the R-factor was less than 0.05, (iv) there was no disorder, and (v) there was no error. This search yielded a total of 8077 fragments. A subset of this data, 1578 fragments, was obtained after applying the additional constraint that the electronegative atom must simultaneously contact all six carbon atoms of the arene, where each contact distance was less than the sum of van der Waals radii + 1.0 Å (Figure 3.15, Results and Discussion).[27]

RESULTS AND DISCUSSION

TCB CRYSTAL STRUCTURES. Further structural information for the anion-π interaction was obtained by growing single crystals in which TCB interacts with halide anions. TCB, 18-crown-6 and alkali halide salts were dissolved in acetonitrile (KBr) or 9:1 dichloromethane:acetonitrile (KI, NaI) solvent and thoroughly mixed. The purpose of the 18-crown-6 was to enhance the solubility of the salts in organic solvent. Slow evaporation at room temperature yielded single crystals suitable for X-ray diffraction.

Solutions of 18-crown-6 and TCB are colorless. As anticipated,[14] addition of the alkali halide salts produced color changes consistent with the formation of CT complexes. When KBr was added, the solution became bright yellow yielding orange single crystals of $[K(18\text{-crown-6})(TCB)_2]^+Br^-$. When KI or NaI were added, the solution became red yielding dark purple single crystals of $[K(18\text{-crown-6})(TCB)_2]^+I^-$ and $[Na(18\text{-crown-6})(TCB)_2]^+I^-$.

The KBr salt crystallizes in the space group $P2_1/c$ whereas the KI and NaI salts crystallize in the space group $P\ \bar{1}$. All three structures exhibit some common features. The alkali cations are encircled by the 18-crown-6 macrocycle. Two TCB ligands are coordinated to each cation via CN nitrogen atoms, with one above and one below the plane of the macrocycle yielding a total coordination number of 8. As illustrated in Figure 3.4, the crystals pack with alternating cation-bearing layers of 18-crown-6 and anion-bearing layers formed by interlaced axial TCB ligands. The structures differ in the orientation of the TCB groups. In the KBr salt, the planes of the two TCB ligands attached to each cation are roughly perpendicular to one another whereas in the KI and NaI salts, they are roughly parallel to one another.

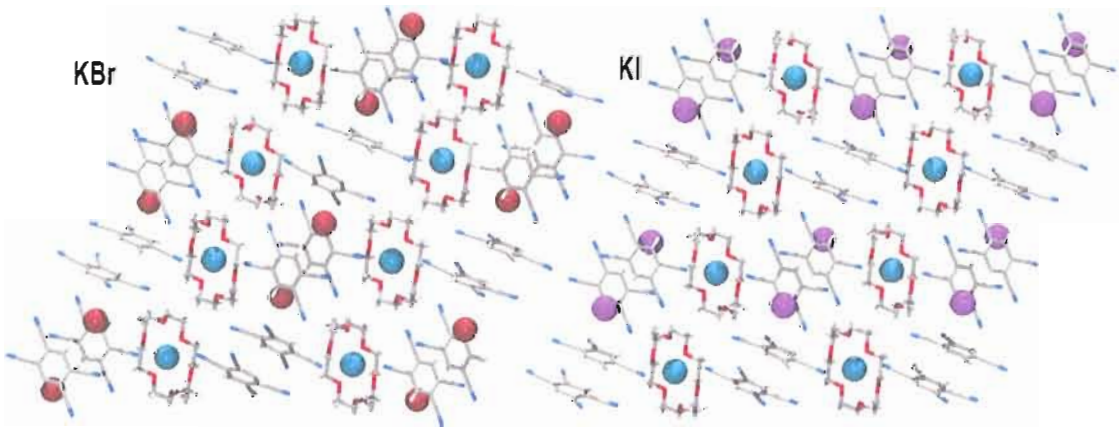

Figure 3.4 View down the *b*-axis of the KBr structure (top) and the *a*-axis of the KI structure (bottom). The NaI structure (not shown) exhibits the same packing as the KI structure. Atom color scheme: C, grey; H, white; N, blue; O, red; K, turquoise; Br, magenta; I, purple.

Despite the packing differences, the local environment about each halide anion is remarkably similar in all three crystals. As illustrated in Figure 3.5, four TCB molecules contact each anion. Distances for these contacts are given in Table 3.1. There are three distinct orientations: above the arene plane nearest to a carbon bearing a CN group (**a** and **b**), above the arene plane nearest to a carbon bearing a hydrogen atom (**c**), and nearly within the plane of the arene, contacting a C–H hydrogen atom (**d**).

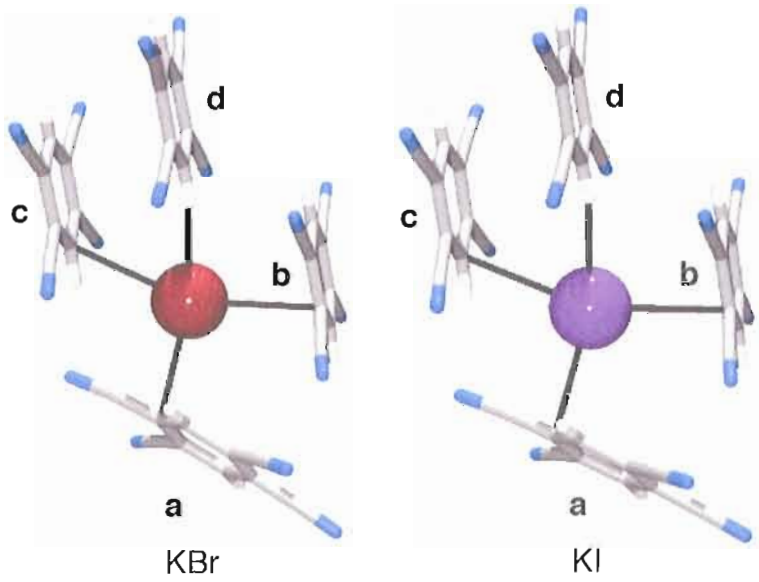

Figure 3.5 Arrangement of four TCB molecules around the anion is remarkably similar in all structures. The closest contact to each arene is indicated by a black bond.

Table 3.1 Observed halide to arene distances (Å).[a]

structure		TCB[b]	d_{carbon}	$d_{centroid}$ d_{plane}
KBr	a	3.34	3.88	3.26
	b	3.42	4.00	3.16
	c	3.48	4.46	2.72
	d	3.73	5.12	0.60
KI	a	3.45	3.97	3.38
	b	3.60	4.02	3.40
	c	3.56	4.47	3.18
	d	3.90	5.28	0.45
NaI	a	3.46	3.99	3.43
	b	3.57	4.03	3.35
	c	3.53	4.39	3.05
	d	3.90	5.29	0.33

[a]Distance between halide and nearest arene carbon atom (d_{carbon}), distance between halide and arene centroid ($d_{centroid}$), and distance between halide and mean plane of arene (d_{plane}). [b]See Figure 3.5 for structures.

Orientation **d** provides a clear example of an aryl C–H•••anion hydrogen bond,[2,28,29] whereas the nature of the interactions represented by the other orientations is not as obvious. In **a** - **c** the anions are located 2.7 to 3.4 Å above the plane of the arene. The anions are not, however, located over the center of the arene as anticipated for the non-covalent anion-π interaction. This is clearly illustrated in Figure 3.6 which shows the halide positions above the TCB plane as well as those previously observed for halide complexes with the similar TCP arene.[14] In every case, the halide anion is positioned either over the periphery of the arene ring or outside the arene ring altogether.

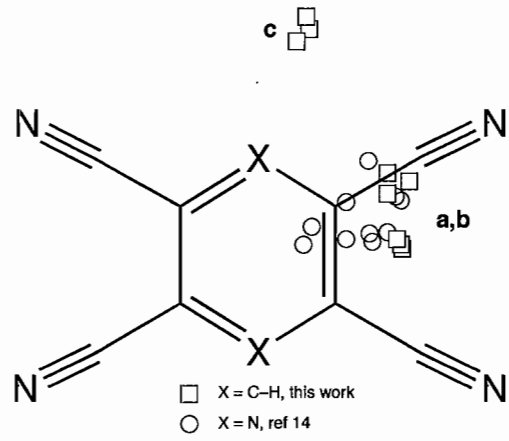

Figure 3.6 The squares (TCB) and circles (TCP) show the locations of halide anions above tetracyanoarene π-systems that have been observed in crystal structures.

ELECTRONIC STRUCTURE CALCULATIONS OF TCB. Electronic structure calculations at the MP2/aug-cc-pVDZ level of theory were performed to evaluate the structure and interaction energies of 1:1 complexes formed between TCB and F^-, Cl^-, and Br^- anions. Four geometries were evaluated for each halide. These include the non-covalent anion-π complex (**1**) a CT complex in which the halide is positioned above a C–H bond (**2**) a CT complex in which the halide is positioned above a C–CN bond (**3**) and a C–H hydrogen bond complex (**4**). Figure 3.7 illustrates these geometries for Cl^- and Table 3.2 summarizes the results obtained for all halides.

Initial calculations focused on the non-covalent anion-π complex, **1**. Somewhat to our surprise, **1** was not a minimum on this potential surface for any of the halides and could only be located by imposing C_{2v} symmetry during the optimization. Prior theoretical studies have established that strongly nucleophilic anions, such as F^-, always interact with electron-deficient arenes by engaging in nucleophilic attack on an arene carbon.[2-8,10] Thus, the required imposition of symmetry constraints to compute anion-π complexes involving F^- is well-established. However, this is the first instance where it has been necessary to impose symmetry constraints to obtain anion-π complexes for Cl^- and Br^-.

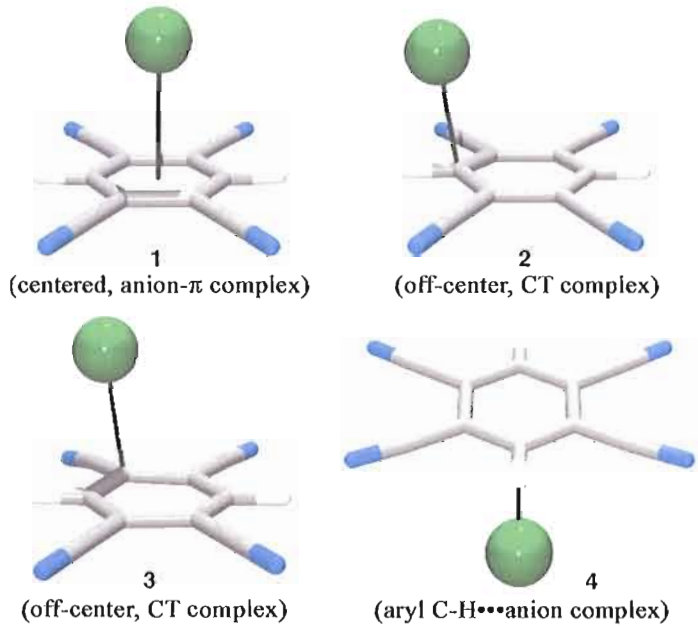

Figure 3.7 MP2/aug-cc-pVDZ optimized geometries for Cl^- complexes with TCB.

Structure **1** is not a stable geometry for halide-TCB complexes, whereas two alternate geometries have been located for complexes in which the halide lies above the arene plane. In the global C_s symmetry minimum (**2**), the halide lies outside the perimeter of the aromatic ring above a C–H bond. This form is observed for F^-, Cl^-, and Br^-. In the less stable C_1 symmetry minimum (**3**) the halide lies outside the perimeter of the aromatic ring above a C–CN bond. This form is observed for F^- and Cl^-, but is not a stationary point for Br^-.

Table 3.2 Calculated halide to arene distances (Å),[a] electronic binding energies (ΔE, kcal mol^{-1}),[b] natural bond order analysis of charge transfer interactions,[c] and charge transfer from the anion to the arene (q_{CT}, e) derived from natural population analysis (NPA) or electrostatic potential fitting (ESP) for complexes of F^-, Cl^-, and Br^- with TCB (**1** - **4**), tricyanobenzene (**5** - **8**), triazine (**9** - **11**), and hexafluorobenzene (**12** - **13**).

complex	d_{carbon}	$d_{centroid}$	d_{plane}	ΔE (binding energy)	Leading CT interaction	$\Delta E^{(2)}$	q_{CT} (NPA)	q_{CT} (ESP)
1(F^-)‡	2.777	2.400	2.400	-33.93(2)[d]		<1	0.008	0.221
2(F^-)	1.500	2.427	1.676	-53.06	$n_4(F^-)\rightarrow\pi^*_{C=C}$	>200	0.477	0.464
3(F^-)	1.575	2.537	1.642	-47.24	$n_4(F^-)\rightarrow\pi^*_{C=C}$	>200	0.461	0.426
4(F^-)	2.590	4.073	0.000	-45.09	$n_4(F^-)\rightarrow\sigma^*_{C-H}$	>200	0.274	0.354
1(Cl^-)‡	3.272	2.962	2.962	-28.34(1)[d]		<1	0.009	0.180
2(Cl^-)	2.603	3.212	2.622	-29.80	$n_4(Cl^-)\rightarrow\pi^*_{C=C}$	21.16	0.120	0.237
3(Cl^-)	2.673	3.206	2.677	-29.13	$n_4(Cl^-)\rightarrow\pi^*_{C=C}$	14.20	0.116	0.244
4(Cl^-)	3.151	4.582	0.000	-27.00	$n_4(Cl^-)\rightarrow\sigma^*_{C-H}$	44.92	0.116	0.103
1(Br^-)‡	3.416	3.122	3.122	-27.70(1)[d]		<1	0.009	0.178
2(Br^-)	2.788	3.349	2.812	-28.68	$n_4(Br^-)\rightarrow\pi^*_{C=C}$	15.76	0.107	0.224
4(Br^-)	3.325	4.753	0.000	-25.33	$n_4(Br^-)\rightarrow\sigma^*_{C-H}$	37.68	0.086	0.097

5(F^-)‡	2.841	2.475	2.475	-25.49(2)[d]		<1	0.007	0.212
6(F^-)	1.500	2.474	1.607	-44.10	$n_4(F^-)\rightarrow\pi^*_{C=C}$	>200	0.477	0.484
7(F^-)	1.791	2.672	1.811	-34.55	$n_4(F^-)\rightarrow\pi^*_{C=C}$	120.0	0.281	0.343
8(F^-)	2.527	3.992	0.000	-35.87	$n_4(F^-)\rightarrow\sigma^*_{C-H}$	153.6	0.175	0.197
5(Cl^-)‡	3.343	3.038	3.038	-21.52(2)[d]		<1	0.007	0.168
6(Cl^-)	2.728	3.370	2.691	-22.72	$n_4(Cl^-)\rightarrow\pi^*_{C=C}$	14.35	0.086	0.205
7(Cl^-)‡	2.837	3.289	2.846	-21.85(1)[d]	$n_4(Cl^-)\rightarrow\pi^*_{C=C}$	3.67	0.049	0.182
8(Cl^-)	3.204	4.638	0.000	-21.63	$n_4(Cl^-)\rightarrow\sigma^*_{C-H}$	36.72	0.078	0.093
5(Br^-)	3.490	3.198	3.198	-21.18		<1	0.007	0.159
6(Br^-)	2.904	3.500	2.876	-21.91	$n_4(Br^-)\rightarrow\pi^*_{C=C}$	11.44	0.078	0.194
8(Br^-)	3.377	4.808	0.000	-20.29	$n_4(Br^-)\rightarrow\sigma^*_{C-H}$	31.07	0.072	0.092
9(F^-)‡	2.845	2.179	2.179	-10.92(2)[d]		<1	0.010	0.155
10(F^-)	1.513	2.321	1.673	-26.34	$n_4(F^-)\rightarrow\pi^*_{N=C}$	>200	0.444	0.382
11(F^-)	2.686	4.034	0.000	-18.54	$n_4(F^-)\rightarrow\sigma^*_{C-H}$	54.13	0.075	0.080
9(Cl^-)	3.397	3.146	3.146	-8.41		<1	0.007	0.110
10(Cl^-)	2.900	3.448	2.896	-8.68	$n_4(Cl^-)\rightarrow\pi^*_{N=C}$	9.60	0.043	0.110
11(Cl^-)	3.408	4.736	0.000	-10.50	$n_4(Cl^-)\rightarrow\sigma^*_{C-H}$	17.54	0.036	0.042

9(Br^-)	3.553	3.313	3.313	-8.33		<1	0.006	0.093
10(Br^-)	3.093	3.569	3.109	-8.27	$n_4(Br^-)\rightarrow\pi^*_{N=C}$	7.30	0.035	0.097
11(Br^-)	3.580	4.906	0.000	-9.83	$n_4(Br^-)\rightarrow\sigma^*_{C-H}$	15.22	0.033	0.041
12(F^-)‡	2.889	2.530	2.530	-19.18(2)[d]		<1	0.004	0.201
13(F^-)	1.478	2.722	1.096	-26.01	$n_4(F^-)\rightarrow\pi^*_{C=C}$	>200	0.501	0.593
12(Cl^-)	3.367	3.064	3.064	-16.03		<1	0.004	0.161
12(Br^-)	3.511	3.223	3.223	-15.55		<1	0.004	0.148

[a]Distance between halide and nearest arene carbon atom (d_{carbon}), distance between halide and arene centroid ($d_{centroid}$), and distance between halide and mean plane of arene (d_{plane}). [b]E(complex) - E(halide) – E(arene) using absolute energies obtained at the MP2/aug-cc-pVDZ level of theory. [c]The leading charge-transfer interaction between the filled halide donor lone pair and unfilled acceptor orbital with associated second-order perturbation energies ($\Delta E^{(2)}$, kcal mol^{-1}). [d]Complex is not a minimum on this potential surface. The number of negative frequencies is given in parentheses.

In the case of F^-, **2** and **3** are much more stable than **1**, by 19 and 13 kcal mol^{-1}, respectively. The F–C distances of 1.50 and 1.58 Å are only slightly longer than the average F–C_{arene} bond length of 1.35 ± 0.02 Å observed in the CSD. The carbon atom bonded to F^- adopts an sp^3 geometry. Such geometries, which indicate a strongly covalent interaction, have been described previously in studies of nucleophilic substitution on aromatic rings and are denoted as Meisenheimer or σ complexes.[30,31]

In the case of Cl^- and Br^-, structures **2** and **3** are close in energy to transition state **1**, but more stable by 0.8 to 1.5 kcal mol^{-1}. The X–C distances are much longer than the average X–C_{arene} distances observed in the CSD: 2.60 and 2.67 Å versus 1.73 ± 0.2 Å for Cl; 2.79 Å versus 1.90 Å for Br. Although there is some distortion to the arene ring, the carbon atom nearest to the halide exhibits a geometry that is closer to that expected for sp^2 hybridization. As will be discussed below, these structures represent weakly covalent donor to π-acceptor complexes with smaller amounts of CT than observed for F^-.

Finally, geometry **4** confirms that halides also form stable complexes with TCB by hydrogen bonding to one of the C–H groups. Recent theoretical studies have established that arene C–H donor groups form moderate to strong hydrogen bonds with anions.[28] The presence of electron-withdrawing substituents increases the acidity of arene C–H donors and, thus strengthens the interaction.[29] The presence of four CN substituents in TCB yields quite acidic C–H groups, so much so that during the optimization of the F^- complex the TCB is actually deprotonated yielding a complex between HF and the TCB anion. Structure **4** contains the strongest arene C–H•••Cl^-

bond yet calculated, with an electronic bonding energy of -27.0 kcal mol^{-1} compared to values of -16.0 kcal mol^{-1} for nitrobenzene and -8.6 kcal mol^{-1} for benzene.[29]

NBO Analysis. Insight into the nature of the bonding interactions in **1** - **4** was obtained by evaluating the extent of CT from the halide donor to the TCB acceptor. Natural Bond Order (NBO) methods[25] can be used to estimate the extent of CT by removing the full set of off-diagonal matrix elements between two fragments of the NBO Fock matrix and recalculating the total energy to determine the associated variational energy change. The leading CT interaction between the filled halide lone pair (n) and unfilled antibonding acceptor orbital (φ^*) of electron deficient aromatics is characterized by the second-order stabilization energy $\Delta E^{(2)}$, which represents the strength of the $n \rightarrow \varphi^*$ CT delocalization.

$\Delta E^{(2)}$ Analysis. Leading interactions and $\Delta E^{(2)}$ values for complexes **1** – **4** with F^-, Cl^-, and Br^- are given in Table 3.2. The $\Delta E^{(2)}$ values are less than 1 kcal mol^{-1} for all halides with **1**, consistent with the view that the interaction is predominantly non-covalent in nature. Significant amounts of CT are observed in all other cases. The $\Delta E^{(2)}$ values for F^- complexes with **2** – **4** exceed 200 kcal mol^{-1}, indicative of strongly covalent bonding. In contrast, $\Delta E^{(2)}$ values for Cl^- and Br^- complexes with **2** – **4** are moderate in value indicating a smaller, but definite, CT interaction.

Electronic Density Surfaces. Covalent bonds can be visualized as regions of electron density between atoms. The lack of CT in **1** and the presence of CT in **2** – **4** can be observed by rendering the electron density surfaces for these complexes. Figure 3.8

shows the electron density surfaces for the Cl^- complexes computed at an isovalue of 0.02 eÅ^{-3}. There is a gap between the halide and TCB surfaces in **1**, but the surface between the halide and TCB is continuous in **2** – **4**. This result clearly illustrates that the degree of covalent bonding between the halide and TCB is significantly greater in **2** – **4** than it is in **1**.

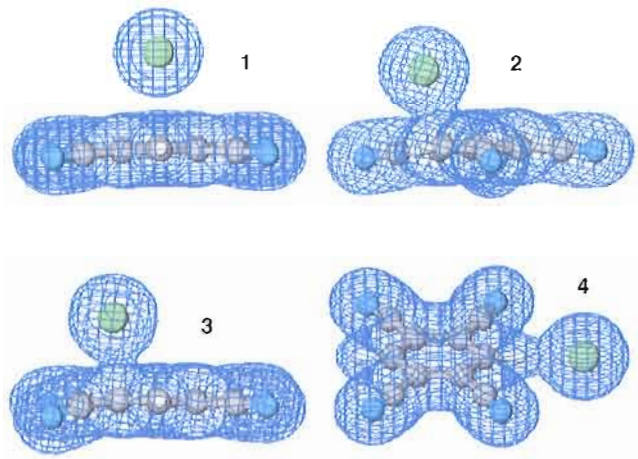

Figure 3.8 Electron density surfaces for Cl^- complexes **1** - **4**, rendered at the same isovalue (0.02 eÅ^{-3}) for comparison, clearly illustrate that the interactions in **2** – **4** possess a higher degree of CT than that in **1**.

Atomic Charge Analysis by NPA and ESP Methods. Atomic charges provide another gauge of the extent of CT. Two different approaches, Natural Population Analysis (NPA) and Electrostatic Potential Fit (ESP), were used to obtain the charge distributions in **1** – **4**. The NPA method derives the charge distribution from the basis functions that are used to represent the wave function.[25] The ESP method, which has been used in prior studies of anion-π interactions,[7-9] derives the charge distribution by

fitting the electrostatic potential of the complex. In either case, the extent of CT from the halide to the arene, q_{CT}, is obtained by subtracting the computed halide charge from the unit charge of the free halide.

q_{CT} Analysis. Values for q_{CT}, given in Table 3.2, reveal that the NPA values differ substantially from the ESP values. The q_{CT} values obtained with the NPA method are fully consistent with both the results of the NBO analysis ($\Delta E^{(2)}$ values in Table 3.2) and the evaluation of electron density surfaces (Figure 3.8). In other words, NPA charges indicate very little CT for **1** and significant CT for **2** – **4**. In contrast, the ESP charges erroneously indicate a significant CT from the halide to TCB in all cases. The greatest discrepancy occurs with **1**, where the ESP method overestimates q_{CT} by more than an order of magnitude. Thus, although ESP charges do an excellent job of reproducing the mid to far range electrostatic potential of a molecule,[32] they fail to adequately describe the extent of CT in the anion-π complex **1**. Failure of the ESP method to represent the charge distribution accurately within other molecules has been noted elsewhere.[33]

ELECTRONIC STRUCTURE CALCULATIONS FOR OTHER ARENES. This theoretical analysis of TCB halide complexes provides the first example in which non-covalent anion-π complexes are not stable for Cl^- and Br^-. These halides do interact with the arene π system, but the interaction involves CT and in the resulting geometries the anion is located over the periphery of the ring rather than over the center of the ring. Since prior studies on Cl^- and Br^- have focused almost exclusively on non-covalent anion-π complexes, there has been virtually no investigation to determine

whether such donor π-acceptor complexes exist for other arenes.[34] To address this question, further calculations were performed on halide complexes with 1,3,5-tricyanobenzene, triazine, and hexafluorobenzene. Geometries investigated are illustrated in Figure 3.9 and results are summarized in Table 3.2.

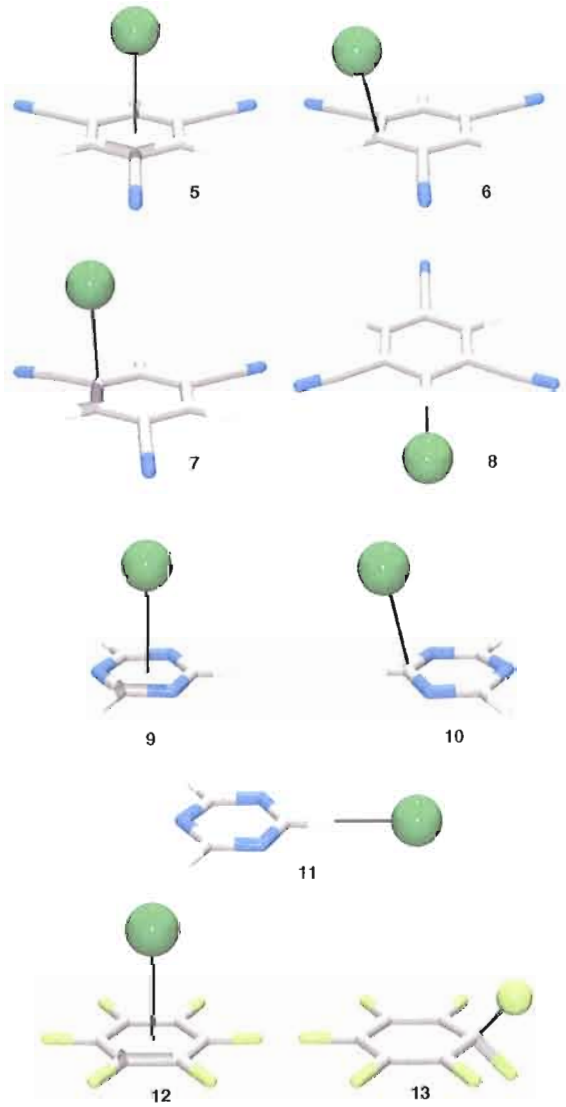

Figure 3.9 MP2/aug-cc-pVDZ optimized geometries for Cl^- complexes with 1,3,5-tricyanobenzene, **5** – **8**, triazine, **9** – **11**, and hexfluorobenzene, **12**, and F^- complex with hexafluorobenzene, **13**.

Results obtained for 1,3,5-tricyanobenzene are similar to those obtained for TCB. The anion-π structure, **5**, is not a minimum for F^- and Cl^-, but is a stable form for Br^-. The alternate CT form (**6**) is the global minimum for all three halides. In **6**, the halide is positioned over a C–H bond. The less stable CT complex (**7**) in which the halide is positioned over a C–CN bond, is a stable structure for F^-, a transition state for Cl^-, and was not located as a stable point for Br^-. A C–H hydrogen bond form (**8**) is also a stable structure for all three halides. A previous study of the 1,3,5-tricyanobenzene complex with Br^- reported only structure **5**.[9]

Three geometries were located for triazine halide complexes. The anion-π structure (**9**) is not a stable point for F^-, but is a stable form for Cl^- and Br^-. The alternate CT form (**10**) and a C–H hydrogen bond form (**11**) are minima for all three halides. The CT form is the global minimum for F^-, but the C–H hydrogen bond forms yield the most stable geometries for Cl^- and Br^-. The latter two halides, **9** and **10** are close in energy, with **10** being the more stable form for Cl^- and **9** being the more stable form for Br^-. The results for F^- are fully consistent with an earlier theoretical study of triazine.[2] Although **9** and **11** have previously been identified as minima for Cl^- and Br^-,[2] none of the prior theoretical studies report the existence of structure **10** for either Cl^- or Br^-.[2,6,7,9,11]

Two geometries were located for hexafluorobenzene complexes. The anion-π structure (**12**) is not a stable point for F^-, but is a stable geometry for Cl^- and Br^-. The

alternate CT form (**13**) is the global minimum for F^-, but was not located as a stable point for either Cl^- or Br^-. These results are completely consistent with prior theoretical studies of this system.[3,5,6,8-10]

NBO Analysis forAdditional Arenes. As with **1** – **4**, the extent of the CT in **5** – **13** was evaluated via NBO methods and charge distributions. Inspection of Table 3.2 reveals that all anion-π complexes, **1**, **5**, **9**, and **12**, are characterized by low $\Delta E^{(2)}$ values and q_{CT} (NPA) values of less than 0.01 *e*. Values of q_{CT} obtained by the ESP method are greatly overestimated for all these structures. Alternate forms have been identified that involve CT from the halide to the π system, **2**, **3**, **6**, **7**, **10**, and **13**. In these cases, F^- yields high $\Delta E^{(2)}$ values and q_{CT} (NPA) values approaching 0.5 *e* indicative of the formation of strong σ bonds. The other halides are characterized by intermediate $\Delta E^{(2)}$ values, ranging from 7.3 to 21.2 kcal mol^{-1} and smaller q_{CT} (NPA) values, ranging from 0.03 to 0.12 *e*.

In three out of the four arenes studied, Cl^- and Br^- are found to form stable, off-center CT complexes with the electron-deficient π system. With one exception, the Br^- complex **10**, these CT complexes are more stable than the non-covalent anion-π complexes. However, the differences in energy are small, ranging from 0.3 to 1.5 kcal mol^{-1}, suggesting a relatively flat potential surface for positioning the halide above the arene plane.

FURTHER ANALYSIS OF SINGLE CRYSTAL STRUCTURE DATA

The preceding theoretical evaluation of halide complexes with electron-deficient arenes has established that (i) the centered non-covalent anion-π complex is not the most stable structure for the majority of systems reported herein and (ii) CT complexes exist in which the halide is positioned over the periphery of the π system. In both types of complexes, Cl^-, Br^-, and I^- lie 2.5 to 3.5 Å above the arene plane as determined from crystal structures and computations. The type of interaction is structurally distinguished by the location of the halide with respect to the arene center. In the anion-π complex, the halide is located directly over the center. In the CT complex, the halide is located over the periphery of the ring.

As shown in Figure 3.10, the distance d_{offset} provides a geometric parameter for describing the location of the halide anion. d_{offset} is readily obtained from two other distances, the distance to the centroid, $d_{centroid}$, and the distance to the average plane of the arene, d_{arene}. The d_{offset} parameter has a value of 0 Å for an idealized, centered anion-π complex. If a halide were positioned directly above a carbon atom in benzene, d_{offset} would be 1.4 Å. Thus, d_{offset} values < 0.7 Å are closer to the arene center and would indicate an anion-π interaction and d_{offset} values > 0.7 Å are closer to the arene perimeter and would indicate a CT complex. In structures calculated for Cl^- CT complexes **2**, **3**, **6**, **7**, and **10**, d_{offset} ranges from 1.7 to 2.0 Å; in crystal structures determined for 1,2,4,5-tetracyanoarenes (see Figure 3.6, interactions **a** and **b**), d_{offset} ranges from 0.7 to 2.4 Å.

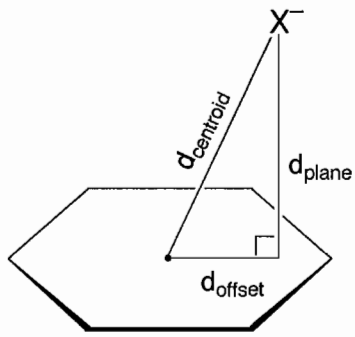

Figure 3.10 The degree of displacement of a halide, X^-, from the center of an arene is given by d_{offset}. This parameter is calculated from distances ($d_{centroid}$ and d_{plane}) that can be queried in a CSD search to provide $d_{offset} = (d_{centroid}^2 - d_{plane}^2)^{1/2}$

SURVEYS OF THE CAMBRIDGE STRUCTURAL DATABASE

Further evidence for CT interactions between halides and electron-deficient arenes is provided from a survey of the Cambridge Structural Database (CSD). A search for halide anions located within 4.0 Å of the centroid of six-membered ring π systems yielded nearly 600 examples. In most of these cases, however, the π system was either positively charged or bonded directly to a positively charged atom. Retaining only charge-neutral π systems yielded the much smaller set of 19 structures shown in Figure 3.11. Within these structures there are 30 halide-arene complexes. Distances for these complexes were evaluated yielding the following ranges: $d_{centroid}$, 3.2 to 4.0 Å; d_{plane}, 3.0 to 3.9 Å; d_{offset}, 0.2 to 2.5 Å. The frequency of d_{offset} values is presented as a histogram in Figure 3.12. Few structures show the halide positioned near the center of the ring; rather, the distribution exhibits a maximum centered at d_{offset} = 1.5 Å, just outside the ring perimeter. In fact, 84% of the anions in the data set are

closer to the ring carbons ($d_{offset} > 0.7$ Å) than to the centroid. Thus, available structural data indicate the CT motif to be more prevalent than the anion-π motif.

EXPANDED CSD SURVEY. To examine the behavior when the π system is in contact with a positive charge, a larger subset of the data was evaluated. There are 138 examples in which a halide interacts with an arene ring containing a single nitrogen atom bonded to a metal cation. These examples include ligands such as pyridine, bipyridine, 1,10-phenanthroline, etc. Distances for these complexes were evaluated yielding the following ranges: $d_{centroid}$, 3.3 to 4.0 Å; d_{plane}, 2.6 to 3.9 Å; d_{offset}, 0.3 to 2.7 Å. A histogram of the d_{offset} values for these complexes is shown in Figure 3.13. As with charge-neutral arenes (Figure 3.12), the distribution shows a maximum above the ring perimeter and 84% of the anions observed are closer to a ring carbon than to the centroid. These data again suggest the CT motif to be the predominant mode of interaction.

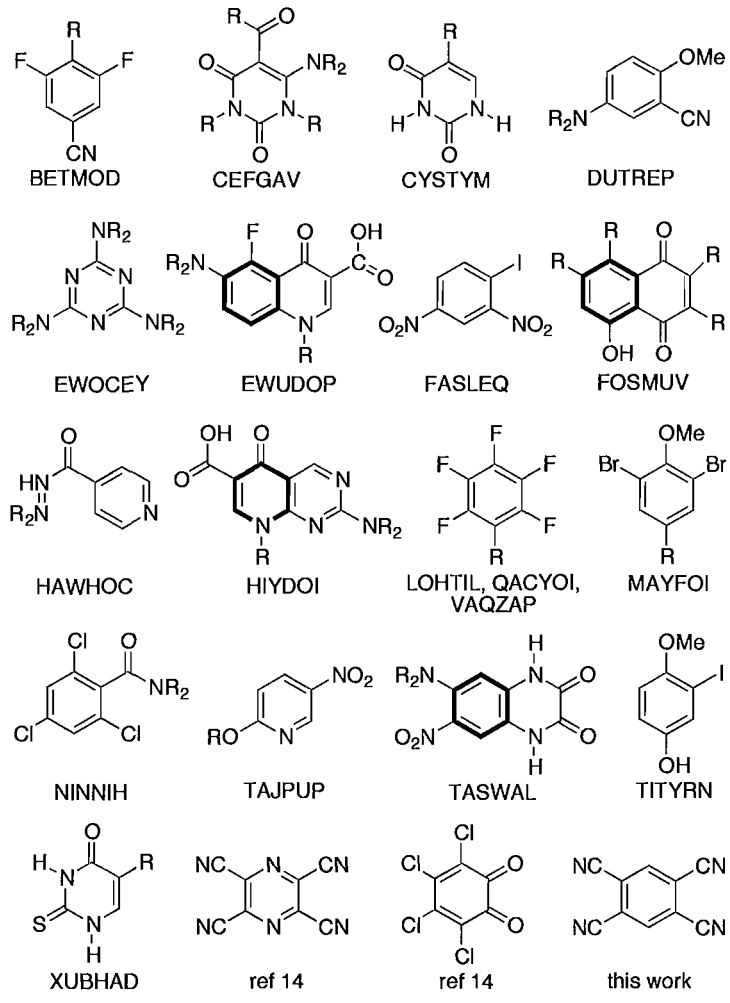

Figure 3.11. Electron-deficient arenes and CSD refcodes for structures in which a halide is located ≤ 4.0 Å from the arene centroid. When more than one ring is present, the ring interacting with the halide is shown in bold.

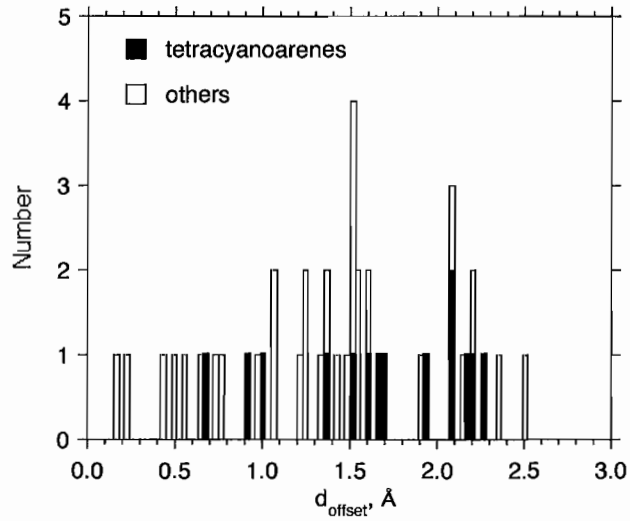

Figure 3.12 Histogram of d_{offset} values (see Figure 3.10) for halide complexes with structures shown in Figure 3.11.

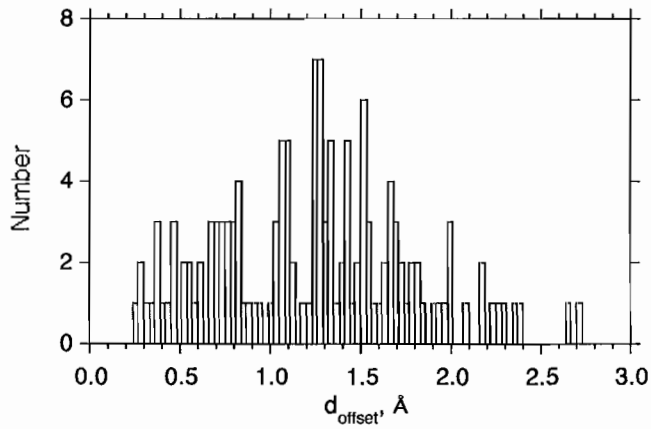

Figure 3.13 Histogram of d_{offset} values (see Figure 3.10) for halide complexes with pyridine fragments that are bound to a metal cation.

STRUCTURAL ANALYSIS OF HALIDE/PYRIDINE COMPLEXES. Further insight into the nature of these interactions is obtained by locating the positions of the halides above the pyridine π systems. A plot of these positions, shown in Figure 3.14, reveals that there is a

preference for the halide to locate over the 2 or 6 carbon atom. This positional predilection is in accord with a previous CSD study[35] of nitrogen heterocycles interacting with NO_3^-, ClO_4^-, BF_4^- and PF_6^- as well as being consistent with a CT bonding motif that is stabilized by the following resonance forms:[36]

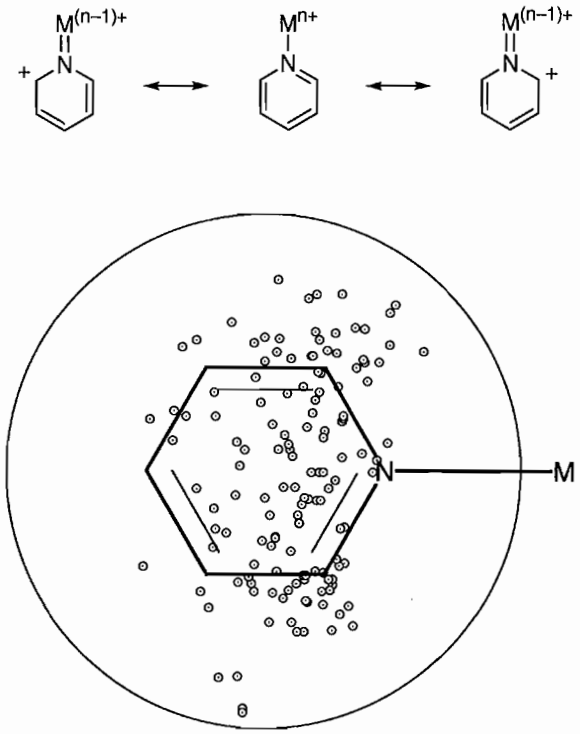

Figure 3.14 Locations of halide anions above the plane of pyridine fragments that are bound to a metal cation. The pyridine metal complex is drawn to scale and the circle represents a d_{offset} value of 3.0 Å.

STRUCTURAL ANALYSIS OF DONOR/PERFLUOROBENZENE COMPLEXES.

The histograms presented in Figures 3.12 and 3.13 lead to the conclusion that halide anions are more likely to interact with an electron-deficient π system through a CT motif rather than the

anion-π motif. This is contrary to two prior analyses of the CSD, which report evidence of a marked preference for *charge-neutral* atoms bearing lone pairs to position themselves over the center of pentafluoroarenes[3] and trinitrobenzene derivatives.[4] In these analyses, the database was searched for instances in which any electronegative atom F, Cl, Br, I, O, S, or N was in contact with all six carbon atoms of the arene, where each contact distance was defined as the sum of van der Waals radii + 1.0 Å.[27] Evidence in support of the anion-π interaction was provided by histograms of atom-centroid-carbon angles showing that data were concentrated at angles close to perpendicular to the ring, consistent with a preference for an electronegative atom to reside above the arene centroid.

In an effort to resolve the inconsistency, this analysis was repeated for pentafluoroarenes. Figure 3.15 shows that it is possible to reproduce the previously reported histogram very closely.[3] However, such data are misleading and give rise to false conclusions regarding the location of electron-rich atoms positioned above electron-deficient arenes. First, the atom-centroid-carbon angle is a poor indicator for the location of an atom above the arene plane. When the atom is off-center, the angle obtained depends on the choice of carbon atom. It is possible for two of the six angles to be near 90°, even when the atom lies well outside the ring perimeter. In addition, these angles are not a very sensitive measure of the degree of displacement. For example, if the atom is constrained to be 3.5 Å above the arene plane and to lie within a perpendicular plane containing a pair of *para* carbon atoms, the atom-centroid-carbon angle involving one of these *para* carbon atoms varies with d_{offset} as follows

(angle, d_{offset}): 90°, 0 Å; 80°, 0.62 Å, 70°, 1.27 Å; 60°, 2.02 Å. Although the atom-centroid-carbon angles are indeed distributed about 90°, the distribution is wide, ranging from 55 to 126°. Evaluation of d_{offset} values for the data in Figure 3.15 reveals that in 65% of the cases the atom is closer to the ring perimeter than to the centroid (> 0.7 Å) and in 17% of the cases, the atom lies outside the ring perimeter (> 1.4 Å).

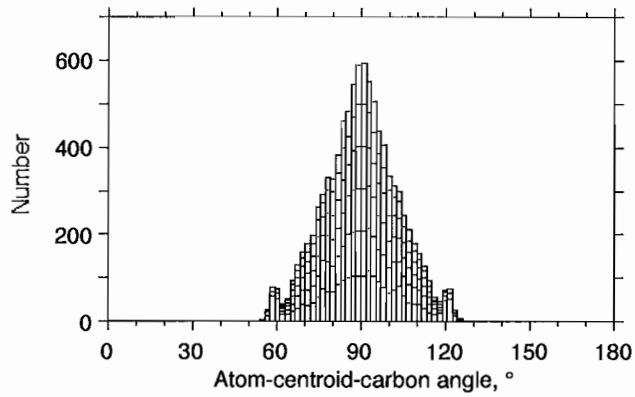

Figure 3.15 Histogram of the distribution of atom-centroid-carbon angles for electronegative atoms in contact with all six carbon atoms of pentafluoroarenes. All six angles for each hit are plotted.

A second, and perhaps more serious, source of confusion stemming from this search is that constraining the electronegative atom to be in simultaneous contact with all six arene carbon atoms biases the search to select data that tend to lie over the arene. A much larger number of hits are obtained when the search criteria are altered such that the electronegative atom must be within 4 Å of the pentafluoroarene centroid. These hits contain the subset of data used to generate Figure 3.15. Distances in these

structures were evaluated yielding the following ranges: $d_{centroid}$, 2.4 to 4.0 Å; d_{plane}, 1.8 to 4.0 Å; d_{offset}, 0 to 3.5 Å. The distribution of the electronegative atoms over the pentafluoroarene plane is illustrated in Figure 3.16. When the atom lies well outside the ring perimeter, a preference to lie in between the ring substituents is apparent. However, for d_{offset} values ranging from 0 to 2 Å, statistical analysis of the data (supporting information) shows that charge-neutral electronegative atoms within 4 Å of a pentafluoroarene centroid are distributed randomly over the arene surface; in other words, these data establish the complete absence of any preferred location over this π system.

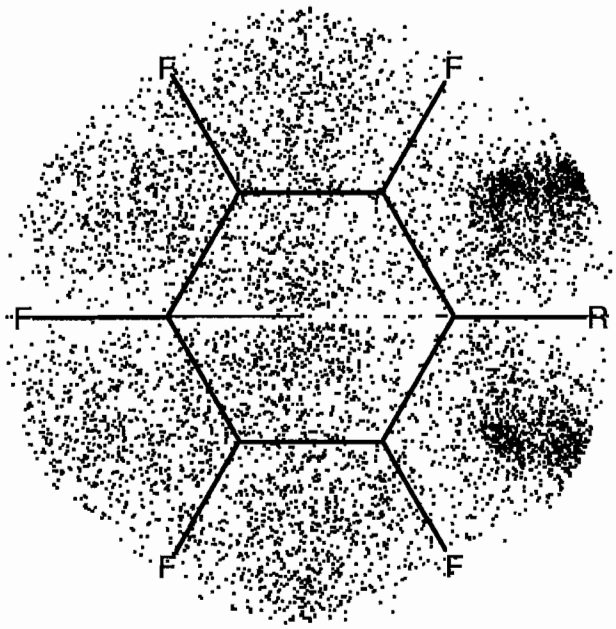

Figure 3.16 Locations of electronegative atoms above the pentafluoroarene plane. The arene is drawn to scale and the outer perimeter represents a d_{offset} value of 3.0 Å.

SUMMARY AND CONCLUSIONS

In this study, we have used electronic structure calculations and crystal structure data to investigate how halides interact with electron-deficient π systems. When the halide lies above the plane of the π system, the results establish that three distinctly different types of complex are possible: strongly covalent σ complexes (**A**), weakly covalent donor π-acceptor complexes (**B**), and non-covalent anion-π complexes (**C**). As shown in Figure 3.17, examples of all three types occur with triazine. These complexes are distinguished from one another by the extent of CT and the position of the halide above the π system.

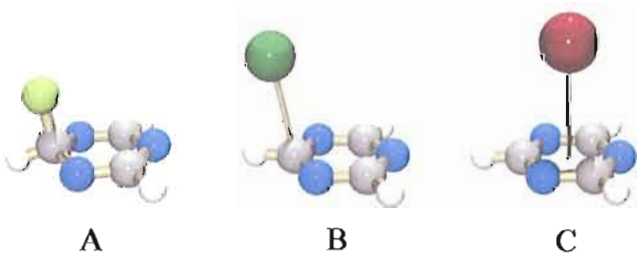

Figure 3.17 When a halide is located above triazine, the most stable forms are a σ complex with F^- (A), a donor π–acceptor complex with Cl^- (B), and an anion-π complex with Br^- (C).

Strongly covalent σ complexes result from nucleophilic attack at a ring carbon. These complexes are characterized by a large amount of CT from the anion to the π system. As established in earlier theoretical studies[2-12] and as confirmed in this study, such complexes represent the only stable geometry that locates F^- above the plane of an aromatic ring. For the complexes investigated here, most F–C bond distances are

short, near 1.5 Å. The ring carbon under attack adopts a tetrahedral geometry and, as a result, the F^- anion is located outside the ring perimeter. There is substantial experimental precedent for the formation of stable σ complexes in studies of nucleophilic substitution reactions of electron-deficient aromatic rings.[30,31] Consistent with these experimental studies, calculations have established that σ complexes also are formed between electron-deficient arenes and other strongly nucleophilic anions. Examples include CN^- and CO_3^{2-} interacting with C_6F_6,[3] and CN^-, NC^- and CO_3^{2-} interacting with triazine.[5,6]

Weakly covalent donor π-acceptor complexes may be formed with less nucleophilic halides. These complexes are characterized by a smaller, but definite, amount of CT from the anion to the π system. Geometries for such complexes are consistent with much less covalent character than in the σ complexes, exhibiting elongated halide–carbon distances and near planar arene carbon atoms. Like σ complexes, the halide is located outside the ring perimeter. Experimental evidence for donor π-acceptor complexes, both in solution and in the solid phase, was provided by a recent study.[14] Further analysis of crystal structure data presented herein confirms that there is a marked preference for halides to lie either over or outside the perimeter of electron-deficient six-membered rings. Results from electronic structure calculations are fully consistent with this result. For example, for three out of the four arenes evaluated in this study calculations show that when Cl^- is located above the π system, the donor π-acceptor motif yields the more stable Cl^- complex.

Non-covalent anion-π complexes may also be formed with less nucleophilic halides. These complexes are characterized by CT values of ≤ 0.01 *e* and a geometry in which the halide is located directly above the arene centroid. Although prior theoretical studies have yielded numerous examples of such complexes in the gas phase,[2-12] crystal structure analysis reveals that there are relatively few clear examples of anion-π complexes for halides in the solid state. Indeed, the current study has established that when an arene becomes sufficiently electron-deficient, non-covalent anion-π complexes may no longer represent stable geometries for halides larger than F^-. For example, the non-covalent anion-π complexes for Cl^- with TCB and 1,3,5-tricyanobenzene are both found as transition states on the MP2/aug-cc-pVDZ potential surface.

Additionally, one should not overlook the fact that electron-deficient arenes bearing C–H groups are potent hydrogen bond donors. As noted elsewhere, even in the absence of electron-withdrawing substituents, simple arenes form C–H hydrogen bonds with anions that can exceed 50% the strength of those formed by O–H and N–H groups.[28] In electron-deficient arenes, aryl C–H groups become much stronger donor groups.[29] As shown in Table 3.2, both tri- and tetracyanobenzene yield hydrogen-bonded complexes with Cl^- and Br^- that are 88 to 95% as strong as corresponding donor π-acceptor complexes, with interaction energies ranging from -20 to -27 kcal mol^{-1}. In the case of triazine, C–H hydrogen bonding yields the most stable complexes with Cl^- and Br^-, 18 to 21% more stable than the corresponding anion-π or donor π-acceptor forms.

The role of aryl C–H binding sites is nicely illustrated in a recent crystal structure.[15] Although attention was drawn to the fact that this structure contains one of the few examples of an anion–π interaction, containing a Cl^- anion positioned above the center of a melamine ring, no mention was made of the interactions with the other electron-deficient arenes lining the binding cavity. As illustrated in Figure 3.18, C–H groups of Cu(II)-coordinated pyridine rings form six hydrogen bonds with the Cl^- guest. Because each of these aryl C–H groups offers a more powerful binding site than the melamine π system,[37] it likely that the six C–H hydrogen bonds play the dominant role in determining the position of the anion within this cavity.

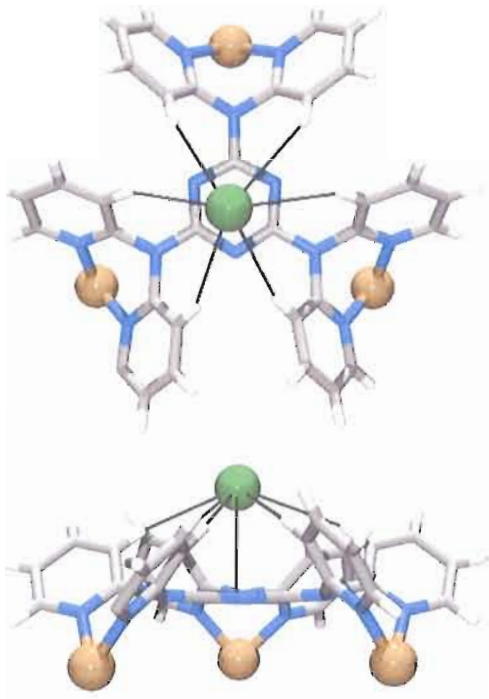

Figure 3.18 Views of a fragment of a Cl^- receptor[15] crystal structure showing six hydrogen-bonding interactions with aryl C–H groups of Cu(II)-coordinated pyridine rings and one anion-π interaction with a melamine ring. Interaction geometries are near ideal with all C-H•••Cl^- angles ≥ 150° and Cl^- to C distances ranging from 3.9 to 4.3 Å.

This study has refined our understanding of how halides interact with arenes. Existence of four potential binding motifs establishes electron-deficient arenes to be versatile building blocks, augmenting the arsenal of conventional hydrogen bonding and electrostatic components that have been used widely in the construction of anion receptors.[1] The results indicate that molecular design strategies for incorporating electron-deficient arenes within anionophore architectures should consider the quite different geometries encountered for the various interactions. The optimal binding motif for a given arene–anion pair may not be immediately obvious, suggesting that new systems should be evaluated on a case-by-case basis.

Knowledge of preferred binding motifs provides a basis for optimizing host architectures for specific anions. For example, in cases where substantial covalent character is anticipated, such as with strongly nucleophilic anions and/or highly electron-deficient arenes (Figure 3.3), optimal interaction with the π system will be achieved when the arene building block is oriented so that the anion is able to adopt a position outside the ring perimeter. Constraining host architecture so that the guest is only permitted to interact with the edges of the arene could lead to enhanced selectivity for such anions.

The influence of arene orientation is expected to decrease as the extent of CT decreases. Comparison of interaction energies for various binding motifs for Cl^- and Br^- with cyanide-substituted arenes reveals that although the strongest bonding is attained when the halide is positioned outside the ring perimeter, substantial stabilization is retained when the anion is held over the ring centroid. The insensitivity

of interaction energy to anion position is most pronounced in the Br^- complexes with triazine. Although the anion-π and donor π-acceptor complexes exhibit d_{offset} values of 0 and 1.75 Å, respectively, these two orientations yield essentially the same interaction energy (Table 3.2).

SUPPORTING INFORMATION AVAILABLE

Crystallographic data for the complexes $[K(18\text{-crown-}6)(TCB)_2]^+Br^-$, $[K(18\text{-crown-}6)(TCB)_2]^+I^-$ and $[Na(18\text{-crown-}6)(TCB)_2]^+I^-$. The full citation for ref 22, Cartesian coordinates and energies (Hartrees) for the MP2/aug-cc-pVDZ optimized geometries for **1 - 13**, and a statistical analysis showing that the data in Figure 3.16 is randomly distributed over the arene. This material is available in Appendix B.

BRIDGE TO CHAPTER IV

Through the crystallographic and computational investigation presented in chapter III we have refined the nature of the interactions between electron-deficient arenes and halides anions. The importance of considering multiple binding geometries for these systems is also highlighted. Specifically, new crystal structures containing 1,2,4,5-tetracyanobenzene and alkali halide salts as well as evaluation of structures found in the Cambridge Structure Database and MP2/aug-cc-pVDZ calculations of halide complexes with TCB, 1,3,5-tricyanobenzene, triazine, and hexafluorobenzene establish that multiple binding modes are present in these systems. Moreover, in most cases the preferred binding geometry is actually over the edge of the electron-deficient aromatic ring.

Chapter IV explores our efforts at designing, synthesizing and studying anion receptors that take into consideration the information that was acquired in the above investigation. Tripodal anion receptors with appended electron-deficient aromatic rings were designed to bind halide anions utilizing only electron-deficient aromatic rings while allowing enough space to access off-center binding geometries. The receptor scaffold was based off a 1,3,5-triethylbenzene core utilizing steric gearing to assist in preorganizing the electron-deficient aromatic rings in solution.

CHAPTER IV

SOLUTION PHASE MEASUREMENT OF *BOTH* WEAK SIGMA *AND* C–H•••X⁻ HYDROGEN BONDING INTERACTIONS IN SYNTHETIC ANION RECEPTORS

INTRODUCTION TO ELECTRON-DEFICIENT ARENE CONTAINING TRIPODAL ANION RECEPTORS

This chapter was co-authored with Aaron C. Sather, Dr. Benjamin P. Hay, Jeffrey S. Meisner and Professor Darren W. Johnson. Aaron Sather and Jeffrey Meisner assisted in synthesis and titration experiments to determine association constants. Dr. Hay completed the quantum calculations within and provided editorial assistance. Prof. Johnson devised the project and provided editorial assistance. Orion Berryman wrote this chapter, performed literature searches, assisted in synthesis and titration experiments, calculated association constants, isolated and solved the single crystal X-ray structures.

Electron-deficient arenes offer a variety of interaction motifs complementing traditional anion binding strategies. We have shown crystallographically and computationally that three distinct binding motifs are possible.[1,2] These binding motifs, illustrated for Cl^- complexes with 1,2,4,5-tetracyanobenzene are (i) the centered noncovalent anion-π interaction (**A**), (ii) off-center or 'weak σ' interactions (**B**

and C), and (iii) C-H•••X– hydrogen bonds (when acidic hydrogenss are available, **D**) (Figure 4.1). Although much recent attention has focused on the anion-π interaction,[3] there is evidence to suggest that this is not the predominant binding mode for many highly electron-deficient arenes.[2] In prior work we found that strongly electron-deficient arenes, such as the tetracyano-substituted example, exhibit stable weak σ and H-bonded geometries **B** – **D**, whereas the anion-π motif (**A**) was not a stable form in the solid and gas phases.

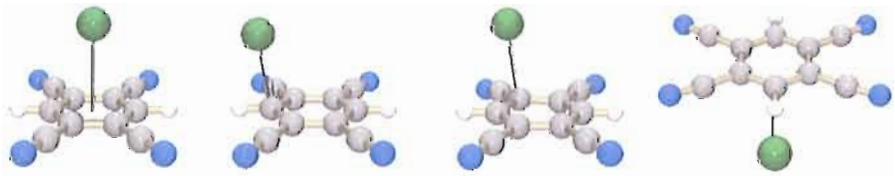

Figure 4.1 MP2/aug-cc-pVDZ optimized geometries for Cl^- interactions with 1,2,4,5-tetracyanobenzene include an unstable anion-π complex (**A**), weak σ complexes (**B** and **C**), and an aryl H-bond complex (**D**).[1] Atom colors: carbon gray, hydrogen white, nitrogen blue, and chloride green.

The majority of prior computational studies on anion-arene interactions have been representative of the molecules in the gas phase. When moving from in silico to solution other factors need to be considered;[4-6] therefore, solution phase association constants (K_a) must be measured to understand fully the selectivity that will emerge in binding anions with electron-deficient arenes. In one case K_as have been determined for model electron-deficient aromatic rings from UV-Vis titrations with halides.[7]

NMR spectroscopy can provide complementary structural information that is not obtainable with UV-Vis spectroscopy. A handful of examples use ^{1}H NMR spectroscopy to characterize anion interactions with electron-deficient aromatic rings in solution, but in many cases additional attractive interactions are present (such as π-stacking, ion pairing or hydrogen bonding).[8-11]

RESEARCH SUMMARY

We present experimental and theoretical results on a series of neutral tripodal receptors that utilize *only* electron-deficient arenes to bind halides in solution (Figure 4.2). These receptors employ steric gearing to preorganize electron-deficient arenes, and ^{1}H NMR spectroscopic titrations and DFT calculations confirm that receptors **1-3** bind anions in a 1:1 stoichiometry. These studies highlight three key aspects that had not been observed previously for anions interacting with electron-deficient aromatic rings in solution: (i) ^{1}H NMR spectroscopy provides sensitive data for determining both the magnitude of anion binding (K_a) and the structure (π contacts versus hydrogen bonding), even in cases of weak binding, (ii) the first observation of receptors binding anions in solution using only electron-deficient aromatic rings with either weak σ or C-H•••X^- hydrogen bonding interactions,[12] and (iii) the first quantitative measurement of the relative stabilities for such interactions in solution.

DESIGN AND SYNTHESIS OF TRIPODAL ANION RECEPTORS

RECEPTOR DESIGN. The cavity present in *syn* conformers of 2,4,6-trisubstituted-1,3,5-triethylbenzene[13] derivatives provides access for monoatomic anions to interact with the electron-deficient dinitroarenes via the π-system or hydrogen bonding (Figure 4.2). Receptors **1-3** are structural isomers composed of three electron-deficient arenes differing only in the position of their nitro substituents, which allows for an understanding of the effect of substitution pattern on receptor function. A key feature of the design strategy is that receptor **2** *cannot* form hydrogen bonds to anions (due to the bulky nitro groups being positioned ortho to each acidic aryl hydrogen) allowing us to study only the interaction between the anion and the π-system. Receptor **4**, lacking electron-deficient aromatic rings, was also prepared as a control.

RECEPTOR SYNTHESIS. Receptors **1-4** were synthesized in good yields from CsF-Celite assisted esterification of known 1,3,5-tris(bromomethyl)-2,4,6-triethylbenzene **5** with the corresponding benzoic acids (Figure 4.2) (see Appendix C).[14] Colorless single crystals of **1** and **2** were grown from slowly evaporating DMSO solutions. **1** and **2** crystallize in space groups *P*-1 and $P2_1/n$, respectively, with four independent molecules per unit cell.[15,16] Interestingly, in the solid state receptors **1** and **2** crystallize with one electron-deficient functional group *anti* with respect to the other aromatic rings (Figure 4.2). Nevertheless, receptors **1-4** exhibit time-averaged C_{3v} symmetry in solution on the NMR timescale suggesting that the up, up, down conformation does not dominate.

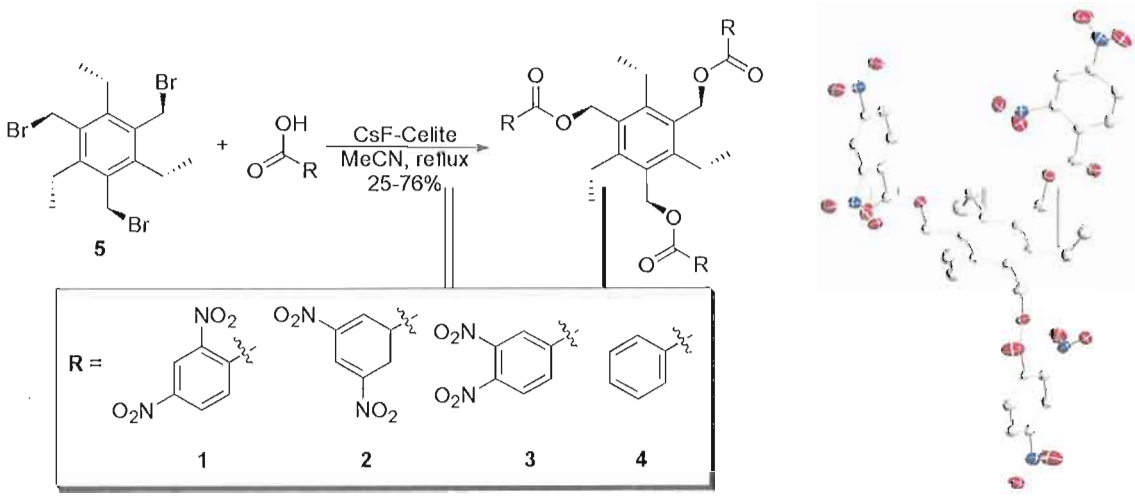

Figure 4.2 Synthesis of tripodal anion receptors **1-3** (left) and ORTEP representation of the crystal structure of receptor **1** (right, 50% probability ellipsoids with hydrogens omitted, carbon depicted as gray, hydrogen white, nitrogen blue and oxygen red).

SOLUTION EQUILIBRIA OF RECEPTOR/ANION COMPLEXES

^{1}H NMR TITRATION EXPERIMENTS. A previous study of strongly electron-deficient aromatic rings illustrated that UV-Vis spectroscopy is a suitable method to determine association constants for weak attractive interactions between halides and electron-deficient aromatic rings.[7,17] We chose to investigate the utility of ^{1}H NMR spectroscopy to determine association constants between halides (Cl^-, Br^- and I^-) and electron-deficient arenes in benzene, in part for the structural information provided by this technique. It is necessary when performing titration experiments to obtain data

where there is maximal change in the binding isotherm.[18] For solubility reasons, it was challenging to find an organic solvent where subtle interactions could be measured and the anion concentration could reach a large excess of the receptor concentration. The low solubility of $NBu_4^+I^-$ and $NBu_4^+Cl^-$ in C_6D_6 prompted us to perform titration experiments with tetra-*n*-heptylammonium halide salts ($NHep_4^+Cl^-$, $NHep_4^+Br^-$ and $NHep_4^+I^-$) at 27 °C. All three electron-deficient receptors **1**-**3** turned pale yellow upon addition of Br^- (see Appendix C, Figure C.5, middle. The picture exemplifies 90 equivalents of tetra-*n*-butylammonium bromide, $NBu_4^+Br^-$). Whereas **2** showed relatively little change in the ^1H NMR spectrum, significant changes occurred with receptors **1** and **3** when $NHep_4^+Br^-$ was titrated into C_6D_6 solution of receptors. Association constants determined for receptors **1** and **2** with $NHep_4^+Br^-$ in d_6-benzene at 27 °C wear 18-35 M^{-1},[19] while control receptor **4**—distinctly lacking electron-deficient arenes—exhibited no measurable binding by NMR and no visible color change (Table 4.1). These results lend support to our hypothesis that electron-deficient aromatic rings are required to bind anions in this neutral system.

Table 4.1 Average K_a (M^{-1}) for receptors **1**, **2**, and **4**[b] with halides

	[c]Cl^-	[c]Br^-	[c]I^-
1	26	18	11
2	53	35	26
4	<1[d]	<1[d]	<1[d]

[a]Average K_a reported from two or three titration experiments (not including receptor **4**). [b]All titrations were performed in C_6D_6 with initial receptor concentrations of ~2 mM; errors are estimated at ± 10%. Receptor **3** was not soluble at 1 mM in C_6D_6 at room temperature but a titration performed with $NBu_4^+Br^-$ and slight heat (to increase solubility) yielded a K_a = 12 M^{-1}. [c]Tetra-*n*-heptylammonium halides were used as the salt sources for each experiment and titrations were performed at 27 °C due to the insolubility of $NHep_4^+I^-$ at room temperature. [d]Chemical shift changes for control receptor **4** were too small to determine K_a's from ^1H NMR spectroscopic titrations.

SOLUTION DATA FOR TETRA-N-BUTYLAMMONIUM BROMIDE. Titrations of receptors **1** and **3** with $NBu_4^+Br^-$ displayed changes in chemical shifts of over 1 ppm,[20] and in the case of receptor **1** with $NBu_4^+Br^-$ the peaks juxtaposition even changed over the course of the titrations (Figure 4.3).[12] Conversely, 3,5-dinitro substituted receptor **2** exhibited much smaller chemical shift changes (maximum of 0.038 ppm for $NHep_4^+Br^-$), but binding constants were determined to be on the same order of magnitude. The striking differences in Δδ for receptors **1** and **3** versus receptor **2** indicate that different binding modes are occurring in solution for these receptors.

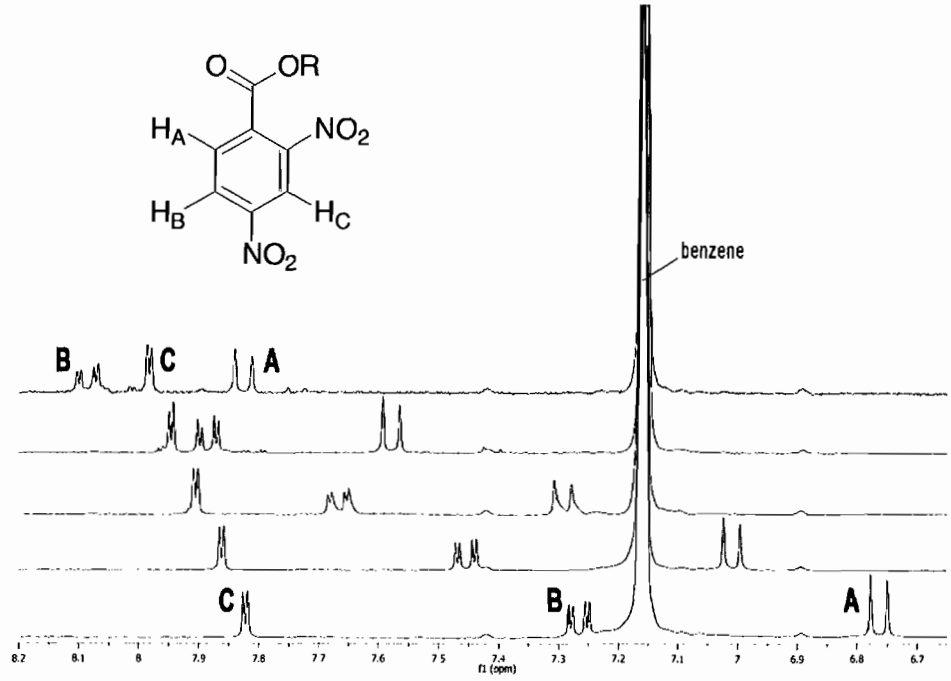

Figure 4.3 ^{1}H NMR spectra from titrations of receptor **1** (4.95 mM) with $NBu_4^+Br^-$ highlighting the chemical shift changes for this system. The ^{1}H NMR spectrum of **1** is compared to spectra of **1** in the presence of 7, 31, 51 and 101 equivalents of $NBu_4^+Br^-$ in ascending order.

COMPUTATIONAL STUDIES

DFT CALCULATIONS OF MODEL COMPOUNDS. Further evidence for the identity of these binding modes is provided by DFT calculations (B3LYP/DZVP).[21] Initial calculations performed on 1:1 complexes between Br^- and models of the arene donors in **1** and **2**, that possess the same substitution patterns but with methyl ester substituents, yielded the interesting results shown in Figure 4.4. Starting from an idealized anion-π geometry, with the Br^- anion located directly over the arene centroid at a distance of 3.2 Å,[2] in both cases optimization failed to yield an anion-π complex;

the model corresponding to **1** gave a bifurcated H-bonded form (ΔE = -20.7 kcal/mol)[22] and the model corresponding to **2** gave a weak σ complex, with the Br^- located above a carbon atom *ortho* to the ester substituent (ΔE = -19.7 kcal/mol). This behavior is consistent with that exhibited by other highly electron-deficient arenes;[1,2] it indicates that the anion-π interaction is not a preferred binding motif for the arene donors in **1** and **2**.

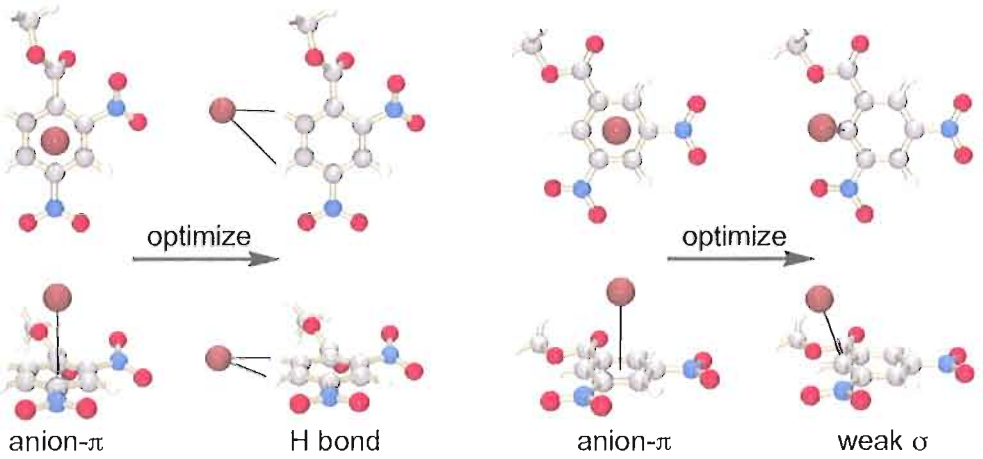

Figure 4.4 B3LYP/DZVP optimizations starting from idealized atomic coordinates for anion-π geometries with Br^- yielded an H-bonded complex for the arene in **1** (left) and a weak σ complex for the arene in **2** (right). Atom colors: carbon gray, hydrogen white, nitrogen blue, oxygen red, and bromide rust.

DFT CALCULATIONS OF RECEPTOR/Br⁻ COMPLEXES. The calculations of the 1:1 complexes with model arenes forecast the results of calculations on Br^- complexes of **1** and **2**. The lowest energy forms obtained for these complexes (Figure 4.5) are fully consistent with the NMR evidence. In **1**, Br^- forms bifurcated H-bonds to each

arene, with H•••Br^- distances of 2.72 Å (proton A, Figure 4.3) and 3.18 Å (proton B, Figure 4.3). In agreement with the spectra, the shortest hydrogen bonding interaction yields the largest chemical shift.[23] In **2**, where H-bonding to the arene is not possible due to steric repulsions, Br^- binds to the arenes via weak σ interactions, with distances of 3.31 Å to the nearest carbon atom in each arene. Lacking direct interaction with aryl hydrogen atoms, this binding motif is consistent with the small chemical shifts observed in the ^{1}H NMR spectrum for **2**•Br^-.

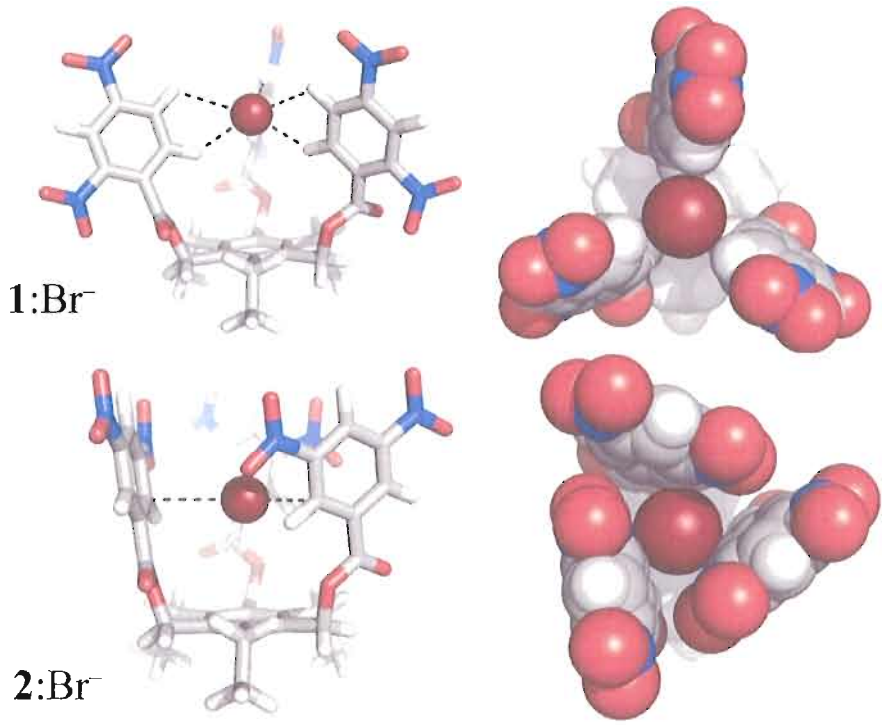

Figure 4.5 Optimized geometries (B3LYP/DZVP) comparing the aryl C-H hydrogen bonding mode of **1** (top) with the weak σ binding mode of **2** (bottom). Atom colors: carbon gray, hydrogen white, nitrogen blue, oxygen red, and bromide rust.

SOLUTION STUDIES WITH CHLORIDE AND IODIDE

Further solution studies, conducted with $NHep_4^+Cl^-$ and $NHep_4^+I^-$ (see Appendix C), yield results that further support conclusions obtained from the Br^- studies. Whereas the **1**•Cl^- complex is colorless in d_6-benzene, the **2**•Cl^- complex presents a pale yellow color in solution. An orange color change was observed for all receptors **1-3** with $NHep_4^+I^-$ (Appendix C, Figure C.5, right demonstrates the color observed when 84 equivalents of $NHep_4^+I^-$ are present at 27 °C).[24] Analogous to the Br^- titration experiments in C_6D_6, significantly larger chemical shift changes were observed for **1** over those of **2**, again consistent with the fact that **1** can form aryl CH•••X^- H-bonds while **2** cannot. Titrations of **1** and **2** with $NHep_4^+Cl^-$ exhibited the largest K_a values (ranging from 26-53 M^{-1}, Table 4.1). I^- ^{1}H NMR titrations at 27 °C reveal association constants ranging from 11-26 M^{-1}.[25] As with Br^-, control receptor **4** fails to form colored complexes with Cl^- or I^- and exhibits no measurable association in C_6D_6.

CONCLUDING REMARKS

Through a series of receptors utilizing only electron-deficient aromatic rings to bind anions, we have shown that ^{1}H NMR spectroscopy is a practical means to measure these subtle interactions in solution. DFT calculations and ^{1}H NMR titrations establish that the nitro group substitution pattern plays a critical role in the binding

mode adopted by the receptor. The 2,4- and 3,4-substitution patterns in **1** and **3** engender the interaction with anions through aryl C-H•••X^- hydrogen bonding, while the 3,5-substitution pattern in **2** promotes weak σ interactions.[24] With two NO_2 and one ester substituent, these highly electron-deficient arenes adopt binding motifs of weak σ and aryl H-bonding instead of the anion-π motif. The differences in binding modes between isomeric receptors **1** and **2** has allowed us to quantify for the first time distinction between aryl H-bonds and anion/arene π contacts, which are inherently in conflict when acidic aryl hydrogens are present. Receptors **1** and **2** exhibit the strongest interactions with Cl^-, followed by Br^- and I^-. Larger association constants are observed when the halide is restricted to interact solely through contacts to the π-system (receptor **2**). Does this approach hint at an emerging selectivity for anion binding in solution using electron-deficient arenes? Receptors that exhibit larger binding constants with more striking differences will need to be studied to further address this issue. We are currently developing new systems to elucidate further how electron-deficient aromatic rings can be integrated into receptor design for anions.

EXPERIMENTAL DETAILS

Full experimental details, including synthesis and structural details for all compounds described, a general X-ray diffraction experimental (including discussion of disorder modeling), syntheses of all receptors from key intermediate **5**, details of DFT calculations, general titration experimental, raw titration data, binding isotherms

as fit from non-linear regression curve fitting software and any associated references are available in Appendix C. CCDC #s 661394-661395 contain supplementary crystallographic data for this paper. These data can be obtained free of charge via http://www.ccdc.cam.ac.uk/conts/retrieving.html.

BRIDGE TO CHAPTER V

In Chapter IV, we demonstrated that subtle changes in receptor design can dramatically influence the preferred anion/arene binding geometry. In particular, anion receptors built from triethylbenzene scaffolds incorporating dinitroarene substituents exhibit modest halide binding in solution. DFT calculations corroborate our observation that 2,4-dinitro and 3,4-dinitro substituted receptors interact with halides via aryl C-H hydrogen bonds while 3,5-dinitro substituted receptors utilize contacts with the π-system.

The conformational flexibility and resulting modest association constants measured for this system with halides prompted us to investigate alternative receptor scaffolds to probe anion/arene interactions in solution. We aimed to rigidify the receptor scaffold and thus produce stronger anion/arene interactions. It was hypothesized that a structurally rigid scaffold would lead to a better understanding of anion/arene binding geometries in solution as well as help answer the question of preferred anion binding selectivity when utilizing electron-deficient aromatic rings.

Chapter V describes our effort in designing, preparing and studying tripodal anion receptors that utilize hydrogen bonds to conformationally stabilize pendant electron-deficient aromatic rings. With the proper receptor design, competing anion/receptor hydrogen bonds will be negligible and the anions will be free to interact with the appropriately positioned electron-deficient arenes.

CHAPTER V

INVESTIGATING THE USE OF INTRAMOLECULAR HYDROGEN BONDS TO STABILIZE RECEPTOR CONFORMATIONS; DESIGNING RECEPTORS FOR ANION/ARENE INTERACTIONS

INTRODUCTION

Chapters II-IV have shown the progression of designing receptors that incorporate electron-deficient aromatic rings to bind anions. Our first foray into anion/arene interactions utilized tandem hydrogen bonding and electron-deficient arenes to attract monoatomic anions in solution. Initial investigations prompted us to study crystallographically and computationally the preferred binding geometry of anion/arene interactions. With this new understanding of anion/arene interactions we developed tripodal anion receptors that utilize steric gearing to preorganize electron-deficient aromatic rings. We found these receptors to exhibit very specific binding modes depending on the substitution pattern of the nitro groups, resulting in modest anion binding in solution. It is our interest to design structurally rigid anion receptors that utilize only electron-deficient aromatic rings to bind anions. Ultimately, in these systems we will address the question of preferred anion binding selectivity for anion/arene interactions.

Hydrogen bonds have long been a favored method of attracting complementary donor or acceptor functionality.[1-4] The directionality and non covalent character of hydrogen bonding makes it an appealing technique for molecular recognition.[5-7] As emphasis, nature—The archetype for molecular recognition—uses hydrogen bonding to control the structure of DNA, protein folding, enzyme active centers, formation of membranes and proton transport. In the early 1900s hydrogen bonding was originally recognized from its unique property imparting capacity, as observed for solvents such as water. Progress has moved from observance to intelligent design and synthetic variants of hydrogen bonding receptors run rampant in the current literature. One particularly interesting application for hydrogen bonding is its capability to control the conformation of otherwise flexible molecules through intramolecular hydrogen bonds. Many elegant receptors have been presented with remarkable properties owing to intramolecular hydrogen bonds.[8-13] We hypothesized that intramolecular hydrogen bonding could be utilized to study anion/arene interactions in solution. One of the challenges associated with this approach is preventing competing hydrogen bonds with the anion in study. This concern will be met by proper receptor design, enticing the receptor to form intramolecular hydrogen bonds rather than hydrogen bonds with the anion.

TRIPODAL RECEPTOR DESIGN; INCORPORATING HYDROGEN BOND DONORS

The tripodal receptor molecules presented herein are designed to present three electron-deficient aromatic rings in close proximity through stabilization from intramolecular hydrogen bonds between neighboring amide substituents. We have focused on attaching electron-deficient aromatic rings to an apical atom by means of amide coupling reactions. A series of linking atoms have been investigated but this chapter will focus on the nitrogen and phosphorous analogs. The receptor core is designed to be admittedly flexible. However, we hypothesize that the conformational variability for the receptor will be severely restricted by intramolecular hydrogen bonds. Two classes of receptors are presented which differ by the apical atom (Figure 5.1). Changing the type of atom that links the electron-deficient arenes together will allow the intramolecular hydrogen bonding distances to be fine tuned. Furthermore, subtle changes in intramolecular hydrogen bonding distances can also be achieved by altering the number of linking atoms. Finally, the strength of anion/arene interactions will be addressed by synthesizing aromatic rings of variable electron-deficiency.

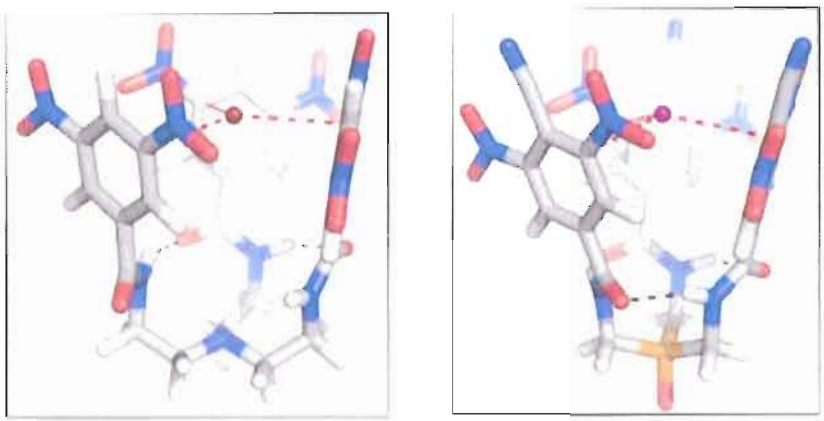

Figure 5.1 Computational studies (CAChe MM3) suggest that tripodal anion receptor/Br^- complexes can form intramolecular hydrogen bonds to stabilize the receptor conformation.

NITROGEN BASED SCAFFOLDS FOR ANION RECOGNITION

SYNTHESIS OF NITROGEN BASED ANION RECEPTORS. Trisamide tripodal anion receptors **1** and **2** based off amine linkers are synthesized in good yield from commercially available starting materials in one step. Tris(2-aminoethyl)amine (TREN) or tris(3-aminopropyl)amine (TRPN) and 3,5-dinitrobenzyl chloride are dissolved in dry dimethylformamide (DMF) and heated to 160 °C. Pouring this mixture over ice and subsequent washes with methanol affords the pure HCl receptor salts tan powders in 50-80% yield (Scheme 5.1). The parent receptors are not readily soluble in chlorinated solvents but dissolve readily in dimethylsulfoxide (DMSO) or

acetonitrile (MeCN). Recent evidence presented in the proceeding sections suggests that these receptors are isolated as the corresponding HCl salt by soaking up the HCl generated in the reaction mixture.

Scheme 5.1 Synthesis of TREN and TRPN based tripodal amide receptors **1** and **2**.

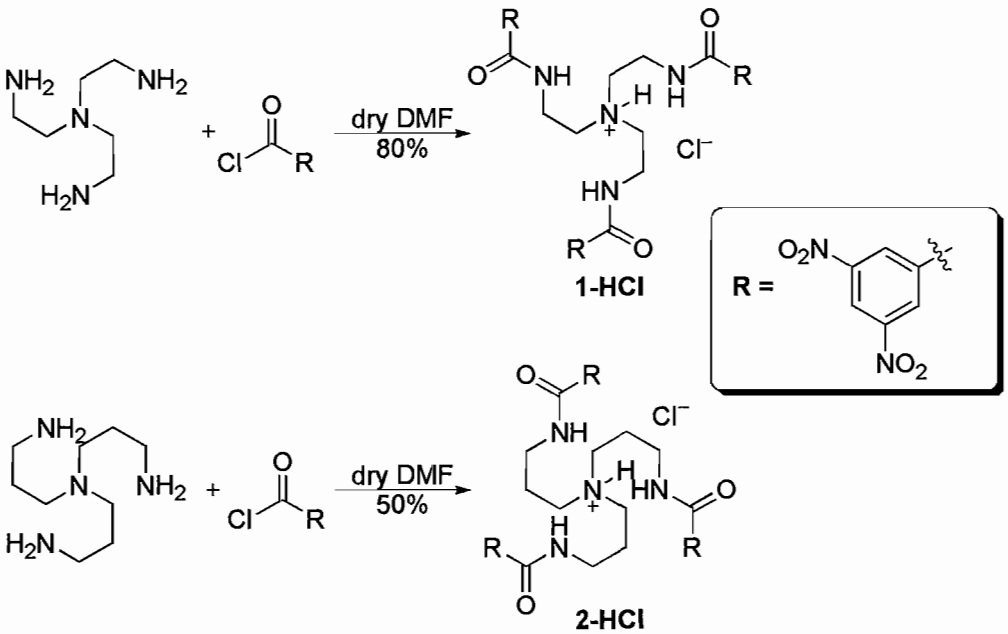

SOLID STATE BEHAVIOR OF NEUTRAL AMINE BASED RECEPTORS. Single crystals of receptor **1** suitable for X-ray diffraction are grown from slow evaporation of MeCN solutions of the isolated product from the reaction mixture. Receptor **1** crystallizes in the *P*-1 symmetry setting with 4 molecules per unit cell. Interestingly, upon close inspection of the crystal structure it is revealed that **1** crystallizes with chloride anion and no counter cation indicating that the product isolated is actually the

HCl salt of receptor **1**. Further solid state analysis of receptor **1**•HCl is provided in the following section.

Colorless single crystals of the TRPN based trisamide receptor were also grown from evaporating MeCN solutions. Unfortunately, all attempts at obtaining single crystal X-ray diffraction data were thwarted by poor diffraction. Presumably, the lack of diffraction in this system arises from the predilection of this molecule to crystallize in sheets.

SOLID STATE BEHAVIOR OF PROTONATED AMINE BASED RECEPTORS. We hypothesized that the anion binding capacity of amine based tripodal trisamide receptors would be enhanced upon protonation of the apical nitrogen. Protonating this system is not ideal for solution measurements of anion/arene interactions where we would prefer to measure only the interaction of the anion with the electron-deficient aromatic ring. However, the added columbic attraction should make isolating single crystals with anions a more profitable endeavor. Single crystal growth revolved around dissolving TREN and TRPN receptors in MeCN followed by subsequent addition of an acid source such as; HCl, HBr, HI, H_2SO_4, HNO_3, $HReO_4$, HBF_4 and $HClO_4$. Both the TREN and TRPN based receptors yielded large colorless block crystals from the HCl solutions, presumably because our starting materials were the HCl salts. No evidence of anion exchange was observed for any of the other anions. Data from single crystal X-ray diffraction studies was collected for the TREN receptor/Cl^- mixture while the TRPN receptor again produced poor diffraction. The X-ray structure of the TREN/Cl^-

complex is strikingly similar to the structure obtained from the product isolated from the reaction mixture. Closer inspection reveals that both structures are actually the same. Receptor **1**•HCl crystallizes in the space group *P*-1 with 4 molecules per unit cell. Interestingly, one Cl^- atom accepts hydrogen bonds from two of the receptor arms in the solid state (3.11 Å and 3.41 Å) while the third arm donates a hydrogen bond to another Cl^- atom (3.25 Å). This hydrogen bonding network extends throughout the structure forming an infinite hydrogen bonding chain (Figure 5.2). The exo bound Cl^- atoms in this crystal structure indicate that the distances between amide substituents in this system are not ideal for intramolecular hydrogen bonds (N–N distances, 3.79 – 4.99 Å) thus nullifying our design strategy to stabilize receptor conformations with intramolecular hydrogen bonds.

In the solid state the receptor arms are all located on the same side of the molecule with the lone pair of the linking nitrogen pointing into the receptor cavity. This conformation bodes well for future anion binding studies as it places all three electron-deficient aromatic rings close enough to interact with one monoatomic anion. However, it is noted in the solid state that all three aromatic rings are roughly parallel. In this conformation the anion would be limited to form anion/arene π-contacts with two arms and aryl C-H hydrogen bonds with the other arm. In order to achieve three π-contacts, one of the aromatic rings would be forced to rotate out of conjugation with the amide. However, we see no evidence of such a rigid conformation by ^{1}H NMR spectroscopy in water containing solvents.

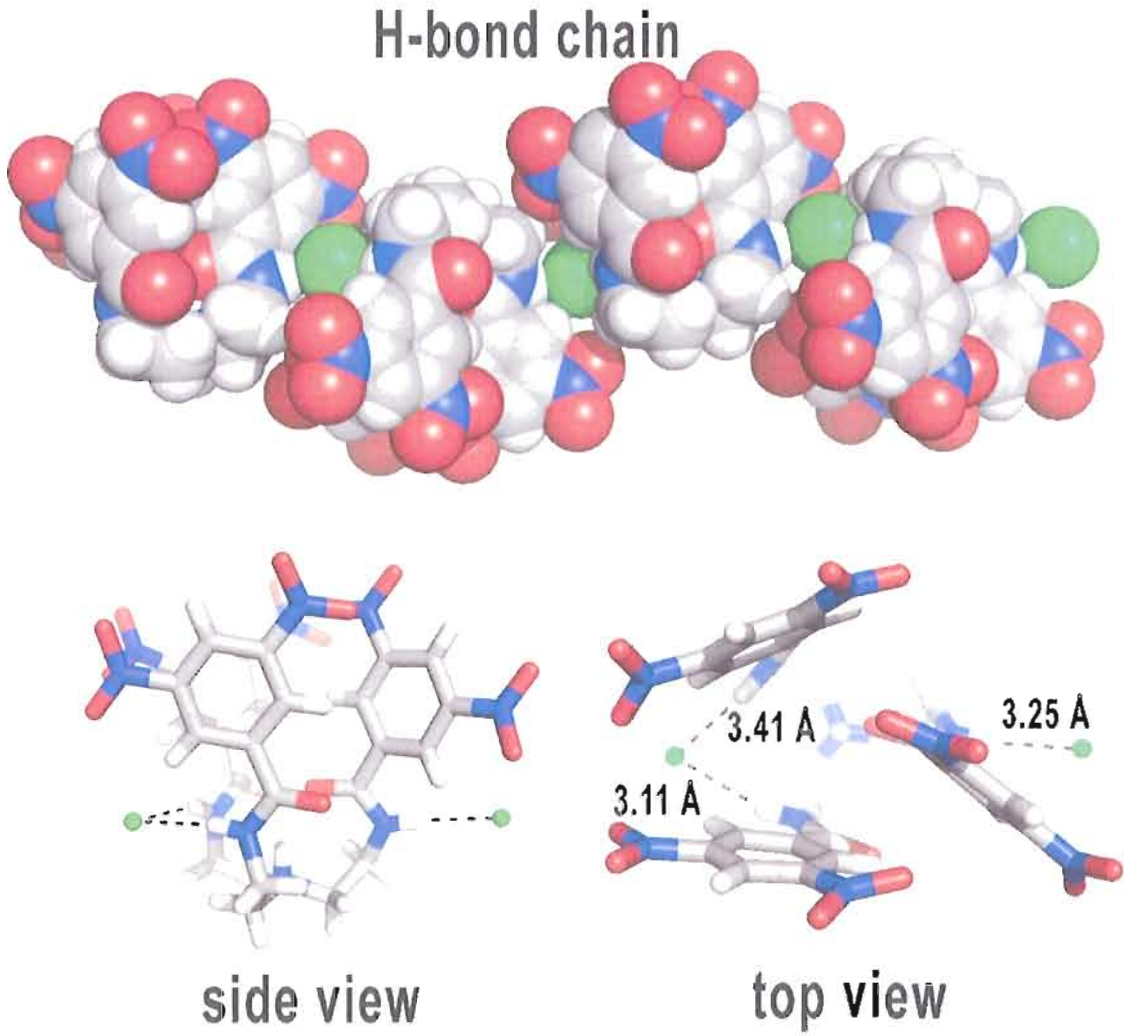

Figure 5.2 Stick and CPK crystal structure representations of the HCl salt of TREN based trisamide receptor **1**.

PHOSPHORUS BASED RECEPTORS FOR ANION RECOGNITION

In an effort to introduce intramolecular hydrogen bonding that was not observed for the TREN and TRPN based tripodal receptors **1** and **2** we chose to investigate phosphorous based receptors. Phosphorous was chosen as the linker atom in this

system for two reasons 1) the synthetic ease of building receptors with only one carbon between the apical atom and the amide linker and 2) the potential to do chemistry with the phosphorus lone pair and thus introduce new functionality into the receptor.

SYNTHESIS OF PHOSPHORUS BASED RECEPTORS. Phosphorus based receptors are synthesized in two steps from commercially available material.[14, 15] The synthesis is amenable to large scale preparation and starting materials can be synthesized in 100+ gram quantities. Tripodal phosphine receptor **3** and phosphine oxide receptor **4** are synthesized by first reacting 1,3,5-triaza-7-phosphaadamantane or the oxide derivative with hydrobromic acid. The resulting crystalline triamine hydrobromide is reacted with 3,5-dinitrobenzoyl chloride in biphasic conditions resulting in isolation of pure receptor **3** and **4** as a white powder (Scheme 5.2). Once removed from solution, receptors **3** and **4** are sparingly soluble in most organic solvents but dissolve readily in DMSO or DMF. Interestingly, the addition of an electron acceptor such as Na^+ or K^+ greatly enhances the receptor's solubility. Both receptors **3** and **4** can be isolated cleanly from the reaction mixture. However, under an oxygen atmosphere phosphine based receptor **3** begins to turn color in a matter of hours, suggesting oxidation of the phosphorus is taking place. Because of this complication we performed initial studies on phosphine oxide based receptor **4**.

Scheme 5.2 Synthesis of phosphine and phosphine oxide tripodal amide receptors **3** and **4**.

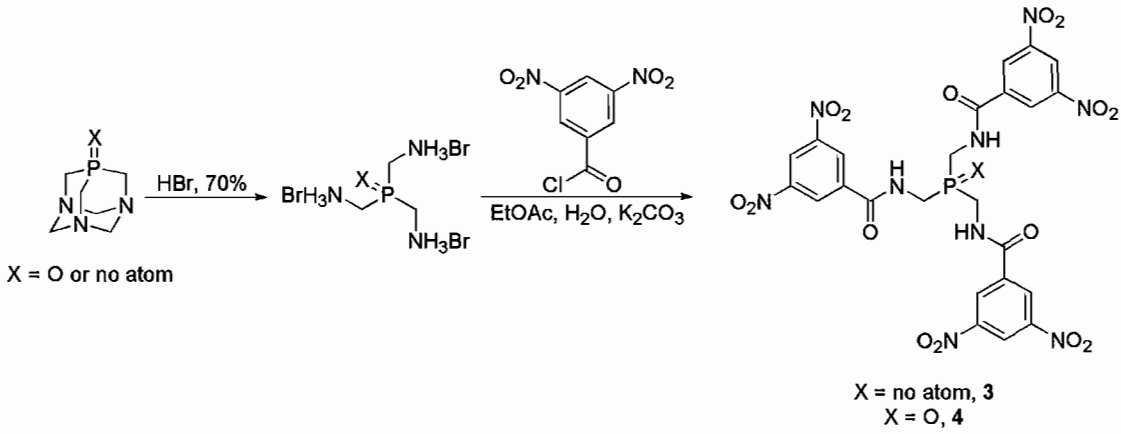

SOLID STATE BEHAVIOR OF TRIPODAL TRISAMIDE PHOSPHINE OXIDE BASED RECEPTOR. The solid state behavior of receptor **4** was investigated by single crystal X-ray diffraction. Long colorless needles suitable for single crystal X-ray diffraction were grown from slowly evaporating DMSO. Receptor **4** crystallizes in the space group *R*3 with one receptor molecule per unit cell and three DMSO solvent molecules. Phosphine oxide based receptor **4** exhibits some similar solid state characteristics to the TREN based receptor **1**. Namely, receptor **4** crystallizes with all three arms on the same side of the molecule and the phoshine oxide functionality directed toward the interior of this cavity (Figure 5.3). One striking difference between the two structures is that phosphine oxide receptor **4** crystallizes with three larger DMSO solvent molecules per receptor. This effectively opens the receptor cavity up creating an appealing bowl conformation with inward directed functionality. Also aiding in the bowl conformation is the nested packing arrangement which serves to fill

the cavity created from this conformation, as well as align the phosphine oxygen dipoles. Creating synthetic systems with inward directional functionality has long been the aspiration of many supramolecular chemists. Our initial efforts aimed to profit from this serendipitous discovery by surveying potential guest molecules for this concave surface. Initial guests screened included the spherical molecule C60, hydrogen bond donors such as urea, pyrazinium bromide and iodide. Interestingly, when NaI or KI are added to receptor **4** the solubility in organic solvents is greatly enhanced (presumably as a result of disrupting the 'nesting' capability of the receptor in the solid state). Moreover, receptor **4**/NaI solutions turn orange upon mixing suggesting possible anion/arene interactions in solution. Unfortunately, changes in ^{1}H NMR chemical shifts were negligible and no further solution characterization was undertaken. Attempts at crystallizing this colored species also met failure.

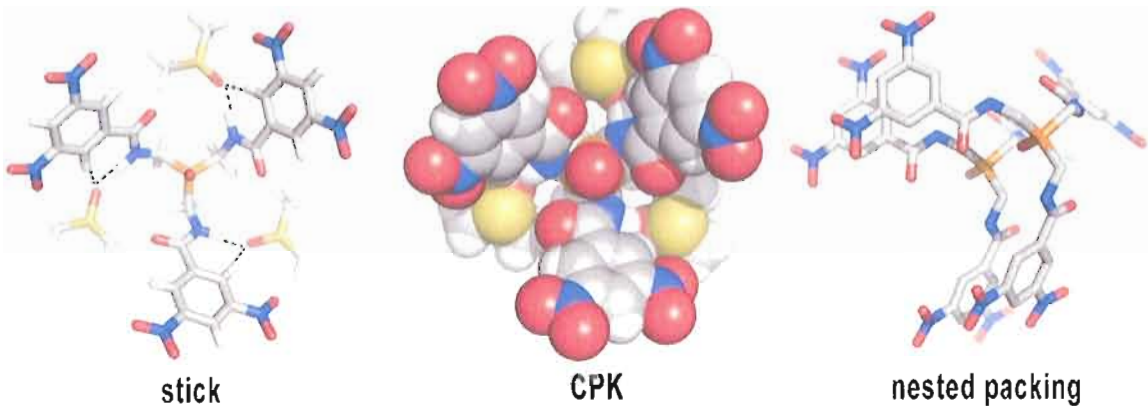

Figure 5.3 Stick, CPK and nested representations of receptor **4** in the crystalline state highlighting the bowl conformation.

SYNTHESIS AND STRUCTURE OF HIGHLY ELECTRON-DEFICIENT AROMATIC RINGS

Endeavoring to develop electron-deficient aromatic rings that are amenable to modular receptor synthesis we designed the nitro-cyano-nitro functionalized benzoic acid **5** (Figure 5.4). The strongly electron withdrawing nitro and cyano substituents were incorporated to enhance anion binding and the benzoic acid functionality serves to withdraw electron density in addition to providing a site for attachment to receptor scaffolds. *Extreme caution should be taken when working and developing new electron-deficient aromatic rings as they have the potential to be explosive and/or shock sensitive. A note to future researchers interested in electron-deficient aromatic rings—as the electron-deficiency increases for these aromatic rings they become especially sensitive to base producing either nucleophilic attack on the ring or deprotonation. Even so, they remain stable to acidic conditions.*

Electron-deficient aromatic ring **5** is synthesized in four steps from commercially available 4-chlorobenzoic acid **6**. 4-chlorobenzoic acid **6** is nitrated in the 3 and 5 positions with fuming nitric acid in excellent yield (92%) producing crystalline **7**. Subsequent esterfication of **7** with $SOCl_2$ and EtOH results in 4-chloro-3,5-dinitrobezoic acid ethyl ester **8** in 92% yield. The cyano functionality is introduced with Rosenmund-von Braun conditions producing 4-cyano-3,5-dinitrobenzoic acid ethyl ester **9** as orange needles in good yield (52%). The desired benzoic acid **5** is produced in 95 % yield from deprotection of **9** with HCl and AcOH. ^{1}H NMR is useful

for characterization however there are notably few protons on benzoic acid **5**. To aid in characterization we grew single crystals suitable for X-ray diffraction from evaporating DMSO. Benzoic acid **5** crystallizes in the space group *P*(2)1/c with four acid molecules and four DMSO solvent molecules per unit cell. We have also shown by ^{1}H NMR that we can convert benzoic acid **5** to the corresponding acid chloride by refluxing in $SOCl_2$ under an inert atmosphere. Once the appropriate receptor scaffold is developed the acid chloride of **5** will be attached to produce receptors that bind anions with highly electron-deficient aromatic rings.

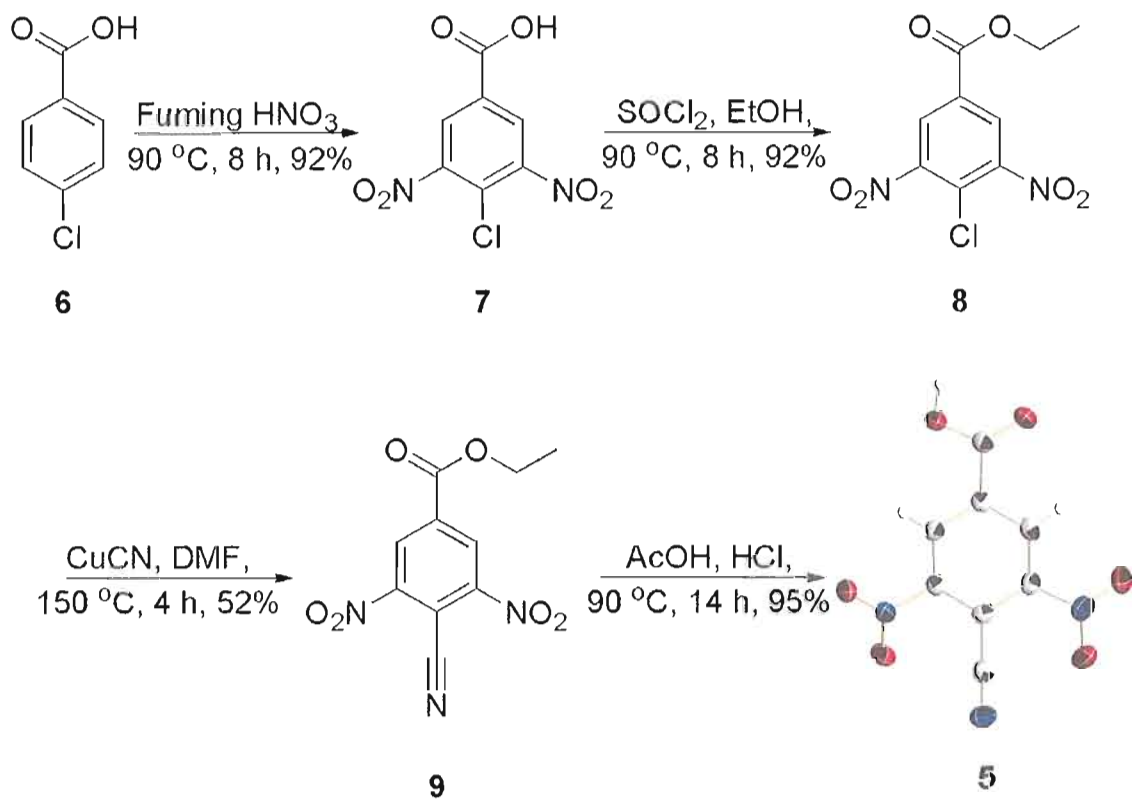

Figure 5.4 Synthesis and crystal structure of nitro-cyano-nitro functionalized benzoic acid **5**.

CONCLUSION

In summary, this chapter has laid the foundation for the next generation of anion receptors. We have investigated the possibility of using intramolecular hydrogen bonds to rigidify receptor scaffolds for anion binding. In particular, we have shown that TREN based tripodal amide receptors are not optimized for intramolecular hydrogen bonds in the solid state. The shorter phosphine oxide receptor also does not exhibit intramolecular hydrogen bonds when crystallized from DMSO. However the receptor does crystallize in a bowl conformation in the solid state, suggesting that this molecule may be an excellent precursor for developing cavities with inward directed functionality. Finally, we have developed and characterized a new electron-deficient aromatic binding motif that promises to produce improved receptors for anion recognition.

Improved receptor design will result in conformationally rigid molecules with stronger anion associations. The synthesis of highly electron-deficient aromatic rings with functionality suitable for receptor production will also aid in enhancing anion/arene interactions in solution and the solid state. Developing improved receptors that utilize only anion/arene interactions to attract anions is paramount in answering the fundamentally important question—do anion/arene interactions exhibit selectivities uncharacteristic of traditional anion binding techniques?

BRIDGE TO CHAPTER VI

Chapter VI shifts focus from studying direct anion/arene interactions to studying the affect that anion binding by hydrogen bonding has on highly conjugated aromatic receptors. This work was inspired by discussions between Prof. Johnson and Prof. Haley aimed at merging their two chemistries. Initial synthetic work by Dr. Charles A. Johnson (Haley Laboratory) led to solid and solution state investigation by Orion B. Berryman (Johnson laboratory). Initial research focused on developing ethynyl pyridine hydrogen bonding receptors for anion and small molecule recognition. Subsequent studies investigated developing larger scaffolds. Sulfonamide appended receptors of this class exhibit interesting water/halide recognition capabilities and all receptors show promise as fluorescent or colorimetric sensors for small molecule and anion recognition.

CHAPTER VI

A CONFORMATIONALLY DIVERSE SERIES OF MOLECULES; 2,6-BIS(ETHYNYL)PYRIDINE, BIPYRIDINE AND THIOPHENE AS SCAFFOLDS FOR MODULAR RECEPTOR DESIGN

INTRODUCTION

This chapter was co-authored with Dr. Charles A. Johnson II, Dr. Lev N. Zakharov, Prof. Michael M. Haley and Prof. Darren W. Johnson. The molecules studied in this chapter were synthesized by Dr. C. A. Johnson who also fully characterized each molecule and isolated two of the single crystals. Dr. Zakharov solved and assisted in solving the single crystal X-ray structures contained in this chapter. Professors Haley and Johnson and Dr. C. A. Johnson conceptualized this project and provided editorial assistance. Orion B. Berryman wrote this chapter, performed the solution studies and isolated and assisted in characterizing the single crystal X-ray structures. This chapter includes work that was published in *Angewandte Chemie International Edition* (**2008**, 47, 117-120, © 2008 Wiley-VCH GmbH and Co. KGaA, Weinheim). Also contained in this chapter for completeness is work from the dissertation of Dr. Charles Andrew Johnson II.

2,6-bis(ethynyl)pyridines have found utility in numerous areas of chemistry. The inherent properties of 2,6-bis(ethynyl)pyridines (conjugation, absorption/emission, mechanical, high spin states, pH dependence, metal binding capability, rigidity etc.) have been exploited for applications such as; liquid crystals, light-emitting materials, rotaxane-type structures, molecular magnets, antiangiogenic activity, polymer composites and coordination complexes.[1-5] In contrast, the supramolecular chemistry of 2,6-bis(ethynyl)pyridines has received negligible attention. Most of the host/guest studies have focused on exploiting the pyridine lone pair to bind metal ions[6] or organoiodides[3]. Alternatively, we hypothesized that the unique absorption/emission properties in tandem with the structural rigidity of 2,6-bis(ethynyl)pyridines aptly positions them to function as small molecule or ion receptors. Moreover, we envisioned that the 2,6-bis(ethynyl)pyridine scaffold and its derivatives would serve as a versatile building block for the development of receptor molecules that target a variety of guests depending on the protonation state of the pyridine and the style of functional groups appended to the alkyne (Figure 6.5).

Supramolecular self-assembly reactions have provided a diverse collection of hosts with remarkable shapes, sizes and tailored properties, including catalysis, enzyme mimicry and sensing, among others.[7-11] Reversible interactions such as metal coordination, hydrogen bonding and electrostatic attractions stabilize the multiple components of these discrete assemblies. Here we disclose a class of hydrogen bonding sulfonamide receptors based off of a 2,6-bis(2-anilinoethynyl)pyridine

scaffold that exhibits a new self-assembly motif: 2+2 dimers consisting of two receptors stitched together by either two water molecules, two halides, *or one of each*, depending on the protonation state of the receptor. We also highlight the modular synthesis of this receptor class with report of a family of amide receptors based off the same receptor scaffold. Additionally the pyridine moiety can be substituted for other heteroaromatic rings to adjust the size of the binding cavity. Cations are now recognized as important structural features in proteins, and it is becoming increasingly apparent that water also plays a vital structural role in proteins and complex self-assembled synthetic molecules.[12] Anions, on the other hand, tend not to share this structural diversity. Although a few proteins are known to self-assemble into oligomers with the aid of anions (often under very high salt concentrations),[13,14] very few synthetic examples exist of anion binding driving the self-assembly of larger structures.[15] The interchangeable use of water *or* halides to drive self-assembly is highly unusual, if not unprecedented. The sulfonamide receptors reported here form 2+2 dimers in solution and in the crystalline state, creating a binding pocket that houses water, hydrogen halides, or both, highlighting the strong directing force *both* water and halides can exert in complex self-assembling systems.

2,6-BIS(2-ANILINOETHYNYL)PYRIDINE SULFONAMIDES

The complex hydrogen bonding interactions of the water molecule are remarkable: water plays a vital role in a number of systems ranging from the formation

of hydrogen-bonded water oligomers[16] to the increased conformational stability of proteins[12] and the crucial synergistic hydrogen bonds formed in enzymatic[17,18] or biomimetic[19] active sites. In many cases these hydrogen bonds dictate both structure and function. In supramolecular chemistry, synergistic hydrogen bonding between water and organic molecules has helped to stabilize vase-like conformations of hosts for organic molecules[20] and induce the formation of intricate hexameric nanoscale capsules stitched together with the aid of eight water molecules.[21,22] In both cases these hosts can be stabilized in wet organic or purely aqueous solvents.[23,24] Anions, on the other hand, tend not to share the structural hydrogen bonding diversity of water, in part as a result of the weak basicity of anions and often a lack of directionality in their hydrogen bond formation.[15,25] Nevertheless, there is an emerging use of anions as directing elements in self-assembly reactions. Notable examples include a double-stranded helix wrapped around two sulfate anions,[26] catenanes and other structures templated by the formation of hydrogen bonds to anions,[27] and supramolecular dimers, oligomers and polymers linked together by anions.[28-30] Herein we report new receptors based on a 2,6-bis(2-anilinoethynyl)pyridine scaffold that surprisingly form 2+2 dimers with *either water, halides or both* depending on the protonation state of the receptor. To the best of our knowledge this is the first example of both halides and water molecules serving the same structural hydrogen bonding roles in a synthetic self-assembled system.[31]

Our initial venture into the use of aryl-ethynyl scaffolds as receptor molecules focused on sulfonamide bearing 2,6-bis(2-anilinoethynyl)pyridines **1** and **2** (Scheme 6.1), designed to target hydrogen bonding guest molecules (see Appendix E). CAChe semi-empirical minimized molecular models suggested that selectivity for different guest molecules could be tailored by protonating the pyridine nitrogen, thus altering the cavity size, or by exchanging the binding substituents. The aryl-ethynyl core **3** is prepared from known 2-iodo-4-*t*-butylaniline[32] in 3 steps in 60% overall yield. Conversion to sulfonamides **1** and **2** was accomplished in excellent yield by treatment of **3** with the respective sulfonyl chlorides (Scheme 6.1).

Scheme 6.1 Synthesis of 2,6-bis(2-anilinoethynyl)pyridine sulfonamides

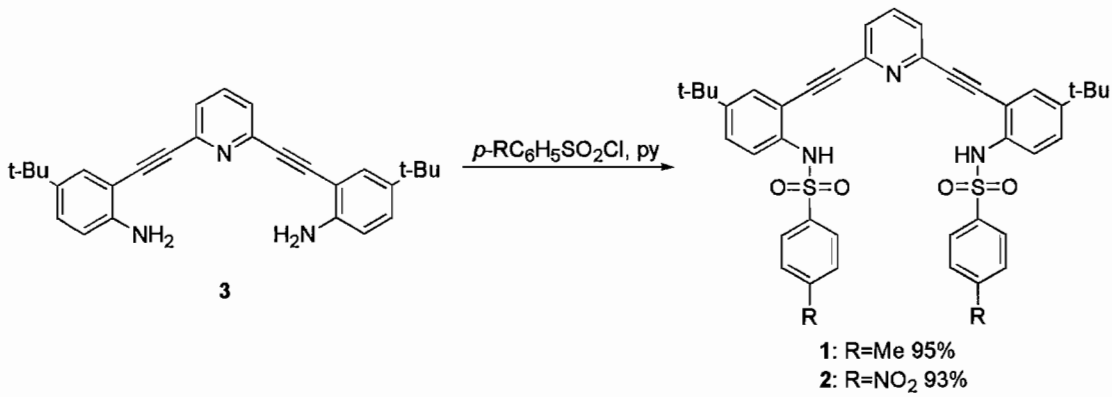

Receptor molecules **1** and **2** have been characterized by ^{1}H and ^{13}C NMR, UV-Vis, fluorescence and IR spectroscopy, melting point and single crystal X-ray diffraction (Experimental and Appendix E). Interestingly, the ^{1}H NMR signals of receptors **1** and **2** exhibit considerable concentration dependence in organic solvents. Furthermore, the sharp singlet typically observed at ca. 1.5 ppm for residual water in $CDCl_3$ appears as a broad downfield singlet (observed as far downfield as ca. 4 ppm depending on concentration), hinting at the hydrogen bonding capability of receptors **1** and **2** in solution. This fact was confirmed by single crystal X-ray diffraction analysis of neutral receptors **1** and **2** (Figure 6.1).[33,34]

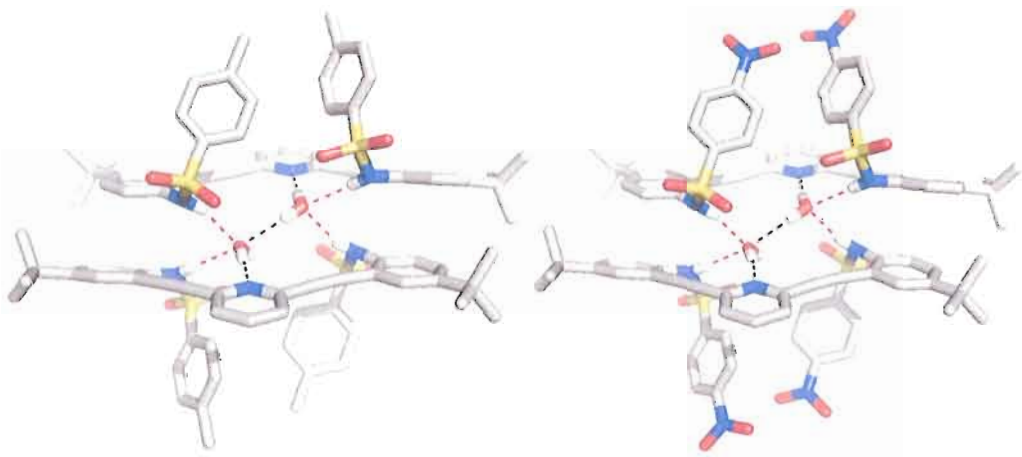

Figure 6.1 Crystal structures of receptors (**1**•H_2O)$_2$ (left) and (**2**•H_2O)$_2$ (right) illustrate the 2+2 dimer formed with water. The hydrogen bonds involving water as the donor atom form a helical twist through the center of the binding cavity. All hydrogen bonds are depicted as dashes. (H atoms not involved in hydrogen bonds were omitted and only one position for the disordered H atom in the bridging solvent water molecule is shown for clarity).

Colorless single crystals of receptors **1** and **2** suitable for X-ray diffraction were grown by layering hexane onto ethyl acetate solutions of each receptor. As suggested from the ^{1}H NMR spectroscopic data, complexes (**1**•H_2O)$_2$ and (**2**•H_2O)$_2$ both crystallize as dimers in space group *P*-1 with two receptor molecules and two water molecules per unit cell; consequently, each dimer has crystallographic inversion symmetry. A prominent feature of each crystal structure is the presence of two hydrogen bonding water molecules stitching the receptor dimers together. Both pyridine nitrogens accept hydrogen bonds from a different water molecule [2.797(4)-2.804(2) Å, O-H···N angles 172(4)-175(3)°], while one water-water hydrogen bond is present [2.917(5)-3.006(7) Å, O-H···O angles 164(4)-178(6)°]. All of the N-substituted sulfonamides adopt the energetically most-favored 'staggered' conformation,[35] and both sulfonamide protons on each receptor donate a hydrogen bond to a different water molecule [2.855(4)-2.860(3) Å, 157(2)-164(3)° and 3.028(4)-3.039(3) Å, 158(2)-164(3)°] such that the 2+2 dimer structure is held together by four sulfonamide-water hydrogen bonds, two pyridine-water hydrogen bonds, one water-water hydrogen bond and two π-stacking interactions between receptors ranging from 3.42-3.44 Å (Figure 6.1).

The dimerization of receptor **1** was further investigated in $CDCl_3$ solutions. Receptor **1** was dissolved in water-saturated $CDCl_3$ to a concentration of 197 mM. Monitoring the sulfonamide N-H and water ^{1}H NMR resonances following a series of dilutions resulted in data that could be fit to a 1:1 dimerization with the non-linear

regression curve fitting software WinEQNMR[36] (Appendix E). In $CDCl_3$ solutions receptor **1** is shown to dimerize with a modest $K_{dim} = 42\ M^{-1}$. Supporting evidence of dimerization in $CDCl_3$ solutions resulted from the NOE observed between the protons on the guest water molecules and the sulfonamide protons of the receptor (Appendix E). Receptor **1** exhibits a propensity to crystallize as a dimer with H_2O even in the presence of other potential neutral guest molecules[37] and in solvents dried over 3 Å molecular sieves.

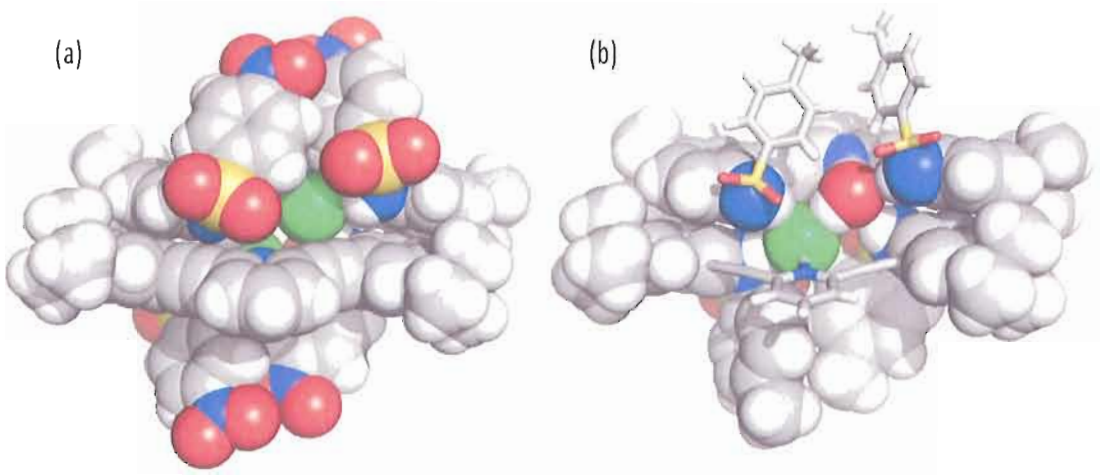

Figure 6.2 (a) Space filling representation of the crystal structure of $(\mathbf{H2}^{+}\bullet Cl^{-})_2$. Hydrogen bonds are depicted as red dots and chloride is shown in green. (b) Crystal structure representation of the water-chloride heterodimer $(\mathbf{H1}^{+}\bullet Cl^{-})\bullet(\mathbf{1}\bullet H_2O)$. *Both* water and hydrogen chloride stabilize dimer formation with seven hydrogen bonds within the binding cavity of the heterodimer. Only one position of the disordered water and chloride atoms is shown for clarity.

Receptor molecules **1** and **2** share a common design trait: their ability to alter guest selectivity by simple changes in the protonation state of the receptors. By

protonating the pyridine nitrogen of receptors **1** and **2**, the anion binding capacity of these receptors is activated. The halide binding properties of $\mathbf{H1}^+$ have been investigated in the solid state: single crystals of the chloride and bromide complexes are prepared by dissolving receptor **1** or **2** in ethyl acetate and bubbling HCl or HBr gas through the solution. Crystallization is induced by layering hexanes onto the yellow ethyl acetate solutions. Strikingly, the single crystal structures of the $\mathbf{H2}^+\bullet Cl^-$ and $\mathbf{H1}^+\bullet Br^-$complexes revealed nearly isostructural dimers to those observed for the neutral $(\mathbf{1}\bullet H_2O)_2$ and $(\mathbf{2}\bullet H_2O)_2$ water dimers.[38,39] In the solid state the $(\mathbf{H2}^+\bullet Cl^-)_2$ and $(\mathbf{H1}^+\bullet Br^-)_2$ dimers (Figure 6.2a and Figure 6.3d, respectively) are held together by four sulfonamide hydrogen bonds [3.156(2)-3.229(2) Å, N-H···Cl angles 151(2)-171(3)°; 3.338(5)-3.440(6) Å, N-H···Br angles 136(4)-168(4)°], two pyridinium N-H hydrogen bonds to the anions [3.022(2) Å, 175(3)° for $(\mathbf{H2}^+\bullet Cl^-)_2$ and 3.127(6) Å, 173(4)° for $(\mathbf{H1}^+\bullet Br^-)_2$], two C_{aryl}-H···X hydrogen bonds (3.69–3.90 Å), and two π-stacking interactions between receptors (3.49 Å for $(\mathbf{H2}^+\bullet Cl^-)_2$ and 3.61 Å for $(\mathbf{H1}^+\bullet Br^-)_2$. The numerous hydrogen bonds and unique dimerization bring the negatively charged halides into close proximity with halide–halide distances of 3.92 Å for $(\mathbf{H2}^+\bullet Cl^-)_2$ and 4.08 Å for $(\mathbf{H1}^+\bullet Br^-)_2$.

CAChe semi-empirical calculations of the 2,6-bis(2-anilinoethynyl)pyridine receptors suggested that larger polyatomic anions would not fit within the binding pocket of the receptor. As predicted, the single crystal X-ray structure of the HBF_4 salt $(\mathbf{H1}^+\bullet BF_4^-)$ reveals that the binding pocket is too small to accommodate the interaction

of the large BF_4^- guest with either sulfonamide proton. Dilution experiments of **H1**$^+$•BF_4^- revealed minimal change in the ^{1}H NMR spectrum upon addition with $CDCl_3$, indicating negligible dimerization in solution as predicted by the receptor conformation observed in the crystal structure. However, titrations of **H1**$^+$•BF_4^- with tetra-*n*-butylammonium halide salts do indicate anion binding occurs in solution between the receptor and halides.[40] Furthermore, the concentration dependence observed in the ^{1}H NMR spectrum upon dilution of (**H1**$^+$•Cl^-)$_2$ in $CDCl_3$ indicates the presence of a receptor/halide dimer in solution. A supersaturated solution of (**H1**$^+$•Cl^-)$_2$ (60 mM) was obtained by passing HCl gas through a $CDCl_3$ solution of neutral receptor **1**. Plotting the changes in chemical shift upon dilution and subsequent fitting of this data to a 1:1 dimerization model with the non-linear least squares regression program WinEQNMR resulted in a $K_{dim} = 250\ M^{-1}$ in $CDCl_3$.[41] Further evidence of dimerization was obtained by mixing a 1:1 ratio of receptor **1** and a *p*-methoxyphenyl sulfonamide derivative. When equimolar mixtures of these receptors are prepared at 10 mM in $CDCl_3$ and HCl gas is passed through the solution, the resulting ^{1}H NMR signals are shifted from the signals observed for either of the analogous homodimers prepared in the same way at the same concentration. This result suggests that both homodimers and a third species – the heterodimer – are present in solution, but equilibrating quickly on the NMR timescale. From all of these experiments it is evident that dimerization of both the neutral and protonated forms of 2,6-bis(2-anilinoethynyl)pyridine receptors occurs in the solid state and in solution.

Remarkably, a different type of "heterodimer" (**H1**$^+$•Cl^-) •(**1**•H_2O) was also crystallized in the presence of concentrated HCl with one water and one chloride in the binding pocket (Figure 6.2b and Figure 6.3b).[42] The heterodimer contains one protonated receptor that binds a chloride anion while the other receptor in the dimer is neutral and bound to a water molecule. Water and hydrogen chloride are freely exchangeable in this binding pocket and provide intermediate structural features to the H_2O and hydrogen halide dimers. Analogous to the other dimers presented, the heterodimer is stabilized by π-stacking interactions between the two receptors (3.43 Å) and a series of seven guest assisted hydrogen bonds. Each guest molecule—water and chloride—accepts two sulfonamide N-H hydrogen bonds (3.157(3)-3.181(3) Å, N-H···X angles 158(3)-167(3)^o) and additionally forms a helical hydrogen bonding pattern running between the pyridinium, chloride, water and pyridine heteroatoms (2.926(3)-3.10 Å, 164(3)-176(4)^o). Two C_{aryl}-H···Cl hydrogen bonds (3.76-3.93 Å) also stabilize the dimer.

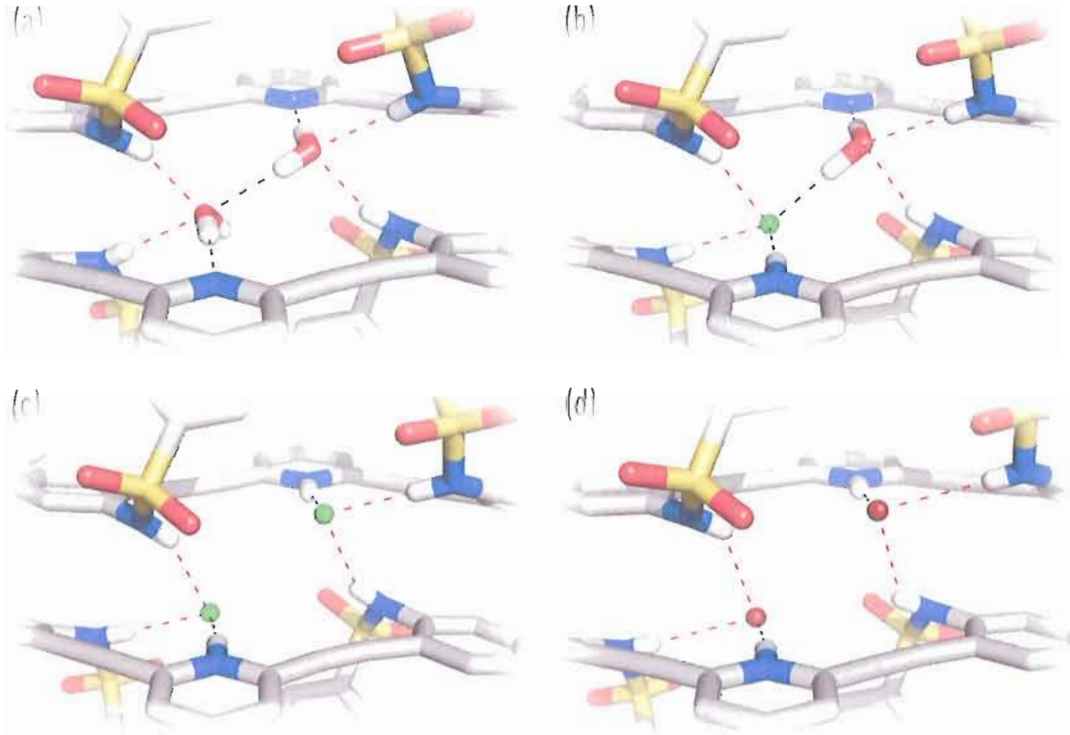

Figure 6.3 Wireframe representations of the crystal structures of $(\mathbf{1}\bullet H_2O)_2$ (a), $(\mathbf{H1}^+\bullet Cl^-)\bullet(\mathbf{1}\bullet H_2O)$ (b), $(\mathbf{H2}^+\bullet Cl^-)_2$ (c), and $(\mathbf{H1}^+\bullet Br^-)_2$ (d) highlighting the interchangeable role that halides and water play in the dimerization of 2,6-bis(2-anilinoethynyl)pyridine sulfonamide receptors. Hydrogen bonds are illustrated as dashes—sulfonamide in red and all others in black. (Hydrogen atoms not involved in H-bonds are omitted for clarity).

In conclusion, we have investigated the host/guest chemistry of a new class of hydrogen bonding receptors. Sulfonamide substituted 2,6-bis(2-anilinoethynyl)pyridines exhibit guest-assisted dimerization with H_2O and/or hydrogen halides, where water and halide anions surprisingly share the same structural role depending on the protonation state of the receptor. In fact, water and hydrogen chloride appear to be completely interchangeable structural partners in facilitating the

dimerization based on the discovery of the heterodimer, (**H1**$^+$•Cl^-)•(**1**•H_2O) (Figure 6.3). The persistence of guest-assisted dimerization has also been observed in solution. In particular, ^{1}H NMR dilution experiments have been used to observe the dimerization behavior of the neutral sulfonamide with water and the protonated sulfonamide with chloride. Both UV-Vis and ^{1}H NMR spectroscopy have been used to assess the association of **H1**$^+$ with anions in solution (Cl^-, Br^- and I^-) and further investigations are underway to quantify the strength of the interactions in solution. We are interested in using our modular approach to synthesize 2,6-bis(2-anilinoethynyl)pyridines designed to target different guest molecules depending on the binding substituent attached to the receptor. The extended conjugation inherent in 2,6-bis(2-anilinoethynyl)pyridines derivatives produces distinct emission properties that will be used to monitor interactions with guest molecules. This observation bodes well for the use of 2,6-bis(2-anilinoethynyl)pyridines derivatives as sensors for the selective recognition of guest molecules.

We recently reported two 2,6-bis(2-anilinoethynyl)pyridine sulfonamides which form hydrogen bonded dimers with water and/or hydrogen halides. Isostructural 2 + 2 dimers were shown to form in solution and in the solid state with two water molecules two halides or one water and one halide. For the remainder of the chapter, we report the synthesis, crystal structures, electronic properties and binding studies for an expanded series of 2,6-bis(2-anilinoethynyl)pyridine Sulfonamides. In addition, we communicate the versatility of this modular ligand class with alternative hydrogen

bonding donors such as a 2,6-bis(2-anilinoethynyl)pyridine amide and expanded core structures 6,6'-bis(2-anilinoethynyl)bipyridine sulfonamide and 6,6'-bis(2-anilinoethynyl)thiophene sulfonamide.

RESULTS AND DISCUSSION

LIGAND DESIGN. Our recent investigation of the structural and electronic properties of pyridine-based cyclynes and metallacycles[8] (Figure 6.4) has prompted further consideration for their use in coordination chemistry applications. We hypothesized that a highly conjugated, structurally rigid phenylacetylene scaffold incorporating the lone pair coordination potential of pyridine moieties should afford a pre-organized ligand capable of an electronic response (e.g., change in absorption) upon guest complexation. Described herein is design and production of a new class of highly conjugated heterophenyl-acetylene ligands designed for host-guest complexation of ions utilizing a multi-coordinate hydrogen bonding motif. Crystallographic and binding studies indicate promise for selective ion coordination.

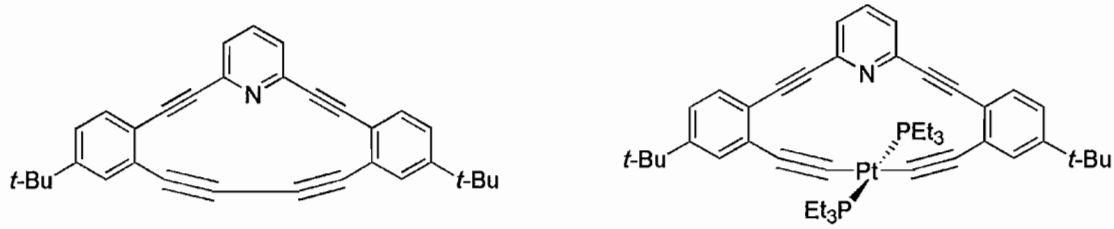

Figure 6.4 Macrocycles **4** and **4a**.

A key aspect for design of our new phenylacetylene-based ligand arises from examination of the structural features of macrocycles **4** and **4a** from a coordination chemistry standpoint. Specifically, the internal cavity of both cycles, which are incapable of housing even small guest ions due to lack of space, and the positioning of the Pt complex in cycle **4a**, which is oriented outside bonding range with the pyridine-N due to the geometry of the phenylacetylene scaffold, led us to consider a more universal acyclic design capable of adapting to a range of guest sizes via a three-coordinate binding motif (Figure 6.5). Computer modeling (CAChe MM3) to determine suitable functional groups (X) capable of non-covalent coordination to guest molecules indicated that amide groups as well as sulfonamide and urea functionalities provided suitable geometric and electronic properties to bind both ions and small organic molecules.

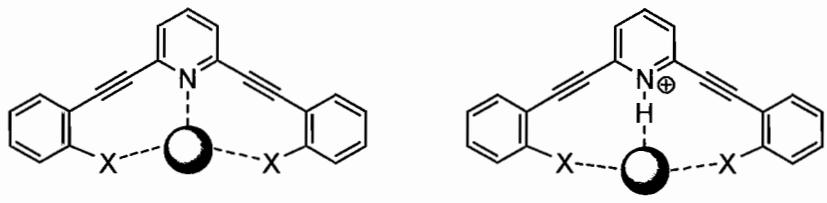

Figure 6.5 Three-coordinate ligand design.

Retrosynthetic analysis of the target ligands indicated that a key dianiline intermediate (**5**) would provide access to all three functionalized ligand analogs via reaction with the appropriate acyl chloride, sulfonyl chloride, or isocyanate (Scheme 6.2). Dianiline **5**, first reported by us (see above), should likewise be available from ethynylaniline **6** and 2,6-dibromopyridine. *Tert*-butyl groups were incorporated into the receptor design to enhance solubility, facilitate the *ortho*-halogenation required to produce **6**, and provide a readily discernable spectroscopic handle. Our proposed synthetic route for the target ligand will additionally allow substitution of different core arenes (e.g., bipyridine) via cross-coupling of the respective dihaloheterocycle to desilylated **6**, a facile method to tailor the ligand cavity to a range of guest sizes.

Scheme 6.2 Retrosynthetic breakdown of receptor scaffold.

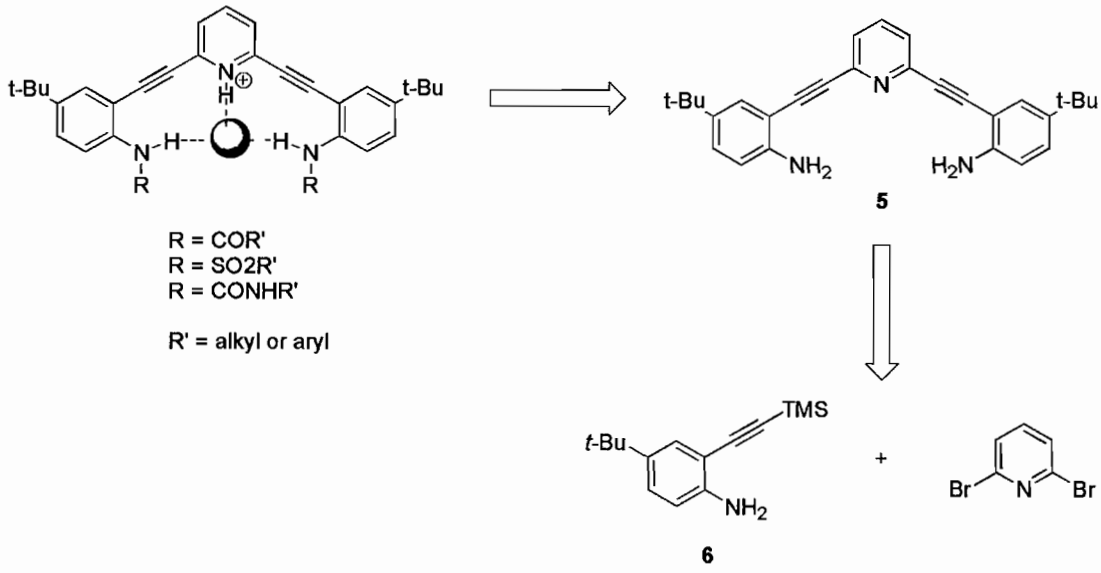

EXPANDED SERIES OF SULFONAMIDE RECEPTORS. Our initial publication of the hydrogen bonding capability of two sulfonamide receptors built from bis(ethynyl)pyridine cores reported the synthesis, solution behavior and solid state characteristics exhibited by these receptors. In the following section we expand this series of receptors with the synthesis of three more sulfonamide receptors. By simply changing the functional groups appended to the sulfonamide we observe drastic changes in the electronic absorption spectra. We also report, through a crystallographic study, the solid state behavior for the whole series of sulfonamides.

Synthesis of 2,6-bis(2-anilinoethynyl)pyridine sulfonamides. Synthesis began with previously reported 2-iodo-4-*t*-butylaniline,[9] available in 73% yield via

iodination of 4-*t*-butylaniline (Scheme 6.3). Pd-catalyzed cross-coupling[10] of 2-iodo-4-*t*-butylaniline with trimethylsilylacetylene (TMSA) afforded ethynylarene **6** in 86% yield. Dianiline **5** was obtained in 79% yield by desilylation of **6** with weak base[11] followed by two-fold cross-coupling to 2,6-dibromopyridine. Sulfonamide receptor analogs **1, 2, 7a** and **7b** were obtained in good yield (89-95%, Scheme 6.3) by treatment of dianiline **5** with an excess of the respective phenylsulfonyl chloride in pyridine.[14] Incorporation of substituents ranging from electron donating (OMe) to electron withdrawing (NO_2) into the 4-position of the sulfonamide phenyl rings was proposed to investigate electronic properties of the ligands as well as effects on guest binding.

Sulfonamide **7c** was additionally considered to examine solid-state and solution effects of a different substitution pattern and increased electron deficiency of the peripheral phenyl rings. The initial attempt to produce a 3,5-bis(trifluoromethyl)-sulfonamide receptor (**7c**) resulted only in isolation of tetra- (**7d,** Figure 6.8) and trisubstituted (**7e**) compounds, the result of enhanced reactivity of the electron deficient bis(trifluoromethyl)sulfonyl chloride. Subsequent efforts to control substitution via stoichiometric treatment with sulfonyl chloride afforded only a mixture of mono-, di-, and trisubstituted adducts, out of which the desired product (**7c**) was difficult to separate from monosubstituted byproduct. The fortuitous isolation of **7d**, which does not contain sulfonamide hydrogens, provides solution evidence for the importance of water in sulfonamide receptors **1, 2, 7a** and **7b**. The

lack of any effect on the water resonance in the ^{1}H NMR spectrum of **7d** is in stark contrast to the ^{1}H NMR spectra observed for receptors **1, 2, 7a** and **7b**, providing further evidence for a solution based hydrogen bonding phenomena.

Scheme 6.3 Synthesis of 2,6-bis(2-anilinoethynyl)pyridine sulfomaide receptors.

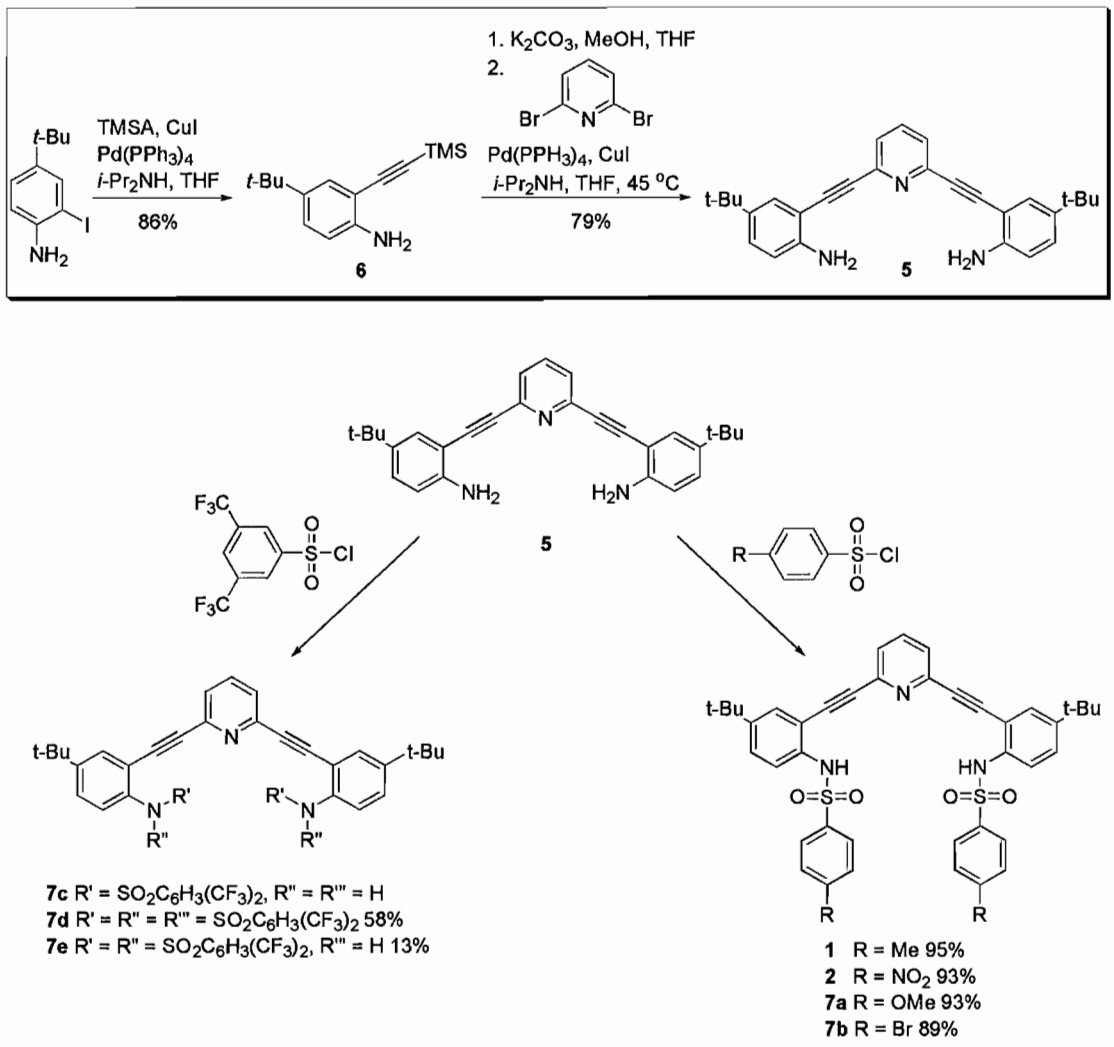

Solid state investigation of 2,6-bis(2-anilinoethynyl)pyridine sulfonamide receptors. Neutral receptors **1, 2, 7a** and **7b** all exhibit the same propensity to crystallize as hydrogen bonded 2+2 dimers with water in the solid state. The solid state structure is very similar throughout the series of receptors differing only in minor adjustments to the hydrogen bonding and π-stacking distances. Figure 6.6 illustrates the similarity between receptors **1, 2, 7a** and **7b** in the solid state with four different representations of the single crystal X-ray structures.

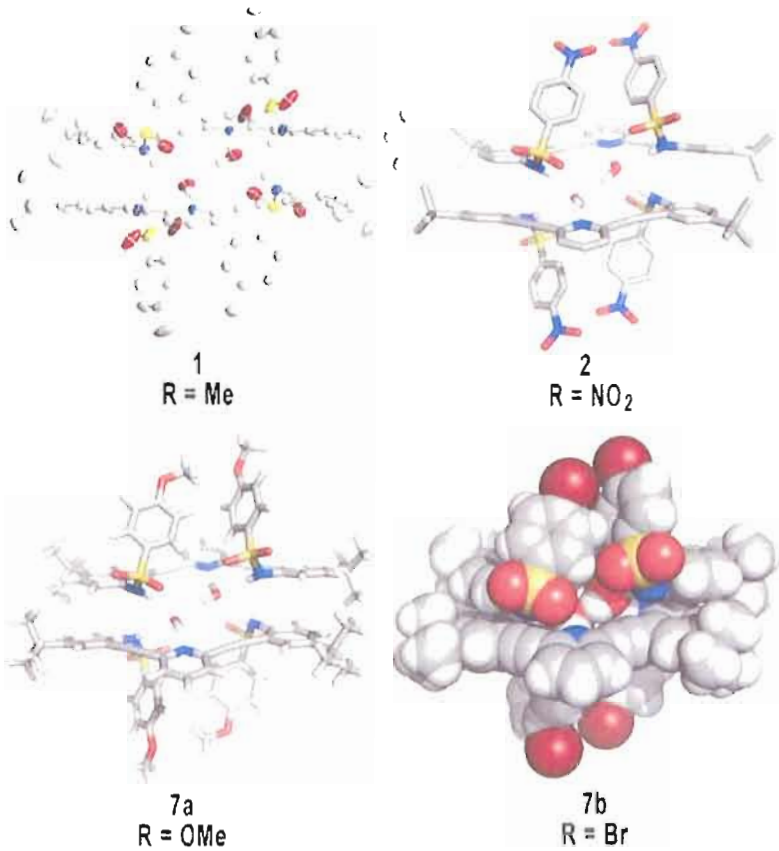

Figure 6.6 Four different representations of the 2+2 water dimer formed when **1, 2, 7a** and **7b** are crystallized in its neutral form.

In one isolated instance a polymorph of receptor **2** was isolated. Attempts were being made to isolate co-crystals of **2** and tetra-*n*-butylammonium iodide with $CHCl_3$/pentane diffusion conditions. The Receptors in this structure form a dimeric pair and with each receptor exhibiting the same helical arrangement. A single sulfonamide functionality from each receptor is interlocked with the neighboring molecule while the second sulfonamide functionality hydrogen bonds to a separate dimeric pair in the solid state. The key driving forces for the solid state structure are the hydrogen bonds between the pyridine-N and sulfonamide hydrogens from the adjacent receptor as well as intermolecular π-stacking (Figure 6.7). This structure remains the only example of dimer formation in these receptors without assisting water molecules. Unfortunately, the poor crystal quality resulted in data unsuitable for publication and only worthy of understanding connectivity and spacial arrangement.

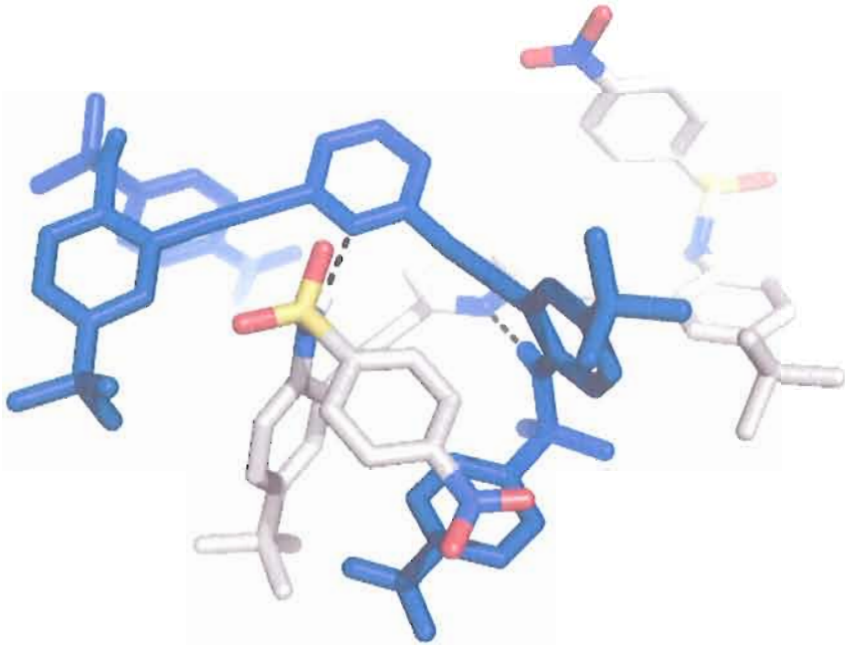

Figure 6.7 Polymorph of **2** dimer notably lacking assisting water molecules. Each molecule colored differently and non H-bonding hydrogens removed for clarity.

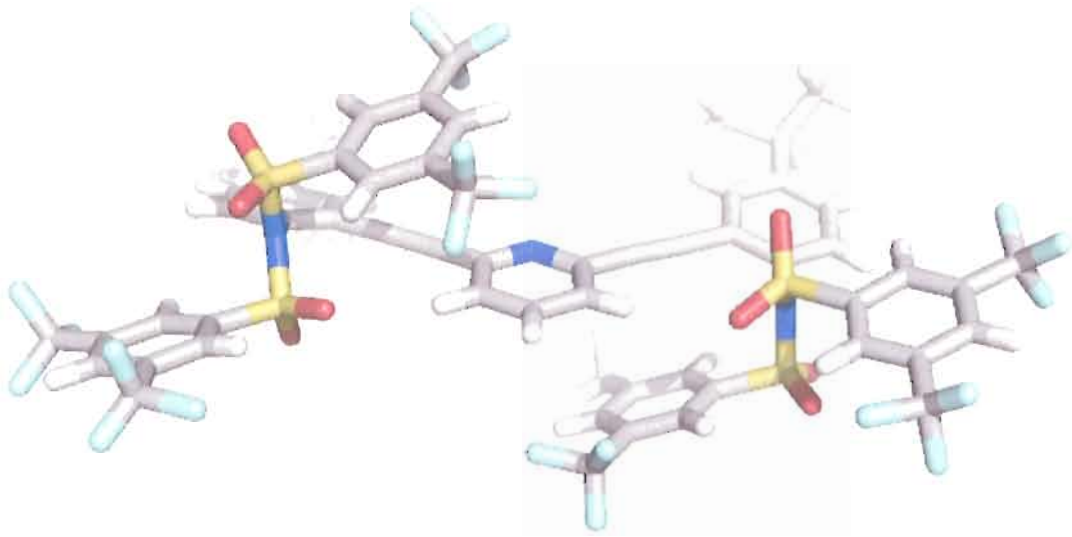

Figure 6.8 Tetra substituted receptor **7d** exhibits no interactions with water molecules in the solid state.

We reported previously that sulfonamide receptors **1** and **2** form 2+2 dimers in the solid state with water, halides or both water and halides. We have also found that larger guest molecules eliminate the 2+2 dimer formed in the solid state. Single crystals of $\mathbf{H1}^{+}\bullet BF_4^{-}$ are isolated by dissolving receptor **1** in ethyl acetate and adding aqueous HBF_4 while stirring vigorously. Crystallization is induced by layering with hexane. The larger size of the BF_4^{-} anion forces the receptor arms to the opposite side of the pyridine N in order to maintain a strong pyridinium hydrogen bond with the BF_4 anion. One receptor sulfonamide forms a head-to-tail intermolecular hydrogen bond with an adjacent receptor molecule while the other sulfonamide hydrogen bonds to the BF_4 anion of a second receptor. This sequence of hydrogen bonds forms a polymeric hydrogen bonding chain in the solid state (Figure 6.9).

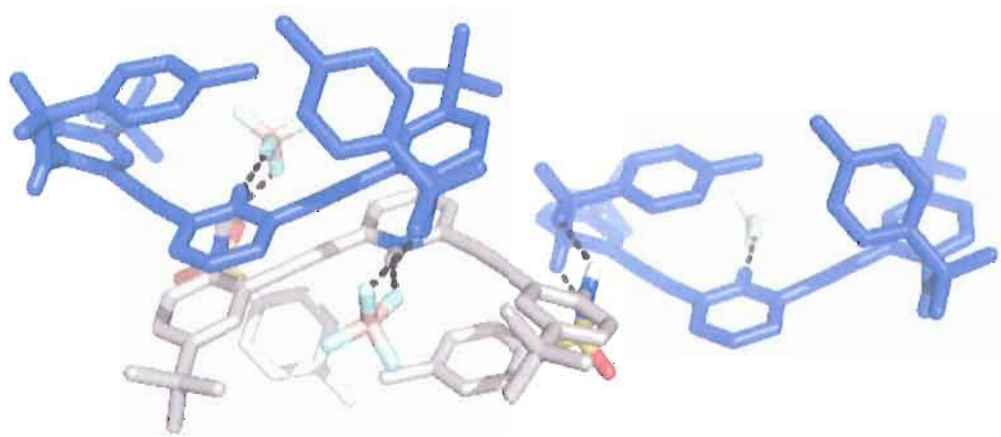

Figure 6.9 Stick representation of the polymeric hydrogen bonding chain present in the solid state structure of $\mathbf{H1}^{+}\bullet\mathbf{BF}_4^{-}$.

The solid state structure of $\mathbf{H1}^+ \bullet HSO_4^-$ also deviates from the 2+2 structure observed for smaller guests. Single crystals of $\mathbf{H1}^+ \bullet HSO_4^-$ were grown from THF solutions of receptor mixed with H_2SO_4. Crystallization is aided by diffusing pentane and the $\mathbf{H1}^+ \bullet HSO_4^-$ salt crystallizes in the *P*-1 space group with two receptor molecules and three THF solvent molecules per unit cell. Similar to the $\mathbf{H1}^+ \bullet BF_4^-$ structure the counter anion forms a strong hydrogen bond with the pyridinium nitrogen resulting in a conformation that puts the receptor arms on the opposite side of the molecule. However, the $\mathbf{H1}^+ \bullet HSO_4^-$ structure is complicated by additional solvents of crystallization. Each sulfonamide also hydrogen bonds to a different HSO_4 anion which in turn donates a hydrogen bond to a THF solvent molecule (Figure 6.10).

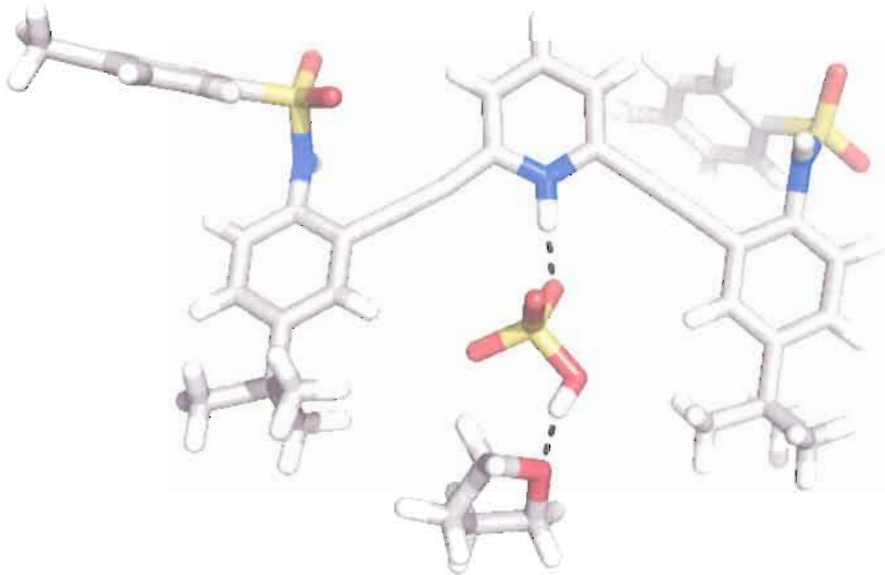

Figure 6.10 Stick representation of a portion of the $\mathbf{H1}^+ \bullet HSO_4^-$ crystal structure highlighting some of the hydrogen bonds present in the solid state.

Synthesis of core analogs. As mentioned above, the synthetic route for key intermediate **5** allows facile modification to investigate other core arenes in place of pyridine. Examination of both bipyridine and pyrrole cores indicated the potential to target larger guest molecules, a direct result of the change in bonding angle of the functionalized phenylacetylene arms. Dihalo-analogs of both heterocycles are known;[16] however, 2,5-dibromopyrrole has been reported to decompose rapidly upon concentration.[16b] Due to the well established chemistry of 2,5-functionalized thiophenes,[17] a thiophene core was proposed as a simple substitute to model the pyrrole core and determine if further examination of pyrrole analogs was warranted, specifically via examination of the solid-state structure.

Synthesis of both core analogs began with desilylation of **6** followed by two-fold Pd-catalyzed cross-coupling with commercially available 6,6'-dibromo-2,2'-bipyridyl or 2,5-dibromothiophene, which afforded compounds **8** and **9**, respectively (Scheme 6.4). While compound **9** was readily purified and characterized, intermediate **8** proved problematic due to extremely poor solubility in common organic solvents (< 0.1 mM) and was isolated only as a 5:1 mixture with mono-coupled byproduct. Independent treatment of dianilines **8** and **9** with *p*-toluenesulfonyl chloride in pyridine provided sulfonamide receptors **10** and **11** in moderate to good yield.

Scheme 6.4 Synthesis of core analogs.

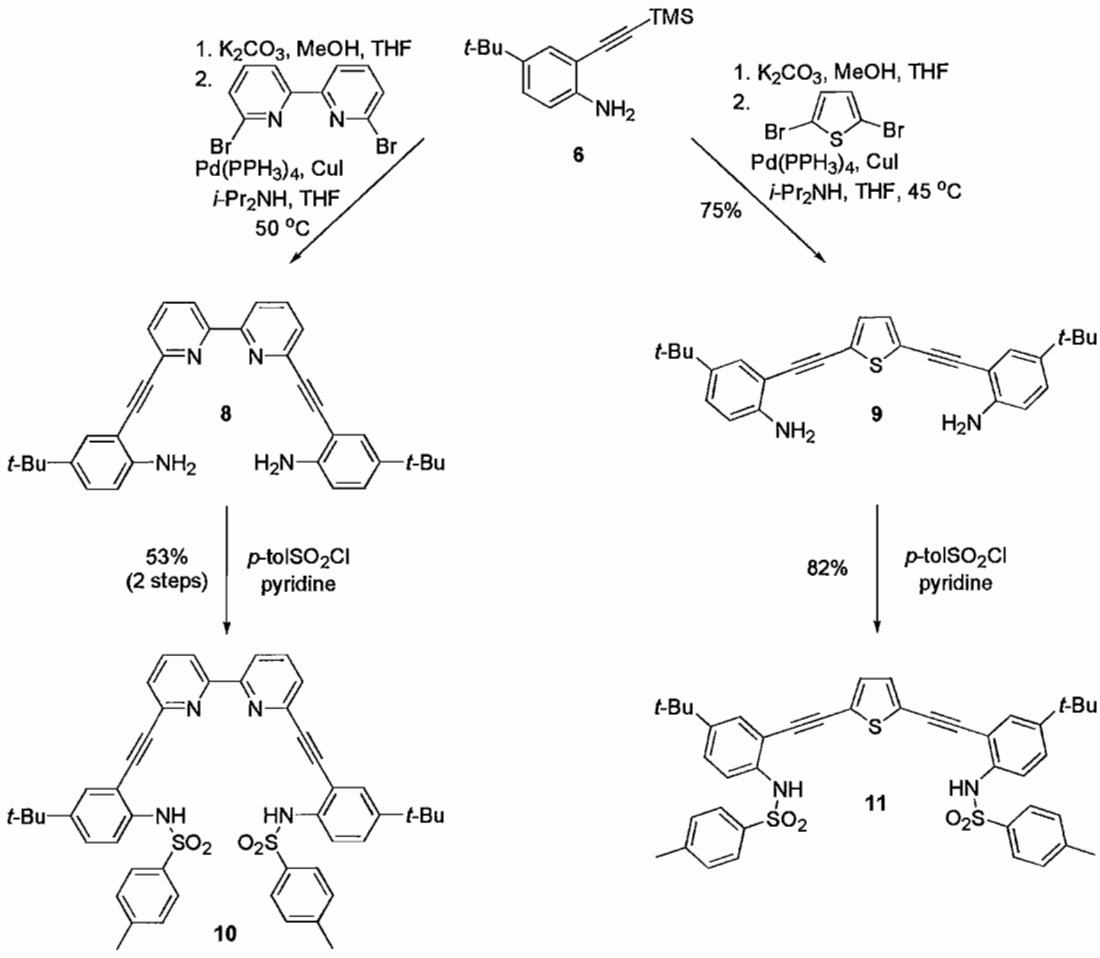

Solid state investigations of core analog sulfonamide receptors. X-ray diffraction structures of core analogs **10** and **11** are shown in Figures 6.11 and 6.12, respectively. Substitution of bipyridine and thiophene into the ligand backbone clearly increases the binding cavity size and will allow exploration of binding larger polyatomic ions and small molecules compared to pyridine-based system. Single crystals of receptor **10** are grown from slowly diffusing hexane into ethyl acetate solutions of receptor resulting in

crystals of the *P*-1 space group with 1 molecule contained in the unit cell. In the solid-state, the bipyridine core of sulfonamide **10** is highly planar with *anti* N-atoms, a factor which results in rotation of a single sulfonamide arm away from the proposed binding cavity. Intermolecular π-stacking interactions are observed between receptors and each sulfonamide functionality hydrogen bonds in a head-to-tail fashion with different adjacent molecules forming an infinite hydrogen bonding chain in the solid state.

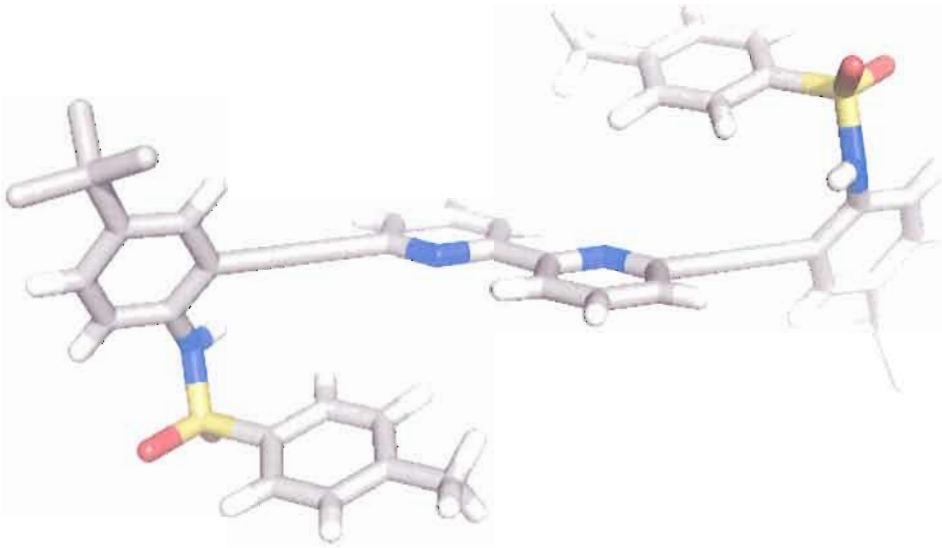

Figure 6.11 Stick representation of the single crystal X-ray structure of sulfonamide **10** with expanded bipyridine core.

Single crystals of receptor **11** are also isolated from diffusing hexane/ethyl acetate mixtures. Receptor **11** crystallizes with 2 molecules per unit cell in the *P*-1 space group Conversely, sulfonamide **11** exhibits a solid-state conformation with both receptor

arms rotated away from the binding cavity due to its participation in multiple intermolecular hydrogen bonds with adjacent receptors.

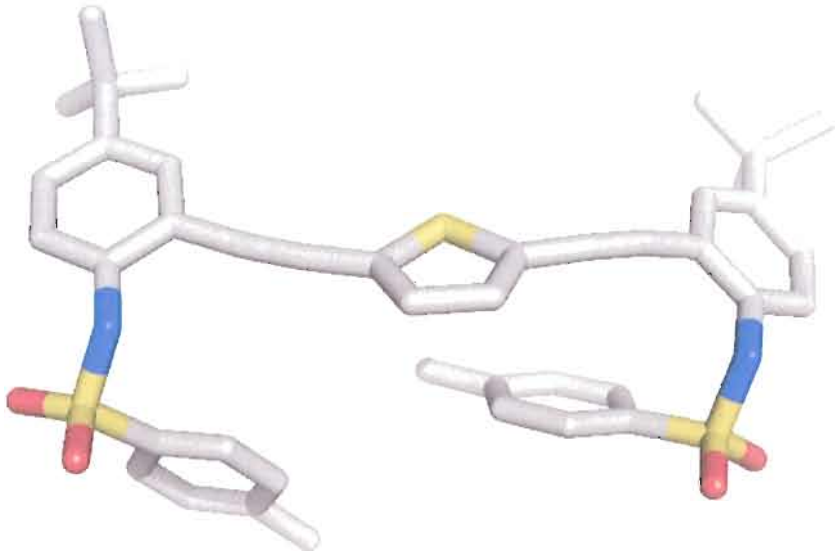

Figure 6.12 Stick representation of the single crystal X-ray structure of sulfonamide **11** with expanded thiophene core. Only one molecule is shown and hydrogen atoms are removed for clarity.

AMIDE FUNCTIONALIZED RECEPTORS. The modular design of this receptor class facilitates the production of a number of receptor types. We have shown above that sulfonamide receptors based off of 2,6-bis(2-anilinoethynyl)pyridine cores express a diverse array of host/guest interactions both in the solid state and in solution. We have also illustrated that the size of the receptor binding pocket can be adjusted by substituting the pyridine core with alternative heterocycles. This next section highlights another key aspect to our modular design. In addition to adjusting the

receptor cavity we can also dictate the terminal substituents attached to the receptor core and subsequently control the properties of the host and its potential guest interactions.

Synthesis of 2,6-bis(2-anilinoethynyl)pyridine amide receptors. Treatment of dianiline **5** with chloroacetyl chloride and Et_3N in CH_2Cl_2[12] afforded diamide **12** in very good yield. Reaction of arene **12** with potassium thioacetate in DMF[12] resulted in acetyl-protected receptor **13**. Treatment of **13** with K_2CO_3 in MeOH and THF under both air-free and ambient conditions afforded the intramolecular disulfide analog **14** in 77% yield instead of desired dithiol **15** (Scheme 6.5).

Scheme 6.5 Synthesis of amide receptors.

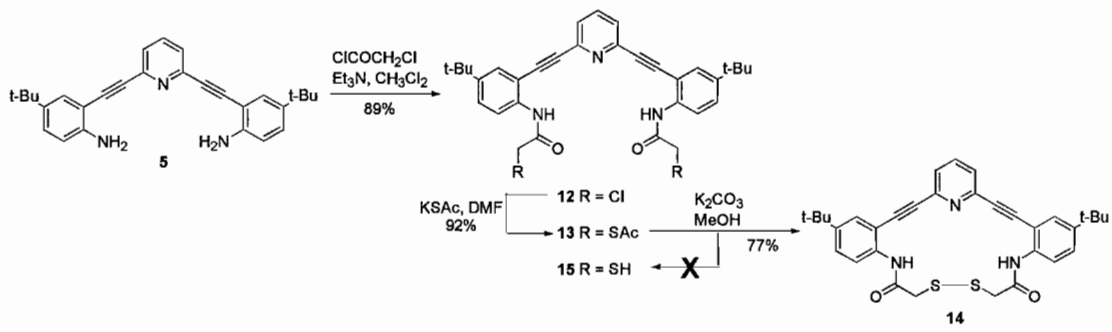

In an initiative to investigate possible anion/arene interactions in these systems amide receptor **16**, containing electron-deficient 3,5-dinitrobenzene substituents, was synthesized. The synthesis of **16** was achieved in fair yield (51%) utilizing biphasic

reaction conditions in one step from key intermediate **5** (Scheme 6.6). Unfortunately, amide **16** is rather insoluble common organic solvents. Several attempts to crystallize both the neutral and protonated forms of **16** met failure. Frequently receptor **16** was isolated as tiny hair-like needles unsuitable for X-ray diffraction studies.

Scheme 6.6 Synthesis of electron-deficient arene containing amide **16**.

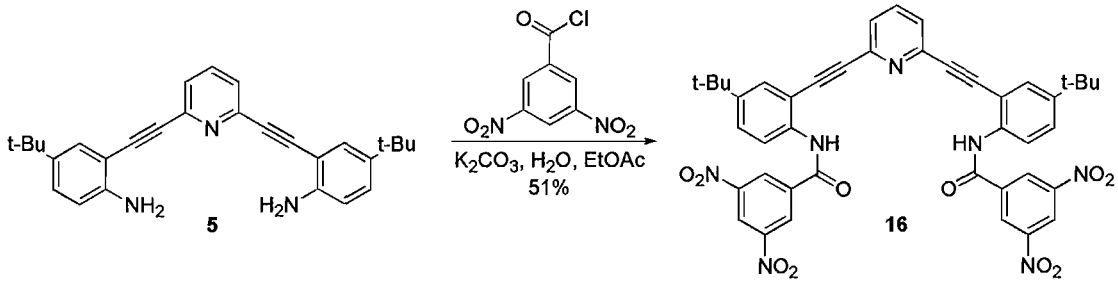

Solid state investigations of 2,6-bis(2-anilinoethynyl)pyridine amide receptors. Crystals of arene **13** suitable for single crystal X-ray diffraction were obtained from slow diffusion of hexanes into a concentrated solution of **13** in EtOAc. Arene **13** crystallizes in the *Pc* space group and displays dimeric association with intermolecular hydrogen bonding between amide hydrogen and carbonyl oxygen ranging from 2.85–3.01 Å (Figure 6.13). The dimeric pair consists of two molecules in an *anti*-relationship with amide arms rotated away from the desired binding cavity. Also noted in the crystal structure is a long C-H•••N hydrogen bond between a solvent dichloromethane molecule and a pyridine nitrogen on the receptor (3.29 Å).

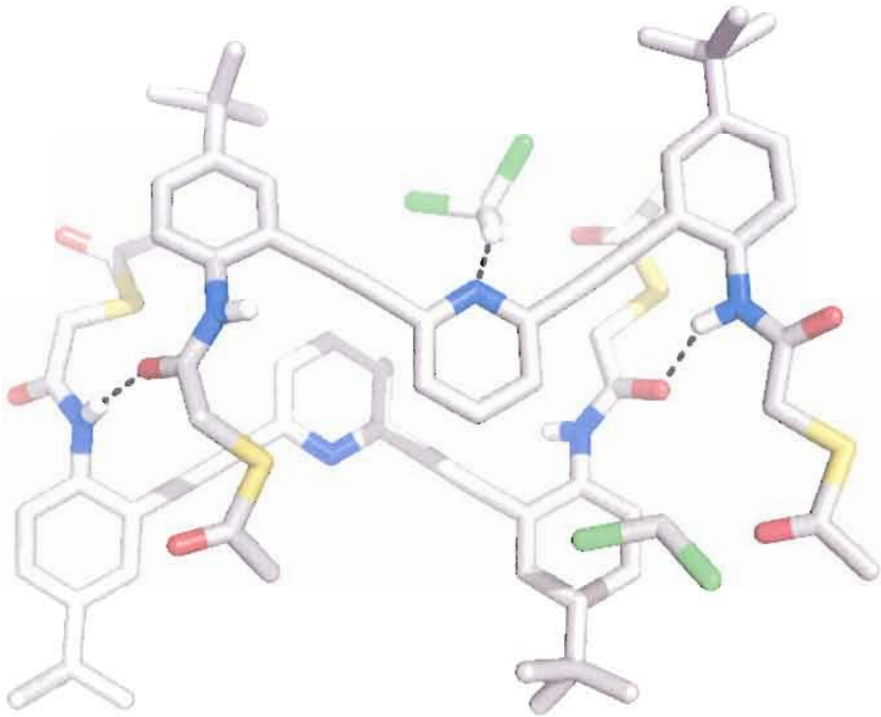

Figure 6.13 Stick representation of the single crystal X-ray structure of arene **13**. Non H-bonding hydrogens have been removed for clarity.

We report that we can influence the receptor conformation in the solid state by protonating the pyridine nitrogen and using an appropriately sized counter anion. In an unrelated experiment attempting to target metal ions with Arene **13**, yellow single crystals were isolated from pentane diffused into THF solutions of the reaction mixture. Close inspection of the single crystal data revealed that the compound isolated was $\mathbf{H13}^{+}\bullet Cl^{-}$ (Figure 6.14). $\mathbf{H13}^{+}\bullet Cl^{-}$ crystallizes in the *P*-1 space group with 2 receptor molecules and 4 THF molecules per unit cell. Remarkably, $\mathbf{H13}^{+}\bullet Cl^{-}$ forms a helical twist conformation around the Cl^{-} anion. Numerous hydrogen bonds serve to

stabilize the Cl^- in the solid state. One strong pyridinium N•••Cl^- hydrogen bond (3.00 Å) and two amide N•••Cl^- hydrogen bonds (3.25 Å and 3.27 Å) are observed in the solid state. This solid state example nicely illustrates how drastic conformational control can be achieved by simple changes in the protonation state of the receptor.

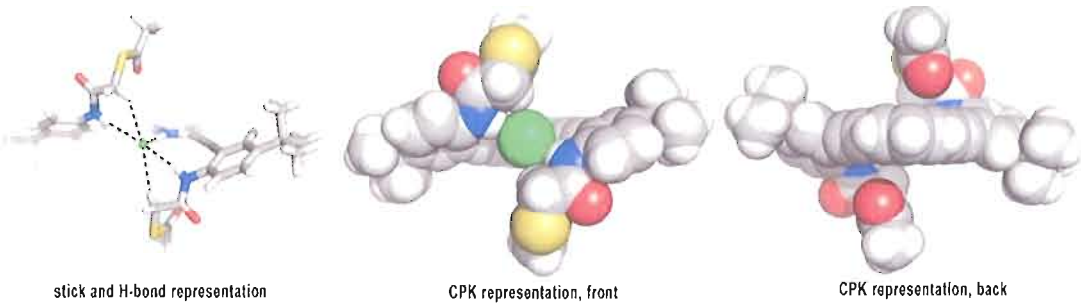

Figure 6.14 Stick (left) and CPK (middle and right) representations of the **H13**$^+$•Cl^- crystal structure highlighting the hydrogen bonding interactions observed in the solid state and the helical conformation formed around the Cl^- anion.

Again we illustrate that we can affect the conformation of the molecule. X-ray diffraction quality single crystals of **14** were grown from evaporating EtOAc/Hexane solutions. Arene **14** crystallizes in the *P*-1 space group with two molecules per unit cell. Unlike arene **13**, inspection of the X-ray data of neutral arene **14** revealed that the disulfide bond enforces a pre-organization of the amide hydrogen, disulfide linkage, and pyridine-N into the desired conformation, although space-filling models indicate that location of the disulfide bond prevents sufficient space for guests (Figure 6.15).

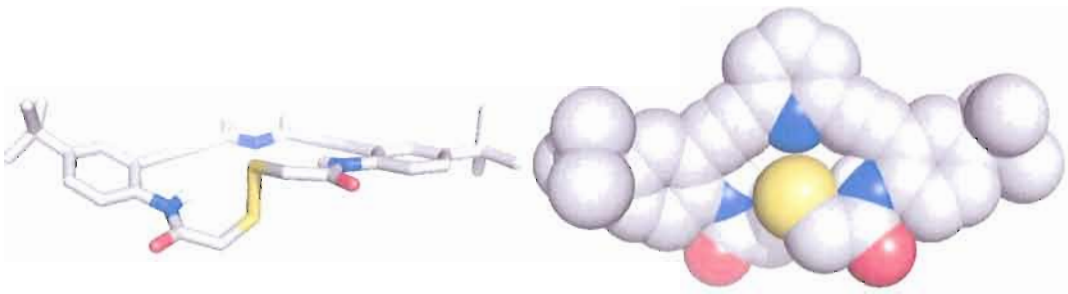

Figure 6.15 Stick (left) and space filling (right) representations of the crystal structure of disulfide **14**. Note that the disulfide linkage inhibits the formation of intermolecular hydrogen bonds between amide substituents.

RECEPTOR ELECTRONIC PROPERTIES. Key elements of the electronic absorption spectra of the new sulfonamide and amide receptors are presented in Table 6.1. In general, the spectra of the pyridine-core receptors all contain a characteristic pattern of three peaks with minimal change upon substitution beyond dianiline **5**, a factor which suggests that electron density is localized in the pyridylacetylene scaffold. The differential substitution of the terminal arene rings of sulfonamides **1, 2, 7a** and **7b** is as expected: the strongest electron donating substituent (OMe, **7a**) exhibited the lowest energy λ_{max} while the most hypsochromically shifted sulfonamide is NO_2-substituted **2**. The small change in λ_{max} (24 nm) between strong donor and acceptor further supports the notion of limited intramolecular charge transfer, likely the result of non-planarity, length of conjugation pathway, and localization of electron density in the π-rich scaffolding. Of note, protonation of the pyridine core by addition of a slight

excess of TFA to receptor solutions in CH_2Cl_2 resulted in a synonymous absorption redshift for all receptors, with disulfide **14** exhibiting the greatest change. Additionally, the solution color changed from colorless to bright yellow. Initial modeling studies suggest an enhanced intramolecular charge transfer model due to a significant increase in electron deficiency of the pyridinium core as the rationale for this occurrence.

Table 6.1 Electronic absorption data for compounds **1**, **2**, **5**, **7a-b**, **9-14** in CH_2Cl_2 at 25 °C

Compound	$\lambda_{max}{}^{a}$ $(\varepsilon)^{b}$	$\lambda_{cutoff}{}^{a}$	$\lambda_{cutoff}{}^{a}$ (+TFA)
1	330 (27,600)	432	480
2	319 (23,000)	425	453
5	359 (22,500)	401	---
7a	343 (23,000)	385	478
7b	342 (19,900)	374	465
9	378 (37,000)	432	---
10	315 (46,100)	363	457
11	357 (37,200)	442	---
12	335 (27,600)	445	---
13	330 (21,600)	362	---
14	337 (17,500)	362	499

[a] Units: nm. [b] Units: M^{-1} cm^{-1}.

The sulfonamide receptors all exhibited weak fluorescent emission ($\Phi_F < 0.05$) with little to no discernable visual fluorescence, a factor attributed to replacement of the

electron donating amino substituents of precursors **5**, **8**, and **9** with electron deficient carbonyl and sulfonyl functionalities. In contrast to electronic absorption, a clear delineation was noted between emission behavior for terminal phenyl substitution for **1, 2** and **7a-b** (Figure 6.16). An inverse relationship was noted between donors (**1** and **7a**), which exhibited a bathochromic shift and quenching upon protonation, and acceptors (**2** and **7b**), which exhibited an increase in intensity and bathochromic shift upon protonation. The assertion of substituent effect is confirmed by considering bromophenyl **7b**. The terminal halo group, which can inductively withdraw electron density but donate via resonance, caused the overall emission behavior to match that of **2** but with a blue-shifted λ_{em} in the absence of acid, one that is in fact equivalent to donors **1** and **7b**. Further investigation via modeling will be required to confirm this assertion.

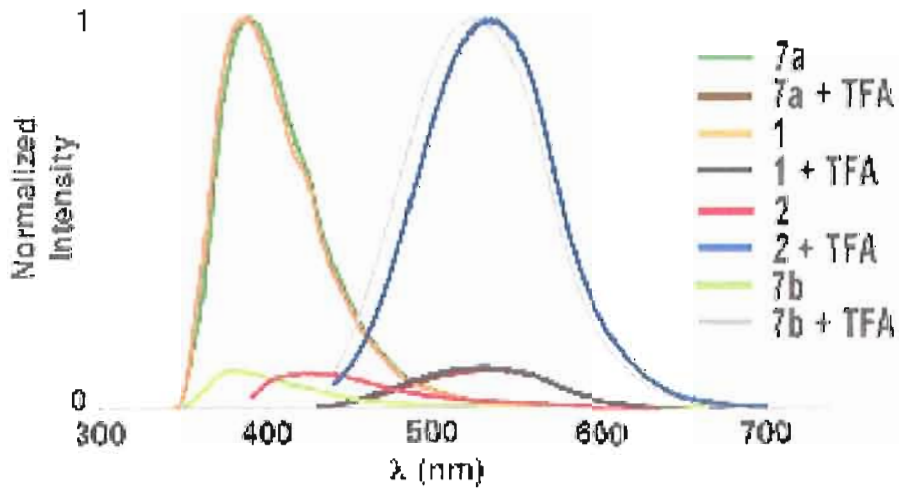

Figure 6.16 Emission spectra of receptors **1, 2** and **7a-b** in $CHCl_3$ at 25 °C.

CONCLUSION

In summary, we have presented a new series of heterophenylacetylene ligands designed for small molecule and ion recognition. The receptors are designed in a modular fashion capable of simple exchange of binding substituents and core motifs. The facile synthesis has produced a series of sulfonamide and amide bearing receptors that show a predilection for interacting with small molecules (H_2O, THF, EtOAc and CH_2Cl_2) or anions (Cl^-, Br^-, BF_4^- and HSO_4^-) in solution and the solid state. The receptors presented adopt conformationally different binding motifs depending on the guest present as well as the heterocyclic core. Solid state conformations are largely dominated by hydrogen bonding interactions and π-stacking. 2,6-bis(2-anilinoethynyl)pyridine sulfonamides form 2+2 dimers in solution and the solid state with H_2O, halides or both H_2O and halides. Sulfonamide receptors based on larger heterocyclic core molecules exhibit larger cavity sizes in the solid state and show no propensity to form 2+2 dimers. The solid state structures of three different amide bearing receptors based off of the 2,6-bis(2-anilinoethynyl)pyridine scaffold illustrate the conformational control possible by altering the guest molecule or the binding substituents. The shapes adopted by the amide receptors in the solid state range from macrocycles, to U-shaped molecules, to a helix formed around Cl^-. The efficiency of our new system, directly attributed to a straightforward synthesis and facile derivatization, bodes well for future receptor development to target remediation and sensing applications for environmental contaminants.

EXPERIMENTAL SECTION

GENERAL. Full experimental details, including sa general X-ray diffraction experimental (including discussion of disorder modelling), syntheses of all receptors from key intermediate **5**, NOE spectrum of $(\mathbf{1}\bullet H_2O)_2$, details of crystallization and dimerization experiments and any associated references are available in Appendix E. CCDC #s 657490-657494 also contain part of the supplementary crystallographic data for this paper. These data can be obtained free of charge via www.ccdc.cam.ac.uk/conts/retrieving.html.

^1H and ^{13}C NMR spectra were recorded using a Varian Inova 300 (^1H 299.95 MHz, ^{13}C 75.43 MHz) or Inova 500 (^1H 500.10 MHz, ^{13}C 125.75 MHz) spectrometer. Chemical shifts (δ) are expressed in ppm downfield from tetramethylsilane using the residual non-deuterated solvent as internal standard ($CDCl_3$: ^1H 7.26 ppm, ^{13}C 77.0 ppm; THF-d_8: ^1H 3.58 ppm, ^{13}C 67.57 ppm). UV-Vis spectra were recorded using a Hewlett-Packard 8453 spectrophotometer and extinction coefficients are expressed in $M^{-1}cm^{-1}$. Mass spectra were recorded using an Agilent 1100 Series LC/MSD. Emission spectra were recorded on a Hitachi F-4500 fluorescence spectrophotometer. Melting points were determined with a Meltemp II apparatus or a TA Instruments DSC 2920 Modulated DSC. THF, Et_3N, and CH_2Cl_2 were distilled from either potassium or CaH_2 prior to use. All chemicals were of reagent grade and used as obtained from manufacturers. Column chromatography was performed on Whatman reagent grade

silica gel (230-400 mesh). Rotary chromatography was performed on a Harrison Research Chromatotron model 7924T with EM-Science $60PF_{254}$ silica gel. Precoated silica gel plates (Sorbent Technology, UV_{254}, 200 μm, 5 × 20 cm) were used for analytical thin-layer chromatography.

GENERAL PREPARATION OF SULFONAMIDES. A solution of arene **5** (1 equiv) and sulfonyl chloride (5 equiv) in pyridine (8-15 mM) was stirred for 3 h under an N_2 environment. Following concentration in vacuo, the crude oil was filtered through a 2.5 cm silica plug and then chromatographed on silica gel.

Sulfonamide 1. Arene **5** (150 mg, 0.36 mmol) was reacted with *p*-toluenesulfonyl chloride according to General Preparation for Sulfonamides. Purification by chromatography (1:1 hexanes:EtOAc) afforded **1** (249 mg, 95%) as a pale yellow solid. Recrystallization by diffusion (hexanes:EtOAc) afforded colorless crystals. Mp: 133-135 °C. ^{1}H NMR (300 MHz, $CDCl_3$): δ 7.85-7.71 (m, 5H), 7.52-7.43 (m, 6H), 7.35 (dd, J = 8.5, 2.3 Hz, 2H), 7.15 (d, J = 8.5 Hz, 4H), 2.34 (s, 6H), 1.26 (s, 18H). ^{13}C NMR (75 MHz, $CDCl_3$): δ 147.53, 143.73, 142.85, 136.93, 136.49, 135.84, 129.54 (2C), 127.89, 127.25, 126.29, 120.52, 112.89, 93.20, 85.56, 34.29, 31.03, 21.45. UV-Vis (CH_2Cl_2): λ_{max} (ε) 234 (58,000), 287 (31,000), 330 (27,600) nm. Fluorescent emission ([**1**] ≤ 0.057 mM in $CHCl_3$; 354 nm excitation): λ_{max} 388 nm. IR (neat): ν 3266, 2961, 2899, 2877, 2213, 1555, 1156 cm^{-1}. MS (CI pos) *m/z* (%): 732 (M^++2, 21), 731 (MH^+, 56), 730 (M^+, 100); $C_{43}H_{43}N_3O_4S_2$ (729.95).

Sulfonamide 2. Arene **5** (150 mg, 0.36 mmol) was reacted with *p*-nitrobenzenesulfonyl chloride according to General Preparation for Sulfonamides. Purification by chromatography (20:1 CH_2Cl_2:EtOAc) afforded **2** (285 mg, 93%) as a pale yellow solid. Recrystallization by diffusion (pentane:$CHCl_3$ or hexanes:EtOAc) afforded pale yellow crystals. Mp: 136-139 °C. ^{1}H NMR (300 MHz, $CDCl_3$): δ 8.15 (d, J = 8.7 Hz, 4H), 8.03 (d, J = 8.7 Hz, 4H), 7.74 (t, J = 7.8 Hz, 1H), 7.55 (d, J = 8.7 Hz, 2H), 7.48-7.37 (m, 6H), 1.29 (s, 18H). ^{13}C NMR (75 MHz, $CDCl_3$): δ 150.10, 149.33, 145.32, 142.68, 137.20, 134.63, 129.82, 128.68, 128.28, 126.31, 124.12, 123.31, 114.59, 92.68, 85.71, 34.51, 31.05. UV-Vis (CH_2Cl_2): λ_{max} (ε) 242 (56,200), 285 (35,500), 319 (23,000) nm. Fluorescent emission ([**2**] ≤ 0.057 mM in $CHCl_3$; 364 nm excitation): λ_{max} 428 nm. IR (neat): ν 3271, 2964, 2869, 2213, 1348, 1171 cm^{-1}. MS (CI pos) *m/z* (%): 794 (M^++2, 24), 793 (MH^+, 53), 792 (M^+, 100), 608 (17), 607 (44); $C_{41}H_{37}N_5O_8S_2$ (791.89).

Arene 5. A suspension of ethynylarene **6** (206 mg, 0.84 mmol) and K_2CO_3 (5 equiv) in MeOH (20 mL) and Et_2O (10 mL) was stirred at rt and monitored by TLC until reaction completion (15-30 min). The solution was diluted with Et_2O and washed with water and brine. The organic layer was dried over $MgSO_4$ and concentrated in vacuo. Without further purification, the residue was dissolved in THF (10 mL) and added dropwise over a period of 12 h to a stirred, deoxygenated suspension of 2,6-dibromopyridine (50 mg, 0.21 mmol), $Pd(PPh_3)_4$ (25 mg, 0.02 mmol), and CuI (8 mg, 0.04 mmol) in THF (50 mL) and *i*-Pr_2NH (50 mL) at 45 °C. After an additional 3 h of

stirring, the suspension was filtered and the insoluble salts washed twice with Et_2O. The filtrate was combined with the Et_2O washes, concentrated, and purified by Chromatotron (3:2 hexanes:EtOAc) to afford **5** (70 mg, 79%) as a pale yellow crystalline solid. Mp: 226 °C. ^{1}H NMR (300 MHz, $CDCl_3$): δ 7.64 (t, J = 8.1 Hz, 1H), 7.45-7.43 (m, 4H), 7.20 (dd, J = 8.7, 1.8 Hz, 2H), 6.67 (d, J = 8.7 Hz, 2H), 4.35 (br s, 4H), 1.27 (s, 18H). ^{13}C NMR (75 MHz, $CDCl_3$): δ 146.31, 143.84, 140.56, 136.36, 129.24, 128.04, 125.73, 114.34, 105.82, 93.11, 87.59, 33.85, 31.31. IR (neat) ν 3451, 3355, 2957, 2866, 2199, 1500 cm^{-1}. UV-Vis (CH_2Cl_2): λ_{max} (ε) 249 (44,200), 295 (24,300), 359 (22,500) nm. MS (CI pos) *m/z* (%): 423 (M^++2, 100), 422 (MH^+, 100); $C_{29}H_{31}N_3$ (421.58).

4-*tert*-butyl-2-(2-trimethylsilylethynyl)aniline (6). A suspension consisting of 2-iodo-4-*t*-butylaniline (800 mg, 2.9 mmol), $Pd(PPh_3)_4$ (168 mg, 0.15 mmol), and CuI (55 mg, 0.29 mmol) in *i*-Pr_2NH (50 mL) and THF (50 mL) was degassed by bubbling Ar. TMSA (1.3 mL, 9 mmol) was added and the suspension was stirred at rt for 12 h under N_2. The suspension was filtered and the insoluble salts washed twice with Et_2O. The filtrate was combined with the Et_2O washes, concentrated, and purified by Chromatotron (3:2 hexanes:CH_2Cl_2) to afford **6** (611 mg, 86%) as a light brown solid. Mp: 41-42 °C. ^{1}H NMR (300 MHz, $CDCl_3$): δ 7.32 (d, J = 2.1 Hz, 1H), 7.17 (dd, J = 8.4, 2.1 Hz, 1H), 6.65 (d, J = 8.4 Hz, 1H), 4.13 (br s, 2H), 1.27 (s, 9H), 0.29 (s, 9H). ^{13}C NMR (75 MHz, $CDCl_3$): δ 145.87, 140.55, 128.68, 127.21, 114.09, 107.25, 102.40, 98.99, 33.79, 31.33, 0.16. IR (neat) ν 3476, 3381, 2960, 2868, 2147, 1500 cm^{-}

[1]. MS (CI pos) *m/z* (%): 317 (M^++THF, 38), 279 (M^++Na^+, 35), 247 (M^++2, 23), 246 (MH^+, 100); $C_{15}H_{23}NSi$ (245.44).

Sulfonamide 7a. Arene **5** (110 mg, 0.26 mmol) was reacted with *p*-methoxybenzenesulfonyl chloride according to General Preparation for Sulfonamides. Purification by chromatography (20:1 CH_2Cl_2:EtOAc) afforded **7a** (185 mg, 93%) as a white crystalline solid. Recrystallization by diffusion (hexanes:CH_2Cl_2) afforded colorless crystals. Mp: 141-143 °C. ^{1}H NMR (300 MHz, $CDCl_3$): δ 7.77 (d, J = 9 Hz, 4H), 7.72 (t, J = 7.7 Hz, 1H), 7.54-7.44 (m, 8H), 7.33 (dd, J = 9.2, 2.4 Hz, 2H), 6.81 (d, J = 9 Hz, 4H), 3.72 (s, 6H), 1.24 (s, 18H). ^{13}C NMR (75 MHz, $CDCl_3$): δ 163.06, 147.62, 142.93, 136.75, 135.70, 130.85, 129.60, 129.43, 127.85, 126.44, 120.64, 114.09, 113.02, 93.28, 85.33, 55.45, 34.31, 31.03. UV-Vis (CH_2Cl_2): λ_{max} (ε) 239 (71,700), 292 (30,200), 343 (23,000) nm. Fluorescent emission ([**7a**] ≤ 0.05 mM in $CHCl_3$; 353 nm excitation): λ_{max} 389 nm. IR (neat): ν 3248, 2962, 2902, 2870, 2214, 1498, 1161 cm^{-1}. MS (CI pos) *m/z* (%): 764 (M^++2, 22), 763 (MH^+, 49), 762 (M^+, 100); $C_{43}H_{43}N_3O_6S_2$ (761.95).

Sulfonamide 7b. Arene **5** (100 mg, 0.24 mmol) was reacted with *p*-bromobenzenesulfonyl chloride according to General Preparation for Sulfonamides. Purification by chromatography (2.5:1 hexanes:EtOAc) followed by recrystallization by diffusion (hexanes:EtOAc) afforded **7b** (183 mg, 89%) as colorless crystals. Mp: 152-154 °C. ^{1}H NMR (300 MHz, $CDCl_3$): δ 8.00 (br s, 2H), 7.82-7.71 (m, 5H), 7.53-7.37 (m, 12H), 1.29 (s, 18H). ^{13}C NMR (75 MHz, $CDCl_3$): δ 148.25, 142.72, 138.65,

137.16, 135.52, 132.22, 129.59, 128.88, 128.18, 127.96, 126.19, 121.56, 113.46, 92.97, 85.89, 34.43, 31.08. UV-Vis (CH_2Cl_2): λ_{max} (ε) 243 (64,000), 291 (29,100), 342 (19,900) nm. Fluorescent emission ([**7b**] ≤ 0.05 mM in $CHCl_3$; 308 nm excitation): λ_{max} 381 nm. IR (neat): ν 3178, 2963, 2873, 2214, 1498, 1170 cm^{-1}. MS (CI pos) *m/z* (%): 863 (M^++6, 24), 862 (M^++5, 61), 861 (M^++4, 42), 860 (M^++3, 100), 859 (M^++2, 21), 858 (MH^+, 49); $C_{41}H_{37}Br_2N_3O_4S_2$ (857.06).

Sulfonamides 7d and **7e.** Arene **5** (100 mg, 0.24 mmol) was reacted with 3,5-bis(trifluoromethyl)benzenesulfonyl chloride according to General Preparation for Sulfonamides. Purification by chromatography (2:1 CH_2Cl_2:hexanes) afforded **7d** (212 mg, 58%) as a crystalline colorless solid and **7e** (36 mg, 13%) as a waxy light yellow solid. Recrystallization of **7d** by diffusion (hexanes:CH_2Cl_2) afforded white needles. **7d**: Mp: 87-90 °C. ^{1}H NMR (300 MHz, $CDCl_3$): δ 8.42 (s, 8H), 8.07 (s, 4H), 7.81 (d, *J* = 2.4 Hz, 2H), 7.55 (dd, *J* = 8.4, 2.4 Hz, 2H), 7.47 (t, *J* = 8.1 Hz, 1H), 7.15 (d, *J* = 8.4 Hz, 2H), 7.09 (d, *J* = 8.1 Hz, 2H), 1.39 (s, 18H). ^{13}C NMR (75 MHz, $CDCl_3$): δ 155.41, 142.22, 141.70, 136.33, 133.17, 132.70, 132.10, 131.66, 131.23, 129.20, 127.94, 126.96, 124.55, 123.97, 120.35, 92.44, 85.07, 35.20, 31.02. IR (neat): ν 2961, 2902, 2873, 2219, 1279, 1181 cm^{-1}. MS (CI pos) *m/z* (%): 1530 (M^++4, 11), 1529 (M^++3, 17), 1528 (M^++2, 41), 1527 (MH^+, 75), 1526 (M^+, 100); $C_{63}H_{47}F_{24}N_3O_8S_4$ (1526.2). **7e**: ^{1}H NMR (300 MHz, $CDCl_3$): δ 8.42 (s, 4H), 8.10 (s, 3H), 8.08 (s, 2H), 7.93 (s, 1H), 7.77 (d, *J* = 1.8 Hz, 1H), 7.65-7.46 (m, 5H), 7.30-7.14 (m, 3H), 1.39 (s,

9H), 1.30 (s, 9H). MS (CI pos) *m/z* (%): 1252 (M^++2, 39), 1251 (MH^+, 61), 1250 (M^+, 100); $C_{53}H_{37}F_{18}N_3O_6S_3$ (1250.04).

Arene 8. A suspension of ethynylarene **6** (391 mg, 1.6 mmol) and K_2CO_3 (5 equiv) in MeOH (20 mL) and Et_2O (10 mL) was stirred at rt and monitored by TLC until reaction completion (15-30 min). The solution was diluted with Et_2O and washed with water and brine. The organic layer was dried over $MgSO_4$ and concentrated in vacuo. Without further purification, the residue was dissolved in THF (10 mL) and added dropwise over a period of 12 h to a stirred, deoxygenated suspension of 6,6'-dibromo-2,2'-dipyridyl (200 mg, 0.64 mmol), $Pd(PPh_3)_4$ (173 mg, 0.2 mmol), and CuI (60 mg, 0.3 mmol) in THF (100 mL) and *i*-Pr_2NH (100 mL) at 50 °C. After an additional 3 h of stirring, the suspension was concentrated and filtered through a 2.5 cm silica plug (1:1 hexanes:EtOAc). Purification by column chromatography (CH_2Cl_2) afforded **8** as a 5:1 mixture with mono-coupled byproduct. ^1H NMR (300 MHz, $CDCl_3$): δ 8.45 (d, J = 7.2 Hz, 2H), 7.81 (t, J = 8.1 Hz, 2H), 7.55 (d, J = 8.1 Hz, 2H), 7.48 (d, J = 2.3 Hz, 2H), 7.22 (dd, J = 8.4, 2.3 Hz, 2H), 6.70 (d, J = 8.4 Hz, 2H), 4.29 (br s, 4H), 1.30 (s, 18H).

Arene 9. A suspension of ethynylarene **6** (500 mg, 2 mmol) and K_2CO_3 (5 equiv) in MeOH (20 mL) and Et_2O (10 mL) was stirred at rt and monitored by TLC until reaction completion (15-30 min). The solution was diluted with Et_2O and washed with water and brine. The organic layer was dried over $MgSO_4$ and concentrated in vacuo. Without further purification, the residue was dissolved in THF (10 mL) and added dropwise over a period of 12 h to a stirred, deoxygenated suspension of 2,5-

dibromothiophene (225 mg, 0.93 mmol), $Pd(PPh_3)_4$ (231 mg, 0.2 mmol), and CuI (76 mg, 0.4 mmol) in THF (50 mL) and *i*-Pr_2NH (50 mL) at 45 °C. After an additional 3 h of stirring, the suspension was concentrated and filtered through a 2.5 cm silica plug (CH_2Cl_2). Purification by column chromatography (CH_2Cl_2) afforded **9** (297 mg, 75%) as a bright yellow, crystalline solid. Mp: 144-145 °C. ^{1}H NMR (300 MHz, $CDCl_3$): δ 7.37 (d, J = 2.1 Hz, 2H), 7.21 (dd, J = 8.5, 2.1 Hz, 2H), 7.15 (s, 2H), 6.68 (d, J = 8.5 Hz, 2H), 4.16 (br s, 4H), 1.29 (s, 18H). ^{13}C NMR (75 MHz, $CDCl_3$): δ 145.52, 140.92, 131.49, 128.62, 127.63, 124.52, 114.38, 106.67, 91.25, 86.75, 33.89, 31.33. UV-Vis (CH_2Cl_2): λ_{max} (ε) 230 (62,000), 323 (25,200), 378 (37,000) nm. IR (neat): ν 3473, 3376, 2961, 2906, 2866, 2193, 1499 cm^{-1}. MS (CI pos) *m/z* (%): 498 (M^++THF, 100), 428 (M^++2, 18), 427 (MH^+, 53); $C_{28}H_{30}N_2S$ (426.21).

Sulfonamide 10. Arene **8** (25 mg, 0.05 mmol) was reacted with *p*-toluenesulfonyl chloride according to General Preparation for Sulfonamides. Chromatography on silica gel (3:1 hexanes:EtOAc) afforded **10** (38 mg, 53% for 2 steps) as a pale yellow solid. Recrystallization by diffusion (hexanes:EtOAc) afforded colorless crystals. Mp: 251-252 °C. ^{1}H NMR (300 MHz, $CDCl_3$): δ 8.58 (d, J = 7.8 Hz, 2H), 7.90 (t, J = 7.8 Hz, 2H), 7.77 (d, J = 8.4 Hz, 4H), 7.58-7.42 (m, 8H), 7.37 (dd, J = 8.8, 2.4 Hz, 2H), 7.14 (d, J = 7.8 Hz, 4H), 2.32 (s, 6H), 1.29 (s, 18H). ^{13}C NMR (125 MHz, $CDCl_3$): δ 155.86, 147.77, 143.85, 141.95, 137.44, 136.36, 135.74, 129.54, 129.18, 127.75, 127.40, 127.29, 121.15, 120.63, 113.34, 94.77, 84.26, 34.40, 31.13, 21.52. UV-Vis (CH_2Cl_2): λ_{max} (ε) 236 (96,000), 291 (56,000), 315 (46,100) nm. Fluorescent emission

([**10**] ≤ 0.057 mM in $CHCl_3$; 343 nm excitation): λ_{max} 390 nm. IR (neat): ν 3313, 2961, 2902, 2866, 2213, 1558, 1165 cm^{-1}. MS (CI pos) *m/z* (%): 809 (M^++2, 29), 808 (MH^+, 63), 807 (M^+, 100); $C_{48}H_{46}N_4O_4S_2$ (807.03).

Sulfonamide 11. A solution of arene **9** (90 mg, 0.2 mmol) was reacted with *p*-toluenesulfonyl chloride according to General Preparation for Sulfonamides. Chromatography on silica gel (CH_2Cl_2) afforded **11** (123 mg, 82%) as a pale yellow solid. Mp: 89-91 °C. ^1H NMR (300 MHz, $CDCl_3$): δ 7.68 (d, J = 8.7 Hz, 4H), 7.54 (d, J = 8.4 Hz, 2H), 7.39-7.34 (m, 4H), 7.22 (d, J = 8.7 Hz, 4H), 7.16 (s, 2H), 7.03 (s, 2H), 2.38 (s, 6H), 1.28 (s, 18H). ^{13}C NMR (75 MHz, $CDCl_3$): δ 147.99, 144.00, 136.21, 134.96, 132.48, 129.66, 128.98, 127.63, 127.20, 124.09, 120.98, 113.79, 89.54, 87.36, 34.39, 31.10, 21.58. UV-Vis (CH_2Cl_2): λ_{max} (ε) 230 (71,000), 287 (31,000), 357 (37,200) nm. Fluorescent emission ([**11**] ≤ 0.057 mM in $CHCl_3$; 289 nm excitation): λ_{max} 424 nm. IR (neat): ν 3248, 2921, 2870, 2852, 2198, 1162 cm^{-1}. MS (CI pos) *m/z* (%): 807 (M^++THF, 16), 737 (M^++2, 21), 736 (MH^+, 37), 735 (M^+, 71), 595 (100), 580 (89); $C_{42}H_{42}N_2O_4S_3$ (734.99).

Arene 12. A solution of chloroacetyl chloride (571 mg, 5.1 mmol) in CH_2Cl_2 (10 mL) was added to a stirred, deoxygenated solution of arene **5** (395 mg, 0.94 mmol) and Et_3N (379 mg, 3.76 mmol) in CH_2Cl_2 (10 mL). The reaction was stirred for 12 h at rt under N_2 and then concentrated in vacuo. CH_2Cl_2 was added and the organic layer was washed thrice with water, dried over $MgSO_4$, and concentrated in vacuo. The crude material was filtered through a 2.5 cm silica plug (1:1 hexanes:EtOAc) and

concentrated to afford **12** (476 mg, 89%) as a pale brown solid. Mp: 193 °C. ^{1}H NMR (300 MHz, $CDCl_3$): δ 9.23 (br s, 2H), 8.30 (d, J = 8.3 Hz, 2H), 7.72 (t, J = 8.3 Hz, 1H), 7.64 (d, J = 2.1 Hz, 2H), 7.52 (d, J = 8.1 Hz, 2H), 7.43 (dd, J = 8.1, 2.1 Hz, 2H), 4.27 (s, 4H), 1.31 (s, 18H). ^{13}C NMR (75 MHz, $CDCl_3$): δ 163.62, 147.46, 143.19, 136.83, 135.83, 129.32, 127.87, 126.20, 119.07, 111.15, 94.78, 84.80, 43.21, 34.41, 31.10. IR (neat) ν 3363, 2962, 2868, 2207, 1691, 1523 cm^{-1}. UV-Vis (CH_2Cl_2): λ_{max} (ε) 254 (52,600), 293 (27,700), 335 (27,600) nm. MS (CI pos) *m/z* (%): 578 (M^++4, 15), 577 (M^++3, 23), 576 (M^++2, 75), 575 (MH^+, 38), 574 (M^+, 100); $C_{33}H_{33}Cl_2N_3O_2$ (574.54).

Arene 13. Potassium thioacetate (16 mg, 0.14 mmol) was added to a stirred, deoxygenated solution of arene **12** (34 mg, 0.06 mmol) in DMF (3 mL). The reaction was stirred for 12 h at rt under N_2 and then concentrated in vacuo. The crude material was filtered through a 2.5 cm silica plug (1:1 hexanes:EtOAc) and purified via Chromatotron (2:1 hexanes: EtOAc) to afford **13** (35 mg, 92%) as a spongy light yellow solid. Recrystallization by diffusion (hexanes:EtOAc) afforded colorless crystals. Mp: 94 °C. ^{1}H NMR (300 MHz, $CDCl_3$): δ 8.75 (br s, 2H), 8.28 (d, J = 8.7 Hz, 2H), 7.75 (br s, 3H), 7.58 (d, J = 2.4 Hz, 2H), 7.39 (dd, J = 8.7, 2.4 Hz, 2H), 3.76 (s, 4H), 2.34 (s, 6H), 1.28 (s, 18H). ^{13}C NMR (75 MHz, $CDCl_3$): δ 195.20, 166.16, 146.81, 143.31, 136.59, 136.54, 129.38, 127.68, 126.57, 119.45, 110.79, 94.31, 85.15, 34.27, 33.99, 31.05, 30.13. IR (neat) ν 3339, 3058, 2962, 2868, 2208, 1693, 1518 cm^{-1}. UV-Vis (CH_2Cl_2): λ_{max} (ε) 253 (48,200), 291 (24,500), 330 (21,600) nm. MS (CI pos) *m/z* (%): 656 (M^++2, 19), 655 (MH^+, 44), 654 (M^+, 100); $C_{37}H_{39}N_3O_4S_2$ (653.85).

Disulfide 14. K_2CO_3 (3 equiv) was added to a deoxygenated solution of **13** (23 mg, 0.03 mmol) in MeOH (5 mL) and THF (3 mL). The suspension was stirred at rt under N_2 for 30 min and completion was monitored by TLC. Et_2O was added and the reaction mixture was washed with water and/or a saturated solution of NH_4Cl. The aqueous layer was further washed with Et_2O twice. The organics were combined and dried over $MgSO_4$. Concentration and purification via Chromatotron (3:2 hexanes:EtOAc) afforded **14** (17 mg, 77%) as a crystalline, white solid. Mp: 247 °C. ^{1}H NMR (300 MHz, $CDCl_3$): δ 9.79 (br s, 2H), 8.47 (d, J = 8.4 Hz, 2H), 7.72 (t, J = 8.4 Hz, 1H), 7.57 (d, J = 2.1 Hz, 2H), 7.51 (d, J = 8.1 Hz, 2H), 7.46 (dd, J = 8.1, 2.1 Hz, 2H), 3.70 (s, 4H), 1.34 (s, 18H). IR (neat) ν 3318, 2959, 2925, 2855, 2207, 1687, 1515 cm^{-1}. UV-Vis (CH_2Cl_2): λ_{max} (ε) 254 (52,200), 296 (24,800), 323 (17,800), 337 (17,500) nm. MS (CI pos) *m/z* (%): 570 (M^++2, 19), 569 (MH^+, 38), 568 (M^+, 100); $C_{33}H_{33}N_3O_2S_2$ (567.76).

Amide 16. Diamine **6** (0.10 g, 0.24 mmol) and K_2CO_3 (0.070 g, 0.50 mmol) were weighted into a round bottom flask (100 ml) and dissolve with 1:1 ethyl acetate:water (20 ml). In a separate container, 3,5-dinitrobenzoyl chloride (0.11 g, 0.48 mmol) was weighed out and dissolve in ethyl acetate (2 ml). This solution was transferred dropwise to the reaction mixture while stirring vigorously. After 2 hours a white precipitate was filtered from the reaction mixture and the solid was dried under vacuum. The reaction yielded a clean white powder (0.1g, 51% yield). Further product can be obtained by recrystallization from hot ethylacetate. ^{1}H NMR (300 MHz,

$CDCl_3$): δ 9.09 (d, J = 3 Hz, 4H), 8.91 (b s, 2H), 8.80 (b t, 2H), 8.39 (d, J = 6.0 Hz, 2H), 7.86 (t, J = 9.0 Hz, 1H), 7.58 (m, 6H), 1.40 (s, 18H).

GENERAL CRYSTALLOGRAPHIC DATA. Single-crystal X-ray diffraction data for compounds **1**, **H1**$^+$•Cl^-, **H1**$^+$•BF_4^-, **H1**$^+$•HSO_4^-, **2**, **2 polymorph no water**, (**7a**•H_2O)$_2$, (**7b**•H_2O)$_2$, **7d**, **10**, **11**, **13**, **H13**$^+$•Cl^- **and 14** were collected on a Bruker-AXS SMART APEX/CCD diffractometer using $Mo_{k\alpha}$ radiation (λ = 0.7107 Å) at 152 K. Diffracted data have been corrected for Lorentz and polarization effects, and for absorption using the SADABS v2.02 area-detector absorption correction program (Siemens Industrial Automation, Inc., © 1996). The structures were solved by direct methods and the structure solution and refinement was based on $|F|^2$. All non-hydrogen atoms were refined with anisotropic displacement parameters whereas hydrogen atoms were placed in calculated positions when possible and given isotropic U values 1.2 times that of the atom to which they are bonded. All crystallographic calculations were conducted with the SHELXTL v.6.1 program package (Bruker AXS Inc., © 2001).

(1•H_2O)$_2$**:** ($C_{43}H_{45}N_3O_5S_2$)$_2$, M_r = 1495.88 , 0.31 x 0.18 x 0.15 mm, triclinic, P-1, a = 10.0377(17) Å, b = 12.755(2) Å, c = 17.357(3) Å, α = 111.270(3)°, β = 96.113(3)°, γ = 102.966(3)°, V = 1974.4(6) Å^3, Z = 1 (i.e., one dimer per unit cell), ρ_{calcd} = 1.258 g mL^{-1}, μ = 0.183 mm^{-1}, $2\theta_{max}$ = 54.00°, T = 173(2) K, $R1$ = 0.0470 for 6966 reflections (662 parameters) with $I > 2\sigma(I)$, and $R1$ = 0.0580, $wR2$ = 0.1222, and GOF = 1.028 for all 8480 data, max/min residual electron density +0.502/-0.682 e Å^{-3}.

(**H1**$^{+}$•Cl^{-})•(**1**•H_2O): $(C_{43}H_{43}N_3O_4S_2)_2$•$H_2O$•HCl, M_r = 1514.32, 0.20 x 0.08 x 0.02 mm, triclinic, *P*-1, a = 9.9702(13) Å, b = 12.8868(17) Å, c = 17.363(2) Å, α = 111.314(2)°, β = 95.475(3)°, γ = 103.737(2)°, V = 1977.7(4) Å^3, Z = 1, ρ_{calcd} = 1.271 g mL^{-1}, μ = 0.215 mm^{-1}, $2\theta_{max}$ = 54.00°, T = 173(2) K, $R1$ = 0.0671 for 5583 reflections (559 parameters) with $I > 2\sigma(I)$, and $R1$ = 0.1074, $wR2$ = 0.1673, and GOF = 1.027 for all 8485 data, max/min residual electron density +0.842/-0.723 e Å^{-3}

H1^{+}•BF_4^{-}**:** $C_{43}H_{44}BF_4N_3O_4S_2$, M = 817.74, triclinic, *P*-1, a = 11.6480(18) Å, b = 13.432(2) Å, c = 15.472(2) Å, α = 105.643(2)°, β = 109.855(2)°, γ = 98.858(3)°, V = 2110.4(6) Å^3, Z = 2, Absorption coefficient = 0.188 mm^{-1}. Final residuals (700 parameters) $R1$ = 0.0439 for 9043 reflections with $I > 2\sigma(I)$, and $R1$ = 0.0519, $wR2$ = 0.1251, GooF = 1.022 for all 17842 data.

H1^{+}•HSO_4^{-}**:** $(C_{86}H_{88}N_6O_8S_4)$• $(C_4H_8O)_3$•$(HSO_4^{-})_2$, M = 413.36, triclinic, *P*-1, a = 14.727(4) Å, b = 15.082(4) Å, c = 21.992(6) Å, α = 83.367(5)°, β = 89.980(5)°, γ = 84.521(5)°, V = 4829(2) Å^3, Z = 2, Absorption coefficient = 0.212 mm^{-1}. Final residuals (1231 parameters) $R1$ = 0.0939 for 21772 reflections with $I > 2\sigma(I)$, and $R1$ = 0.2385, $wR2$ = 0.2466, GooF = 0.979 for all 41939 data.

(**2**•H_2O)$_2$**:** $(C_{41}H_{39}N_5O_9S_2)_2$, M_r = 1619.78 , 0.30 x 0.20 x 0.01 mm, triclinic, *P*-1, a = 10.1068(15) Å, b = 12/5999(19) Å, c = 17.186(3) Å, α = 110.709(3)°, β = 97.006(3)°, γ = 100.306(3)°, V = 1972.9(5) Å^3, Z = 1, ρ_{calcd} = 1.363 g mL^{-1}, μ = 0.198 mm^{-1}, $2\theta_{max}$ = 54.00°, T = 173(2) K, $R1$ = 0.0642 for 4980 reflections (674 parameters) with $I > 2\sigma(I)$,

and $R1$ = 0.1233, $wR2$ = 0.1462, and GOF = 1.034 for all 8413 data, max/min residual electron density +0.312/-0.432 e Å^{-3}.

(**H2**$^{+}$•Cl^{-})$_2$: ($C_{41}H_{38}ClN_5O_8S_2$)$_2$, M_r = 1656.66, 0.30 x 0.25 x 0.02 mm, triclinic, P-1, a = 9.8907(13) Å, b = 12.9533(17) Å, c = 17.012(2) Å, α = 107.831(2)°, β = 95.845(2)°, γ = 103.618(2)°, V = 1980.5(4) Å^3, Z = 1, ρ_{calcd} = 1.389 g mL^{-1}, μ = 0.262 mm^{-1}, $2\theta_{max}$ = 54.00°, T = 173(2) K, $R1$ = 0.0572 for 6572 reflections (594 parameters) with $I > 2\sigma(I)$, and $R1$ = 0.0744, $wR2$ = 0.1594, and GOF = 1.045 for all 8472 data, max/min residual electron density +0.564/-0.290 e Å^{-3}.

(**H2**$^{+}$•Br^{-})$_2$: ($C_{43}H_{44}BrN_3O_4S_2$)$_2$, M_r = 1621.68, 0.21 x 0.07 x 0.02 mm, triclinic, P-1, a = 9.632(16) Å, b = 13.33(2) Å, c = 17.47(3) Å, α = 108.39(4)°, β = 94.56(5)°, γ = 106.51(4)°, V = 2005(6) Å^3, Z = 1, ρ_{calcd} = 1.343 g mL^{-1}, μ = 1.175 mm^{-1}, $2\theta_{max}$ = 54.00°, T = 173(2) K, $R1$ = 0.0598 for 5748 reflections (599 parameters) with $I > 2\sigma(I)$, and $R1$ = 0.1021, $wR2$ = 0.1527, and GOF = 1.035 for all 8622 data, max/min residual electron density +0.680/-0.371 e Å^{-3}.

2 no water: $C_{340}H_{308}Cl_{136}N_{40}O_{64}S_{16}$, M = 7767.42, orthorhombic, Pcba, a = 27.226(4), b = 20.765(3), c = 31.191(4) Å, α = 90°, β = 90°, γ = 90°, V = 17634(4) Å^3, Z = 2, Absorption coefficient = 0.452 mm^{-1}. Final residuals (1138 parameters) $R1$ = 0.1272 for 21121 reflections with $I > 2\sigma(I)$, and $R1$ = 0.1872, $wR2$ = 0.4228, GooF = 1.460 for all 99616 data.

(7a•H$_2$O)$_2$: ($C_{43}H_{45}N_3O_7S_2$)$_2$, M = 1559.88, triclinic, P-1, a = 9.8389(19) Å, b = 13.094(3) Å, c = 17.479(3) Å, α = 68.463(3)°, β = 75.262(3)°, γ = 80.671(3)°, V = 2019.7(7) Å^3, Z = 1, Absorption coefficient = 0.185 mm^{-1}. Final residuals (680 parameters) $R1$ = 0.0498 for 9074 reflections with $I > 2\sigma(I)$, and $R1$ = 0.0676, $wR2$ = 0.1351, GooF = 0.987 for all 17590 data.

(7b•H$_2$O)$_2$: $C_{41}H_{39}Br_2N_3O_5S_2$, M = 755.38, triclinic, P-1, a = 10.0725(7) Å, b = 12.7166(8) Å, c = 17.3538(11) Å, α = 111.3340(10)°, β = 96.3670(10)°, γ = 101.7700(10)°, V = 1984.8(2) Å^3, Z = 1, Absorption coefficient = 2.195 mm^{-1}. Final residuals (638 parameters) $R1$ = 0.0351 for 8599 reflections with $I > 2\sigma(I)$, and $R1$ = 0.0430, $wR2$ = 0.0974, GooF = 1.052 for all 22389 data.

7d: $C_{42.5}H_{47.5}F_{12}N_{1.5}O_4S_2$, M = 934.55, monoclinic, C2/c, a = 9.986(3) Å, b = 54.639(16) Å, c = 31.711(10) Å, α = 99.004(6)°, β = 90°, γ = 90°, V = 17090(9) Å^3, Z = 16, Absorption coefficient = 0.221 mm^{-1}. Final residuals (977 parameters) $R1$ = 0.0839 for 20434 reflections with $I > 2\sigma(I)$, and $R1$ = 0.2161, $wR2$ = 0.2269, GooF = 0.867 for all 98547 data.

10: $C_{48}H_{28}N_4O_4S_2$, M = 788.86, triclinic, P-1, a = 7.960(3) Å, b = 10.860(4) Å, c = 12.852(4) Å, α = 101.699(7)°, β = 97.680(7)°, γ = 95.720(6)°, V = 1068.9(6) Å^3, Z = 1, Absorption coefficient = 1.226 mm^{-1}. Final residuals (318 parameters) $R1$ = 0.0779 for 4783 reflections with $I > 2\sigma(I)$, and $R1$ = 0.1359, $wR2$ = 0.2033, GooF = 1.219 for all 9270 data.

11: $C_{42}H_{42}N_2O_4S_3$, M = 734.96, triclinic, P-1, a = 11.748(5) Å, b = 12.750(5) Å, c = 13.028(6) Å, α = 97.514(9)°, β = 95.518(10)°, γ = 94.730(8)°, V = 1916.8(15) Å^3, Z = 2, Absorption coefficient = 1.273 mm^{-1}. Final residuals (466 parameters) $R1$ = 0.1271 for 6692 reflections with $I > 2\sigma(I)$, and $R1$ = 0.2568, $wR2$ = 0.3612, GooF = 1.079 for all 13924 data.

13: $C_{75}H_{80}Cl_2N_6O_8S_4$, M = 1392.59, monoclinic, Pc, a = 16.1430(15) Å, b = 9.5995(9) Å, c = 25.146(2) Å, α = 90°, β = 103.677(2)°, γ = 90°, V = 3786.2(6) Å^3, Z = 2, Absorption coefficient = 0.252 mm^{-1}. Final residuals (884 parameters) $R1$ = 0.0799 for 13075 reflections with $I > 2\sigma(I)$, and $R1$ = 0.1057, $wR2$ = 0.2317, GooF = 1.064 for all 27274 data.

H13$^+$•Cl$^-$: $(C_{37}H_{39}ClN_3O_4S_2)(C4H8O)_2$, M = 278.17, triclinic, P-1, a = 12.050(4) Å, b = 14.724(5) Å, c = 14.751(5) Å, α = 110.303(6)°, β = 110.984(6)°, γ = 91.054(6)°, V = 2261.2(12) Å^3, Z = 2, Absorption coefficient = 0.225 mm^{-1}. Final residuals (608 parameters) $R1$ = 0.0807 for 5298 reflections with $I > 2\sigma(I)$, and $R1$ = 0.1557, $wR2$ = 0.2477, GooF = 0.991 for all 10149 data.

14: $C_{35}H_{37}N_3O_3S_2$, M = 611.80, triclinic, P-1, a = 9.5029(18) Å, b = 12.881(2) Å, c = 13.585(3) Å, α = 79.321(3)°, β = 86.979(3)°, γ = 88.986(3)°, V = 1631.8(5) Å^3, Z = 2, Absorption coefficient = 0.202 mm^{-1}. Final residuals (467 parameters) $R1$ = 0.0484 for 7398 reflections with $I > 2\sigma(I)$, and $R1$ = 0.0552, $wR2$ = 0.1374, GooF = 1.047 for all 14264 data.

CHAPTER VII

CONCLUDING REMARKS AND FUTURE PERSPECTIVES

CONCLUDING REMARKS

The new millennium has brought with it a rebirth of anion/arene chemistry. This dissertation has chronicled the early exploration of this field and reviewed the many paths that researchers have taken to understanding the interactions between anions and electron-deficient aromatic rings. Initial investigations in the Johnson laboratory have illustrated that it is possible to develop anion receptors capable of interacting with anions by way of electron-deficient aromatic rings. This initial research led to the detailed crystallographic and computational study of the preferred binding mode for halide anions interacting with electron-deficient aromatic rings. The importance of considering multiple binding modes in these systems was highlighted. The following tripodal anion receptors—bearing electron-deficient aromatic rings—showed that it is possible to develop anion receptors capable of attracting anions using only electron-deficient aromatic rings. Furthermore, very subtle changes in binding orientations can be observed by ^{1}H NMR in these systems. The development of intramolecular hydrogen bonding receptors and highly electron-deficient binding motifs were

presented in an effort to increase the strength of anion/arene interactions. Finally, in collaboration with the Haley lab (UO), a crystallographic expedition was presented highlighting a conformationally diverse series of conjugated receptor molecules that show a predilection to bind anions and small molecules. Despite the rich history of anion/arene interactions and the recent resurgence of interest in these attractive forces, there remain many complexities to be understood.

FUTURE PERSPECTIVES

In short, this dissertation has established the necessary foundation for critical evaluation of anion/arene interactions. One of the exciting prospects of anion/arene interacts is their potential to deviate from trends in traditional anion binding selectivities. In particular, by improving receptor design (conformationally rigid host molecules containing newly developed electron-deficient aromatic rings) it will be possible to evaluate selectivity trends for anions interacting with electron-deficient aromatic rings.

Scheme 7.1 presents a representative example of improving our first generation receptor design by removing the conformational flexibility from the receptor. Initial progress has been made toward this receptor but clearly more synthetic work needs to be achieved before quantitative studies are undertaken.

Scheme 7.1 Synthesis of improved conformationally rigid sulfamide receptor will aid in understanding the selectivity of anion/arene interactions.

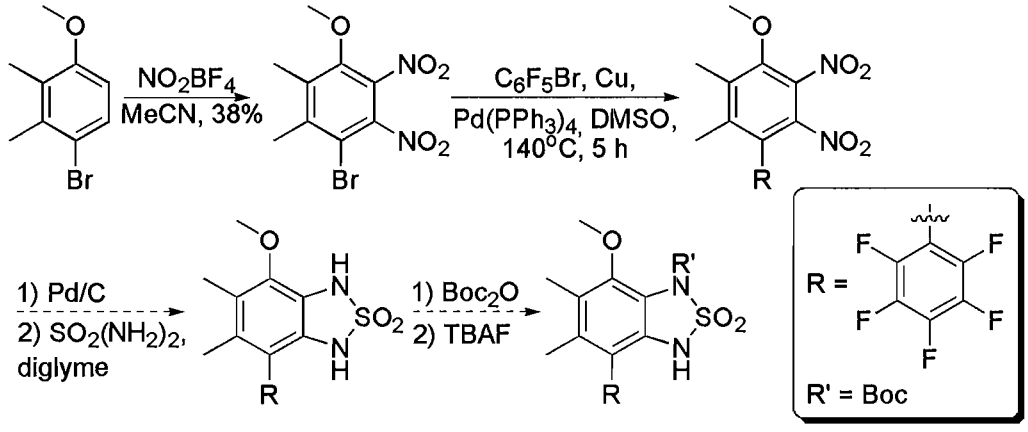

Another exciting prospective receptor class is highlighted in chapter V. The phosphine and phosphine oxide based receptors need further evaluation to determine whether intramolecular hydrogen bonds are established in solution or the solid state. Additionally, conformationally locking these bowl shaped architectures will result in an exciting new class of molecules that enlist the function of inward directed functionality (Figure 7.1).

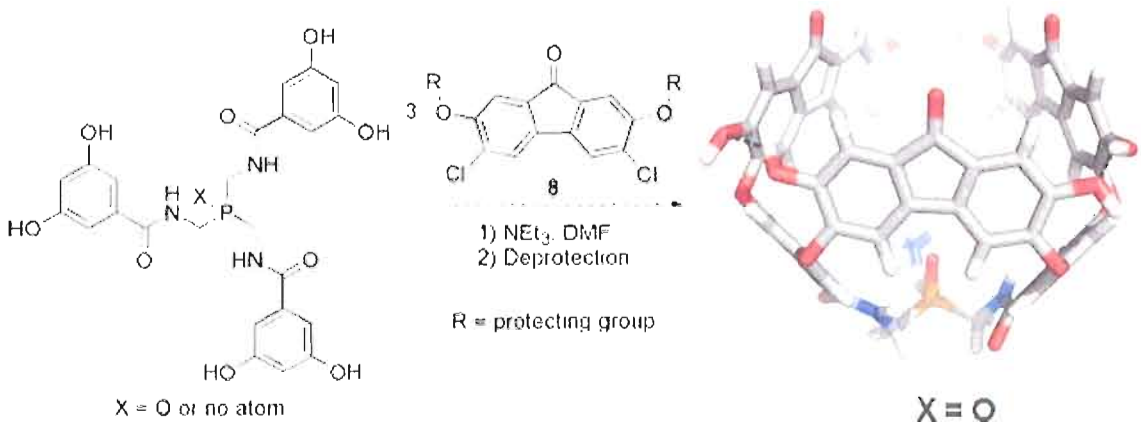

Figure 7.1 'Conformationally locked' bowl-shaped molecule with inward directed functionality. Molecular design is based off of the X-ray structure of **4** shown in Chapter V, Figure 5.3.

Now that we have presented a keen understanding of binding modes available for anion/arene interactions we can begin to look into the role of solvent affects on anion/arene interactions. It has yet to be illustrated whether the energy of anion/arene interactions is solvent dependent and proof of this statement would surely interest current readers.

Another hypothesis is that electron-deficient aromatic rings can be used to alter traditional reaction rates. For instance this hypothesis could be simply tested by adding the appropriate electron-deficient aromatic ring to a reaction involving a polar or anionic transition state. If the electron-deficient arene has a role in stabilizing the transition state then the corresponding reaction rate should be increased. Alternatively, this theory could be tested intramolecularly with the leaving group and the electron-deficient aromatic ring incorporated into the same receptor. The correct receptor design would position the

electron-deficient aromatic ring appropriately to stabilize the leaving group during the reaction. An example receptor design is provided in Figure 7.2.

Figure 7.2 Example receptor exhibiting tethered electron-deficient aromatic ring and leaving group.

The vast majority of solution, solid state and computational studies of anion/arene interactions have focused on monoatomic anions. Clearly, further studies must be done on larger biologically and environmentally relevant anions for the importance of this interaction to be fully understood.

APPENDIX A

SUPPORTING INFORMATION FOR CHAPTER II: ANION-π INTERACTION AUGMENTS HALIDE BINDING IN SOLUTION

EXPERIMENTAL

GENERAL. Pyridine, *d*-chloroform and acetonitrile was dried over 3Å molecular sieves. Tetra-*n*-butylammonium salts were dried under a vacuum at 50°C and stored in a desicator. All other materials were obtained from TCI-America, Sigma-Aldrich, Acros and Strem. Nuclear Magnetic Resonance ^{1}H NMR, ^{13}C NMR and ^{19}F NMR spectra were recorded on a Varian INOVA 300 (299.935), 125 (125.751) and 282 (282.224) MHz spectrometer respectively. Chemical shifts (δ) expressed as ppm downfield from tetramethylsilane using either the residual solvent peak as an internal standard ($CDCl_3$ ^{1}H: 7.27 ppm) or using $CDCl_3$ spiked with 1% trimethylsilane for the ^{1}H NMR spectra. For the ^{13}C NMR spectra the middle $CDCl_3$ peak (δ 77.00 ppm) was used as the internal standard. For the ^{19}F NMR spectra C_6F_6 (δ -164.9 ppm) was used as the internal standard Signal patterns are indicated as b, broad; s, singlet; d, doublet; t, triplet; m, multiplet. Coupling constants (*J*) are given in hertz.

Single-crystal X-ray diffraction data for compounds **1** and **1**·nBu_4^+·Cl^- were collected on a Bruker-AXS SMART APEX/CCD diffractometer using $Mo_{k\alpha}$ radiation (λ = 0.7107 Å) at 152 K. Diffracted data have been corrected for Lorentz and polarization effects, and for absorption using the SADABS v2.02 area-detector absorption correction program (Siemens Industrial Automation, Inc., © 1996). The structures were solved by direct methods and the structure solution and refinement was based on $|F|^2$. All non-hydrogen atoms were refined with anisotropic displacement parameters whereas hydrogen atoms were placed in calculated positions when possible and given isotropic *U* values 1.2 times that of the atom to which they are bonded. Hydrogen atoms of the amino groups in **1** and **1**·nBu_4^+·Cl^- were located via difference Fourier map inspection and refined with riding coordinates and isotropic thermal parameters based upon the corresponding N atoms [U(H) = 1.2Ueq (O)]. All crystallographic calculations were conducted with the SHELXTL v.6.1 program package (Bruker AXS Inc., © 2001).

2-*p*-toluenesulfonamide-2', 3', 4', 5', 6'-pentafluorobiphenyl (1). An oven dried 100 mL round bottom Schlenk flask was charged with N-(2-iodophenyl)-4-methylbenzenesulfonamide (3.68 g, 14.9 mmol), copper powder (4.77 g, 75.1 mmol) and tetrakistriphenylphosphine palladium (0) (0.86o g, 0.741 mmol). Dry dimethylsulfoxide (46 mL) was added via a syringe to the reaction mixture. The mixture was degassed purging with N_2 (3×) and then bromopentafluorobenzene (3.70

mL, 29.7 mmol) was added. The solution was again degassed and then was heated at 115-120°C for 5.5 h. under a N_2 atmosphere. The reaction was cooled to room temperature and was diluted with DCM (50 mL) and water (50 mL). The resulting foamy mixture was then filtered through a glass frit containing celite and silica gel. The remaining celite/silica gel pad was washed with DCM (3 × 50 mL). The resulting pale green solution was transferred to a 150 mL separatory funnel and washed with water (3 × 100 mL) followed by brine (1 × 100 mL). The separated organic layer was dried over $MgSO_4$. Removal of the DCM in vacuo left a crude pale green solid that was later purified by flash column chromatography (silica gel, 3:1 hexanes: ethyl acetate) to yield a colorless product (1.64 g, 26.7% yield) that crystallized overnight upon standing in the column eluent. Structure was determined by single crystal X-ray diffraction. Single crystals suitable for data collection were grown by diffusing pentane into a chloroform solution of **1** at –30 °C. ^{1}H NMR (300 MHz, $CDCl_3$; 25°C): δ 7.56 (d, J = 8.1 Hz, 1H, C*H*), 7.48 (t, J = 4.5 Hz, 1H, ArC*H*), 7.41 (d, J = 4.6 Hz, 2H, ArC*H*), 7.35 (t, J = 4.2 Hz, 1H, ArC*H*), 7.17 (m, 3H, ArC*H*), 6.35 (b, 1H, N*H*), 2.41 (s, 3H, CH_3); ^{19}F NMR (282 MHz, $CDCl_3$; 25°C): δ –191.51 (q, J = 16.2 Hz, 2F C*F*), -205.54 (t, J = 22.2 Hz, 1F, C*F*), -213.14 (m, 2F, C*F*). ^{13}C NMR (125 MHz, $CDCl_3$; 25°C): δ 144.37, 144.45, 136.36, 134.57, 131.90, 131.04, 129.73, 127.39, 127.25, 127.04, 122.46, 21.62, 0.202.

***N*-biphenyl-2-yl-4-methyl-benzenesulfonamide (2).** Similar to literature procedure,[1] an oven dried 50 mL round bottom flask was charged with 2-aminobiphenyl (0.330 g, 2.00 mmol) and pyridine (7.5 mL). To this stirred solution *p*-toluenesulfonylchloride (0.570 g, 3.00 mmol) was added and stirred for 4 h. The resulting pale pink solution with white precipitate was concentrated down in vacuo and diluted with dichloromethane (50 mL) and water (50 mL). The organic layer was separated and washed with 3M HCl (3 × 50 mL) and 1M $NaHCO_3$ (3 × 50 mL). Removal of the organic layer in vacuo resulted in a pale pink solid that was later crystallized from an 8:1 mixture of hexanes and dichloromethane. Crystallization yielded colorless crystals (0.56 g, 87%). The structure was determined by single crystal X-ray diffraction. Single crystals suitable for data collection were grown by diffusing pentane into a chloroform solution of **2** at –30°C. ^{1}H NMR (300 MHz, $CDCl_3$; 25°C): δ 7.80 (d, J = 8.1 Hz, 2H, ArC*H*), 7.72 (d, J = 8.1 Hz, 1H, ArC*H*), 7.48 (d, J = 8.7 Hz, 1H, ArC*H*), 7.35 (m, 4H, ArC*H*), 7.20 (d, J = 8.4 Hz, 2H, ArC*H*), 7.12 (m, 1H, ArC*H*), 6.86 (m, 2H, ArC*H*), 6.58 (b, 1H, N*H*), 2.41 (s, 3H, CH_3).

NMR TITRATION EXPERIMENTS

GENERAL. ^{1}H NMR spectra were recorded on a Varian 300 or 500 MHz spectrometer. Each titration was performed with 8 to 14 measurements in $CDCl_3$ at room temperature. $CDCl_3$ was passed through activated alumina and dried over 3Å molecular sieves. Aliquots from a stock solution of tetra-*n*-butylammonium salts (60 –

200 mM) were added to the initial solution of receptor (9 – 25 mM). All additions were done through septa with a syringe to minimize evaporation. All proton signals were referenced to an internal TMS standard. The association constants Ka were calculated by the non-linear regression curve fitting program WinEQNMR

Table A.1 ^{1}H NMR Titration data for receptor **1** and TBACl trial 1

		fromGuest Stock				
Additio n	δ ppm	Vol. Guest added (ml)	Total Vol. (ml)	[R]		[G]
0	6.2480	0	0.6	9.677E-03		0.000E+00
1	6.3005	0.01	0.61	9.518E-03		1.039E-03
2	6.3483	0.02	0.62	9.365E-03		2.044E-03
3	6.3937	0.03	0.63	9.216E-03		3.017E-03
4	6.4360	0.04	0.64	9.072E-03		3.960E-03
5	6.5128	0.06	0.66	8.797E-03		5.760E-03
6	6.5816	0.08	0.68	8.538E-03		7.455E-03
7	6.6474	0.1	0.7	8.294E-03		9.052E-03
8	6.7038	0.12	0.72	8.064E-03		1.056E-02
9	6.7789	0.15	0.75	7.741E-03		1.267E-02
10	6.8479	0.18	0.78	7.444E-03		1.462E-02
11	6.9067	0.21	0.81	7.168E-03		1.643E-02
12	6.9735	0.25	0.85	6.831E-03		1.864E-02
13	7.0401	0.3	0.9	6.451E-03		2.112E-02
14	7.1055	0.35	0.95	6.112E-03		2.334E-02

initial vol. (G)	Receptor Stock (M)	Guest Stock (M)	Mol Guest
0.6	0.009676678	0.063363558	0.000126727

mol Receptor	
9.67668E-06	

TBACl MW	Receptor 2 MW
277.92	413.365

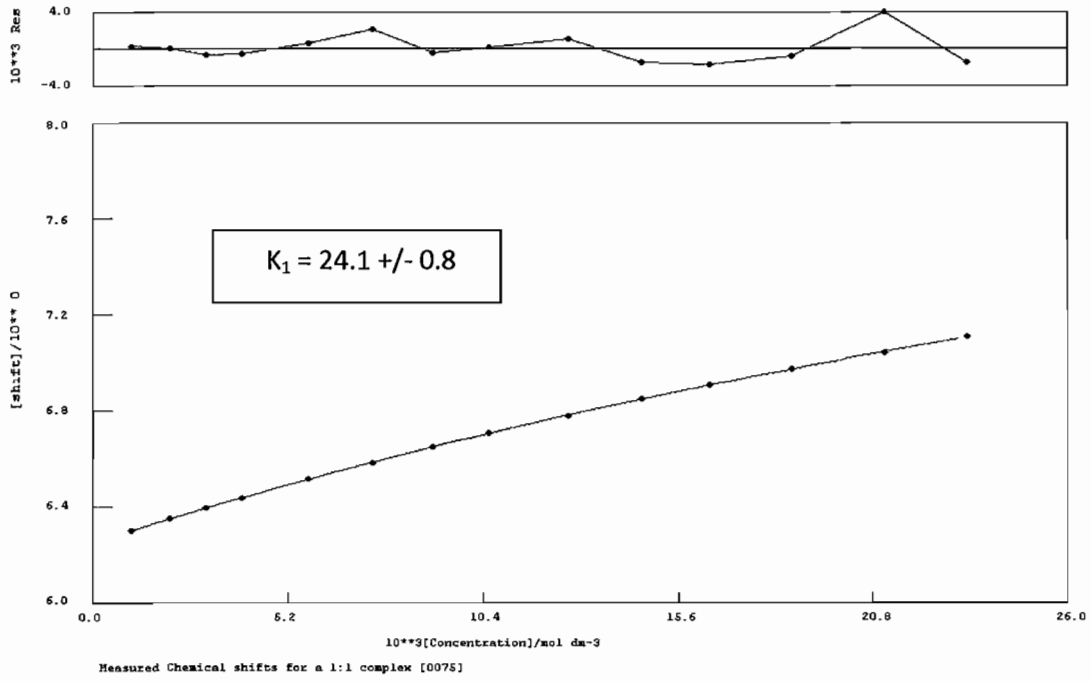

Graph A.1 Binding isotherm from receptor **1** titration with TBACl trial 1

Table A.2 ^{1}H NMR Titration data for receptor **1** and TBACl trial 2

		from Guest Stock				
Additio n	δ ppm	Vol. Guest added (ml)	Total Vol. (ml)	[R]		[G]
0	6.2414	0	0.6	9.822E-03		0.000E+00
1	6.2950	0.01	0.61	9.661E-03		9.874E-04
2	6.3465	0.02	0.62	9.505E-03		1.943E-03
3	6.3969	0.03	0.63	9.354E-03		2.868E-03
4	6.4392	0.04	0.64	9.208E-03		3.765E-03
5	6.5203	0.06	0.66	8.929E-03		5.476E-03
6	6.5929	0.08	0.68	8.666E-03		7.086E-03
7	6.6544	0.1	0.7	8.419E-03		8.605E-03
8	6.7396	0.13	0.73	8.073E-03		1.073E-02
9	6.8080	0.16	0.76	7.754E-03		1.268E-02
10	6.8934	0.2	0.8	7.366E-03		1.506E-02
11	6.9692	0.25	0.85	6.933E-03		1.772E-02
12	7.0955	0.35	0.95	6.203E-03		2.219E-02

initial vol. (R)	Receptor Stock (M)	Guest Stock (M)	mol Guest (G)
0.6	0.009821828	0.060233161	0.000120466
	mol Receptor		
	9.82183E-06		
	TBACl MW	Receptor 2 MW	
	277.92	413.365	

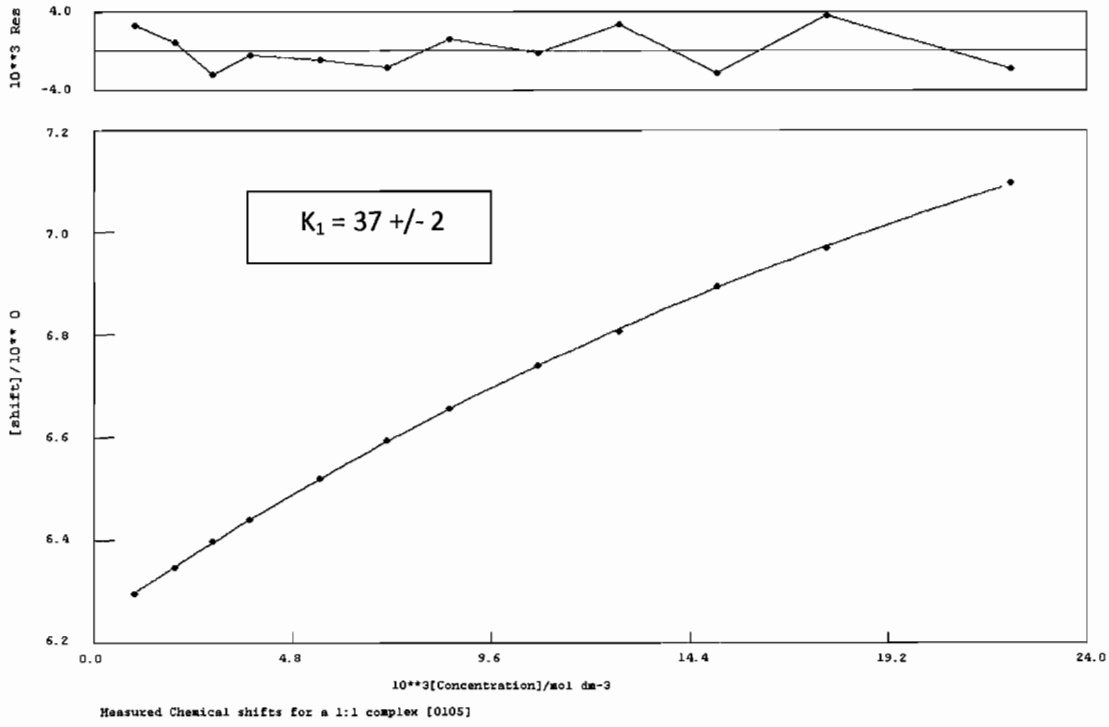

Graph A.2 Binding isotherm from receptor **1** titration with TBACl trial 2

Table A.3 ^{1}H NMR Titration data for receptor **1** + TBACl trial 3

		from Guest Stock				
Addition	δ ppm	Vol. Guest added (ml)	Total Vol. (ml)	[R]		[G]
0	6.2463	0	0.6	1.040E-02		0.000E+00
1	6.3003	0.01	0.61	1.023E-02		1.051E-03
2	6.3488	0.02	0.62	1.007E-02		2.069E-03
3	6.3962	0.03	0.63	9.907E-03		3.054E-03
4	6.4799	0.05	0.65	9.602E-03		4.934E-03
5	6.5543	0.07	0.67	9.316E-03		6.701E-03
6	6.6207	0.09	0.69	9.046E-03		8.366E-03
7	6.6811	0.11	0.71	8.791E-03		9.937E-03
8	6.7608	0.14	0.74	8.434E-03		1.213E-02
9	6.8279	0.17	0.77	8.106E-03		1.416E-02
10	6.9045	0.21	0.81	7.706E-03		1.663E-02
11	6.9863	0.26	0.86	7.258E-03		1.939E-02
12	7.1104	0.36	0.96	6.502E-03		2.405E-02

initial vol. (R)	Receptor Stock (M)	Guest Stock (M)	mol Guest (G)
0.6	0.010402429	0.064137162	0.000128274
	mol Receptor		
	1.04024E-05		
	TBACl MW	Receptor 2 MW	
	277.92	413.365	

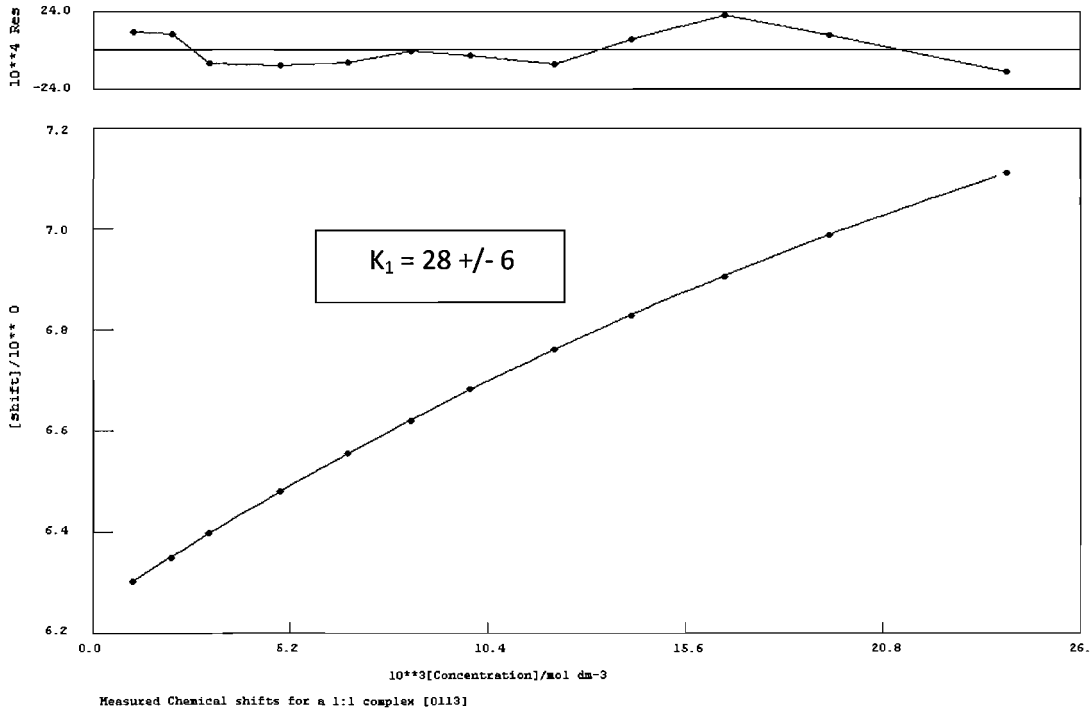

Graph A.3 Binding isotherm from receptor **1** titration with TBACl trial 3

Table A.4 ^{1}H NMR Titration data for receptor **1** + TBABr trial 1

		from Guest Stock				
Addition	δ ppm	Vol. Guest added (ml)	Total Vol. (ml)	[R]		[G]
0	6.358	0	0.6	2.035E-02		0.000E+00
1	6.359	0.01	0.61	2.001E-02		3.260E-03
2	6.453	0.03	0.63	1.938E-02		9.470E-03
3	6.53	0.05	0.65	1.878E-02		1.530E-02
4	6.593	0.07	0.67	1.822E-02		2.078E-02
5	6.67	0.1	0.7	1.744E-02		2.841E-02
6	6.736	0.13	0.73	1.672E-02		3.541E-02
7	6.785	0.16	0.76	1.606E-02		4.187E-02
8	6.847	0.2	0.8	1.526E-02		4.972E-02
9	6.91	0.25	0.85	1.436E-02		5.849E-02
10	7.019	0.35	0.95	1.285E-02		7.327E-02
11	7.086	0.45	1.05	1.163E-02		8.523E-02

initial vol. (G)	Receptor Stock (M)	Guest Stock (M)	mol Guest
0.6	0.020345215	0.198867778	0.0003977 4

mol Receptor
2.03E-05

TBABr MW	Receptor MW
322.375	413.365

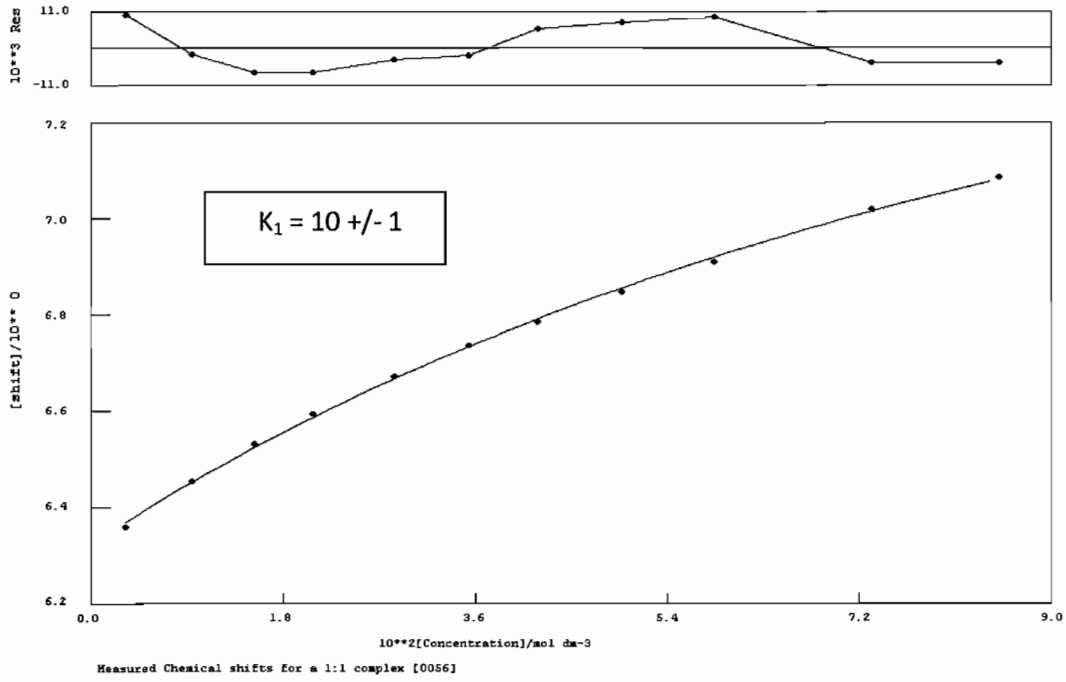

Graph A.4 Binding isotherm from receptor **1** titration with TBABr trial 1

Table A.5 ^{1}H NMR Titration data for receptor **1** + TBABr trial 2

		from Guest Stock				
Addition	δ ppm	Vol. Guest added (ml)	Total Vol. (ml)	[R]		[G]
0	6.284	0	0.6	0.01982719		0
1	6.315	0.01	0.61	0.019502154		0.001980689
2	6.327	0.02	0.62	0.019187603		0.003897485
3	6.346	0.04	0.64	0.018587991		0.007551377
4	6.365	0.06	0.66	0.018024718		0.01098382
5	6.389	0.09	0.69	0.017241035		0.015759394
6	6.409	0.12	0.72	0.016522658		0.020137004
7	6.431	0.16	0.76	0.015653045		0.025436216
8	6.45	0.21	0.81	0.014686807		0.031324228
9	6.477	0.31	0.91	0.013072872		0.041159151

initial vol. (R)	Receptor Stock (M)	Guest Stock (M)	mol Guest
0.6	1.98E-02	0.120822024	0.000241644
	mol Receptor		
	1.98E-05		
	TBABr MW	Receptor MW	
	322.375	413.365	

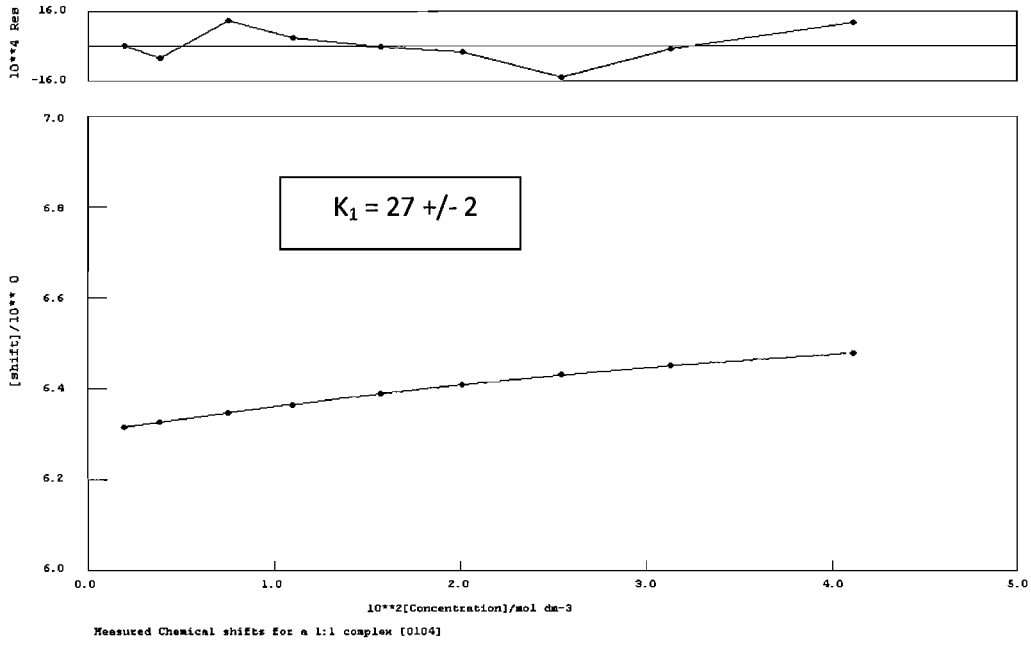

Graph A.5 Binding isotherm from receptor **1** titration with TBABr trial 2

Table A.6 ^{1}H NMR Titration data for receptor **1** + TBABr trial 3

		from Guest Stock				
Addition	δ ppm	Vol. Guest added (ml)	Total Vol. (ml)	[R]		[G]
0	6.297	0	0.6	2.032E-02		0
1	6.299	0.01	0.61	1.999E-02		0.001977638
2	6.366	0.02	0.62	1.967E-02		0.003891481
3	6.398	0.03	0.63	1.935E-02		0.005744567
4	6.452	0.05	0.65	1.876E-02		0.009279685
5	6.497	0.07	0.67	1.820E-02		0.012603751
6	6.557	0.1	0.7	1.742E-02		0.017233701
7	6.606	0.13	0.73	1.670E-02		0.021483106
8	6.659	0.17	0.77	1.583E-02		0.026633901
9	6.710	0.22	0.82	1.487E-02		0.032365731
10	6.793	0.32	0.92	1.325E-02		0.041960315

initial vol. (R)	Receptor Stock (M)	Guest Stock (M)	mol Guest
0.6	2.03E-02	0.120635905	0.000241272
	mol Receptor		
	2.03E-05		
	TBABr MW	Receptor MW	
	322.375	413.365	

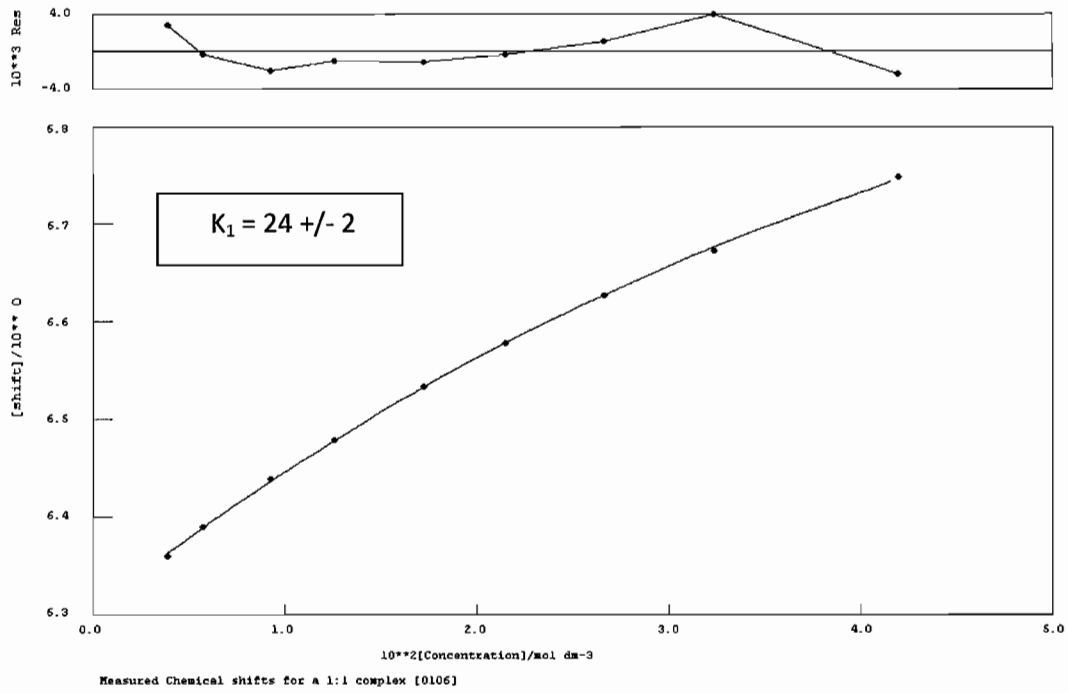

Graph A.6 Binding isotherm from receptor **1** titration with TBABr trial 3

Table A.7 ^{1}H NMR titration data for receptor **1** + TBAI trial 1

		from Guest Stock				
Add.	δ ppm	Vol. Guest added (ml)	Total Vol. (ml)	[R]		[G]
0	6.295	0	0.6	0.01911143		0.0000E+00
1	6.309	0.01	0.61	0.01879813		1.9872E-03
2	6.329	0.03	0.63	0.01820137		5.7724E-03
3	6.356	0.06	0.66	0.01737403		1.1020E-02
4	6.377	0.09	0.69	0.01661864		1.5811E-02
5	6.392	0.12	0.72	0.01592619		2.0203E-02
6	6.405	0.15	0.75	0.01528915		2.4244E-02
7	6.42	0.19	0.79	0.01451501		2.9154E-02
8	6.435	0.24	0.84	0.01365102		3.4634E-02
9	6.445	0.28	0.88	0.01303052		3.8570E-02
10	6.457	0.35	0.93	0.01232996		4.5620E-02

initial vol. (G)	Receptor Stock (M)	Guest Stock (M)	mol Guest
0.6	0.019111439	0.121219915	0.00024244
	mol Receptor		
	1.91114E-05		
	TBAI MW	Receptor MW	
	369.37	413.365	

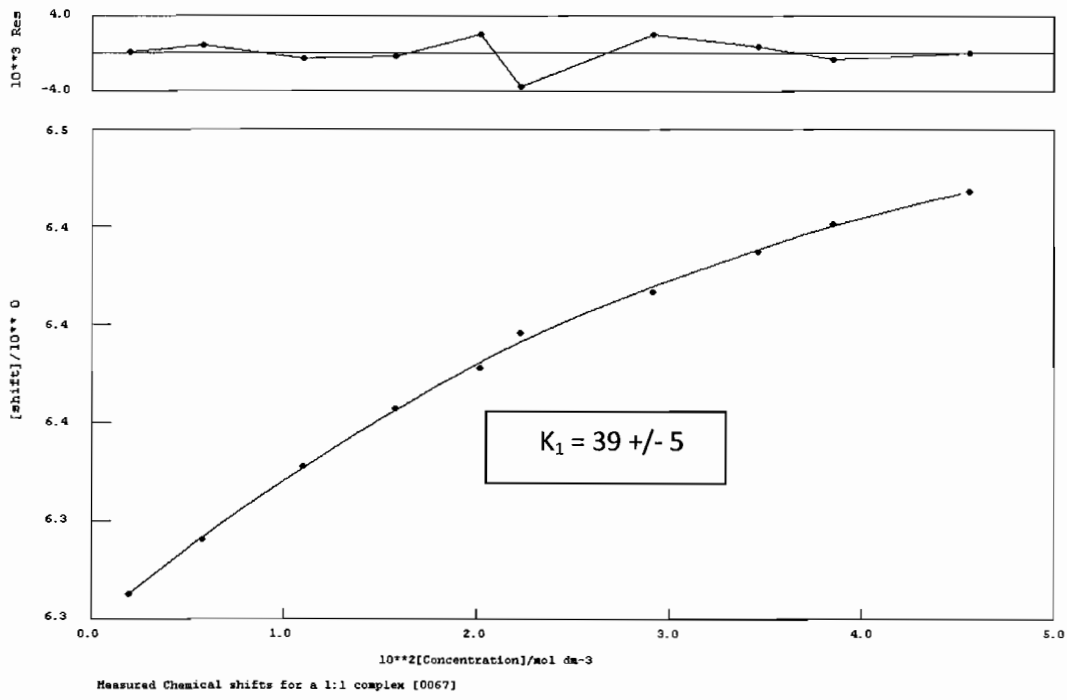

Graph A.7 Binding isotherm from receptor **1** titration with TBAI trial 1

Table A.8 ^{1}H NMR titration data for receptor **1** + TBAI trial 2

		from Guest Stock				
Addition	δ ppm	Vol. Guest added (ml)	Total Vol. (ml)	[R]		[G]
0	6.303	0	0.6	2.032E-02		0.000E+00
1	6.318	0.01	0.61	1.999E-02		1.934E-03
2	6.336	0.03	0.63	1.935E-02		5.616E-03
3	6.361	0.06	0.66	1.847E-02		1.072E-02
4	6.378	0.09	0.69	1.767E-02		1.538E-02
5	6.393	0.12	0.72	1.693E-02		1.966E-02
6	6.404	0.15	0.75	1.626E-02		2.359E-02
7	6.417	0.19	0.79	1.543E-02		2.837E-02
8	6.431	0.24	0.84	1.452E-02		3.370E-02
9	6.442	0.28	0.88	1.386E-02		3.753E-02

initial vol. (G)	Receptor Stock (M)	Guest Stock (M)	mol Guest
0.6	0.020321024	0.117944067	0.0002358 9

mol Receptor
1.22E-05

TBAI MW	Receptor MW
369.37	413.365

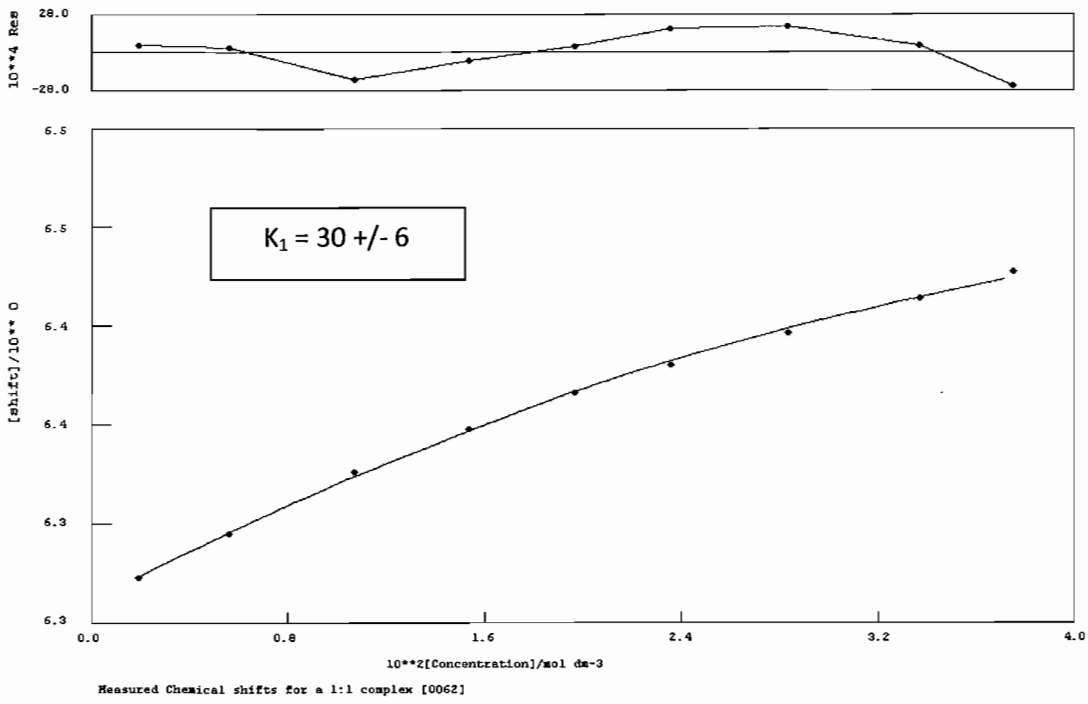

Graph A.8 Binding isotherm from receptor **1** titration with TBAI trial 2

Table A.9 ^{1}H NMR titration data for receptor **1** + TBAI trial 3

		from Guest Stock				
Addition	δ ppm	Vol. Guest added (ml)	Total Vol. (ml)	[R]		[G]
0	6.293	0	0.6	0.019498506		0.0000E+00
1	6.306	0.01	0.61	0.019178859		1.9675E-03
2	6.326	0.03	0.63	0.018570006		5.7150E-03
3	6.344	0.05	0.65	0.017998621		9.2319E-03
4	6.364	0.08	0.68	0.017204564		1.4119E-02
5	6.379	0.11	0.71	0.016477611		1.8594E-02
6	6.395	0.14	0.74	0.0158096		2.2706E-02
7	6.41	0.18	0.78	0.014998851		2.7696E-02
8	6.421	0.23	0.83	0.014095306		3.3257E-02
9	6.442	0.28	0.88	0.013294436		3.8187E-02

initial vol. (G)	Receptor Stock (M)	Guest Stock (M)	mol Guest
0.6	0.019498506	0.120015161	0.00024003
	mol Receptor		
	1.94985E-05		
	TBAI MW	Receptor MW	
	369.37	413.365	

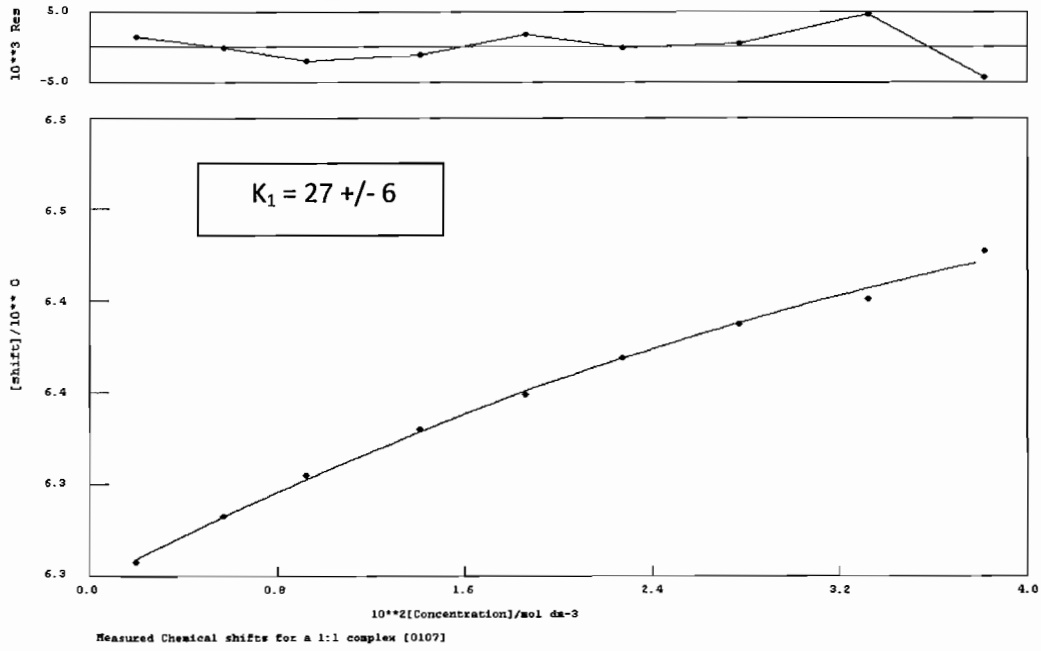

Graph A.9 Binding isotherm from receptor **1** titration with TBAI trial 3

pK_a DETERMINATION

GENERAL. The pKa measurements were made with an Orion model 230Aplus pH meter equipped with a Triode 9107BN pH electrode. The pH meter was calibrated with 1:1 stock solutions of acetonitrile/water buffered at 7.00 and 10.00 pH. The electrode was allowed to soak in acetonitrile for 2 hours prior to any measurements. Initial receptor concentrations were made to 10^{-3} M in acetonitrile and 0.06 g tetra-*n*-butylammonium iodide was added as a supporting electrolyte. A stock solution of tetramethylammonium hydroxide in ethanol 0.05 M (to avoid precipitation) was prepared under nitrogen. Aliquots of the stock tetramethylammonium hydroxide were added to the receptor solution under nitrogen and the resulting potential was measured. Titration curves were prepared by plotting the potential vs the total amount of stock tetramethylammonium hydroxide added. The relative pKa was taken as the pH at the half-neutralization potential.

Table A.10 pK_a determination for receptor **1** trial 1

Addition	Total Added	pH	RelmV
0	0	7.97	-99.6
1	50	8.51	-135.5
2	100	8.76	-150.7
3	150	8.89	-158.7
4	200	9	-165.8
5	250	9.09	-171.3
6	300	9.17	-176
7	350	9.24	-180.3
8	400	9.3	-183.9
9	450	9.36	-187.6
10	500	9.41	-190.8
11	750	9.66	-206.2
12	800	9.74	-210.7
13	850	9.84	-216.9
14	900	9.92	-221.6
15	950	10	-226.9
16	1000	10.09	-232.5
17	1050	10.18	-237.7
18	1100	10.45	-255.4
19	1150	10.8	-278.3
20	1200	13.45	-442.5
21	1250	13.85	-468.9
22	1300	14.26	-493.5
23	1400	14.47	-507.7
24	1600	14.98	-540.3
25	1900	15.36	-564.1

HNP = -380 mV = pH 13.3

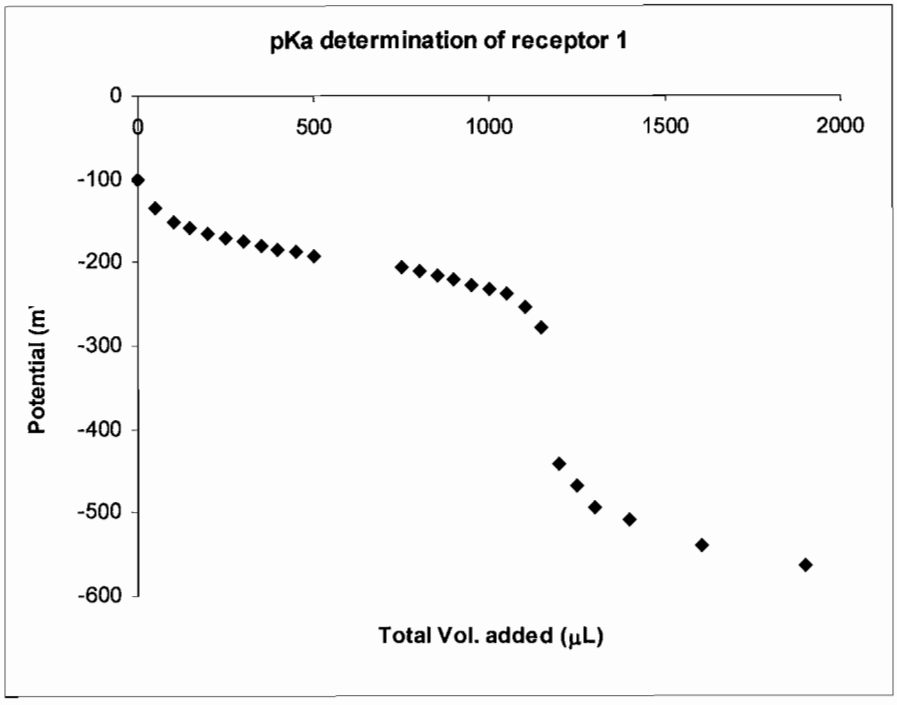

Graph A.10 pKa titration of receptor **1** trial 1

Table A.11 pK_a determination for receptor **1** trial 2

Addition	Total Added	pH	RelmV
0	0	8.15	-101
1	30	9.39	-177.2
2	60	9.8	-202.6
3	90	10.19	-227.4
4	105	10.5	-246.5
5	115	10.88	-270.8
6	120	11.48	-308.6
7	125	13.52	-436.5
8	130	15.02	-532.3
9	140	17.46	-678
10	150	17.84	-711.3
11	165	18.18	-733.3
12	195	18.49	-753.7
13	245	18.67	-766.3
14	295	18.73	-769.8
15	345	18.72	-770.6

HNP = -505 mV = pH 14.2

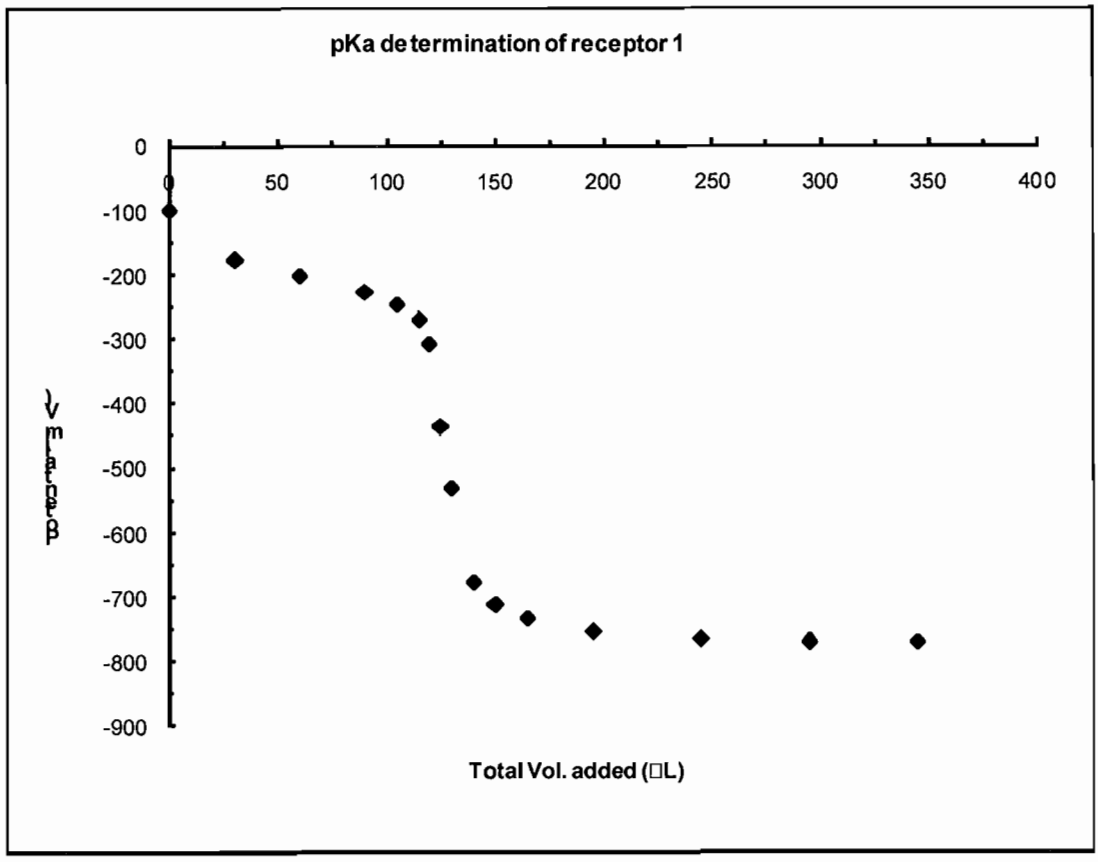

Graph A.11 pKa titration of receptor **1** trial 2

Table A.12 pK_a determination for receptor **2** trial 1

Addition	Total Added	pH	RelmV
0	0	8.56	-127.4
1	30	10.83	-268.2
2	40	10.97	-278
3	50	11.09	-286.2
4	55	11.15	-290.4
5	65	11.25	-297.6
6	75	11.35	-304.4
7	85	11.45	-311.4
8	100	11.62	-322.2
9	110	11.76	-331.9
10	120	11.95	-344.3
11	125	12.07	-352
12	130	12.27	-364.8
13	135	12.61	-386.8
14	140	13.17	-422.5
15	145	13.95	-472.8
16	150	14.5	-508.2
17	155	15.25	-556.6
18	160	16.36	-580.7
19	170	17.07	-666.8
20	180	17.6	-700
21	190	17.83	-720
22	200	17.93	-726
23	220	18.04	-736.8
24	250	18.22	-747.5
25	300	18.35	-755.8
26	350	18.39	-757.7
27	400	18.39	-757.7

HNP = -540 mV = pH 15.1

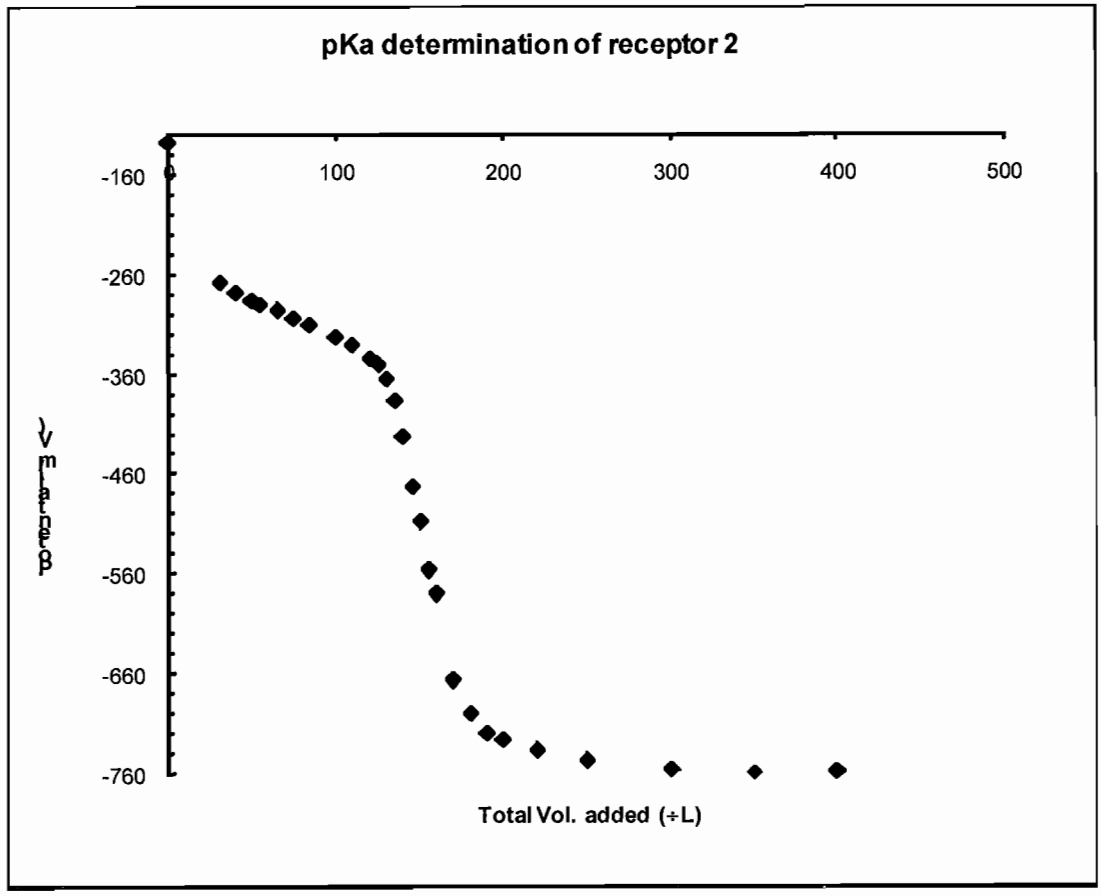

Graph A.12 pKa titration of receptor **2** trial 1

Table A.13 pK_a determination for receptor **2** trial 2

0	0	9.7	-201.8
1	20	10.76	-266.9
2	40	11.06	-285.7
3	60	11.28	-299.7
4	80	11.47	-312.2
5	100	11.68	-325.9
6	120	11.95	-343.6
7	130	12.16	-359.4
8	140	12.57	-385.3
9	150	13.65	-452.4
10	155	14.57	-510.2
11	160	16.3	-624
12	165	16.81	-652
13	170	17.12	-670.2
14	175	17.4	687.5
15	185	17.75	710.1
16	195	17.96	-724.3
17	215	18.15	-736.2
18	245	18.29	-745.5
19	295	18.38	-751.5
20	345	18.42	-753.8

HNP = -550 mV = pH 14.7

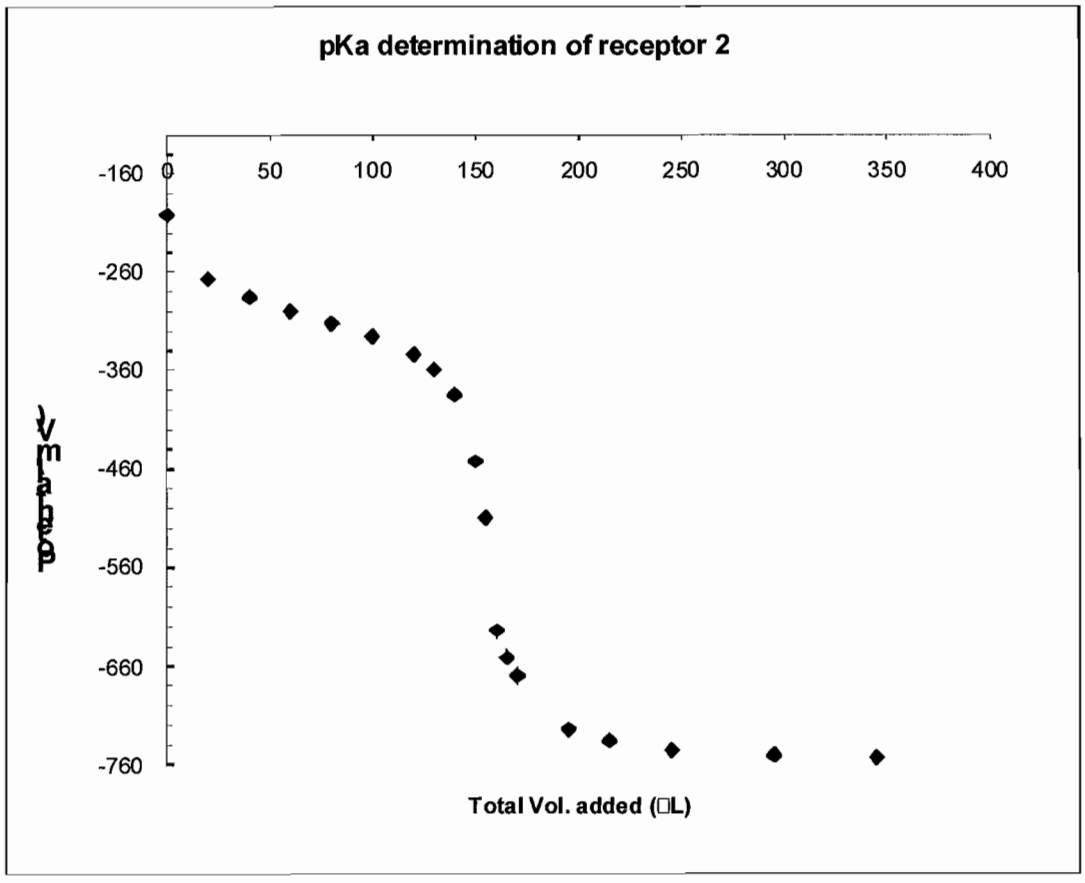

Graph A.13 pKa titration of receptor **2** trial 2

REFERENCE

1 Sakamoto, T.; Kondo, Y.; Iwashita, S.; Nagano, T.; Yamanaka, H. *Chem. Pharm. Bull.* **1988**, 36, 1305-1308.

APPENDIX B

SUPPORTING INFORMATION FOR CHAPTER III: STRUCTURAL CRITERIA FOR THE DESIGN OF ANION RECEPTORS: THE INTERACTION OF HALIDES WITH ELECTRON-DEFICIENT ARENES

CARTESIAN COORDINATES AND ABSOLUTE ENERGIES FOR OPTIMIZED STRUCTURES 1-13 AT THE MP2/aug-cc-pVDZ LEVEL OF THEORY

1, TETRACYANO-FLUORIDE ANION. -699.3309466394 a.u. (-81.9; -62.4 cm^{-1})

C	-0.70843	-1.21592	-0.21924
C	-1.41053	0.00000	-0.20599
C	-1.43917	-2.45539	-0.23382
H	-2.50222	0.00000	-0.17584
N	-2.05830	-3.47195	-0.27329
F	0.00000	0.00000	2.18602
C	0.70843	1.21592	-0.21924
C	-0.70843	1.21592	-0.21924
C	0.70843	-1.21592	-0.21924
C	1.41053	0.00000	-0.20599
C	1.43917	2.45539	-0.23382
C	-1.43917	2.45539	-0.23382
C	1.43917	-2.45539	-0.23382
H	2.50222	0.00000	-0.17584
N	2.05830	3.47195	-0.27329
N	-2.05830	3.47195	-0.27329
N	2.05830	-3.47195	-0.27329

1, TETRACYANO-CHLORIDE ANION. -1059.3766931185 a.u. (-26.9 cm-1)

C	-0.70890	-1.21697	-0.46715
C	-1.41134	0.00000	-0.45187
C	-0.70890	1.21697	-0.46715
C	0.70890	1.21697	-0.46715
C	1.41134	0.00000	-0.45187
C	0.70890	-1.21697	-0.46715
C	-1.43876	-2.45721	-0.48010
H	-2.50276	0.00000	-0.41464
C	-1.43876	2.45721	-0.48010
C	1.43876	2.45721	-0.48010
H	2.50276	0.00000	-0.41464
C	1.43876	-2.45721	-0.48010
N	-2.05549	-3.47476	-0.52632
N	2.05549	-3.47476	-0.52632
N	-2.05549	3.47476	-0.52632
N	2.05549	3.47476	-0.52632
Cl	0.00000	0.00000	2.50012

1, TETRACYANO-BROMIDE ANION. -3172.2621916160 a.u. (-20.1 cm-1)

C	-1.21729	0.70902	-0.91052
C	0.00000	1.41148	-0.89382
C	-2.45759	1.43865	-0.92389
H	0.00000	2.50288	-0.85566
N	-3.47552	2.05464	-0.97155
Br	0.00000	0.00000	2.21709
C	1.21729	-0.70902	-0.91052
C	-1.21729	-0.70902	-0.91052
C	1.21729	0.70902	-0.91052
C	0.00000	-1.41148	-0.89382
C	2.45759	-1.43865	-0.92389
C	-2.45759	-1.43865	-0.92389
C	2.45759	1.43865	-0.92389
H	0.00000	-2.50288	-0.85566
N	3.47552	-2.05464	-0.97155
N	-3.47552	-2.05464	-0.97155
N	3.47552	2.05464	-0.97155

2, TETRACYANO-FLUORIDE ANION. -699.3614274043 a.u.

C	0.86447	-0.09673	-1.20986
C	1.56067	-0.31110	0.00000
C	0.86447	-0.09673	1.20986
C	-0.52385	0.17733	1.21626
C	-1.32733	-0.06252	0.00000
C	-0.52385	0.17733	-1.21626
C	1.60874	-0.07791	-2.44285
H	2.62957	-0.53206	0.00000
C	1.60874	-0.07791	2.44285
C	-1.19632	0.58573	2.41005
H	-2.27659	0.48946	0.00000
C	-1.19632	0.58573	-2.41005
N	2.24413	-0.07006	-3.45191
N	-1.78641	0.94176	-3.38481
N	2.24413	-0.07006	3.45191

N	-1.78641	0.94176	3.38481
F	-1.79054	-1.49009	0.00000

2, TETRACYANO-CHLORIDE ANION. -1059.3790281928 a.u.

C	1.07877	0.03170	-1.21762
C	1.72198	0.33145	0.00000
C	1.07877	0.03170	1.21762
C	-0.22974	-0.51386	1.21830
C	-0.92672	-0.69328	0.00000
C	-0.22974	-0.51386	-1.21830
C	1.77549	0.27039	-2.45508
H	2.72555	0.76308	0.00000
C	1.77549	0.27039	2.45508
C	-0.87283	-0.84699	2.46018
H	-1.91933	-1.14085	0.00000
C	-0.87283	-0.84699	-2.46018
N	2.38100	0.46360	-3.46271
N	-1.37731	-1.16688	-3.49063
N	2.38100	0.46360	3.46271
N	-1.37731	-1.16688	3.49063
Cl	-2.27641	1.53200	0.00000

2, TETRACYANO-BROMIDE ANION. -3172.2637577693 a.u.

C	-1.48027	0.15209	1.21812
C	-2.02462	0.60588	0.00000
C	-1.48027	0.15209	-1.21812
C	-0.35328	-0.70793	-1.21890
C	0.26891	-1.06297	0.00000
C	-0.35328	-0.70793	1.21890
C	-2.09287	0.56087	2.45550
H	-2.88409	1.28029	0.00000
C	-2.09287	0.56087	-2.45550
C	0.18637	-1.19149	-2.46056
H	1.12851	-1.73207	0.00000
C	0.18637	-1.19149	2.46056
N	-2.62961	0.90050	3.46330
N	0.59377	-1.62813	3.49117
N	-2.62961	0.90050	-3.46330
N	0.59377	-1.62813	-3.49117
Br	2.23011	0.91913	0.00000

3, TETRACYANO-FLUORIDE ANION. -699.3521595236 a.u.

C	-0.61766	1.16203	0.13783
C	-1.31440	-0.07872	-0.19364
C	-0.65790	-1.31304	-0.13947
C	0.75411	-1.39791	0.03852
C	1.48363	-0.19228	0.05715
C	0.84104	1.05063	-0.00022
C	-1.20788	2.34685	-0.51233
H	-2.38726	-0.04285	-0.39871
C	-1.43140	-2.51412	-0.33543
C	1.43150	-2.66047	0.09305
H	2.57736	-0.22313	0.07506
C	1.62980	2.24810	-0.08222

N	-1.69281	3.27178	-1.08207
N	2.29878	3.23092	-0.16252
N	-2.08174	-3.49960	-0.49737
N	2.01140	-3.70044	0.14318
F	-0.93297	1.50100	1.64296

3, TETRACYANO-CHLORIDE ANION. -1059.3779531793 a.u.

C	0.24838	1.00415	0.55978
C	1.06596	-0.13649	0.73022
C	0.57533	-1.41156	0.41597
C	-0.75761	-1.56628	-0.06607
C	-1.59437	-0.44052	-0.17007
C	-1.11157	0.83363	0.17949
C	0.70970	2.28475	1.03427
H	2.09924	-0.01025	1.05934
C	1.42341	-2.56347	0.57818
C	-1.26799	-2.86732	-0.40738
H	-2.62449	-0.55709	-0.51603
C	-1.99499	1.96570	0.09413
N	1.03749	3.30327	1.55802
N	-2.76639	2.87179	0.04616
N	2.11971	-3.51769	0.73205
N	-1.70972	-3.93869	-0.68335
Cl	1.39006	1.51096	-1.80345

4, TETRACYANO-FLUORIDE ANION. -699.3487321985 a.u.

C	1.21282	0.00000	-1.09941
C	0.00000	0.00000	-1.81358
C	-1.21282	0.00000	-1.09941
C	-1.19026	0.00000	0.32990
C	0.00000	0.00000	1.10902
C	1.19026	0.00000	0.32990
C	2.45048	0.00000	-1.83834
H	0.00000	0.00000	-2.90677
C	-2.45048	0.00000	-1.83834
C	-2.47307	0.00000	1.00498
H	0.00000	0.00000	2.66098
C	2.47307	0.00000	1.00498
N	3.45935	0.00000	-2.47266
N	3.54811	0.00000	1.51728
N	-3.45935	0.00000	-2.47266
N	-3.54811	0.00000	1.51728
F	0.00000	0.00000	3.69945

4, TETRACYANO-CHLORIDE ANION. -1059.3745631877 a.u.

C	0.00000	-1.21706	-1.40589
C	0.00000	0.00000	-2.11354
C	0.00000	1.21706	-1.40589
C	0.00000	1.21208	0.01862
C	0.00000	0.00000	0.74016
C	0.00000	-1.21208	0.01862
C	0.00000	-2.45293	-2.14754
H	0.00000	0.00000	-3.20642
C	0.00000	2.45293	-2.14754

C	0.00000	2.48092	0.70701
H	0.00000	0.00000	1.86730
C	0.00000	-2.48092	0.70701
N	0.00000	-3.45420	-2.79229
N	0.00000	-3.57333	1.18052
N	0.00000	3.45420	-2.79229
N	0.00000	3.57333	1.18052
Cl	0.00000	0.00000	3.89116

4, TETRACYANO-BROMIDE ANION. -3172.2584167556 a.u.

C	0.00000	-1.21743	-2.01870
C	0.00000	0.00000	-2.72576
C	0.00000	1.21743	-2.01870
C	0.00000	1.21322	-0.59442
C	0.00000	0.00000	0.12390
C	0.00000	-1.21322	-0.59442
C	0.00000	-2.45327	-2.76026
H	0.00000	0.00000	-3.81863
C	0.00000	2.45327	-2.76026
C	0.00000	2.48132	0.09459
H	0.00000	0.00000	1.24304
C	0.00000	-2.48132	0.09459
N	0.00000	-3.45419	-3.40548
N	0.00000	-3.57493	0.56554
N	0.00000	3.45419	-3.40548
N	0.00000	3.57493	0.56554
Br	0.00000	0.00000	3.44846

5, TRICYANO-FLUORIDE ANION. -607.3049199007 a.u. (-65.3; -65.3 cm^{-1})

C	-1.39585	-0.03206	0.25636
C	-0.67858	-1.24028	0.25873
C	-2.83959	-0.06522	0.26349
H	-1.20256	-2.19795	0.22911
N	-4.02808	-0.09225	0.29872
F	-0.00000	0.00000	-2.21789
C	0.72568	-1.19281	0.25636
C	0.67016	1.22487	0.25636
C	1.41340	0.03247	0.25873
C	-0.73482	1.20781	0.25873
C	1.47628	-2.42655	0.26349
C	1.36331	2.49177	0.26349
H	2.50476	0.05753	0.22911
H	-1.30220	2.14042	0.22911
N	2.09393	-3.44230	0.29872
N	1.93415	3.53454	0.29872

5, TRICYANO-CHLORIDE ANION. -967.3532302847 a.u. (-14,0; -14.0 cm^{-1})

C	-1.40820	0.13617	-0.53119
C	-0.57908	1.27204	-0.52997
C	-1.17819	2.58614	-0.53652
H	-2.49461	0.24115	-0.49813
N	-1.67188	3.66711	-0.57980
Cl	0.00000	0.00000	2.50722
C	0.58617	-1.28763	-0.53119

C	0.82203	1.15145	-0.53119
C	-0.81207	-1.13752	-0.52997
C	1.39116	-0.13452	-0.52997
C	-1.65057	-2.31341	-0.53652
C	2.82875	-0.27273	-0.53652
H	1.03846	-2.28097	-0.49813
H	1.45615	2.03982	-0.49813
N	-2.33987	-3.28144	-0.57980
N	4.01175	-0.38566	-0.57980

5, TRICYANO-BROMIDE ANION. -3080.2392284262 a.u.

C	0.97527	1.02520	-0.94149
C	1.35903	-0.32803	-0.94041
C	2.76286	-0.66687	-0.94781
H	1.72755	1.81599	-0.90894
N	3.91800	-0.94569	-0.99274
Br	0.00000	-0.00000	2.25694
C	-1.37548	0.33201	-0.94149
C	0.40021	-1.35721	-0.94149
C	-0.39543	1.34097	-0.94041
C	-0.96360	-1.01294	-0.94041
C	-0.80390	2.72615	-0.94781
C	-1.95896	-2.05927	-0.94781
H	-2.43647	0.58811	-0.90894
H	0.70892	-2.40410	-0.90894
N	-1.14001	3.86593	-0.99274
N	-2.77799	-2.92025	-0.99274

6, TRICYANO-FLUORIDE ANION. -607.3345811788 a.u.

C	0.21537	0.47631	1.22244
C	0.02308	-0.90605	1.21822
C	-0.14211	-1.61094	0.00000
C	0.02308	-0.90605	-1.21822
C	0.21537	0.47631	-1.22244
C	0.01050	1.28902	0.00000
C	-0.33299	-3.03186	0.00000
C	0.51968	1.15738	2.44707
H	0.06173	-1.45683	2.16401
H	0.06173	-1.45683	-2.16401
C	0.51968	1.15738	-2.44707
H	0.58428	2.22657	0.00000
N	0.78920	1.73510	3.45536
N	0.78920	1.73510	-3.45536
N	-0.49391	-4.21370	0.00000
F	-1.39846	1.80349	0.00000

6, TRICYANO-CHLORIDE ANION. -967.3551621007 a.u.

C	1.20097	0.30555	0.52102
C	1.23840	-1.06860	0.22316
C	0.02470	-1.76524	0.05198
C	-1.21189	-1.10704	0.21095
C	-1.22056	0.26756	0.50897
C	-0.02155	1.00524	0.61282
C	0.04835	-3.17628	-0.25164

C	2.44482	1.01038	0.72158
H	2.19490	-1.58678	0.11943
H	-2.15059	-1.65495	0.09778
C	-2.48784	0.93300	0.69702
H	-0.03940	2.06779	0.84858
N	3.48381	1.54769	0.93647
N	-3.54526	1.43742	0.90145
N	0.06782	-4.34203	-0.48930
Cl	-0.02678	2.13884	-1.86844

6, TRICYANO-BROMIDE ANION. -3080.2403988245 a.u.

C	0.78572	0.31724	-1.21154
C	0.11898	1.55560	-1.22583
C	-0.22796	2.15965	0.00000
C	0.11898	1.55560	1.22583
C	0.78572	0.31724	1.21154
C	1.07995	-0.34398	0.00000
C	-0.91037	3.43182	0.00000
C	1.16223	-0.28860	-2.46658
H	-0.13400	2.03771	-2.17323
H	-0.13400	2.03771	2.17323
C	1.16223	-0.28860	2.46658
H	1.58973	-1.30633	0.00000
N	1.50950	-0.73266	-3.51381
N	1.50950	-0.73266	3.51381
N	-1.46000	4.48712	0.00000
Br	-1.16930	-2.18052	0.00000

7, TRICYANO-FLUORIDE ANION. -607.3193609577 a.u.

C	-0.01112	-1.25677	-0.05443
C	1.21564	-0.51893	-0.18535
C	1.21409	0.88363	-0.07260
C	0.01291	1.62432	0.01929
C	-1.20073	0.90365	-0.06775
C	-1.22599	-0.49868	-0.18044
C	2.47098	1.59221	-0.09625
C	-0.02347	-2.60868	-0.60503
H	2.15896	-1.06001	-0.29333
H	0.02210	2.71349	0.09745
C	-2.44579	1.63298	-0.08635
H	-2.17859	-1.02405	-0.28459
N	-0.03375	-3.67719	-1.12864
N	-3.46854	2.24366	-0.10557
N	3.50363	2.18585	-0.11962
F	-0.01264	-1.85118	1.63476

7, TRICYANO-CHLORIDE ANION. -967.3537734340 a.u. (-14.64 cm^{-1})

C	-0.00703	-0.98129	-0.66243
C	1.22223	-0.30335	-0.53519
C	1.21477	1.06337	-0.20483
C	0.00620	1.76737	-0.02485
C	-1.20902	1.07470	-0.20285
C	-1.22965	-0.29188	-0.53403
C	2.46695	1.76901	-0.05691

C	-0.01393	-2.36635	-1.07495
H	2.16218	-0.84943	-0.63336
H	0.01134	2.82689	0.24124
C	-2.45444	1.79181	-0.05298
H	-2.17491	-0.82884	-0.63184
N	-0.02037	-3.45542	-1.55248
N	-3.47302	2.39749	0.05091
N	3.49100	2.36570	0.04517
Cl	0.00783	-1.86801	2.03245

8, TRICYANO-FLUORIDE ANION. -607.3214706194 a.u.

C	0.00000	1.19185	-0.28526
C	0.00000	1.22166	1.12901
C	0.00000	0.00000	1.82998
C	0.00000	-1.22166	1.12901
C	0.00000	-1.19185	-0.28526
C	0.00000	0.00000	-1.05401
C	0.00000	0.00000	3.27486
C	0.00000	2.48125	-0.95429
H	0.00000	2.17123	1.67255
H	0.00000	-2.17123	1.67255
C	0.00000	-2.48125	-0.95429
H	0.00000	0.00000	-2.33954
N	0.00000	3.57621	-1.41841
N	0.00000	-3.57621	-1.41841
N	0.00000	0.00000	4.46455
F	0.00000	0.00000	-3.58119

8, TRICYANO-CHLORIDE ANION. -967.3534364159 a.u.

C	-1.19919	-0.10068	-0.00619
C	-1.23842	-1.51264	-0.00043
C	-0.02449	-2.22743	0.00258
C	1.20994	-1.54865	-0.00007
C	1.21222	-0.13614	-0.00583
C	0.01730	0.61492	-0.00900
C	-0.04574	-3.67245	0.00846
C	-2.46959	0.59535	-0.00911
H	-2.19463	-2.04253	0.00164
H	2.15015	-2.10642	0.00229
C	2.50252	0.52227	-0.00836
H	0.03370	1.73441	-0.01367
N	-3.56446	1.05912	-0.01104
N	3.61049	0.95381	-0.00996
N	-0.06322	-4.86173	0.01330
Cl	0.06341	3.81874	-0.02304

8, TRICYANO-BROMIDE ANION. -3080.2378127903 a.u.

C	0.00000	1.20678	0.71727
C	0.00000	1.22461	2.12948
C	0.00000	0.00000	2.82596
C	0.00000	-1.22461	2.12948
C	0.00000	-1.20678	0.71727
C	0.00000	0.00000	-0.01356
C	0.00000	0.00000	4.27115

C	0.00000	2.48647	0.03913
H	0.00000	2.17289	2.67330
H	0.00000	-2.17289	2.67330
C	0.00000	-2.48647	0.03913
H	0.00000	0.00000	-1.12699
N	0.00000	3.58836	-0.40789
N	0.00000	-3.58836	-0.40789
N	0.00000	0.00000	5.46055
Br	0.00000	0.00000	-3.39060

9, TRIAZINE-FLUORIDE ANION. -379.3048274267 a.u. (-49.2; -49.2 cm-1)

N	-0.73730	1.17285	-0.50582
C	-1.29628	-0.04879	-0.48628
N	-0.64706	-1.22495	-0.50582
C	0.69039	-1.09822	-0.48628
N	1.38437	0.05210	-0.50582
C	0.60589	1.14701	-0.48628
H	-2.38960	-0.08993	-0.47589
H	1.27268	-2.02449	-0.47589
H	1.11692	2.11442	-0.47589
F	0.00000	0.00000	2.04619

9, TRIAZINE-CHLORIDE ANION. -739.3554755842 a.u.

N	0.03528	-0.87282	-1.34829
C	-1.10897	-0.82289	-0.64359
N	-1.21647	-0.76717	0.69572
C	-0.03265	-0.71963	1.33188
N	1.18193	-0.76282	0.75625
C	1.14233	-0.81880	-0.58677
H	-2.04183	-0.84183	-1.21389
H	-0.06031	-0.65172	2.42296
H	2.10284	-0.83430	-1.10928
Cl	-0.00142	2.34738	-0.12913

9, TRIAZINE-BROMIDE ANION. -2852.2418712145 a.u.

C	0.91977	0.91977	-1.44029
N	-0.35851	1.33797	-1.45335
H	1.69292	1.69292	-1.42936
Br	0.00000	-0.00000	1.86619
C	-1.25642	0.33666	-1.44029
C	0.33666	-1.25642	-1.44029
N	-0.97947	-0.97947	-1.45335
N	1.33797	-0.35851	-1.45335
H	-2.31257	0.61965	-1.42936
H	0.61965	-2.31257	-1.42936

10, TRIAZINE-FLUORIDE ANION. -379.3294080551 a.u.

N	-0.56710	0.00637	1.22263
C	0.34887	0.96210	1.12353
N	0.94562	1.45177	0.00000
C	0.34887	0.96210	-1.12353
N	-0.56710	0.00637	-1.22263
C	-0.77784	-0.69116	0.00000
H	0.62356	1.46865	2.06048

H	0.62356	1.46865	-2.06048
H	-1.74251	-1.21787	0.00000
F	0.18159	-1.86062	0.00000

10, TRIAZINE-CHLORIDE ANION. -739.3559045234 a.u.

N	-1.20372	-0.46387	-0.67832
C	-1.11808	-1.34345	0.33042
N	0.01491	-1.79790	0.90554
C	1.13327	-1.33198	0.31130
N	1.19281	-0.45163	-0.69865
C	-0.01134	0.01211	-1.09919
H	-2.06041	-1.73599	0.72615
H	2.08614	-1.71490	0.69091
H	-0.02182	0.77440	-1.87661
Cl	-0.01176	2.51131	0.37488

10, TRIAZINE-BROMIDE ANION. -2852.2417747178 a.u.

N	-0.71529	1.18983	1.19852
C	0.37718	1.96523	1.12631
N	1.00297	2.36479	0.00000
C	0.37718	1.96523	-1.12631
N	-0.71529	1.18983	-1.19852
C	-1.17121	0.76780	0.00000
H	0.80330	2.30986	2.07380
H	0.80330	2.30986	-2.07380
H	-2.01742	0.08122	0.00000
Br	0.26485	-1.97202	0.00000

11, TRIAZINE-FLUORIDE ANION. -379.3169709605 a.u.

N	0.00000	1.19305	0.08739
C	0.00000	1.12239	1.42738
N	0.00000	0.00000	2.17792
C	0.00000	-1.12239	1.42738
N	0.00000	-1.19305	0.08739
C	0.00000	0.00000	-0.57682
H	0.00000	2.07246	1.97453
H	0.00000	-2.07246	1.97453
H	0.00000	0.00000	-1.72876
F	0.00000	0.00000	-3.26239

11, TRIAZINE-CHLORIDE ANION. -739.3588083346 a.u.

N	-1.19828	-0.64494	-0.00231
C	-1.10939	-1.98503	0.00339
N	0.02547	-2.71493	0.00620
C	1.14013	-1.95454	0.00264
N	1.19266	-0.61254	-0.00310
C	-0.01149	0.01186	-0.00542
H	-2.05112	-2.54394	0.00602
H	2.09666	-2.48773	0.00464
H	-0.02650	1.11750	-0.01008
Cl	-0.05818	3.41902	-0.01891

11, TRIAZINE-BROMIDE ANION. -2852.2442695895 a.u.

N	0.00000	1.19585	1.48105

C	0.00000	1.12523	2.82241
N	0.00000	0.00000	3.56686
C	0.00000	-1.12523	2.82241
N	0.00000	-1.19585	1.48105
C	0.00000	0.00000	0.84328
H	0.00000	2.07432	3.36838
H	0.00000	-2.07432	3.36838
H	0.00000	0.00000	-0.25968
Br	0.00000	0.00000	-2.73633

12, HEXAFLUOROBENZENE-FLUORIDE ANION. -925.5378550230 a.u.

C	1.28241	-0.54910	-0.24677
F	2.52890	-1.08048	-0.21607
F	0.00000	-0.00000	2.28285
C	-0.16567	1.38514	-0.24677
C	-1.11674	-0.83605	-0.24677
C	-1.28241	0.54910	-0.24677
C	0.16567	-1.38514	-0.24677
C	1.11674	0.83605	-0.24677
F	-0.32873	2.73033	-0.21607
F	-2.20017	-1.64985	-0.21607
F	-2.52890	1.08048	-0.21607
F	0.32873	-2.73033	-0.21607
F	2.20017	1.64985	-0.21607

12, HEXAFLUOROBENZENE-CHLORIDE ANION. -1285.5874924051 a.u.

C	1.37919	-0.13728	0.51326
C	0.54481	-1.24789	0.55225
C	-0.83485	-1.08098	0.54577
C	-1.37995	0.19649	0.50021
C	-0.54554	1.30709	0.46123
C	0.83413	1.14022	0.46771
F	2.70951	-0.29819	0.51952
F	1.07043	-2.47965	0.59619
F	-1.63944	-2.15182	0.58333
F	-2.71024	0.35742	0.49394
F	-1.07116	2.53894	0.41723
F	1.63870	2.21105	0.43014
Cl	0.00194	-0.15680	-2.68269

12, HEXAFLUOROBENZENE-BROMIDE ANION. -3398.4732559122 a.u.

C	-0.98451	0.98451	0.89668
F	-1.94078	1.94078	0.91219
Br	-0.00000	0.00000	-2.32596
C	-0.36036	-1.34487	0.89668
C	1.34487	0.36036	0.89668
C	0.98451	-0.98451	0.89668
C	0.36036	1.34487	0.89668
C	-1.34487	-0.36036	0.89668
F	-0.71038	-2.65116	0.91219
F	2.65116	0.71038	0.91219
F	1.94078	-1.94078	0.91219
F	0.71038	2.65116	0.91219
F	-2.65116	-0.71038	0.91219

13, HEXAFLUOROBENZENE-FLUORIDE ANION. -925.5487386394 a.u.

C	-1.19506	-0.89963	-0.02044
C	-0.00884	-1.64068	-0.00839
C	1.18547	-0.91267	-0.01653
C	1.19173	0.48241	-0.03564
C	0.00736	1.30458	-0.04889
C	-1.18597	0.49543	-0.03970
F	-2.39961	-1.55612	-0.01326
F	-0.01640	-3.01520	0.01058
F	2.38272	-1.58233	-0.00540
F	2.40661	1.12867	-0.04269
F	0.01460	2.28120	-1.15811
F	-2.39367	1.15496	-0.05068
F	0.01105	2.31134	1.03312

TETRACYANOBENZENE. -599.6087673856 a.u.

C	-0.71112	-1.22003	0.00000
C	-1.41505	0.00000	0.00000
C	-0.71112	1.22003	0.00000
C	0.71112	1.22003	0.00000
C	1.41505	0.00000	0.00000
C	0.71112	-1.22003	0.00000
C	-1.43671	-2.46413	0.00000
H	-2.50803	0.00000	0.00000
C	-1.43671	2.46413	0.00000
C	1.43671	2.46413	0.00000
H	2.50803	0.00000	0.00000
C	1.43671	-2.46413	0.00000
N	-2.04537	-3.48749	0.00000
N	2.04537	-3.48749	0.00000
N	-2.04537	3.48749	0.00000
N	2.04537	3.48749	0.00000

TRICYANOBENZENE. -507.5961931348 a.u.

C	1.32557	-0.45834	0.00000
C	0.26867	-1.39173	0.00000
C	-1.05971	-0.91881	0.00000
C	-1.33961	0.46319	0.00000
C	-0.26585	1.37714	0.00000
C	1.07094	0.92854	0.00000
C	-2.15138	-1.86529	0.00000
C	2.69108	-0.93050	0.00000
H	0.47576	-2.46453	0.00000
H	-2.37223	0.82024	0.00000
C	-0.53970	2.79579	0.00000
H	1.89646	1.64429	0.00000
N	3.81487	-1.31915	0.00000
N	-0.76502	3.96335	0.00000
N	-3.04986	-2.64420	0.00000

TRIAZINE. -279.6193158697 a.u.

N	1.33837	-0.35862	0.00000
C	0.92288	0.92288	0.00000

N	-0.35862	1.33837	0.00000
C	-1.26067	0.33780	0.00000
N	-0.97975	-0.97975	0.00000
C	0.33780	-1.26067	0.00000
H	1.69599	1.69599	0.00000
H	-2.31676	0.62077	0.00000
H	0.62077	-2.31676	0.00000

HEXAFLUOROBENZENE. -825.8391823112 a.u.

C	-1.27087	-0.58793	0.00000
C	-1.14460	0.80664	0.00000
C	0.12627	1.39457	0.00000
C	1.27087	0.58793	0.00000
C	1.14460	-0.80664	0.00000
C	-0.12627	-1.39457	0.00000
F	-2.49302	-1.15192	0.00000
F	-2.24410	1.58306	0.00000
F	0.24892	2.73497	0.00000
F	2.49302	1.15192	0.00000
F	2.24410	-1.58306	0.00000
F	-0.24892	-2.73497	0.00000

FLUORIDE ANION. -99.6681122581 a.u.

CHLORIDE ANION. -459.7227643886 a.u.

BROMIDE ANION. -2572.6092871756 a.u.

SUPPORTING MATERIAL REFERENCES

Full citation for NWChem software: Straatsma, T.P.; Apra, E.; Windus, T.L.; Bylaska, E.J.; de Jong, W.; Hirata, S.; Valiev, M.; Hackler, M. T.; Pollack, L.; Harrison, R. J.; Dupuis, M.; Smith, D.M.A; Nieplocha, J.; Tipparaju V.; Krishnan, M.; Auer, A. A.; Brown, E.; Cisneros, G.; Fann, G. I.; Fruchtl, H.; Garza, J.; Hirao, K.; Kendall, R.; Nichols, J.; Tsemekhman, K.; Wolinski, K.; Anchell, J.; Bernholdt, D.; Borowski, P.; Clark, T.; Clerc, D.; Dachsel, H.; Deegan, M.; Dyall, K.; Elwood, D.; Glendening, E.; Gutowski, M.; Hess, A.; Jaffe, J.; Johnson, B.; Ju, J.; Kobayashi, R.; Kutteh, R.; Lin, Z.; Littlefield, R.; Long, X.; Meng, B.; Nakajima, T.; Niu, S.; Rosing, M.; Sandrone, G.; Stave, M.; Taylor, H.; Thomas, G.; van Lenthe, J.; Wong, A.; Zhang, Z.;

"NWChem, A Computational Chemistry Package for Parallel Computers, Version 4.6" (2004), Pacific Northwest National Laboratory, Richland, Washington 99352-0999, USA.

STATISTICAL ANALYSIS OF THE POSITION OF ELECTRONEGATIVE ATOMS ABOVE THE PENTAFLUOROARENES. The experimental probability, expressed as a percent, of locating an atom at a given d(offset) value was determined by binning d(offset) values for the points shown in Figure 16 from 0.0 to 2.0 angstroms using a bin size of 0.05, dividing the number in each bin by the total number of points, and multiplying the result by 100.

The theoretical probablility, expressed as a percent, of finding an atom with a given d(offset) value for a randomly distributed set of atoms was determined by computing the area of a disc with an inner radius of r1 and an outer radius of r1+0.05 angstroms, where r1 ranged from 0 to 1.95 angstroms, dividing this area by the total area of a circle of radius 2.00 angstroms, and multiplying by 100.

A plot of the experimental probability (circles) and the theoretical probability (dashed line) versus the d(offset) value, presented below, shows that the experimental points track the theoretical line over the range of the data.

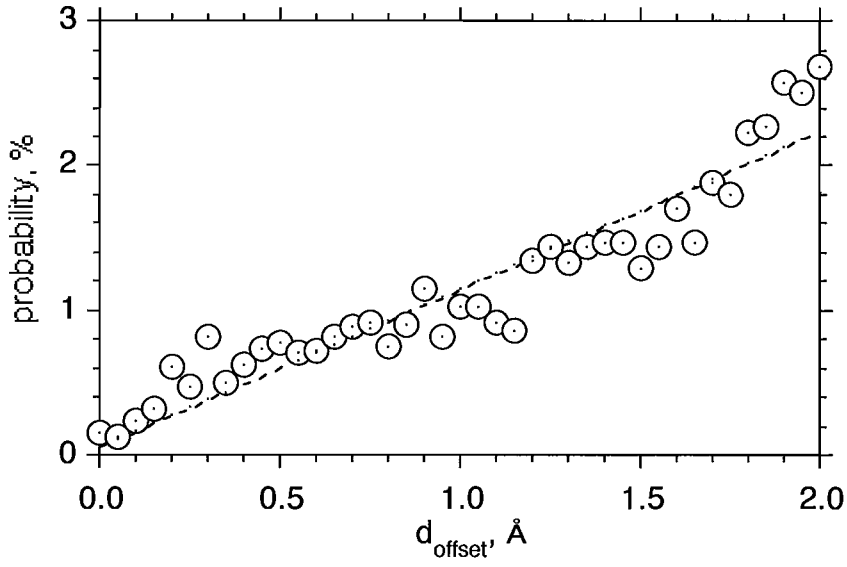

Graph B.1 Statistical analysis of the position of electronegative atoms above pentafluoroarenes.

APPENDIX C

SUPPORTING INFORMATION FOR CHAPTER IV: SOLUTION PHASE MEASUREMENT OF *BOTH* WEAK SIGMA *AND* C–H•••X⁻ HYDROGEN BONDING INTERACTIONS IN SYNTHETIC ANION RECEPTORS

EXPERIMENTAL

GENERAL. *d*-chloroform and acetonitrile were dried over 3Å molecular sieves. Tetra-*n*-alkylammonium salts were dried under a vacuum at 50°C (25°C for the $NHep_4^+Cl^-$) and stored in a calcium carbonate filled dessiccator. All other materials were obtained from TCI-America, Sigma-Aldrich, Acros and Strem and used as received. All glassware was flame dried immediately prior to use. Nuclear Magnetic Resonance ^1H NMR and ^{13}C NMR spectra were recorded on a Varian INOVA 300 (299.935) and 125 (125.751) MHz spectrometer respectively. Chemical shifts (δ) are expressed as ppm downfield from tetramethylsilane using either the residual solvent peak as an internal standard ($CDCl_3$ ^1H: 7.27 ppm, ^{13}C: 77.00 ppm), (C_6D_6 ^1H: 7.16 ppm, ^{13}C: 128.39 ppm) (d_6-DMSO ^1H: 2.50 ppm, ^{13}C: 39.51 ppm) or using $CDCl_3$ spiked with 1%

trimethylsilane for the ^{1}H NMR spectra. Signal patterns are indicated as b, broad; s, singlet; d, doublet; t, triplet; m, multiplet. Coupling constants (*J*) are given in hertz.

1,3,5-tris(bromomethyl)-2,4,6-triethylbenzene (5).[1] To a mixture of paraformaldehyde (16.7 g, 556.3 mmol) and triethylbenzene 2 (10.0 mL, 53.1 mmol) in 100 mL of HBr/AcOH (30 wt %) zinc bromide (19.7 g, 87.5 mmol) was slowly added at room temperature. The mixture was heated to 90 °C for 16.5 h, during which time white crystals formed. The reaction was cooled to room temperature, and the white solid was filtered off. The white crystals were washed with water (3 × 100 ml), and dried under vacuum overnight to give 22.79 g (51.7 mmol, 97%) of **5** as a white solid. Mp 169-170 °C; ^{1}H NMR (0.1 M in $CDCl_3$, 300 MHz) δ 4.58 (s, 6H), 2.94 (q, J = 7.7 Hz, 6H), 1.34 (t, J = 7.7 Hz, 9H); ^{13}C NMR ($CDCl_3$, 300 MHz) δ 145.0, 132.6, 28.5, 22.7, 15.6.

1,3,5-tris(2,4-dinitrobenzoatomethyl)-2,4,6-triethylbenzene (1).[2] 1,3,5-tris(bromomethyl)-2,4,6-triethylbenzene (**5**) (0.441 g, 1.00 mmol) was added to a stirring suspension of 2,4-dinitrobenzoic acid (1.06 g, 5.0 mmol), and CsF-Celite (1.13 g) in 150 ml of acetonitrile. The reaction mixture was heated at reflux for 16 h. After cooling to room temperature the lemon-yellow solution was evaporated under reduced pressure. The remaining yellow powder was dissolved in ethyl acetate and the solid CsF-Celite was filtered off. Evaporation of the remaining organic solvent produced an off-white solid that was dissolved in a minimal amount of dimethylsulfoxide. Water

was added slowly to precipitate out a white solid. The crude product was filtered off and washed with cold methanol to remove residual acid. The white solid was dried in air to yield pure product (0.5 g, 60%). mp 180-181 °C; ^{1}H NMR ($CDCl_3$, 300 MHz) δ 8.825 (sd, 3H), 8.535 (dd, 3H), 7.899 (d, 3H), 5.544 (s, 6H), 2.871 (q, 6H), 1.213 (t, 9H); ^{1}H NMR (0.005M in C_6D_6, 300 MHz) δ 7.81 (sd, 3H), 7.62 (dd, 3H), 6.76 (d, 3H), 5.47 (s, 6H), 2.94 (q, 6H), 1.08 (t, 9H); ^{1}H NMR (d_6-DMSO 300 MHz) δ 8.81 (s, 3H), 8.64 (dd, 3H), 8.15 (d, 3H), 5.50 (s, 6H), 2.86 (q, 6H), 1.16 (t, 9H); ^{13}C NMR (d_6-DMSO, 300 MHz) δ 163.7, 148.9, 147.3, 147.1, 131.5, 131.3, 128.9, 128.6, 120.0, 63.0, 22.3, 16.1

1,3,5-tris(3,5-dinitrobenzoatomethyl)-2,4,6-triethylbenzene (2).[2] 1,3,5-tris(bromomethyl)-2,4,6-triethylbenzene (**5**) (0.441 g, 1.00 mmol) was added to a stirring suspension of 2,4-dinitrobenzoic acid (1.06 g, 5.0 mmol), and CsF-Celite (2.00 g) in 150 ml of acetonitrile. The reaction mixture was heated at reflux for 16 h. After cooling to room temperature the lemon-yellow solution was evaporated under reduced pressure. The remaining yellow powder was dissolved in ethyl acetate and the solid CsF-Celite was filtered off. Evaporation of the remaining organic solvent produced an off-white solid that was dissolved in a minimal amount of dimethylsulfoxide. Water was added slowly to precipitate out a white solid. The crude product was filtered off and washed with cold methanol. Residual 3,5-dinitrobenzoic acid is removed by dissolving the remaining solid in acetone (2 ml) and methanol (4 ml) followed by slow evaporation of the acetone. Pure (**2**) was isolated by filtering off the white solid and

washing with cold methanol (3 ml) yielding a white powder (0.5g, 60%). mp 201.5-202.5 °C; ^{1}H NMR ($CDCl_3$, 300 MHz) δ 9.23 (t, 3H), 9.15 (sd, 6H), 5.62 (s, 6H), 2.97 (q, 6H), 1.23 (t, 9H); ^{1}H NMR (DMSO-d_6, 300 MHz) δ 9.03 (t, 3H), 8.86 (sd, 6H), 5.68 (s, 6H), 3.00 (q, 6H), 1.32 (t, 9H); ^{13}C NMR (d_6-DMSO, 300 MHz) δ 162.6, 148.3, 147.5, 132.5, 129.5, 128.8, 122.6, 62.6, 22.5, 16.3

1,3,5-tris(3,4-dinitrobenzoatomethyl)-2,4,6-triethylbenzene (3).[2] 1,3,5-tris(bromomethyl)-2,4,6-triethylbenzene (**5**) (0.441 g, 1.00 mmol) was added to a stirring suspension of 3,4-dinitrobenzoic acid (1.06 g, 5.0 mmol), and CsF-Celite (1.13 g) in 150 ml of acetonitrile. The reaction mixture was heated at reflux for 16 h. After cooling to room temperature the lemon-yellow solution was evaporated under reduced pressure. The remaining yellow powder was dissolved in ethyl acetate and the solid CsF-Celite was filtered off. Evaporation of the remaining organic solvent produced an off-white solid that was dissolved in a minimal amount of dimethylsulfoxide. Water was added slowly to precipitate out a white solid. The crude product was filtered off and washed with cold methanol to remove residual acid. Pure product was obtained by flash column chromatography with 2:1 hexanes:ethyl acetate as the eluent (20%). mp 230 °C (decomp); ^{1}H NMR ($CDCl_3$, 300 MHz) δ 8.55 (sd, 3H), 8.44 (dd, 3H), 7.99 (d, 3H) 5.61 (s, 6H), 2.91 (q, 6H), 1.27 (t, 9H); ^{1}H NMR (d_6-DMSO, 300 MHz) δ 8.57 (sd, 3H), 8.42 (dd, 3H), 8.33 (d, 3H) 5.56 (s, 6H), 2.92 (q, 6H), 1.18 (t, 9H); ^{1}H NMR (0.001 M in C_6D_6, 300 MHz) δ 7.93 (sd, 3H), 7.42 (d, 3H), 6.61 (dd, 3H), 5.43 (s, 6H), 2.88 (q, 6H), 1.08 (t, 9H).

1,3,5-tris(benzoatomethyl)-2,4,6-triethylbenzene (4).[2] 1,3,5-tris(bromomethyl)-2,4,6-triethylbenzene (**5**) (0.661 g, 1.5 mmol) was added to a stirring suspension of benzoic acid (0.916 g, 7.5 mmol), and CsF-Celite (3.00 g) in 200 ml of acetonitrile. The reaction mixture was heated at reflux for 20 h. After cooling to room temperature the creamy white suspension was filtered and evaporated under reduced pressure. The remaining yellow oil was refluxed with water (200 ml) and the yellow solid was filtered off. The crude product was recrystallized from a minimal amount of acetone (0.605g, 73.7%). mp 139-140 °C; ^{1}H NMR (d_6-DMSO, 300 MHz) δ 7.93 (d, 6H), 7.65 (t, 3H), 7.50 (t, 6H) 5.48 (s, 6H), 2.84 (q, 6H), 1.18 (t, 9H); ^{13}C NMR (d_6-DMSO, 300 MHz) δ 166.8, 147.9, 133.3, 131.1, 131.0, 130.3, 128.9, 61.8, 23.6, 16.9

NMR SPECTROSCOPIC TITRATIONS

GENERAL. ^{1}H NMR spectra were recorded on a Varian 300, 500 or 600 MHz spectrometer. Each titration was performed with 9 to 17 measurements in C_6D_6 at room temperature or 27 °C in a water bath. C_6D_6 was dried over 3Å molecular sieves. Anion stock solutions were prepared by diluting with a known amount of receptor stock solution such that a constant receptor concentration is maintained throughout the titration. Aliquots from a stock solution of tetra-*n*-alkylammonium salts (ca. 200 or 500 mM) were added to the initial solution of receptor (1–5 mM). All additions were done through septa with Hamilton gas tight syringes to minimize evaporation. All proton signals were referenced to the residual solvent peak C_6H_6 (7.16 ppm). The association constants (K_a) were calculated by non-linear regression curve fitting software.[3] The reported association constants were calculated from the proton on the receptor that exhibits the largest change throughout the titration and are presented as an average of two or three measurements.

Table C.1 1,3,5-tris(2,4-dinitrobenzoatomethyl)-2,4,6-triethylbenzene (**1**) and tetra-*n*-heptylammonium bromide trial 1.

Addition	X^- equiv. (M)	Vol. X^- added/aliquot (µL)	Total Vol. in tube(µL)	[X^-] (mol/L)	[R] (mol/L)	peak 1 (ppm)	peak 2 (ppm)	peak 3 (ppm)	peak 4 (ppm)
0	0.000	0	700	0	0.002051425	7.814	7.273	6.764	5.478
1	0.692	5	705	0.001418724	0.002051425	7.822	7.311	6.814	5.486
2	2.046	10	715	0.004196645	0.002051425	7.829	7.34	6.853	5.492
3	3.363	10	725	0.006897934	0.002051425	7.832	7.354	6.874	5.494
4	5.890	20	745	0.012082958	0.002051425	7.836	7.376	6.905	5.499
5	8.285	20	765	0.016996869	0.002051425	7.839	7.394	6.933	5.502
6	11.652	30	795	0.02390416	0.002051425	7.843	7.417	6.967	5.506
7	14.775	30	825	0.030309103	0.002051425	7.846	7.437	6.998	5.51
8	19.503	50	875	0.040008016	0.002051425	-	-	-	-
9	23.719	50	925	0.048658397	0.002051425	7.854	7.486	7.071	5.518
10	27.504	50	975	0.05642156	0.002051425	7.857	7.504	7.098	5.52
11	30.919	50	1025	0.063427342	0.002051425	7.86	7.518	7.12	5.522
12	36.838	100	1125	0.075570696	0.002051425	7.864	7.543	7.155	5.524
13	41.791	100	1225	0.085731462	0.002051425	-	-	-	-
14	45.997	100	1325	0.094358527	0.002051425	7.869	7.577	7.204	5.527
15	52.753	200	1525	0.108218403	0.002051425	7.874	7.599	7.237	5.529
16	59.057	250	1775	0.121151033	0.002051425	7.876	7.619	7.264	5.53

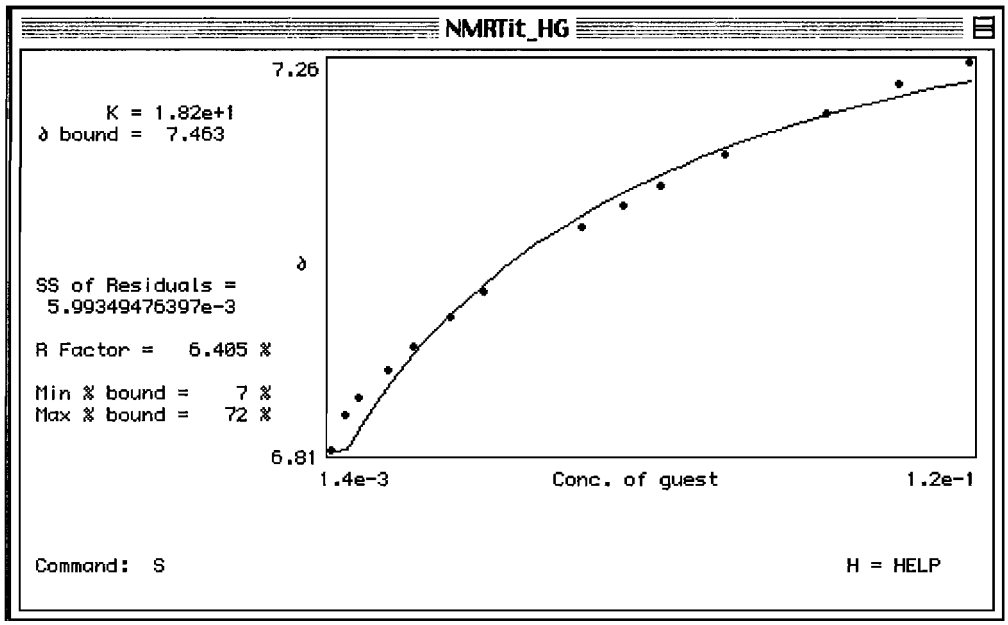

Graph C.1 Binding isotherm for titration of 1,3,5-tris(2,4-dinitrobenzoatomethyl)-2,4,6-triethylbenzene (**1**) and tetra-*n*-heptylammonium bromide trial 1.

Table C.2 1,3,5-tris(2,4-dinitrobenzoatomethyl)-2,4,6-triethylbenzene (**1**) and tetra-*n*-heptylammonium bromide trial 2.

Addition	X^- equiv. (M)	Vol. X^- added/aliquot (µL)	Total Vol. in tube(µL)	[X] (mol/L)	[R] (mol/L)	peak 1 (ppm)	peak 2 (ppm)	peak 3 (ppm)	peak 4 (ppm)
0	0.000	0	700	0	0.002051425	7.814	7.273	6.764	5.478
1	0.692	5	705	0.001418724	0.002051425	7.822	7.312	6.815	5.486
2	2.046	10	715	0.004196645	0.002051425	7.828	7.339	6.852	5.491
3	3.363	10	725	0.006897934	0.002051425	7.831	7.353	6.873	5.494
4	5.890	20	745	0.012082958	0.002051425	7.836	7.376	6.905	5.498
5	8.285	20	765	0.016996869	0.002051425	7.839	7.394	6.933	5.502
6	11.652	30	795	0.02390416	0.002051425	7.843	7.419	6.971	5.506
7	14.775	30	825	0.030309103	0.002051425	7.846	7.439	7.001	5.51
8	19.503	50	875	0.040008016	0.002051425	7.851	7.467	7.042	5.515
9	23.719	50	925	0.048658397	0.002051425	7.854	7.487	7.072	5.518
10	27.504	50	975	0.05642156	0.002051425	7.857	7.505	7.098	5.52
11	30.919	50	1025	0.063427342	0.002051425	7.86	7.518	7.12	5.522
12	36.838	100	1125	0.075570696	0.002051425	7.864	7.544	7.156	5.524
13	41.791	100	1225	0.085731462	0.002051425	-	-	-	-
14	45.997	100	1325	0.094358527	0.002051425	7.87	7.578	7.205	5.527
15	52.753	200	1525	0.108218403	0.002051425	7.874	7.6	7.238	5.529
16	59.057	250	1775	0.121151033	0.002051425	7.877	7.619	7.264	5.53

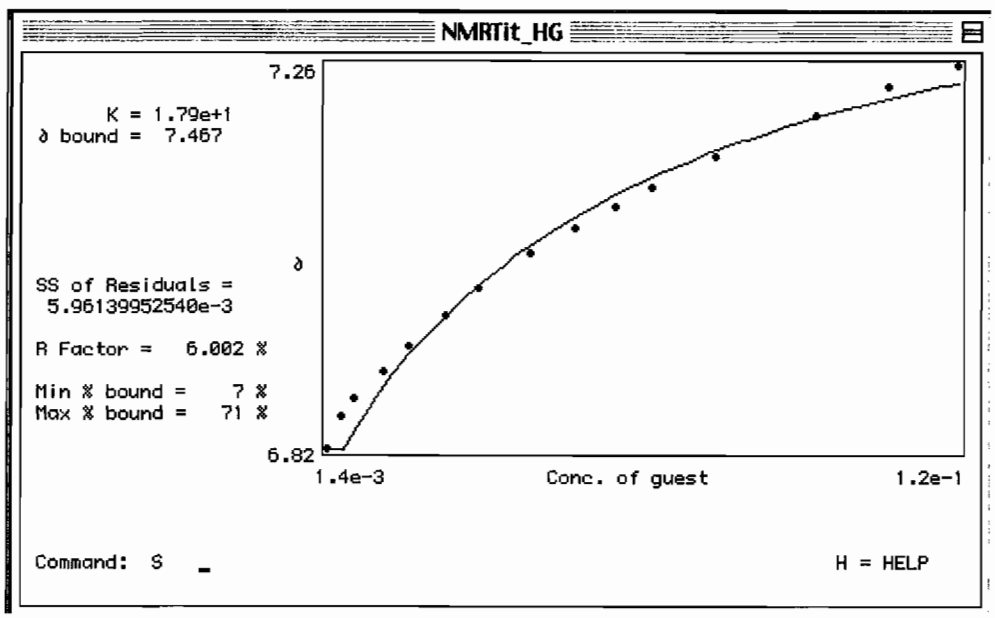

Graph C.2 Binding isotherm for titration of 1,3,5-tris(2,4-dinitrobenzoatomethyl)-2,4,6-triethylbenzene (**1**) and tetra-*n*-heptylammonium bromide trial 2.

Table C.3 1,3,5-tris(2,4-dinitrobenzoatomethyl)-2,4,6-triethylbenzene (**1**) and tetra-*n*-heptylammonium bromide trial 3.

Addition	X^- equiv. (M)	Vol. X^- added/aliquot (µL)	Total Vol. in tube(µL)	$[X^-]$ (mol/L)	[R] (mol/L)	peak 1 (ppm)	peak 2 (ppm)	peak 3 (ppm)	peak 4 (ppm)
0	0.000	0	700	0	0.002051425	7.814	7.273	6.764	5.478
1	0.692	5	705	0.001418724	0.002051425	7.823	7.304	6.818	5.486
2	2.046	10	715	0.004196645	0.002051425	7.828	7.338	6.85	5.491
3	3.363	10	725	0.006897934	0.002051425	7.831	7.351	6.87	5.494
4	5.890	20	745	0.012082958	0.002051425	7.835	7.373	6.9	5.498
5	8.285	20	765	0.016996869	0.002051425	7.838	7.39	6.928	5.501
6	11.652	30	795	0.02390416	0.002051425	7.843	7.415	6.965	5.506
7	14.775	30	825	0.030309103	0.002051425	7.846	7.436	6.997	5.51
8	19.503	50	875	0.040008016	0.002051425	7.85	7.464	7.038	5.514
9	23.719	50	925	0.048658397	0.002051425	7.854	7.485	7.069	5.517
10	27.504	50	975	0.05642156	0.002051425	7.857	7.503	7.096	5.52
11	30.919	50	1025	0.063427342	0.002051425	7.859	7.517	7.118	5.522
12	36.838	100	1125	0.075570696	0.002051425	7.864	7.542	7.154	5.524
13	41.791	100	1225	0.085731462	0.002051425	-	-	-	-
14	45.997	100	1325	0.094358527	0.002051425	7.869	7.576	7.204	5.527
15	52.753	200	1525	0.108218403	0.002051425	7.873	7.599	7.236	5.529
16	59.057	250	1775	0.121151033	0.002051425	7.877	7.619	7.264	5.53

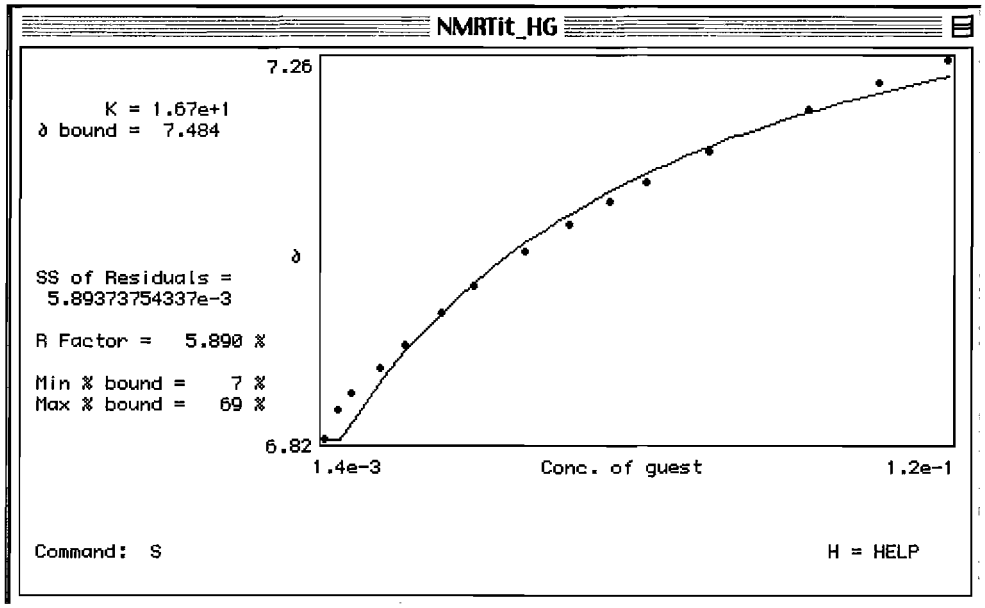

Graph C.3 Binding isotherm for titration of 1,3,5-tris(2,4-dinitrobenzoatomethyl)-2,4,6-triethylbenzene (**1**) and tetra-*n*-heptylammonium bromide trial 3.

Table C.4 1,3,5-tris(3,5-dinitrobenzoatomethyl)-2,4,6-triethylbenzene (**2**) and tetra-*n*-heptylammonium bromide trial 1.

Addition	X^- equiv. (M)	Vol. X^- added/aliquot (µL)	Total Vol. in tube(µL)	[X^-] (mol/L)	[R] (mol/L)	peak 1 (ppm)	peak 2 (ppm)	peak 3 (ppm)
0	0.000	0	700	0	0.001956908	8.59	8.371	5.476
1	0.716	5	705	0.001400971	0.001956908	8.593	8.375	5.482
2	2.118	10	715	0.004144131	0.001956908	8.595	8.376	8.484
3	3.481	10	725	0.006811617	0.001956908	8.597	8.378	5.487
4	6.097	20	745	0.011931759	0.001956908	8.597	8.378	5.489
5	8.577	20	765	0.016784181	0.001956908	8.599	8.379	5.491
6	12.062	30	795	0.023605039	0.001956908	-	-	-
7	15.294	30	825	0.029929834	0.001956908	8.599	8.38	5.496
8	20.189	50	875	0.03950738	0.001956908	8.6	8.381	5.499
9	24.554	50	925	0.048049517	0.001956908	8.601	8.382	5.502
10	28.471	50	975	0.055715537	0.001956908	-	-	-
11	32.006	50	1025	0.062633652	0.001956908	8.602	8.383	5.505
12	38.134	100	1125	0.074625052	0.001956908	8.602	8.383	5.507
13	43.261	100	1225	0.084658672	0.001956908	8.602	8.384	5.509
14	47.615	100	1325	0.093177784	0.001956908	8.602	8.384	5.51
15	54.609	200	1525	0.106864226	0.001956908	8.602	8.385	5.511
16	61.135	250	1775	0.119635025	0.001956908	8.602	8.386	5.513

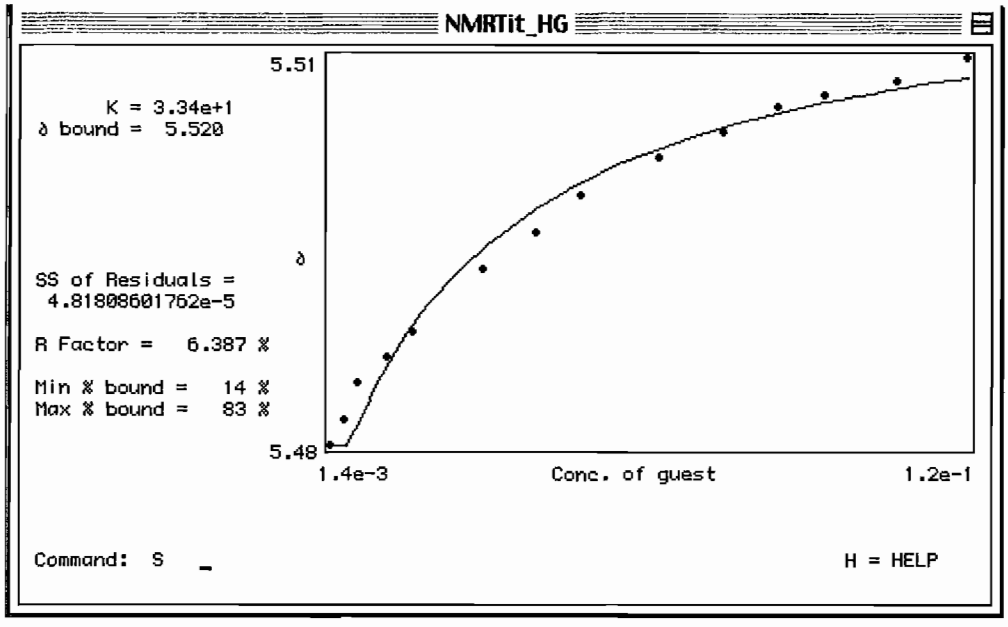

Graph C.4 Binding isotherm for titration of 1,3,5-tris(3,5-dinitrobenzoatomethyl)-2,4,6-triethylbenzene (**2**) and tetra-*n*-heptylammonium bromide trial 1.

Table C.5 1,3,5-tris(3,5-dinitrobenzoatomethyl)-2,4,6-triethylbenzene (**2**) and tetra-*n*-heptylammonium bromide trial 2.

Addition	X^- equiv. (M)	Vol. X^- added/aliquot (µL)	Total Vol. in tube(µL)	[X^-] (mol/L)	[R] (mol/L)	peak 1 (ppm)	peak 2 (ppm)	peak 3 (ppm)
0	0.000	0	700	0	0.001956908	8.589	8.371	5.475
1	0.716	5	705	0.001400971	0.001956908	8.594	8.376	5.482
2	2.118	10	715	0.004144131	0.001956908	8.596	8.377	5.486
3	3.481	10	725	0.006811617	0.001956908	8.597	8.378	5.487
4	6.097	20	745	0.011931759	0.001956908	8.598	8.379	5.489
5	8.577	20	765	0.016784181	0.001956908	8.599	8.379	5.491
6	12.062	30	795	0.023605039	0.001956908	8.599	8.38	5.494
7	15.294	30	825	0.029929834	0.001956908	8.6	8.381	5.496
8	20.189	50	875	0.03950738	0.001956908	8.6	8.381	5.498
9	24.554	50	925	0.048049517	0.001956908	8.601	8.382	5.502
10	28.471	50	975	0.055715537	0.001956908	8.601	8.382	5.502
11	32.006	50	1025	0.062633652	0.001956908	8.602	8.383	5.505
12	38.134	100	1125	0.074625052	0.001956908	8.602	8.383	5.507
13	43.261	100	1225	0.084658672	0.001956908	8.601	8.383	5.507
14	47.615	100	1325	0.093177784	0.001956908	8.602	8.384	5.51
15	54.609	200	1525	0.106864226	0.001956908	8.602	8.385	5.511
16	61.135	250	1775	0.119635025	0.001956908	8.602	8.385	5.513

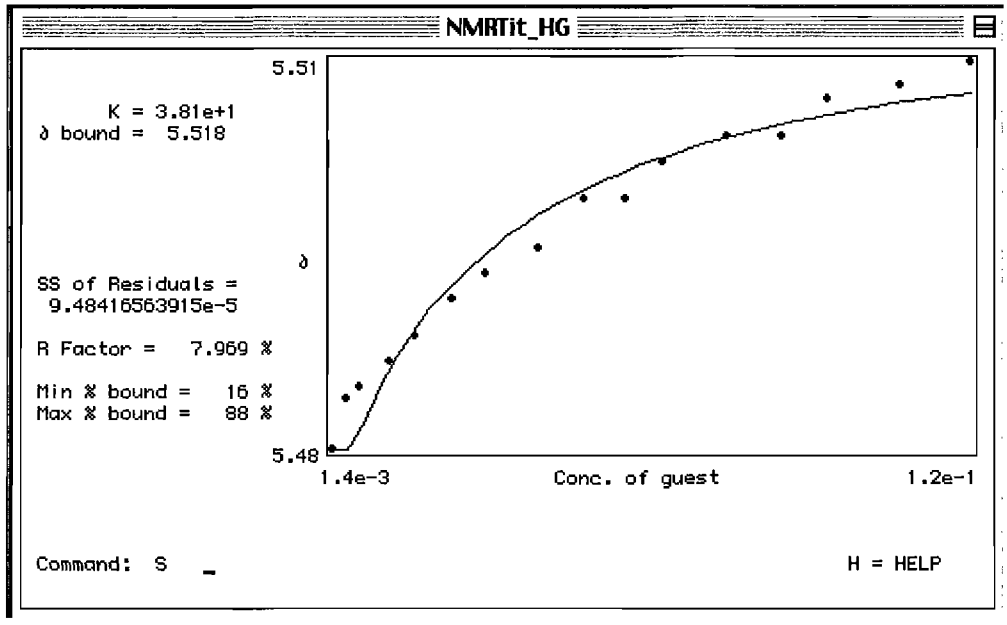

Graph C.5 Binding isotherm for titration of 1,3,5-tris(3,5-dinitrobenzoatomethyl)-2,4,6-triethylbenzene (**2**) and tetra-*n*-heptylammonium bromide trial 2.

Table C.6 1,3,5-tris(3,5-dinitrobenzoatomethyl)-2,4,6-triethylbenzene (**2**) and tetra-*n*-heptylammonium bromide trial 3.

Addition	X^- equiv. (M)	Vol. X^- added/aliquot (µL)	Total Vol. in tube(µL)	[X^-] (mol/L)	[R] (mol/L)	peak 1 (ppm)	peak 2 (ppm)	peak 3 (ppm)
0	0.000	0	650	0	0.001956908	8.59	8.372	5.476
1	0.771	5	655	0.001507915	0.001956908	8.594	8.376	5.482
2	2.277	10	665	0.00445572	0.001956908	8.596	8.377	5.485
3	3.739	10	675	0.007316182	0.001956908	8.598	8.378	5.488
4	6.536	20	695	0.012790159	0.001956908	8.598	8.379	5.491
5	9.177	20	715	0.0179579	0.001956908	8.598	8.379	5.491
6	12.872	30	745	0.025189269	0.001956908	8.6	8.38	5.495
7	16.281	30	775	0.031860791	0.001956908	8.6	8.38	5.496
8	21.412	50	825	0.041901767	0.001956908	8.601	8.382	5.5
9	25.957	50	875	0.050795203	0.001956908	8.601	8.382	5.502
10	30.010	50	925	0.058727187	0.001956908	8.601	8.382	5.503
11	33.648	50	975	0.065845634	0.001956908	8.601	8.382	5.504
12	39.908	100	1075	0.078095985	0.001956908	8.601	8.383	5.506
13	45.102	100	1175	0.088261169	0.001956908	8.601	8.383	5.509
14	49.482	100	1275	0.096831815	0.001956908	8.602	8.384	5.51
15	56.460	200	1475	0.110486742	0.001956908	8.602	8.385	5.512
16	62.907	250	1725	0.123102707	0.001956908	8.602	8.386	5.514

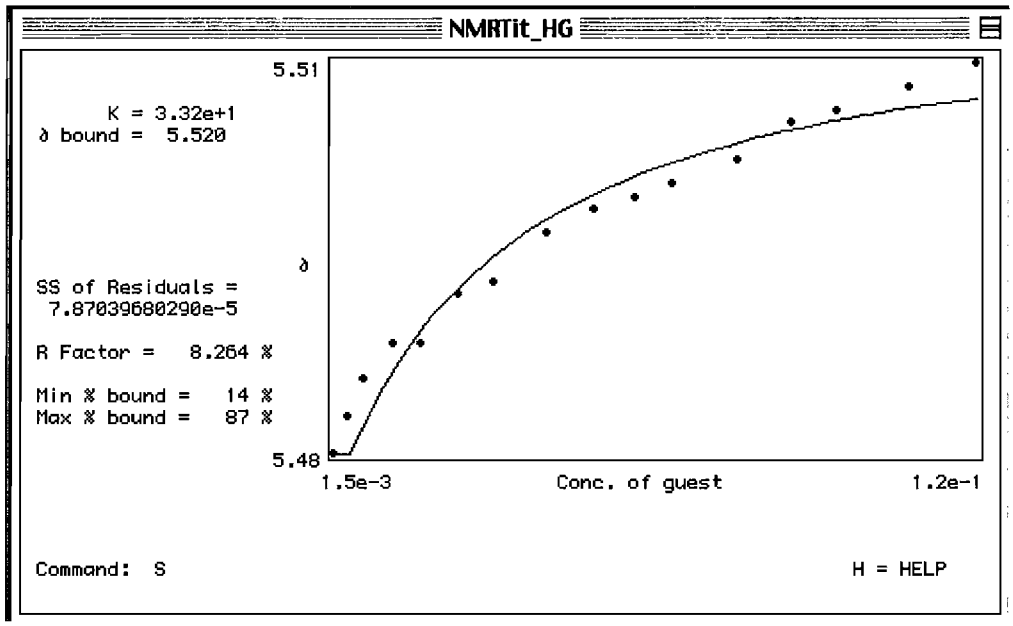

Graph C.6 Binding isotherm for titration of 1,3,5-tris(3,5-dinitrobenzoatomethyl)-2,4,6-triethylbenzene (**2**) and tetra-*n*-heptylammonium bromide trial 3.

Table C.7 1,3,5-tris(3,5-dinitrobenzoatomethyl)-2,4,6-triethylbenzene (**2**) and tetra-*n*-butylammonium bromide.

Addition	X– equiv. (M)	Vol. X– added/aliquot (μL)	Total Vol. in tube(μL)	[X–] (mol/L)	[R] (mol/L)	peak 1 (ppm)	peak 2 (ppm)	peak 3 (ppm)	peak 4 (ppm)
0	0.000	0	600	0	0.004952176	7.826	7.284	6.778	5.481
1	0.716	5	605	0.00413377	0.004952176	7.836	7.335	6.845	5.491
2	2.119	10	615	0.012199661	0.004952176	7.844	7.377	6.9	5.499
3	3.483	10	625	0.020007445	0.004952176	7.852	7.414	6.947	5.505
4	6.101	20	645	0.034896706	0.004952176	7.865	7.472	7.023	5.516
5	8.582	20	665	0.048890372	0.004952176	7.877	7.523	7.092	5.524
6	12.070	30	695	0.068370764	0.004952176	7.889	7.583	7.16	5.534
7	15.304	30	725	0.086238985	0.004952176	7.898	7.631	7.235	5.541
8	20.201	50	775	0.112945252	0.004952176	7.91	7.685	7.307	5.549
9	24.568	50	825	0.136414395	0.004952176	7.92	7.735	7.373	5.556
10	28.488	50	875	0.157201351	0.004952176	7.927	7.771	7.422	5.56
11	32.025	50	925	0.175741068	0.004952176	7.933	7.796	7.463	5.564
12	38.157	100	1025	0.207394243	0.004952176	7.938	7.823	7.496	5.565
13	43.287	100	1125	0.233420187	0.004952176	7.949	7.882	7.564	5.569
14	47.643	100	1225	0.255196998	0.004952176	7.955	7.907	7.597	5.571
15	54.641	200	1425	0.289581435	0.004952176	7.961	7.943	7.642	5.573
16	61.171	250	1675	0.32101497	0.004952176	7.967	7.96	7.681	5.574
17	101.003	stock	stock	0.500186116	0.004952176	7.989	8.106	7.843	5.568

Table C.8 1,3,5-tris(3,4-dinitrobenzoatomethyl)-2,4,6-triethylbenzene (**3**) and tetra-*n*-butylammonium bromide.

Addition	X- equiv. (mol)	Vol [X-] added (μL)	total V (μL)	[X-] (mol/L)	[R] (mol/L)	d (ppm)	c (ppm)	b (ppm)	a (ppm)
0	0.0000	0	600	0.000000	0.001	7.928	7.399	6.609	5.432
1	6.6557	10	610	0.006656	0.001	7.991	7.567	6.867	5.466
2	19.3333	20	630	0.019333	0.001	8.031	7.671	7.047	5.492
3	36.9091	30	660	0.036909	0.001	8.064	7.776	7.211	5.515
4	62.9014	50	710	0.062901	0.001	8.094	7.890	7.397	5.546
5	105.2632	50	760	0.105263	0.001	8.115	7.961	7.512	5.564
6	112.5060	70	830	0.112506	0.001	8.132	8.019	7.610	5.579
7	144.0645	100	930	0.144065	0.001	8.145	8.069	7.697	5.590
8	169.4951	100	1030	0.169495	0.001	8.154	8.103	7.758	5.598
9	199.5593	150	1180	0.199559	0.001	8.162	8.136	7.818	5.606
10	222.8421	150	1330	0.222842	0.001	8.165	8.153	7.850	5.609
11	246.7843	200	1530	0.246784	0.001	8.169	8.169	7.886	5.612
12	331.4607	250	1780	0.331461	0.001	8.175	8.183	7.919	5.613
13	406.0000	stock	stock	0.406000	0.001	8.184	8.265	8.073	5.627

Table C.9 1,3,5-tris(benzoatomethyl)-2,4,6-triethylbenzene (**4**) and tetra-*n*-butylammonium bromide.

Addition	X- equiv. (mol)	Vol [X-] added (µL)	total V (µL)	[X-] (mol/L)	[R] (mol/L)	d (ppm)	c (ppm)	b (ppm)	a (ppm)
0	0.0000	0	600	0.000E+00	4.959E-03	5.522	6.981	7.058	8.083
1	0.8339	5	605	4.135E-03	4.959E-03	5.522	6.982	7.059	8.079
2	2.4611	10	615	1.220E-02	4.959E-03	5.521	6.983	7.060	8.079
3	4.0362	10	625	2.001E-02	4.959E-03	5.520	6.983	7.061	8.077
4	7.0399	20	645	3.491E-02	4.959E-03	5.518	6.984	7.063	8.075
5	9.8630	20	665	4.891E-02	4.959E-03	5.516	6.985	7.064	8.073
6	13.7929	30	695	6.839E-02	4.959E-03	5.514	6.987	7.067	8.071
7	17.3976	30	725	8.627E-02	4.959E-03	5.511	6.988	7.069	8.069
8	22.7852	50	775	1.130E-01	4.959E-03	5.508	6.990	7.073	8.066
9	27.5198	50	825	1.365E-01	4.959E-03	5.504	6.992	7.076	8.063
10	31.7133	50	875	1.573E-01	4.959E-03	5.501	6.994	7.077	8.060
11	35.4534	50	925	1.758E-01	4.959E-03	5.499	6.996	7.082	8.058
12	41.8390	100	1025	2.075E-01	4.959E-03	5.494	6.999	7.087	8.054
13	47.0894	100	1125	2.335E-01	4.959E-03	5.491	7.001	7.091	8.051
14	51.4826	100	1225	2.553E-01	4.959E-03	5.488	7.004	7.094	8.049
15	58.4192	200	1425	2.897E-01	4.959E-03	5.483	7.007	7.099	8.044
16	64.7605	250	1675	3.211E-01	4.959E-03	5.479	7.010	7.104	8.040
17	100.9059	stock	stock	5.004E-01	4.959E-03	5.454	7.030	7.160	8.018

Table C.10 1,3,5-tris(2,4-dinitrobenzoatomethyl)-2,4,6-triethylbenzene (**1**) and tetra-*n*-heptylammonium iodide trial 1.

Addition	X- equiv. (mol)	Vol [X-] added (µL)	total V (µL)	[X-] (mol/L)	[R] (mol/L)	d (ppm)	c (ppm)	b (ppm)	a (ppm)
0	0.0000	0	700	0.000E+00	2.744E-03	5.479	6.770	7.278	7.820
1	0.7752	5	705	2.127E-03	2.744E-03	5.486	6.809	7.307	7.826
2	2.2931	10	715	6.291E-03	2.744E-03	5.489	6.831	7.322	7.829
3	3.7691	10	725	1.034E-02	2.744E-03	5.490	6.842	7.331	7.830
4	6.6023	20	745	1.811E-02	2.744E-03	5.494	6.876	7.353	7.833
5	9.2873	20	765	2.548E-02	2.744E-03	5.497	6.893	7.366	7.836
6	13.0615	30	795	3.584E-02	2.744E-03	5.500	6.926	7.382	7.839
7	16.5612	30	825	4.544E-02	2.744E-03	5.503	6.948	7.402	7.843
8	21.8608	50	875	5.998E-02	2.744E-03	5.506	6.980	7.425	7.845
9	26.5875	50	925	7.295E-02	2.744E-03	5.508	7.000	7.436	7.847
10	30.8294	50	975	8.459E-02	2.744E-03	5.509	7.026	7.456	7.849
11	34.6574	50	1025	9.509E-02	2.744E-03	5.511	7.044	7.469	7.851
12	41.2927	100	1125	1.133E-01	2.744E-03	5.512	7.071	7.488	7.854
13	46.8446	100	1225	1.285E-01	2.744E-03	5.513	7.097	7.506	7.856
14	51.5586	100	1325	1.415E-01	2.744E-03	5.514	7.117	7.519	7.858
15	59.1318	200	1525	1.622E-01	2.744E-03	5.515	7.160	7.540	7.862

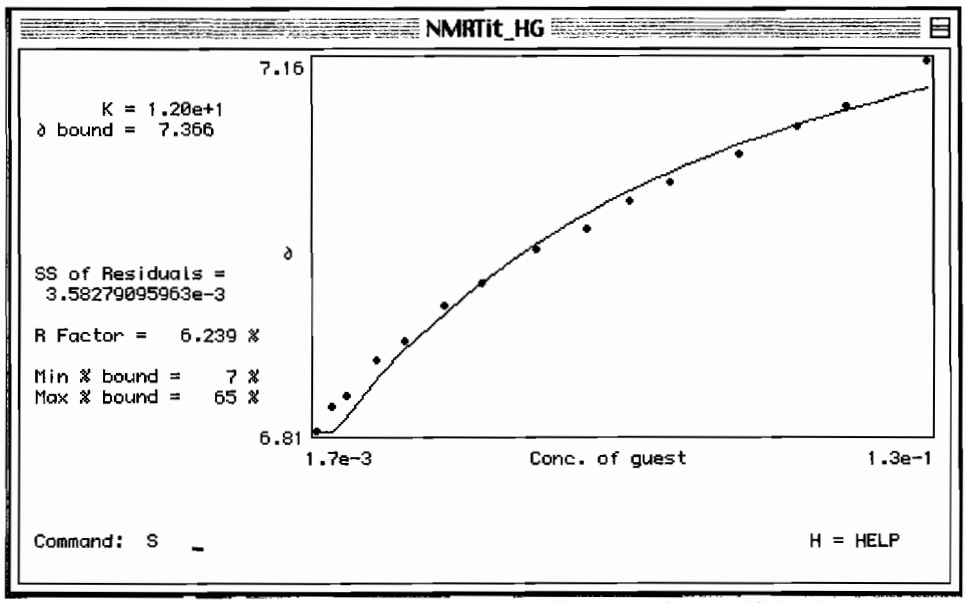

Graph C.7 Binding isotherm for titration of 1,3,5-tris(2,4-dinitrobenzoatomethyl)-2,4,6-triethylbenzene (**1**) and tetra-*n*-heptylammonium iodide trial 1.

Table C.11 1,3,5-tris(2,4-dinitrobenzoatomethyl)-2,4,6-triethylbenzene (**1**) and tetra-*n*-heptylammonium iodide trial 2.

Addition	X- equiv. (mol)	Vol [X-] added (μL)	total V (μL)	[X-] (mol/L)	[R] (mol/L)	d (ppm)	c (ppm)	b (ppm)	a (ppm)
0	0.0000	0	700	0.000E+00	2.484E-03	5.479	6.772	7.279	7.820
1	0.7123	5	705	1.769E-03	2.484E-03	5.486	6.810	7.307	7.826
2	2.1071	10	715	5.234E-03	2.484E-03	5.489	6.834	7.325	7.829
3	3.4633	10	725	8.603E-03	2.484E-03	5.491	6.849	7.335	7.830
4	6.0667	20	745	1.507E-02	2.484E-03	5.495	6.877	7.353	7.834
5	8.5339	20	765	2.120E-02	2.484E-03	5.497	6.898	7.368	7.836
6	12.0019	30	795	2.981E-02	2.484E-03	5.501	6.930	7.389	7.839
7	15.2177	30	825	3.780E-02	2.484E-03	5.503	6.956	7.407	7.842
8	20.0874	50	875	4.990E-02	2.484E-03	5.507	6.991	7.424	7.845
9	24.4306	50	925	6.069E-02	2.484E-03	5.509	7.014	7.448	7.848
10	28.3284	50	975	7.037E-02	2.484E-03	5.511	7.040	7.466	7.850
11	31.8459	50	1025	7.911E-02	2.484E-03	5.512	7.056	7.475	7.851
12	37.9429	100	1125	9.425E-02	2.484E-03	5.513	7.093	7.502	7.854
13	43.0445	100	1225	1.069E-01	2.484E-03	5.514	7.160	7.510	7.856
14	47.3760	100	1325	1.177E-01	2.484E-03	5.515	7.160	7.522	7.860
15	54.3348	200	1525	1.350E-01	2.484E-03	5.516	7.160	7.549	7.862
16	60.8281	250	1775	1.511E-01	2.484E-03	5.516	7.184	7.557	7.864

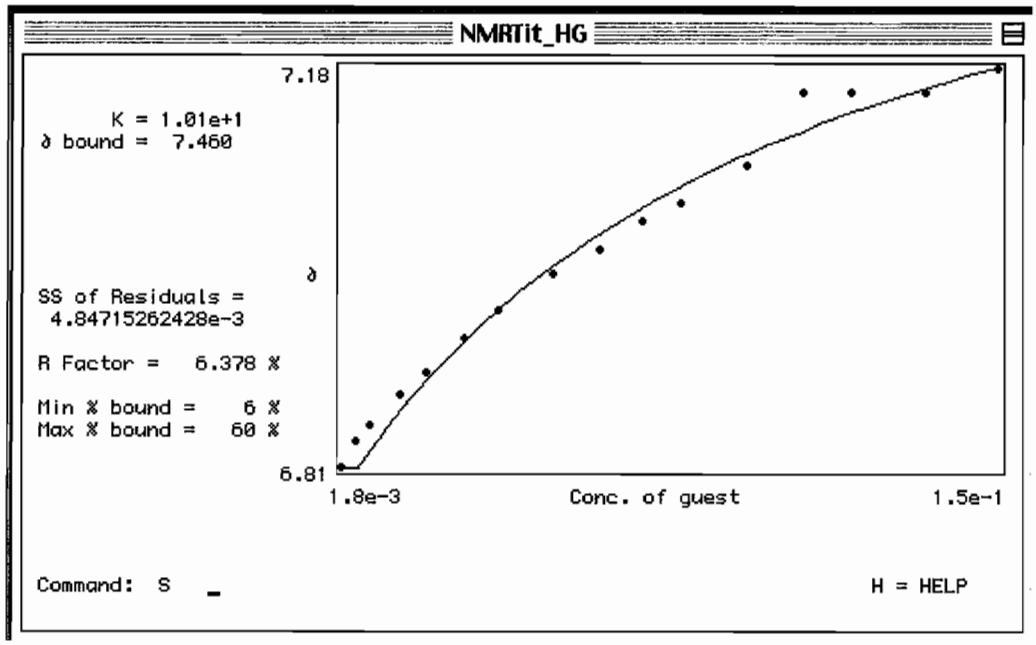

Graph C.8 Binding isotherm for titration of 1,3,5-tris(2,4-dinitrobenzoatomethyl)-2,4,6-triethylbenzene (**1**) and tetra-*n*-heptylammonium iodide trial 2.

Table C.12 1,3,5-tris(3,5-dinitrobenzoatomethyl)-2,4,6-triethylbenzene (**2**) and tetra-*n*-heptylammonium iodide trial 1.

Addition	X- equiv. (mol)	Vol [X-] added (μL)	total V (μL)	[X-] (mol/L)	[R] (mol/L)	d (ppm)	c (ppm)	b (ppm)	a (ppm)
0	0.0000	0	700	0.000E+00	2.484E-03	5.479	6.772	7.279	7.820
1	0.7123	5	705	1.769E-03	2.484E-03	5.486	6.810	7.307	7.826
2	2.1071	10	715	5.234E-03	2.484E-03	5.489	6.834	7.325	7.829
3	3.4633	10	725	8.603E-03	2.484E-03	5.491	6.849	7.335	7.830
4	6.0667	20	745	1.507E-02	2.484E-03	5.495	6.877	7.353	7.834
5	8.5339	20	765	2.120E-02	2.484E-03	5.497	6.898	7.368	7.836
6	12.0019	30	795	2.981E-02	2.484E-03	5.501	6.930	7.389	7.839
7	15.2177	30	825	3.780E-02	2.484E-03	5.503	6.956	7.407	7.842
8	20.0874	50	875	4.990E-02	2.484E-03	5.507	6.991	7.424	7.845
9	24.4306	50	925	6.069E-02	2.484E-03	5.509	7.014	7.448	7.848
10	28.3284	50	975	7.037E-02	2.484E-03	5.511	7.040	7.466	7.850
11	31.8459	50	1025	7.911E-02	2.484E-03	5.512	7.056	7.475	7.851
12	37.9429	100	1125	9.425E-02	2.484E-03	5.513	7.093	7.502	7.854
13	43.0445	100	1225	1.069E-01	2.484E-03	5.514	7.160	7.510	7.856
14	47.3760	100	1325	1.177E-01	2.484E-03	5.515	7.160	7.522	7.860
15	54.3348	200	1525	1.350E-01	2.484E-03	5.516	7.160	7.549	7.862
16	60.8281	250	1775	1.511E-01	2.484E-03	5.516	7.184	7.557	7.864

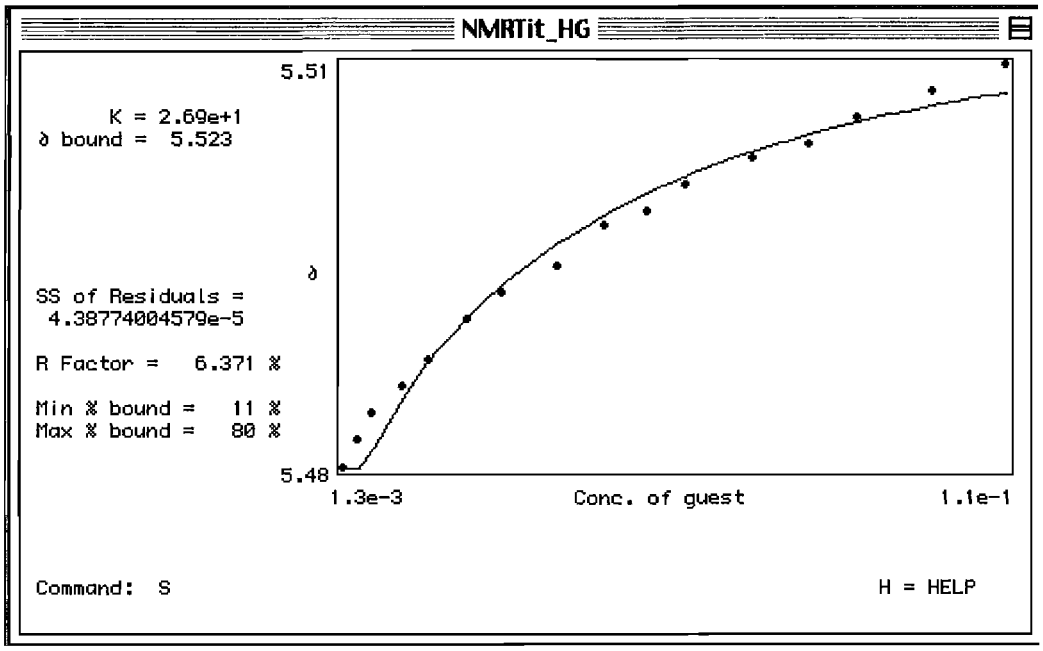

Graph C.9 Binding isotherm for titration of 1,3,5-tris(3,5-dinitrobenzoatomethyl)-2,4,6-triethylbenzene (**2**) and tetra-*n*-heptylammonium iodide trial 1.

Table C.13 1,3,5-tris(3,5-dinitrobenzoatomethyl)-2,4,6-triethylbenzene (**2**) and tetra-*n*-heptylammonium iodide trial 2.

Addition	X-equiv. (mol)	Vol [X-] added (μL)	total V (μL)	[X-] (mol/L)	[R] (mol/L)	c (ppm)	b (ppm)	a (ppm)
0	0.0000	0	700	0.000E+00	2.081E-03	5.479	8.375	8.590
1	0.6595	5	705	1.372E-03	2.081E-03	5.484	8.377	8.594
2	1.9507	10	715	4.059E-03	2.081E-03	5.486	8.378	8.596
3	3.2064	10	725	6.672E-03	2.081E-03	5.488	8.380	8.597
4	5.6166	20	745	1.169E-02	2.081E-03	5.490	8.382	8.598
5	7.9007	20	765	1.644E-02	2.081E-03	5.492	8.382	8.600
6	11.1115	30	795	2.312E-02	2.081E-03	5.495	8.383	8.600
7	14.0887	30	825	2.931E-02	2.081E-03	5.497	8.384	8.600
8	18.5971	50	875	3.870E-02	2.081E-03	5.500	8.386	8.600
9	22.6181	50	925	4.706E-02	2.081E-03	5.502	8.386	8.603
10	26.2266	50	975	5.457E-02	2.081E-03	5.504	8.388	8.604
11	29.4832	50	1025	6.135E-02	2.081E-03	5.505	8.388	8.604
12	35.1278	100	1125	7.309E-02	2.081E-03	5.507	8.390	8.605
13	39.8509	100	1225	8.292E-02	2.081E-03	5.510	8.392	8.606
14	43.8610	100	1325	9.126E-02	2.081E-03	5.510	8.392	8.606
15	50.3036	200	1525	1.047E-01	2.081E-03	5.513	8.393	8.607
16	56.3151	250	1775	1.172E-01	2.081E-03	5.515	8.396	8.607

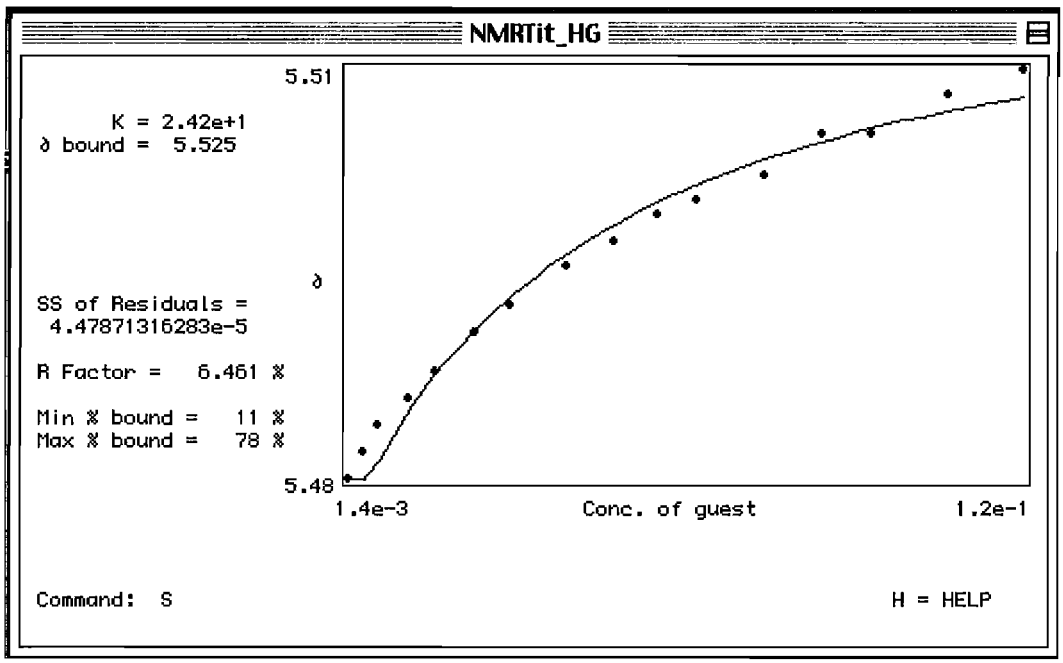

Graph C.10 Binding isotherm for titration of 1,3,5-tris(3,5-dinitrobenzoatomethyl)-2,4,6-triethylbenzene (**2**) and tetra-*n*-heptylammonium iodide trial 2.

Table C.14 1,3,5-tris(benzoatomethyl)-2,4,6-triethylbenzene (**4**) and tetra-*n*-heptylammonium iodide.

Addition	X- equiv. (mol)	Vol [X-] added (μL)	total V (μL)	[X-] (mol/L)	[R] (mol/L)	a (ppm)
0	0.0000	0	700	0.000E+00	3.076E-03	6.973
1	0.4478	5	705	1.377E-03	3.076E-03	6.973
2	1.3247	10	715	4.074E-03	3.076E-03	6.974
3	2.1774	10	725	6.697E-03	3.076E-03	6.974
4	3.8140	20	745	1.173E-02	3.076E-03	6.975
5	5.3652	20	765	1.650E-02	3.076E-03	6.974
6	7.5455	30	795	2.321E-02	3.076E-03	6.974
7	9.5672	30	825	2.942E-02	3.076E-03	6.974
8	12.6287	50	875	3.884E-02	3.076E-03	6.974
9	15.3593	50	925	4.724E-02	3.076E-03	6.975
10	17.8098	50	975	5.477E-02	3.076E-03	6.975
11	20.0212	50	1025	6.158E-02	3.076E-03	6.975
12	23.8543	100	1125	7.336E-02	3.076E-03	6.975
13	27.0616	100	1225	8.323E-02	3.076E-03	6.976
14	29.7848	100	1325	9.160E-02	3.076E-03	6.976
15	34.1597	200	1525	1.051E-01	3.076E-03	6.977
16	38.2420	250	1775	1.176E-01	3.076E-03	6.978
17	63.1437	stock	stock	1.942E-01	3.076E-03	6.938

Table C.15 1,3,5-tris(2,4-dinitrobenzoatomethyl)-2,4,6-triethylbenzene (**1**) and tetra-*n*-heptylammonium chloride trial 1.

Addition	X^- equiv. (M)	Vol. X^- added/aliquot (µL)	Total Vol. in tube(µL)	[X] (mol/L)	[R] (mol/L)	peak 1 (ppm)	peak 2 (ppm)	peak 3 (ppm)	peak 4 (ppm)
0	0.000	0	700	0	0.002028795	7.813	7.27	6.76	5.477
1	0.679	5	705	0.001378421	0.002028795	7.826	7.326	6.83	5.487
2	2.010	10	715	0.004077426	0.002028795	7.838	7.373	6.892	5.496
3	3.303	10	725	0.006701976	0.002028795	7.843	7.394	6.923	5.5
4	5.787	20	745	0.011739702	0.002028795	7.848	7.425	6.965	5.506
5	8.140	20	765	0.016514019	0.002028795	7.853	7.448	6.999	5.51
6	11.448	30	795	0.023225086	0.002028795	7.861	7.48	7.047	5.516
7	14.515	30	825	0.029448075	0.002028795	7.867	7.506	7.084	5.52
8	19.160	50	875	0.038871459	0.002028795	7.873	7.538	7.133	5.525
9	23.303	50	925	0.047276099	0.002028795	7.878	7.564	7.16	5.528
10	27.020	50	975	0.054818725	0.002028795	7.883	7.587	7.203	5.532
11	30.375	50	1025	0.061625484	0.002028795	7.885	7.604	7.228	5.534
12	36.191	100	1125	0.073423868	0.002028795	7.891	7.632	7.269	5.538
13	41.057	100	1225	0.083295984	0.002028795	7.895	7.653	7.299	5.54
14	45.188	100	1325	0.09167797	0.002028795	7.897	7.669	7.322	5.541
15	51.826	200	1525	0.105144111	0.002028795	7.903	7.696	7.36	5.544
16	58.019	250	1775	0.117709349	0.002028795	7.908	7.719	7.392	5.546

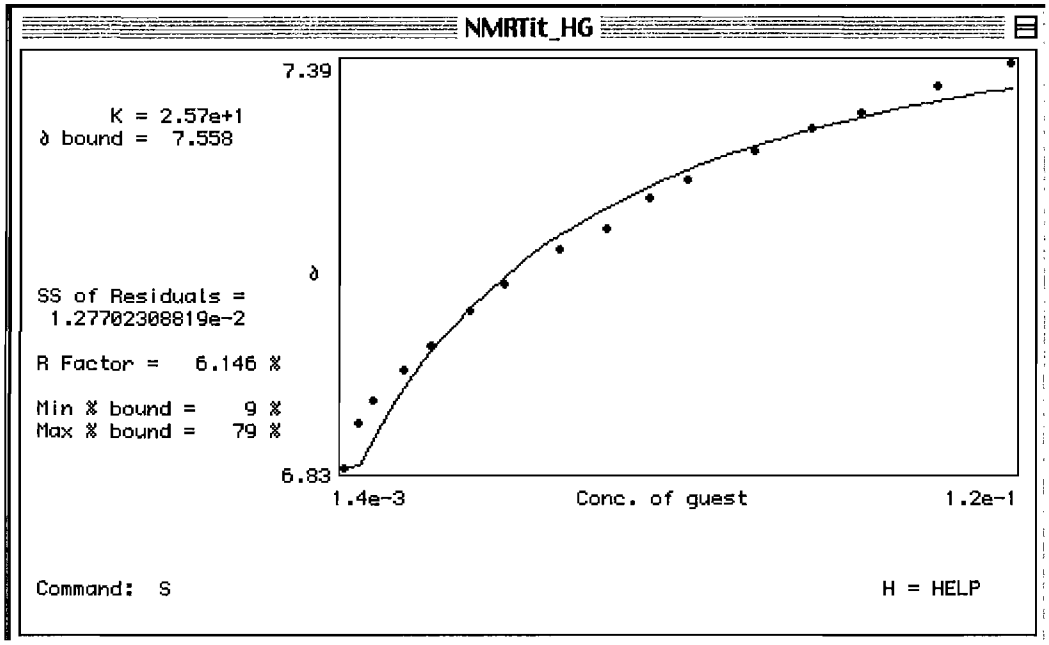

Graph C.11 Binding isotherm for titration of 1,3,5-tris(2,4-dinitrobenzoatomethyl)-2,4,6-triethylbenzene (**1**) and tetra-*n*-heptylammonium chloride trial 1.

Table C.16 1,3,5-tris(2,4-dinitrobenzoatomethyl)-2,4,6-triethylbenzene (**1**) and tetra-*n*-heptylammonium chloride trial 2.

Addition	X^- equiv. (M)	Vol. X^- added/aliquot (µL)	Total Vol. in tube(µL)	[X] (mol/L)	[R] (mol/L)	peak 1 (ppm)	peak 2 (ppm)	peak 3 (ppm)	peak 4 (ppm)
0	0.000	0	700	0	0.002028795	7.813	7.271	6.761	5.478
1	0.679	5	705	0.001378421	0.002028795	7.825	7.321	6.824	5.486
2	2.010	10	715	0.004077426	0.002028795	7.837	7.372	6.891	5.496
3	3.303	10	725	0.006701976	0.002028795	7.843	7.396	6.925	5.501
4	5.787	20	745	0.011739702	0.002028795	7.849	7.426	6.967	5.506
5	8.140	20	765	0.016514019	0.002028795	7.855	7.45	7.002	5.511
6	11.448	30	795	0.023225086	0.002028795	7.861	7.48	7.046	5.517
7	14.515	30	825	0.029448075	0.002028795	7.866	7.504	7.082	5.521
8	19.160	50	875	0.038871459	0.002028795	7.873	7.537	7.132	5.525
9	23.303	50	925	0.047276099	0.002028795	7.878	7.564	7.16	5.529
10	27.020	50	975	0.054818725	0.002028795	7.883	7.586	7.202	5.532
11	30.375	50	1025	0.061625484	0.002028795	7.885	7.602	7.226	5.534
12	36.191	100	1125	0.073423868	0.002028795	7.89	7.631	7.267	5.538
13	41.057	100	1225	0.083295984	0.002028795	7.895	7.652	7.298	5.54
14	45.188	100	1325	0.09167797	0.002028795	7.898	7.67	7.323	5.542
15	51.826	200	1525	0.105144111	0.002028795	7.903	7.695	7.36	5.544
16	58.019	250	1775	0.117709349	0.002028795	7.907	7.718	7.39	5.546

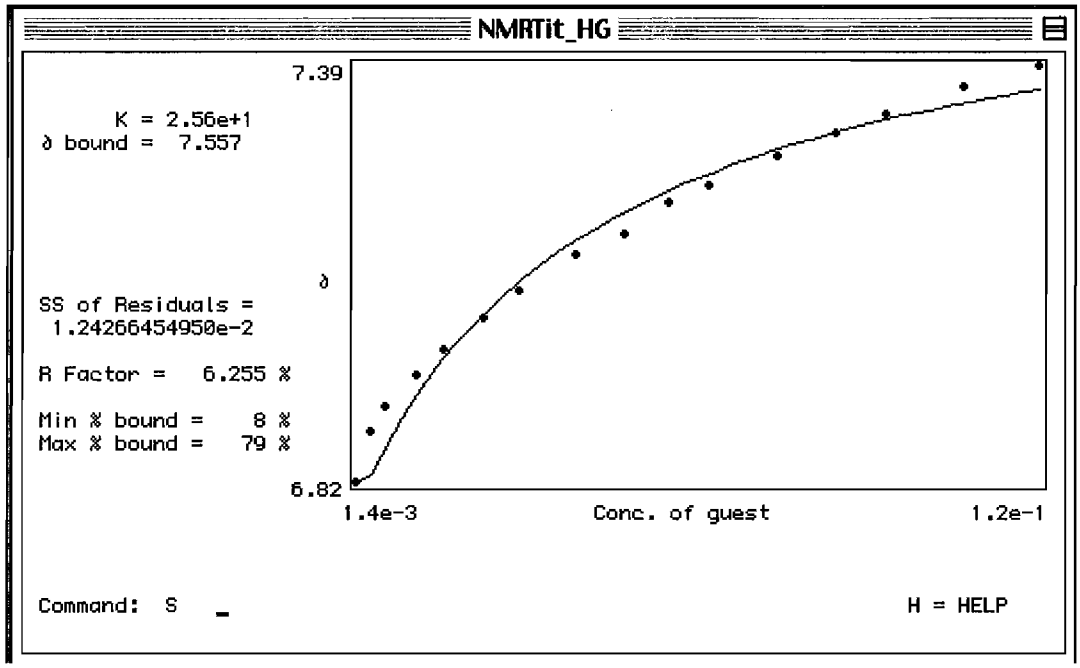

Graph C.12 Binding isotherm for titration of 1,3,5-tris(2,4-dinitrobenzoatomethyl)-2,4,6-triethylbenzene (**1**) and tetra-*n*-heptylammonium chloride trial 2.

Table C.17 1,3,5-tris(2,4-dinitrobenzoatomethyl)-2,4,6-triethylbenzene (**1**) and tetra-*n*-heptylammonium chloride trial 3.

Addition	X^- equiv. (M)	Vol. X^- added/aliquot (µL)	Total Vol. in tube(µL)	[X^-] (mol/L)	[R] (mol/L)	peak 1 (ppm)	peak 2 (ppm)	peak 3 (ppm)	peak 4 (ppm)
0	0.000	0	700	0	0.002028795	7.813	7.271	6.761	5.477
1	1.349	10	710	0.002737427	0.002028795	7.832	7.351	6.864	5.492
2	2.661	10	720	0.005398814	0.002028795	7.841	7.386	6.909	5.499
3	3.937	10	730	0.007987286	0.002028795	7.844	7.404	6.935	5.503
4	6.387	20	750	0.012957153	0.002028795	7.85	7.431	6.974	5.508
5	8.709	20	770	0.017668845	0.002028795	7.856	7.455	7.01	5.512
6	11.975	30	800	0.024294662	0.002028795	7.862	7.484	7.053	5.517
7	15.005	30	830	0.030441504	0.002028795	7.867	7.509	7.089	5.521
8	19.595	50	880	0.039754902	0.002028795	7.873	7.541	7.137	5.526
9	23.692	50	930	0.048066858	0.002028795	7.879	7.567	7.16	5.529
10	27.371	50	980	0.055530656	0.002028795	7.882	7.587	7.204	5.532
11	30.693	50	1030	0.062269813	0.002028795	7.885	7.601	7.228	5.534
12	36.455	100	1130	0.073958971	0.002028795	7.891	7.634	2.27	5.538
13	41.279	100	1230	0.083747453	0.002028795	7.895	7.655	7.302	5.541
14	45.379	100	1330	0.092063983	0.002028795	7.898	7.672	7.325	5.542
15	51.970	200	1530	0.105435658	0.002028795	7.903	7.698	7.361	5.545
16	58.125	250	1780	0.117924652	0.002028795	7.908	7.719	7.393	5.546

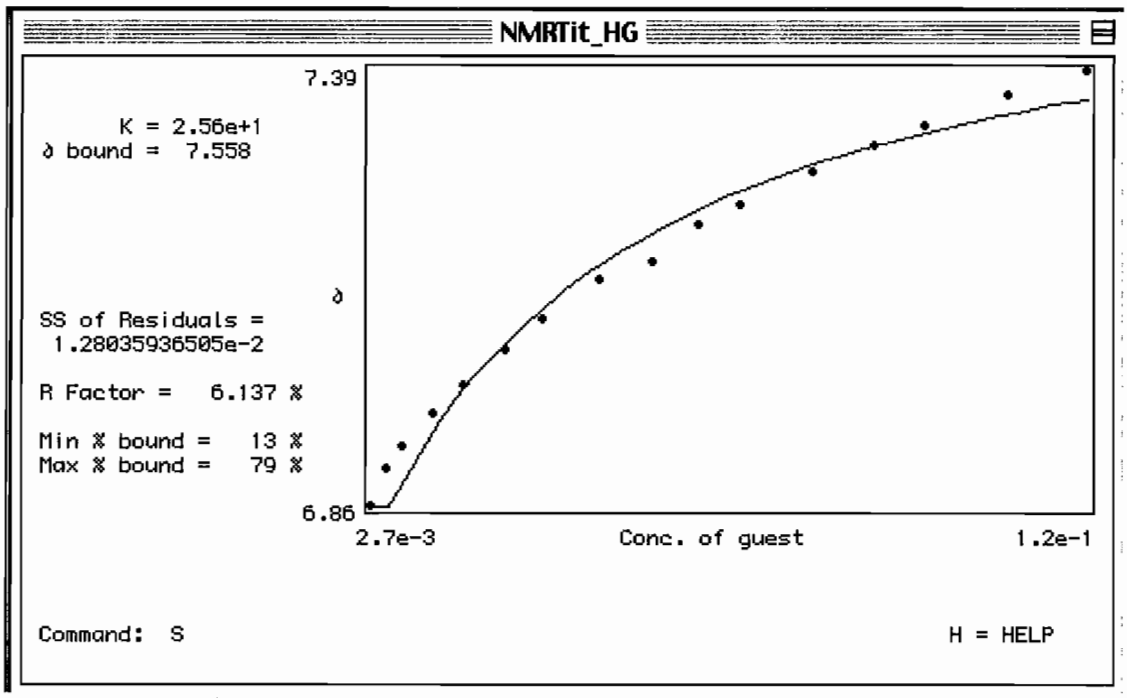

Graph C.13 Binding isotherm for titration of 1,3,5-tris(2,4-dinitrobenzoatomethyl)-2,4,6-triethylbenzene (**1**) and tetra-*n*-heptylammonium chloride trial 3.

Table C.18 1,3,5-tris(3,5-dinitrobenzoatomethyl)-2,4,6-triethylbenzene (**2**) and tetra-*n*-heptylammonium chloride trial 1.

Addition	X^- equiv. (M)	Vol. X^- added/aliquot (µL)	Total Vol. in tube(µL)	[X^-] (mol/L)	[R] (mol/L)	peak 1 (ppm)	peak 2 (ppm)	peak 3 (ppm)
0	0.000	0	700	0	0.002064738	8.589	8.37	5.475
1	0.714	5	705	0.001475157	0.002064738	8.593	8.373	5.482
2	2.113	10	715	0.004363577	0.002064738	8.596	8.376	5.487
3	3.474	10	725	0.007172317	0.002064738	8.598	8.377	5.49
4	6.085	20	745	0.012563589	0.002064738	8.599	8.378	5.493
5	8.559	20	765	0.017672964	0.002064738	8.6	8.378	5.495
6	12.038	30	795	0.02485501	0.002064738	8.601	8.38	5.497
7	15.263	30	825	0.031514726	0.002064738	8.601	8.379	5.5
8	20.148	50	875	0.041599438	0.002064738	8.601	8.38	5.503
9	24.504	50	925	0.050593911	0.002064738	8.6	8.381	5.505
10	28.413	50	975	0.058665874	0.002064738	8.601	8.381	5.506
11	31.941	50	1025	0.065950329	0.002064738	8.601	8.382	5.508
12	38.057	100	1125	0.078576717	0.002064738	8.601	8.382	5.51
13	43.173	100	1225	0.089141653	0.002064738	8.6	8.382	5.511
14	47.518	100	1325	0.098111883	0.002064738	8.6	8.382	5.513
15	54.498	200	1525	0.112523071	0.002064738	8.6	8.383	5.514
16	61.010	250	1775	0.12597013	0.002064738	8.6	8.383	5.516

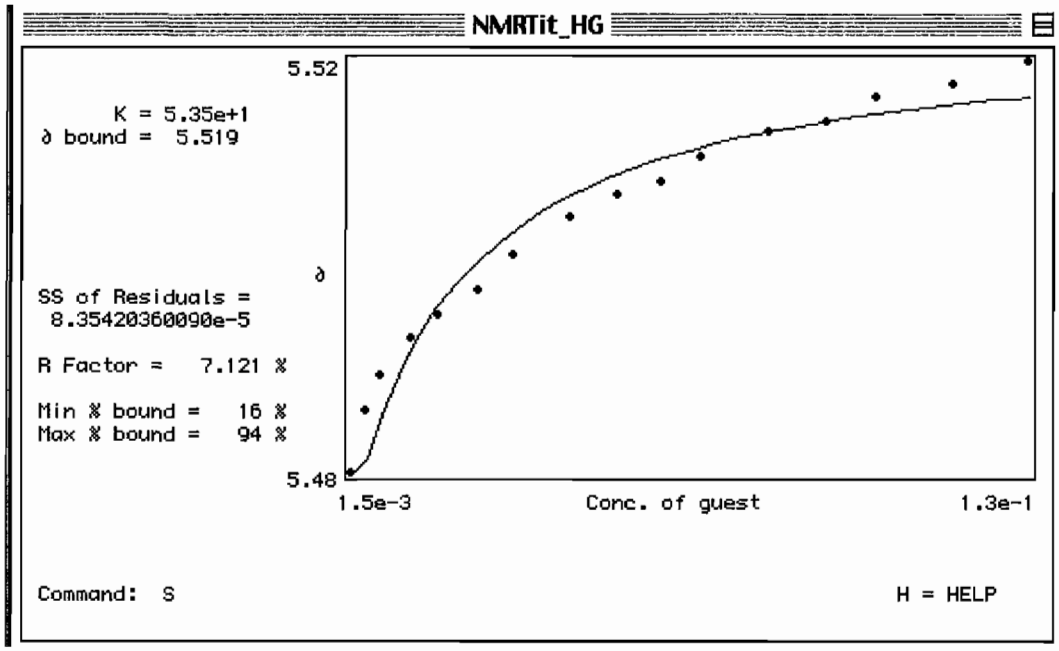

Graph C.14 Binding isotherm for titration of 1,3,5-tris(3,5-dinitrobenzoatomethyl)-2,4,6-triethylbenzene (**2**) and tetra-*n*-heptylammonium chloride trial 1.

Table C.19 1,3,5-tris(3,5-dinitrobenzoatomethyl)-2,4,6-triethylbenzene (**2**) and tetra-*n*-heptylammonium chloride trial 2.

Addition	X^- equiv. (M)	Vol. X^- added/aliquot (µL)	Total Vol. in tube(µL)	[X^-] (mol/L)	[R] (mol/L)	peak 1 (ppm)	peak 2 (ppm)	peak 3 (ppm)
0	0.000	0	700	0	0.002064738	8.589	8.37	5.475
1	0.714	5	705	0.001475157	0.002064738	8.593	8.373	5.482
2	2.113	10	715	0.004363577	0.002064738	8.596	8.376	5.487
3	3.474	10	725	0.007172317	0.002064738	8.598	8.378	5.49
4	6.085	20	745	0.012563589	0.002064738	8.6	8.379	5.493
5	8.559	20	765	0.017672964	0.002064738	8.6	8.379	5.495
6	12.038	30	795	0.02485501	0.002064738	8.6	8.38	8.498
7	15.263	30	825	0.031514726	0.002064738	8.601	8.38	5.5
8	20.148	50	875	0.041599438	0.002064738	8.601	8.38	5.503
9	24.504	50	925	0.050593911	0.002064738	8.601	8.381	5.505
10	28.413	50	975	0.058665874	0.002064738	8.601	8.381	5.506
11	31.941	50	1025	0.065950329	0.002064738	8.601	8.381	5.508
12	38.057	100	1125	0.078576717	0.002064738	8.601	8.382	5.51
13	43.173	100	1225	0.089141653	0.002064738	8.601	8.382	5.511
14	47.518	100	1325	0.098111883	0.002064738	8.6	8.383	5.513
15	54.498	200	1525	0.112523071	0.002064738	8.601	8.383	5.514
16	61.010	250	1775	0.12597013	0.002064738	8.6	8.383	5.516

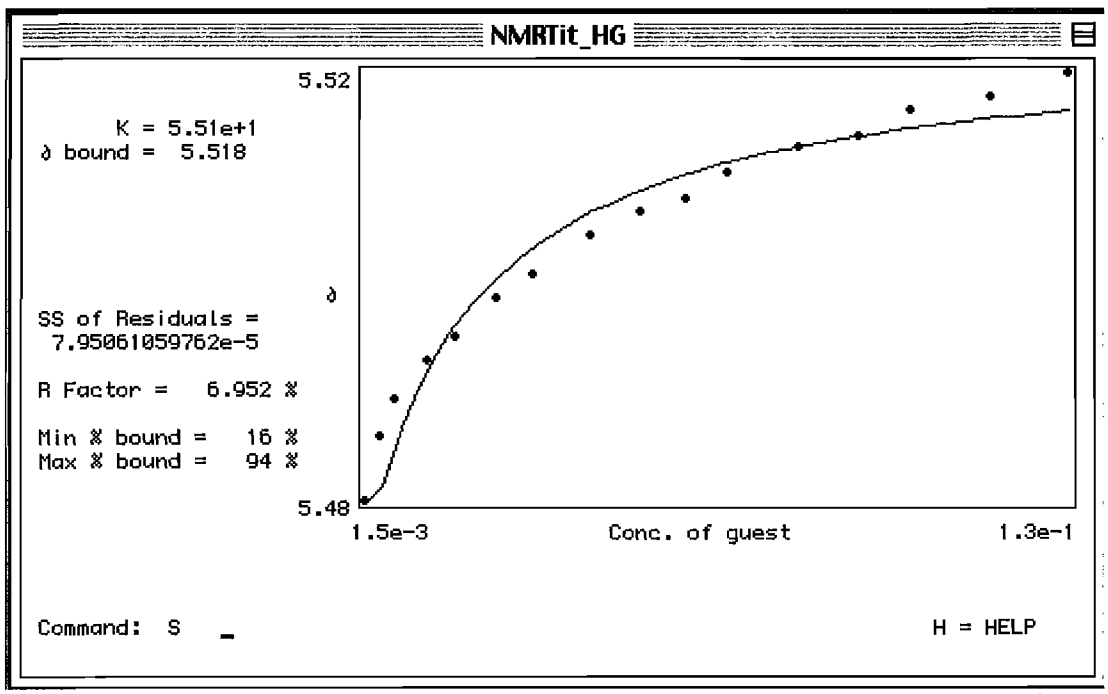

Graph C.15 Binding isotherm for titration of 1,3,5-tris(3,5-dinitrobenzoatomethyl)-2,4,6-triethylbenzene (**2**) and tetra-*n*-heptylammonium chloride trial 2.

Table C.20 1,3,5-tris(3,5-dinitrobenzoatomethyl)-2,4,6-triethylbenzene (**2**) and tetra-*n*-heptylammonium chloride trial 3.

Addition	X^- equiv. (M)	Vol. X^- added/aliquot (µL)	Total Vol. in tube(µL)	[X^-] (mol/L)	[R] (mol/L)	peak 1 (ppm)	peak 2 (ppm)	peak 3 (ppm)
0	0.000	0	700	0	0.002064738	8.59	8.37	5.475
1	0.714	5	705	0.001475157	0.002064738	8.593	8.373	5.482
2	2.113	10	715	0.004363577	0.002064738	8.597	8.376	5.488
3	4.797	20	735	0.009904628	0.002064738	8.599	8.378	5.492
4	7.339	20	755	0.015152113	0.002064738	8.6	8.379	5.494
5	9.749	20	775	0.02012876	0.002064738	8.6	8.379	5.496
6	13.140	30	805	0.027130068	0.002064738	8.601	8.38	8.498
7	16.287	30	835	0.033628288	0.002064738	8.601	8.38	5.5
8	21.058	50	885	0.043479639	0.002064738	8.601	8.381	5.503
9	25.319	50	935	0.052277369	0.002064738	8.601	8.381	5.505
10	29.147	50	985	0.060181928	0.002064738	8.601	8.381	5.507
11	32.606	50	1035	0.067322762	0.002064738	8.602	8.382	5.508
12	38.609	100	1135	0.079716985	0.002064738	8.602	8.383	5.51
13	43.639	100	1235	0.090104046	0.002064738	8.6	8.382	5.511
14	47.916	100	1335	0.098934994	0.002064738	8.6	8.383	5.513
15	54.799	200	1535	0.113145052	0.002064738	8.6	8.383	5.514
16	61.233	250	1785	0.126429665	0.002064738	8.6	8.383	5.516

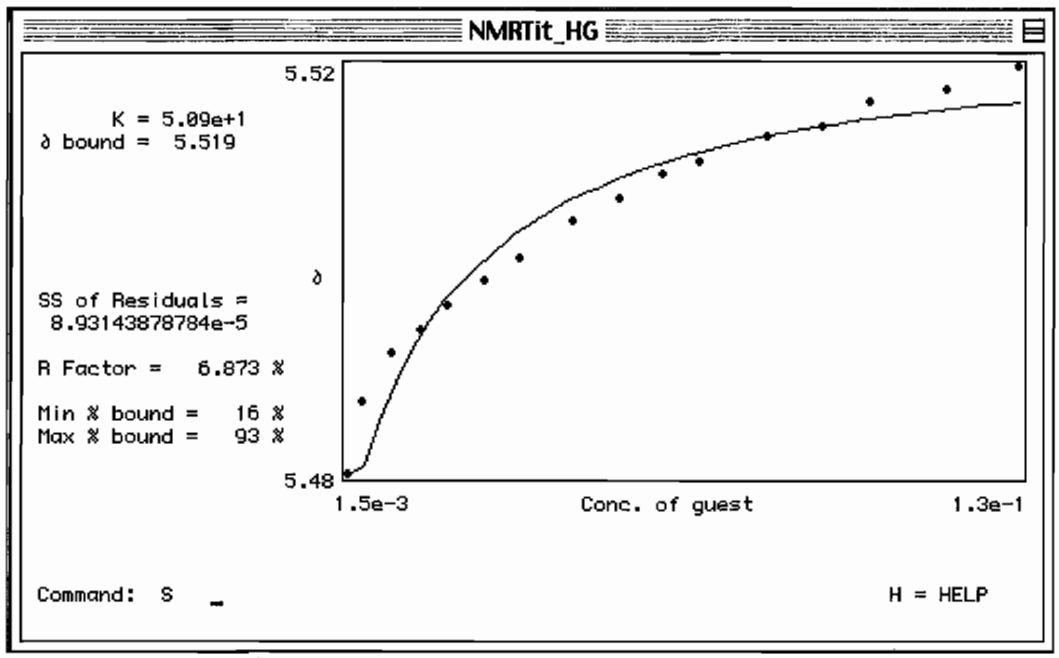

Graph C.16 Binding isotherm for titration of 1,3,5-tris(3,5-dinitrobenzoatomethyl)-2,4,6-triethylbenzene (**2**) and tetra-*n*-heptylammonium chloride trial 3.

Table C.21 1,3,5-tris(benzoatomethyl)-2,4,6-triethylbenzene (**4**) and tetra-*n*-heptylammonium chloride.

Addition	X-equiv. (mol)	Vol [X-] added (µL)	total V (µL)	[X-] (mol/L)	[R] (mol/L)	c (ppm)	b (ppm)	a (ppm)
0	0.0000	0	700	0.000E+00	1.547E-03	5.521	6.955	8.080
1	1.5868	10	710	2.454E-03	1.547E-03	5.521	6.956	8.080
2	4.6301	20	730	7.161E-03	1.547E-03	5.520	6.956	8.079
3	8.8947	30	760	1.376E-02	1.547E-03	5.519	6.957	8.078
4	15.3003	50	810	2.366E-02	1.547E-03	5.517	6.956	8.076
5	20.9611	50	860	3.242E-02	1.547E-03	5.516	6.957	8.079
6	25.9998	50	910	4.021E-02	1.547E-03	5.514	6.957	8.074
7	34.5806	100	1010	5.348E-02	1.547E-03	5.512	6.957	8.071
8	47.4873	200	1210	7.345E-02	1.547E-03	5.509	6.957	8.068
9	58.6480	250	1460	9.071E-02	1.547E-03	5.506	6.958	8.065

Table C.22 Ethyl-3,5-dinitrobenzoate and tetra-*n*-butylammonium bromide.

Addition	X- equiv. (mol)	Vol [X-] added (µL)	total V (µL)	[X-] (mol/L)	[R] (mol/L)	c (ppm)	b (ppm)	a (ppm)
0	0.0000	0	700	0.000E+00	4.330E-03	3.979	8.429	8.609
1	0.8089	5	705	3.503E-03	4.330E-03	3.979	8.431	8.609
2	2.3927	10	715	1.036E-02	4.330E-03	3.981	8.431	8.61
3	3.9328	10	725	1.703E-02	4.330E-03	3.982	8.432	8.611
4	6.8890	20	745	2.983E-02	4.330E-03	3.985	8.436	8.611
5	11.0372	30	775	4.779E-02	4.330E-03	3.988	8.439	8.612
6	16.0931	40	815	6.969E-02	4.330E-03	3.991	8.443	8.613
7	21.7554	50	865	9.421E-02	4.330E-03	3.995	8.448	8.613
8	26.7989	50	915	1.160E-01	4.330E-03	3.997	8.452	8.614
9	35.3952	100	1015	1.533E-01	4.330E-03	4.004	8.457	8.615
10	42.4495	100	1115	1.838E-01	4.330E-03	4.007	8.461	8.615
11	55.5634	250	1365	2.406E-01	4.330E-03	4.014	8.475	8.617
12	64.6172	250	1615	2.798E-01	4.330E-03	4.030	8.488	8.618
13	76.3037	500	2115	3.304E-01	4.330E-03	4.040	8.499	8.62

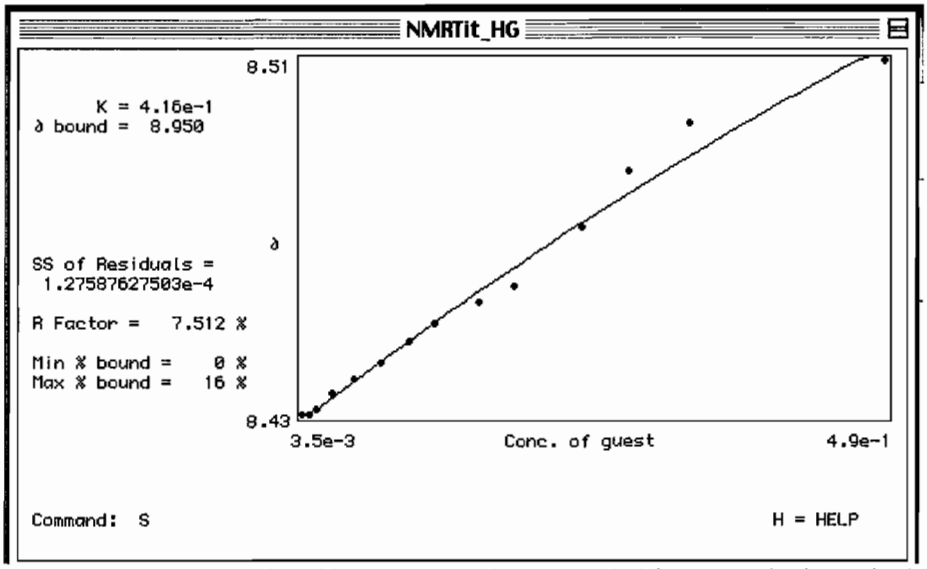

Graph C.17 Near linear relationship obtained when ethyl-3,5-benzoate is titrated with tetra-n-butylammonium bromide.

Ethyl-3,5-dinitrobenzoate and ethyl-2,4-dinitrobenzoate were synthesized as test molecules to understand the role that preorganization plays in this system. ^{1}H NMR titrations of the ethyl-3,5-dinitrobenzoate with $NBu_4^+Br^-$ and $NHep_4^+I^-$ result in complex binding isotherms that do not fit well to a 1:1 binding model (see graph C.17). Unfortunately, the ethyl-2,4-dinitrobenzoate was insoluble in C_6D_6 preventing comparative titrations for this compound.

UV-VIS SPECTROSCOPIC INVESTIGATION OF COMPLEX FORMATION

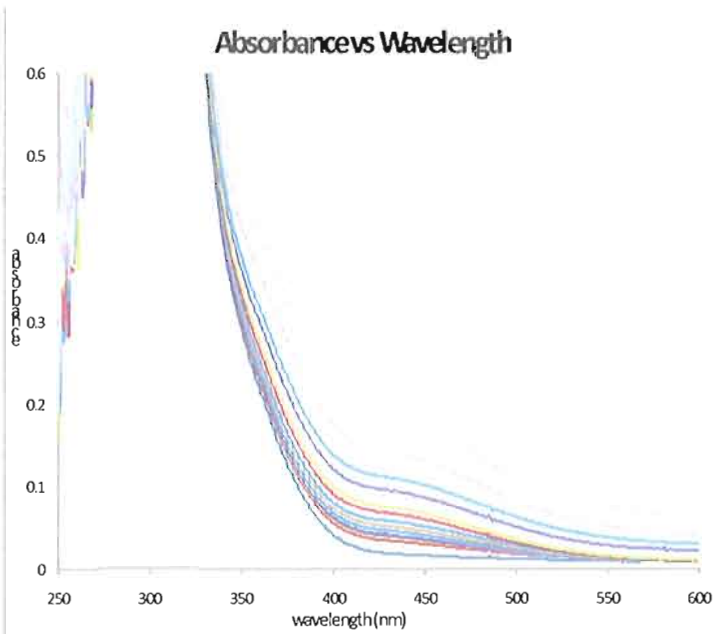

Graph C.18 UV-Vis titration of 1,3,5-tris(3,5-dinitrobenzoatomethyl)-2,4,6-triethylbenzene (**2**) and tetra-*n*-heptylammonium iodide.

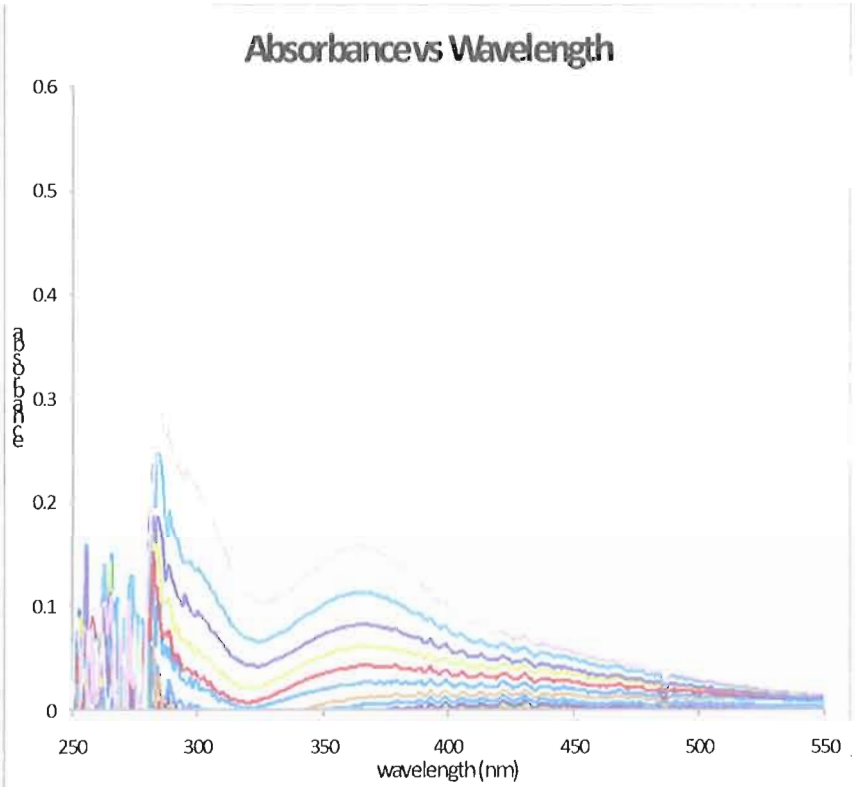

Graph C.19 UV-Vis titration of 1,3,5-tris(2,4-dinitrobenzoatomethyl)-2,4,6-triethylbenzene (**1**) and tetra-*n*-heptylammonium iodide with receptor (**1**) absorbance blanked.

SINGLE CRYSTAL X-RAY DIFFRACTION DATA

GENERAL. Single-crystal X-ray diffraction data for compounds 1,3,5-tris(2,4-dinitrobenzoatomethyl)-2,4,6-triethylbenzene (**1**) and 1,3,5-tris(3,5-dinitrobenzoatomethyl)-2,4,6-triethylbenzene (**2**) were collected on a Bruker-AXS SMART APEX/CCD diffractometer using $Mo_{k\alpha}$ radiation (λ = 0.7107 Å) at 152 K. Diffracted data have been corrected for Lorentz and polarization effects, and for absorption using the SADABS v2.02 area-detector absorption correction program (Siemens Industrial Automation, Inc., © 1996).[4] The structures were solved by direct

methods and the structure solution and refinement was based on $|F|^2$. Hydrogen atoms for **1** were found from the residual density map and refined with isotropic thermal parameters whereas hydrogen atoms for **2** were placed in calculated positions and given isotropic U values 1.2 times that of the atom to which they are bonded. All non-hydrogen atoms were refined with anisotropic displacement parameters. Twelve dimethylsulfoxide molecules per unit cell are highly disordered and were treated by SQUEEZE.[5] The correction of the X-ray data by SQUEEZE, 618 electrons per unit cell, is close to the required value for twelve DMSO molecules in the unit cell, 504 electrons per unit cell. All crystallographic calculations were conducted with the SHELXTL v.6.1 program package (Bruker AXS Inc., © 2001).[6]

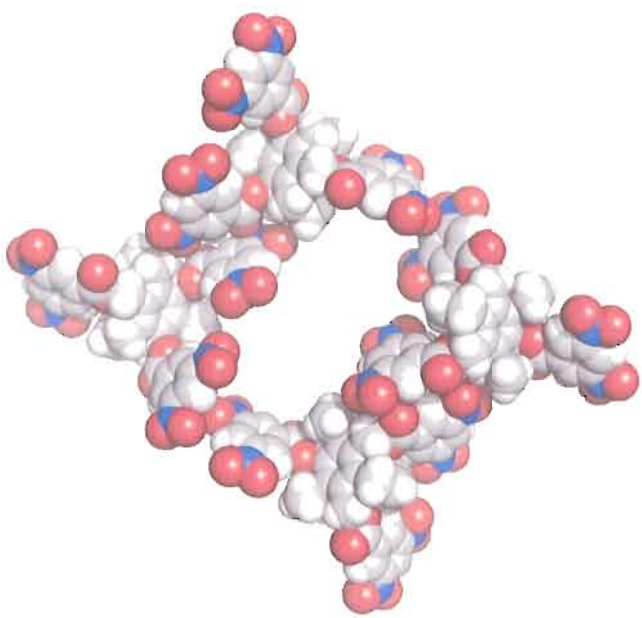

Figure C.1 Packing diagram of receptor **2** illustrating the porous channels formed in the solid state

PACKING DESCRIPTION FOR RECEPTORS 1 AND 2. Receptor **1** crystallizes in a 'nested' type of close pack conformation with one receptor molecule filling the 'cavity' of an adjacent molecule. In the case of receptor **2** a similar self-complementarity is observed; however, the packing arrangement reveals large pores of ca. 12.5 × 19.8 Å.

DFT CALCULATIONS

METHODS. DFT calculations were performed with the NWCHEM program.[7] DFT calculations were done using the B3LYP functional[8] using the DZVP basis set with DGauss A1 coulomb fitting.[9] Optimized geometries and absolute energies for all structures are provided as supporting information.

MODEL COMPOUNDS.

Br anion

Energy –2573.7777630 hartree

METHYL 3,5-DINITROBENZOATE.

Energy -869.2950500 hartree

22

C	0.127000	3.845490	-0.001007
O	-0.177994	2.428497	-0.003006
C	0.888977	1.607498	-0.002000
C	0.490982	0.159500	-0.004013
O	2.045990	1.984497	0.000992
C	-0.847000	-0.245500	-0.012009
C	-1.141998	-1.608490	-0.016006
C	-0.147003	-2.582489	-0.014008
C	1.175980	-2.148483	-0.007004

C	1.511978	-0.797500	-0.003006
N	2.255981	-3.161484	-0.006012
N	-2.558000	-2.037491	-0.022995
O	-2.785004	-3.249496	-0.020996
O	-3.418000	-1.153488	-0.029984
O	3.417984	-2.751495	-0.006012
O	1.918991	-4.348495	-0.004013
H	0.701981	4.106491	0.892990
H	-0.841995	4.348495	0.000000
H	0.700989	4.109497	-0.892990
H	-1.651000	0.482498	-0.014008
H	-0.393997	-3.638489	-0.016998
H	2.551987	-0.483505	0.002000

WEAK-SIGMA COMPLEX OF Br ANION WITH METHYL 3,5-DINITROBENZOATE.

Energy -3443.1041652 hartree

23

C	0.600555	2.932434	-3.087326
O	0.207886	1.833481	-2.248489
C	1.169632	1.357254	-1.430679
C	0.643890	0.343048	-0.472000
O	2.338348	1.707748	-1.493973
C	-0.746872	0.147583	-0.294418
C	-1.159653	-0.879425	0.576400
C	-0.261459	-1.594070	1.357056
C	1.101181	-1.327408	1.207932
C	1.558441	-0.372238	0.286713
N	2.061081	-2.088745	1.990967
N	-2.579758	-1.209198	0.664795
O	-2.940704	-2.019165	1.535660
O	-3.347717	-0.683533	-0.149002
O	3.270203	-1.863113	1.815109
O	1.630554	-2.934586	2.794708

H	0.937836	3.773422	-2.472748
H	-0.297821	3.208008	-3.646347
H	1.404709	2.634995	-3.769119
H	-1.466415	0.640732	-0.929779
H	-0.608322	-2.350891	2.050690
H	2.621140	-0.187546	0.169678
Br	-1.339569	2.592850	1.100967

METHYL 2,4-DINITROBENZOATE.

Energy -869.2821988 hartree

22

C	-1.509979	-3.984985	0.537003
O	-1.335983	-2.549988	0.668000
C	-0.872986	-1.927994	-0.423981
C	-0.716980	-0.439987	-0.188980
O	-0.679977	-2.439987	-1.505981
C	-1.863983	0.359985	-0.248978
C	-1.779984	1.747986	-0.162979
C	-0.524979	2.338989	-0.016998
C	0.638000	1.579987	0.046997
C	0.522995	0.195007	-0.031982
N	1.765000	-0.599991	0.081009
N	-0.423981	3.810989	0.074005
O	0.701004	4.297989	0.208008
O	-1.473984	4.454987	0.007004
O	1.645996	-1.802994	0.321000
O	2.836000	-0.005997	-0.051987
H	-2.227982	-4.211000	-0.256989
H	-1.883987	-4.317993	1.505997
H	-0.548981	-4.454987	0.309006
H	-2.835983	-0.112000	-0.372986
H	-2.667984	2.370987	-0.206985
H	1.608002	2.049988	0.163010

C-H COMPLEX OF Br ANION WITH METHYL 2,4-DINITROBENZOATE.

Energy -3443.0929338 hartree

23

C	0.652893	3.853363	0.387756
O	0.338455	2.474700	0.680405
C	-0.445740	1.855209	-0.209457
C	-0.524948	0.376282	0.075974
O	-0.965927	2.381378	-1.174622
C	0.673019	-0.341431	0.128998
C	0.663559	-1.735382	0.214706
C	-0.558624	-2.406357	0.249741
C	-1.773514	-1.718582	0.210938
C	-1.738266	-0.332321	0.133896
N	-3.029984	0.373276	0.195496
N	-0.589066	-3.875656	0.342697
O	-1.696381	-4.428696	0.407654
O	0.489716	-4.476013	0.349319
O	-3.049698	1.481491	0.737091
O	-4.024887	-0.202209	-0.262787
H	1.151230	3.925354	-0.582794
H	1.329086	4.167831	1.184921
H	-0.259109	4.459213	0.382355
H	1.654053	0.153412	0.093475
H	1.609482	-2.268921	0.255447
H	-2.718033	-2.249115	0.254578
Br	4.120026	0.158112	0.112625

RECEPTOR CALCULATIONS.

COMPLEX OF Br ANION WITH 1 WITHOUT SYMMETRY.

Energy -5646.2918730 hartree

91

C	-0.403885	1.170990	-3.176590
C	-1.121078	-0.035995	-3.039093
C	-0.450516	-1.274994	-3.006622
C	0.950760	-1.304000	-3.168274
C	1.680603	-0.106995	-3.316010
C	0.997757	1.126984	-3.327072
C	3.200531	-0.145004	-3.432602
C	3.701263	-0.252991	-4.888596
C	-1.232956	-2.563995	-2.777756
C	-1.733200	-3.214005	-4.085068
C	-1.142761	2.503983	-3.144455
C	-1.599731	2.981995	-4.538330
C	1.799377	2.408981	-3.400360
O	2.370941	2.695984	-2.076340
C	2.024445	3.835983	-1.462830
C	2.585342	3.888992	-0.060516
O	1.288651	4.696991	-1.904449
C	1.696609	-2.617004	-3.078033
O	2.199570	-2.774002	-1.707626
C	1.927887	-3.914993	-1.053604
C	2.391815	-3.837997	0.381760
O	1.319107	-4.867996	-1.499496
C	-2.610138	0.012009	-2.777344
O	-2.757950	0.119980	-1.328278
C	-3.984329	0.336990	-0.835114
C	-3.914597	0.398987	0.673737
O	-4.983932	0.569992	-1.487061
C	-4.204727	1.625992	1.275452
C	-4.035538	1.809982	2.646545

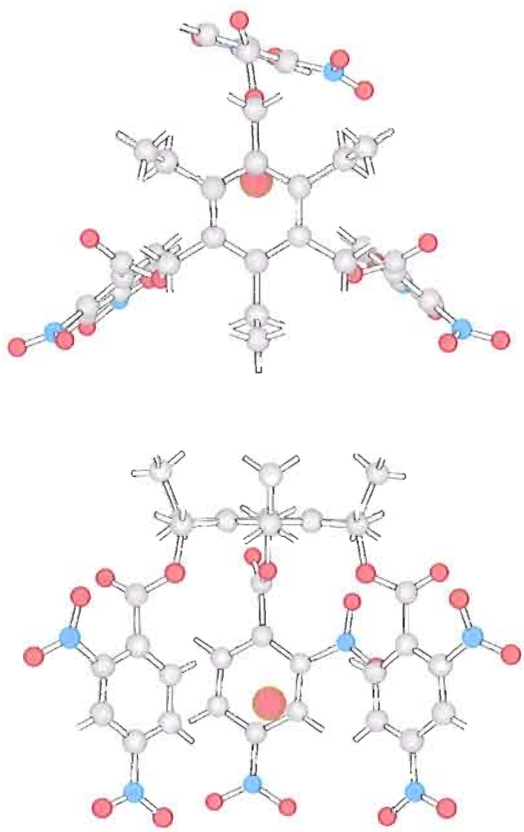

Br–H distances = 2.832, 3.043

Br–H distances = 2.909, 3.021

Br–C distance = 3.432 Å

Figure C.2 Ball and stick representations of receptor **1** DFT minima with Br^- without symmetry

C	-3.556976	0.750992	3.415710
C	-3.242889	-0.481003	2.849945
C	-3.468002	-0.651993	1.487700
C	2.073715	3.004990	0.893326
C	2.445175	3.105988	2.236984
C	3.340210	4.106995	2.614441
C	3.875839	5.001984	1.689453
C	3.495224	4.873993	0.359604
C	3.251724	-4.794998	0.947052
C	3.532837	-4.815002	2.306549
C	2.952316	-3.836990	3.112579
C	2.110565	-2.856003	2.588409
C	1.836000	-2.865997	1.218781
N	-3.264145	-1.996994	0.928680
N	-3.390564	0.934982	4.866257
N	4.130600	5.776993	-0.617218
N	3.751816	4.232986	4.027817
N	3.953003	-5.774994	0.097382
N	3.259216	-3.849000	4.556793
O	4.562057	5.124985	4.309677
O	3.263611	3.444992	4.838547
O	-3.074585	-0.048004	5.539368
O	-3.600723	2.064987	5.325226
O	4.183868	5.397995	-1.792252
O	4.598267	6.840988	-0.201508
O	-3.762268	-2.233002	-0.183151
O	-2.654739	-2.823990	1.607224
O	4.299408	-6.841003	0.614273
O	4.185287	-5.449997	-1.071121
O	4.033813	-4.722000	4.968826
O	2.724869	-2.994003	5.263580
H	3.631424	0.744980	-2.966812
H	3.596725	-0.979996	-2.849655

H	4.797760	-0.276000	-4.918854
H	3.331329	-1.164000	-5.376633
H	3.365341	0.596985	-5.495926
H	-0.620956	-3.289993	-2.238388
H	-2.081100	-2.375992	-2.115875
H	-0.899048	-3.477997	-4.748062
H	-2.291153	-4.132004	-3.863098
H	-2.393707	-2.541000	-4.644852
H	-2.010834	2.428986	-2.484528
H	-0.517609	3.277985	-2.693115
H	-2.270538	2.255981	-5.015717
H	-2.131989	3.937988	-4.461151
H	-0.744858	3.126984	-5.211365
H	2.661835	2.317993	-4.063187
H	1.214127	3.267990	-3.719391
H	2.579987	-2.636993	-3.718491
H	1.082596	-3.479996	-3.326508
H	-3.132721	-0.888000	-3.103165
H	-3.104202	0.862991	-3.246521
H	-4.556961	2.446991	0.655579
H	-4.258087	2.760986	3.120850
H	-2.855759	-1.293000	3.452789
H	1.368317	2.217987	0.627136
H	2.025604	2.401993	2.953842
H	4.579407	5.766983	1.994812
H	4.198227	-5.561005	2.725494
H	1.665710	-2.080994	3.210464
H	1.171677	-2.093002	0.833328
Br	0.040649	0.237991	2.156693

*COMPLEX OF Br ANION WITH **1** AND C3 SYMMETRY IMPOSED.*

Energy -5646.3014218 hartree

91

C	0.819992	0.774490	3.102493
C	2.227982	0.900497	3.108505
C	3.051987	-0.240509	3.102493
C	2.456985	-1.523500	3.108505
C	1.056992	-1.666489	3.102493
C	0.242996	-0.509491	3.108505
C	0.412994	-3.048492	3.104492
C	0.212997	-3.625488	4.522491
C	4.571976	-0.107513	3.104492
C	5.169983	0.008484	4.522491
C	-0.055008	2.023483	3.104492
C	-0.455002	2.484497	4.522491
C	3.352982	-2.745500	3.095505
O	3.919983	-2.949493	1.755493
C	3.598984	-4.069489	1.092500
C	4.209976	-4.073502	-0.290482
O	2.854980	-4.949493	1.481506
C	2.838989	2.287491	3.095505
O	2.731979	2.880493	1.755493
C	3.861984	3.162491	1.092500
C	3.560989	3.693497	-0.290482
O	4.995987	2.958496	1.481506
C	3.033981	2.812485	-1.237488
C	2.860977	3.207489	-2.565491
C	3.224976	4.502487	-2.936493
C	3.749985	5.409485	-2.017487
C	3.901978	4.993484	-0.700485
C	3.709976	-3.176498	-1.237488
C	4.138977	-3.224487	-2.565491
C	5.077988	-4.187500	-2.936493

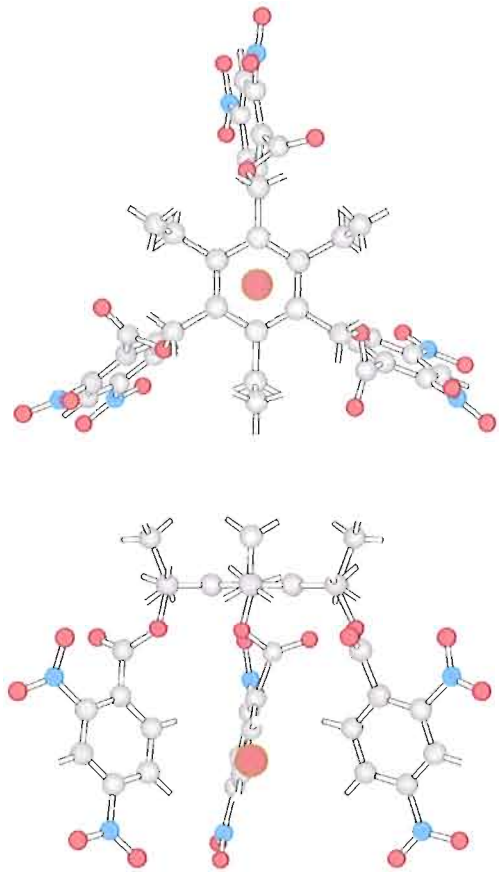

Br–H distances = 2.724, 3.178

Figure C.3 Ball and stick representation of receptor **1** DFT minima with Br^- with symmetry.

C	5.600983	-5.095490	-2.017487
C	5.164978	-5.018494	-0.700485
N	4.382980	5.989487	0.273500
N	3.046982	4.944489	-4.334488
N	5.785980	-5.934494	0.273500
N	5.549988	-4.254500	-4.334488
O	6.396988	-5.113495	-4.612488
O	5.071976	-3.453491	-5.138489
O	3.366989	6.107483	-4.612488
O	2.591980	4.130493	-5.138489
O	5.765976	-5.600494	1.462494
O	6.315979	-6.962494	-0.157500
O	4.104980	5.804489	1.462494
O	5.009979	6.962494	-0.157500
C	-1.263000	-0.674500	3.095505
O	-1.723007	-1.062500	1.755493
C	-2.531998	-0.225510	1.092500
C	-2.841003	-0.752502	-0.290482
O	-2.921997	0.858490	1.481506
C	-1.815002	-0.768494	-1.237488
C	-2.071000	-1.115494	-2.565491
C	-3.374008	-1.447495	-2.936493
C	-4.421997	-1.446487	-2.017487
C	-4.137009	-1.106491	-0.700485
N	-5.240997	-1.187500	0.273500
N	-3.668000	-1.822495	-4.334488
O	-4.835007	-2.126495	-4.612488
O	-2.735000	-1.809494	-5.138489
O	-4.942000	-1.336502	1.462494
O	-6.397003	-1.131500	-0.157500
H	1.013992	-3.748489	2.518494
H	-0.550995	-3.011490	2.591492
H	1.168000	-3.734497	5.052505

H	-0.257004	-4.615494	4.469498
H	-0.425995	-2.979492	5.138504
H	5.020981	-0.960495	2.591492
H	4.876984	0.763489	2.518494
H	4.930984	-0.868500	5.138504
H	6.262985	0.096497	4.469498
H	4.787979	0.889496	5.052505
H	-0.962006	1.852493	2.518494
H	0.459000	2.839493	2.591492
H	-1.027008	1.712494	5.052505
H	-1.076996	3.386490	4.469498
H	0.423996	2.715485	5.138504
H	4.221985	-2.615494	3.742493
H	2.838989	-3.655502	3.393494
H	3.883987	2.297485	3.393494
H	2.290985	2.975494	3.742493
H	2.744980	1.792496	-0.975479
H	2.445984	2.500488	-3.279480
H	4.017990	6.415497	-2.316483
H	2.970978	-2.417496	-0.975479
H	3.733978	-2.511490	-3.279480
H	6.338989	-5.830490	-2.316483
H	-1.584000	-1.492493	3.742493
H	-1.794006	0.225494	3.393494
H	-0.788010	-0.508500	-0.975479
H	-1.251007	-1.121490	-3.279480
H	-5.428009	-1.717500	-2.316483
Br	1.642990	-0.377502	-2.198486

COMPLEX OF Br ANION WITH 2 WITH C3 SYMMETRY IMPOSED.

Energy -5646.3163446 hartree

91

C	0.053986	3.017532	-0.272873
C	1.394730	3.027679	-0.718460
C	2.457382	3.017654	0.202835
C	2.173721	3.009308	1.587021
C	0.843307	2.999069	2.046967
C	-0.212800	3.009247	1.108627
C	0.534409	2.971786	3.540176
C	0.467941	4.380325	4.167831
C	3.905746	3.010284	-0.275085
C	4.469147	4.427353	-0.516251
C	-1.084427	3.010254	-1.288300
C	-1.587723	4.426407	-1.638351
C	3.323441	2.883942	2.566849
O	3.803223	1.498856	2.551102
C	3.597931	0.732162	3.640381
C	3.879395	-0.712082	3.370468
O	3.235092	1.154236	4.726578
C	1.669724	2.921875	-2.205475
O	1.430313	1.539032	-2.628800
C	2.483231	0.787048	-3.003983
C	2.123900	-0.659546	-3.128754
O	3.602280	1.222916	-3.227585
C	0.897324	-1.162613	-2.672500
C	0.639084	-2.527954	-2.807617
C	1.572540	-3.410828	-3.337891
C	2.787643	-2.883987	-3.772797
C	3.077759	-1.524307	-3.669006
C	4.094406	-1.197632	2.072998
C	4.333237	-2.561768	1.897171
C	4.322617	-3.459885	2.957550

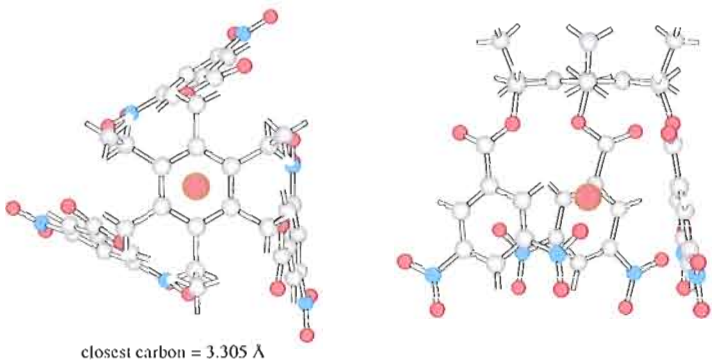

Figure C.4 Ball and stick representation of receptor **2** DFT minima with Br^-

C	4.093338	-2.950211	4.234985
C	3.865921	-1.592422	4.454910
N	3.779602	-3.787125	-4.375031
N	-0.662918	-3.056000	-2.366928
N	4.115021	-3.869995	5.382339
N	4.600830	-3.071716	0.541809
O	4.643448	-4.298370	0.387497
O	4.783203	-2.244705	-0.354630
O	-0.805832	-4.284515	-2.341629
O	-1.539200	-2.241058	-2.067490
O	3.941025	-3.390915	6.508484
O	4.322189	-5.067764	5.156631
O	4.836990	-3.292800	-4.782104
O	3.492844	-4.986984	-4.455292
C	-1.636902	2.883469	1.612747
O	-1.870026	1.493561	2.016266
C	-2.713730	0.741333	1.282745
C	-2.627304	-0.708618	1.640533
O	-3.471207	1.179306	0.431427
C	-1.614105	-1.210953	2.468796
C	-1.587570	-2.579315	2.744675
C	-2.505768	-3.465210	2.191772
C	-3.495300	-2.938843	1.362427
C	-3.564346	-1.576447	1.074768
N	-4.503220	-3.845749	0.794128
N	-0.550446	-3.107239	3.645966
O	-0.444534	-4.335922	3.742310
O	0.139175	-2.292282	4.263992
O	-5.389160	-3.352234	0.087600
O	-4.417145	-5.048004	1.068314
H	1.277725	2.377472	4.074936
H	-0.410950	2.452591	3.717743
H	1.420929	4.913956	4.058289

H	0.240723	4.312759	5.239502
H	-0.306183	4.999054	3.694397
H	4.537308	2.489166	0.447800
H	4.003937	2.427277	-1.194092
H	4.439362	5.035522	0.397491
H	5.510773	4.374069	-0.855896
H	3.892990	4.963928	-1.280823
H	-1.922836	2.414612	-0.919266
H	-0.767900	2.502594	-2.202026
H	-1.967148	4.949203	-0.751587
H	-2.402817	4.373260	-2.372070
H	-0.789000	5.047470	-2.063217
H	4.183563	3.487976	2.271683
H	3.056610	3.148758	3.587494
H	2.684067	3.200012	-2.481384
H	0.977570	3.525742	-2.796082
H	0.154587	-0.513718	-2.226944
H	1.360046	-4.470612	-3.411987
H	4.036819	-1.138794	-3.999069
H	4.082962	-0.536331	1.216278
H	4.487167	-4.518265	2.795837
H	3.673691	-1.220291	5.454941
H	-1.807983	3.475479	2.513947
H	-2.385864	3.162476	0.875046
H	-0.863342	-0.559311	2.896744
H	-2.453278	-4.526962	2.400177
H	-4.332932	-1.191100	0.413589
Br	1.125702	-1.092407	0.623932

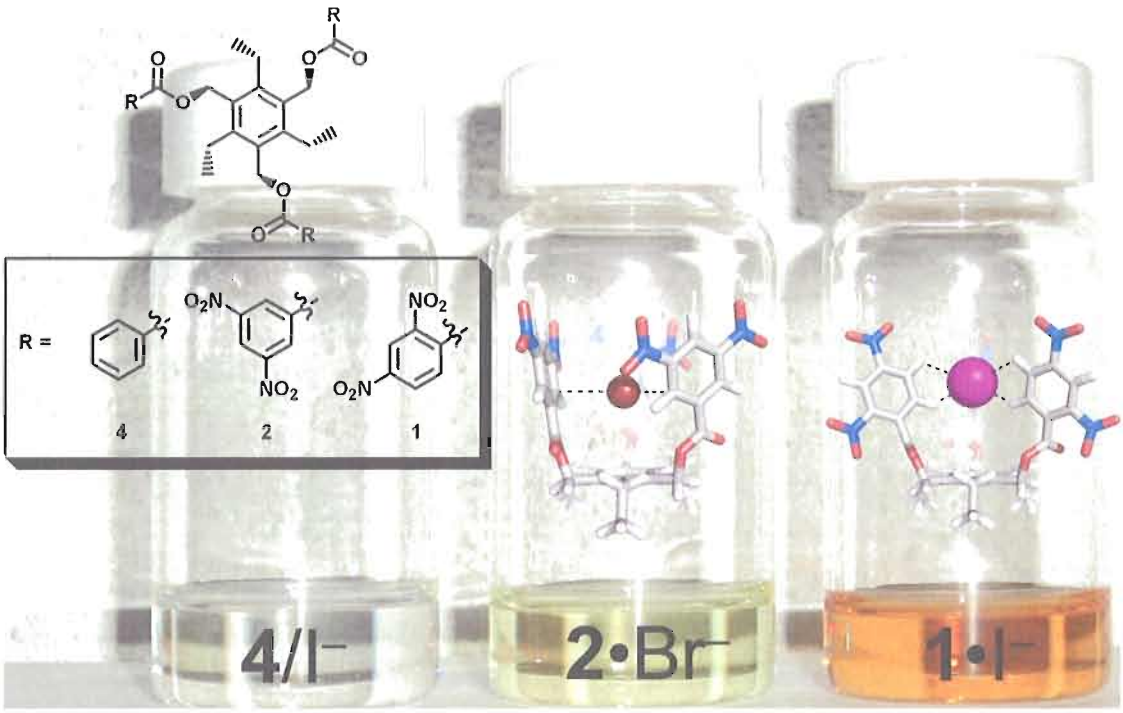

Figure C.5 Vials containing tripodal anion receptors and halides in benzene.

SUPPORTING REFERENCES

1. A. Vacca, C. Nativi, M. Cacciarini, R, Pergoli, S. Roelens, *J. Am. Chem. Soc.* **2004**, *126*, 16456-16465.
2. *Synthetic Communications*. **1998**. *28*(11), 2021-2026.
3. A. P. Bisson, C. A. Hunter, J. C. Morales and K. Young, *Chem. Eur. J.*, **1998**, 4, 845-851
4. G. M. Sheldrick, *SADABS: Area Detector Absorption Correction*; University of Göttingen: Göttingen, Germany, 2001.
5. P. Van der Sluis and A. L. Spek, *Acta Crystallographica, Section A: Foundations of Crystallography*, 1990, A46, 194-201.
6. G. M. Sheldrick, SHELXTL: Program Library for Structure Solution and Molecular Graphics, 5.10; Bruker AXS: Madison, WI, 2000).
7. E. J. Bylaska, W. A. de Jong, K. Kowalski, T. P. Straatsma, M. Valiev, D. Wang, E. Apra, T. L. Windus, S. Hirata, M. T. Hackler, Y. Zhao, P.-D. Fan, R. J. Harrison, M. Dupuis, D. M. A. Smith, J. Nieplocha, V. Tipparaju, M. Krishnan, A. A. Auer, M. Nooijen, E. Brown, G. Cisneros, G. I. Fann, H. Fruchtl, J. Garza, K. Hirao, R. Kendall, J. A. Nichols, K. Tsemekhman, K. Wolinski, J. Anchell, D. Bernholdt, P. Borowski, T. Clark, D. Clerc, H. Dachsel, M. Deegan, K. Dyall, D. Elwood, E. Glendening, M. Gutowski, A. Hess, J. Jaffe, B. Johnson, J. Ju, R. Kobayashi, R. Kutteh, Z. Lin, R. Littlefield, X. Long, B. Meng, T. Nakajima, S. Niu, L. Pollack, M. Rosing, G. Sandrone, M. Stave, H. Taylor, G. Thomas, J. van Lenthe, A. Wong, and Z. Zhang, *NWChem, A Computational Chemistry Package for Parallel Computers, Version 5.0*, 2006, Pacific Northwest National Laboratory, Richland, Washington 99352-0999, USA.
8. (a) Becke, A. D. *Phys. Rev. A* **1988**, *38*, 3098. (b) Becke, A. D. In *The Challenge of d and f Electrons: Theory and Computation*; Salahub, D. R.; Zerner, M. C., Eds.; ACS Symposium Series, No. 394, American Chemical Society: Washington D. C., 1989; p166. (c) Becke, A. D. *Int. J. Quantum Chem. Symp.* **1989**, *23*, 599. (d) Perdew, J. P. *Phys. Rev. B* **1986**, *33*, 8822.
9. Godbout, N.; Salahub, D. R.; Andzelm, J.; Wimmer, E. *Can. J. Chem.* **1992**, *70*, 560.

APPENDIX D

SUPPORTING INFORMATION FOR CHAPTER V: INVESTIGATING THE USE OF INTRAMOLECULAR HYDROGEN BONDS TO STABILIZE RECEPTOR CONFORMATIONS; DESIGNING RECEPTORS FOR ANION/ARENE INTERACTIONS

EXPERIMENTAL

GENERAL. All chemicals were obtained from TCI-America, Sigma-Aldrich, Acros and Strem. Nuclear Magnetic Resonance ^{1}H NMR and ^{13}C NMR spectra were recorded on a Varian INOVA 300 (299.935) and 125 (125.751) MHz spectrometer respectively. Chemical shifts (δ) expressed as ppm downfield from tetramethylsilane using either the residual solvent peak as an internal standard ($CDCl_3$ ^{1}H: 7.27 ppm) or using $CDCl_3$ spiked with 1% trimethylsilane for the ^{1}H NMR spectra. For the ^{13}C NMR spectra the middle $CDCl_3$ peak (δ 77.00 ppm) was used as the internal standard. Signal patterns are indicated as b, broad; s, singlet; d, doublet; t, triplet; m, multiplet. Coupling constants (J) are given in hertz.

Synthesis of TREN based tripodal amide receptor (1•HCl). 3,5-dinitrobenzoyl chloride (3.152 g, 13.67 mmol) is weighed out into a 100 ml oven dried round bottom flask. Dry dimethylformamide (10 ml) is added via syringe and the reaction is stirred at 0 °C. Tris(2-aminoethyl)amine (0.51 ml, 3.40 mmol) is added dropwise and warmed to room temperature overnight. The remaining solution is heated to 160 °C for an additional 2 hours. Upon cooling the reaction mixture is poured over ice and the resulting oily solid is triturated with methanol to yield a tan powder in 80 % yield (1.94 g, 2.71 mmol) ^{1}H NMR (300 MHz, d_6 - DMSO; 25 °C): δ 9.68 (t, 3H), 9.01 (t, J = 3.0 Hz, 3H), 8.95 (d, J = 3.0 Hz, 6H), 3.63 (b).

Synthesis of TRPN based tripodal amide receptor (2•HCl): 3,5-dinitrobenzoyl chloride (2.460 g, 10.67 mmol) is weighed out into a 100 ml oven dried round bottom flask. Dry dimethylformamide (10 ml) is added via syringe and the reaction is stirred at 0 °C. Tris(3-aminopropyl)amine (0.52 ml, 2.62 mmol) is added dropwise and warmed to room temperature overnight. The reaction mixture is poured over ice and the resulting oily solid is sonicated repeatedly with water to yield a tan powder in 50 % yield (1.1244 g, 1.45 mmol) ^{1}H NMR NMR (300 MHz, d_6 - DMSO; 25 °C): δ 9.31 (t, 3H), 9.00 (d, J = 3.0 Hz, 6H), 8.91 (t, J = 3.0 Hz, 3H), 3.60 (m, 2H), 3.38 (m, 2H), 1.76 (m, 2H).

Synthesis of phosphine based receptor (3). Weigh out tris(methylamine) phosphineoxide hydrobromide (0.208 g, 0.57 mmol) and K_2CO_3 (0.408 g, 2.95 mmol) into an oven dried round bottom flask (100 ml) under a nitrogen atmosphere using standard schlenk techniques. A 1:1 mixture of ethyl acetate : water (50 ml) is added to the reaction flask. In a separate container 3,5-dinitrobenzoyl chloride (0.388 g, 1.68 mmol) is dissolve in ethyl acetate 4 ml. This solution is transferred dropwise while stirring the reaction mixture vigorously. The ethyl acetate layer is separated and the solvent removed under vacuum. The resulting product decomposes under an oxygen atmosphere. ^{1}H NMR (300 MHz, d_6 - DMSO; 25 ^{o}C): δ 9.58 (t, J = 6.3 Hz, 3H), 9.07 (d, J = 1.8 Hz, 6H), 8.96 (t, J = 2.1 Hz, 3H), 3.91 (b, 6H).

Synthesis of phosphine oxide based receptor (4). Weigh out tris(methylamine) phosphineoxide hydrobromide (0.107 g, 0.28 mmol) and K_2CO_3 (0.250 g, 0.03 mmol) into a round bottom flask (100 ml) and dissolve with 1:1 ethyl acetate:water (20 ml). In separate container weigh out 3,5-dinitrobenzoyl chloride (0.238 g, 1.03 mmol) and dissolve in ethyl acetate (3 ml). Transfer this solution dropwise to the reaction mixture while stirring vigorously. After 2 hours the ethyl acetate layer separated and the solvent is removed under vacuum yielding a white powder that is sparingly soluble in ethyl acetate, acetonitrile and hot ethyl alcohol. ^{1}H NMR (300 MHz, d_6 - DMSO; 25 ^{o}C): δ 9.64 (t, 3H), 9.03 (t, J = 1.8 Hz, 6H), 8.92 (t, 3H), 4.13 (b, 6H).

FUMING HNO_3. Fuming HNO_3 is prepared by distilling equal parts (v) of HNO_3 and H_2SO_4. The red distillate is collected at standard pressure at 80°C. **CAUTION fuming HNO_3 is a strong oxidizer and should be handled with extreme caution. Highly electron-deficient aromatic rings have the potential to be explosive. Handle with care.**

Synthesis of 4-chloro-3,5-dinitrobenzoic acid (7). Freshly distilled fuming nitric acid (4 ml) and concentrated sulfuric acid (20 ml) are cooled to 0 °C in a round bottom flask equipped with a magnetic stir bar. 4-chlorobenzoic acid (**6**) (5 g, 31.93 mmol) is transferred to the acid solution in 5 portions while stirring vigorously. The reaction mixture is warmed to room temperature and the heat is slowly increased to 90 °C. The yellow solution is heated for 8 hours. The reaction mixture is then cooled to room temperature and poured over 50 ml of ice. The pale yellow/green solid is filtered and washed with copious amounts of distilled water and dried under vacuum. The crystalline product is obtained in 92 % yield (7.25 g, 29.40 mmol) MP 166.1-167.0 °C. ^{1}H NMR (300 MHz, $CDCl_3$; 25 °C): δ 8.66 (s, 2H), 3.29 (b, 1H).

Synthesis of 4-chloro-3,5-dinitrobenzoic acid ethyl ester (8). (procedure adapted from *J. Org. Chem.* Vol. 66 No. 9 **2001**, 2985.) Thionyl chloride (30 ml) is added dropwise to dry ethanol (90 ml) at 0 °C. After solution has returned to 0 °C the 4-chloro-3,5-dinitrobenzoic acid (**7**) is added and the reaction mixture is heated to reflux. After 8 hours of refluxing the colorless solution is removed from heat and cooled to room temperature. The colorless crystals that formed upon cooling are collected and washed with cold ethanol. The ethanol wash is combined with the reaction solution and the solvent is removed under reduced pressure. Additional ester (**8**) is obtained by recrystallization of the reaction residue from hot ethanol (6.11 g, 92 %). MP 85.3-87.3 °C. ^{1}H NMR NMR (300 MHz, $CDCl_3$; 25 °C): δ 8.61 (s, 2H), 4.48 (q, J = X.X Hz, 2H), 1.45 (t, J = X.X Hz, 3H).

Synthesis of 4-cyano-3,5-dinitrobenzoic acid ethyl ester (9). In dry conditions under nitrogen using proper schlenk technique a flame dried 3-neck round bottom flask (100 ml) is charged with 4-chloro-3,5-dinitrobenzoic acid ethyl ester (**8**) (6.11 g, 22.26 mmol) and copper cyanide (2.79 g, 31.17 mmol). Dry dimethylformamide (30 ml) is added via syringe and the yellow solution is heated to 150 °C for 4 hours. After cooling to room temperature the dark green solution is poured over ice (150 ml). The dark green/red precipitate is collected and washed with water until the wash is colorless. The dark precipitate is dissolved in a minimal amount of ethyl acetate and filtered through a plug of silica. The eluent is collected in three portions with most of the

product being collected with the first 200 ml. The eluent is removed under reduced pressure and the resulting orange solid is recrystallized from hot ethyl alcohol in 52 % yield (3.07 g, 11.57 mmol) and the remaining ethyl ester (**9**) is obtained by reducing the ethyl alcohol concentration and fractional crystallization. ^{1}H NMR NMR (300 MHz, $CDCl_3$; 25 °C): δ 9.07 (s, 2H), 4.55 (q, J = 7.2 Hz, 2H), 1.49 (t, J = 7.5 Hz, 3H). ^{1}H NMR NMR (300 MHz, d_6 - DMSO; 25 °C): δ 8.92 (s, 2H), 4.45 (q, J = 6.9 Hz, 2H), 1.38 (t, J = 7.2 Hz, 3H). ^{13}C NMR (125 MHz, d_6 - DMSO; 25 °C): δ 161.75, 151.18, 135.12, 129.59, 110.51, 105.69, 63.01, 13.90.

Synthesis of 4-cyano-3,5-dinitrobenzoic acid (5). A round bottom flask (250 ml) is charged with 4-cyano-3,5-dinitrobenzoic acid ethyl ester (**9**) (5.22 g, 19.69 mmol). Glacial acetic acid (100 ml) and concentrated HCl (30 ml) are added to the round bottom flask and the reaction is heated to 90 °C overnight under a nitrogen atmosphere. After 14 hours the reaction is cooled to room temperature. The acid (**5**) is extracted with diethyl ether (3 x 150 ml) and subsequently dried with Na_2SO_4. The diethyl ether is removed under reduced pressure leaving a yellow solid. Alternatively the product can be collected as a yellow solid (4.43 g, 95%) after removing the acetic acid/HCl under reduced pressure. The acid is 96% pure by ^{1}H NMR and can be purified by washing the yellow solid with dichloromethane. ^{1}H NMR NMR (300 MHz, d_6 - DMSO; 25 °C): δ 8.89 (s, 2H), 3.50 (b, 1H).

X-RAY DIFFRACTION. Single-crystal X-ray diffraction data for compounds **1**•HCl, **4** and **5** were collected on a Bruker-AXS SMART APEX/CCD diffractometer using $Mo_{k\alpha}$ radiation ($\lambda = 0.7107$ Å) at 152 K. Diffracted data have been corrected for Lorentz and polarization effects, and for absorption using the SADABS v2.02 area-detector absorption correction program (Siemens Industrial Automation, Inc., © 1996). The structures were solved by direct methods and the structure solution and refinement was based on $|F|^2$. Hydrogen were found from the residual density map when possible and refined with isotropic thermal parameters and otherwise placed in calculated positions and given isotropic U values 1.2 times that of the atom to which they are bonded. All non-hydrogen atoms were refined with anisotropic displacement parameters. All crystallographic calculations were conducted with the SHELXTL v.6.1 program package (Bruker AXS Inc., © 2001).

Crystal data for **1**•HCl: $C_{27}H_{25}ClN_{10}O_{15}$, $M = 765.02$, triclinic, P-1, $a = 12.3142(13)$ Å, $b = 13.2582(15)$ Å, $c = 20.049(2)$ Å, $\alpha = 92.948(2)°$, $\beta = 95.577(2)°$, $\gamma = 92.771(2)°$, $V = 3248.9(6)$ Å^3, $Z = 4$, μ(Mo-Kα) = 0.208 mm^{-1}. Final residuals (1155 parameters) $R1 = 0.0430$ for 13528 reflections with $I > 2\sigma(I)$, and $R1 = 0.0716$, $wR2 = 0.1238$, GooF = 0.978 for all 25458 data.

Crystal data for **4**: $C_8H_6N_3O_{5.3}P_{0.3}$ (C_2H_6OS), $M = 953.83$, Rhombohedral, $R3$, $a = 26.969(4)$ Å, $b = 26.969(4)$ Å, $c = 4.7896(9)$ Å, $\alpha = 90.00°$, $\beta = 90.00°$, $\gamma = 120.00°$, $V = 3016.8(8)$ Å^3, $Z = 3$, μ(Mo-Kα) = 0.315 mm^{-1}. Final residuals (213 parameters) $R1 =$

0.0543 for 2974 reflections with $I > 2\sigma(I)$, and $R1 = 0.1004$, $wR2 = 0.0864$, GooF = 0.801 for all 9960 data.

Crystal data for **5**: $C_8H_3N_3O_6 \bullet (C_2H_6OS)$, $M = 252.21$, monoclinic, $P(2)1/c$, $a = 9.9021(17)$ Å, $b = 5.9929(10)$ Å, $c = 22.218(4)$ Å, $\alpha = 90.00°$, $\beta = 96.386(3)°$, $\gamma = 90.00°$, $V = 1310.3(4)$ Å^3, $Z = 4$, μ(Mo-Kα) = 0.287 mm^{-1}. Final residuals (226 parameters) $R1 = 0.0460$ for 3029 reflections with $I > 2\sigma(I)$, and $R1 = 0.0622$, $wR2 = 0.1062$, GooF = 1.053 for all 10638 data.

APPENDIX E

SUPPORTING INFORMATION FOR CHAPTER VI: A CONFORMATIONALLY DIVERSE SERIES OF MOLECULES; 2,6-BIS(ETHYNYL)PYRIDINE, BIPYRIDINE AND THIOPHENE AS SCAFFOLDS FOR MODULAR RECEPTOR DESIGN

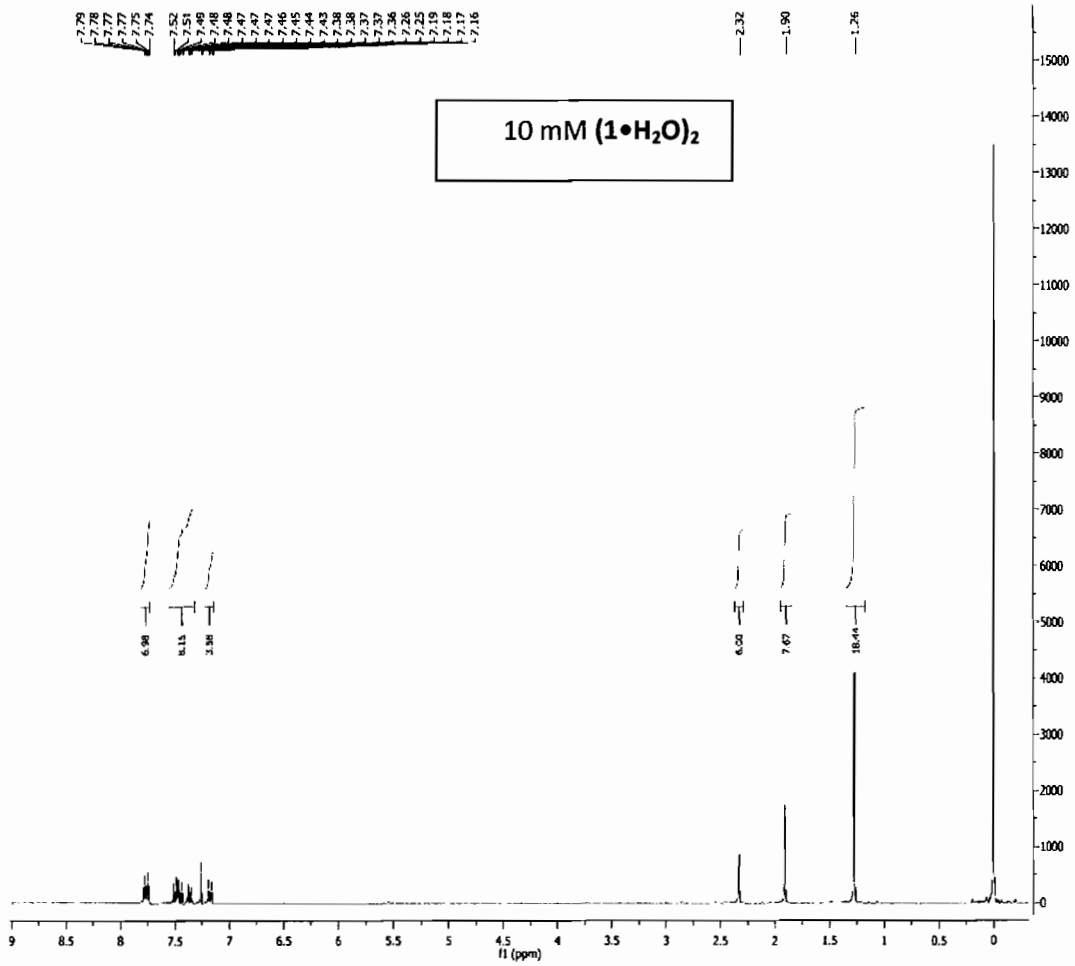

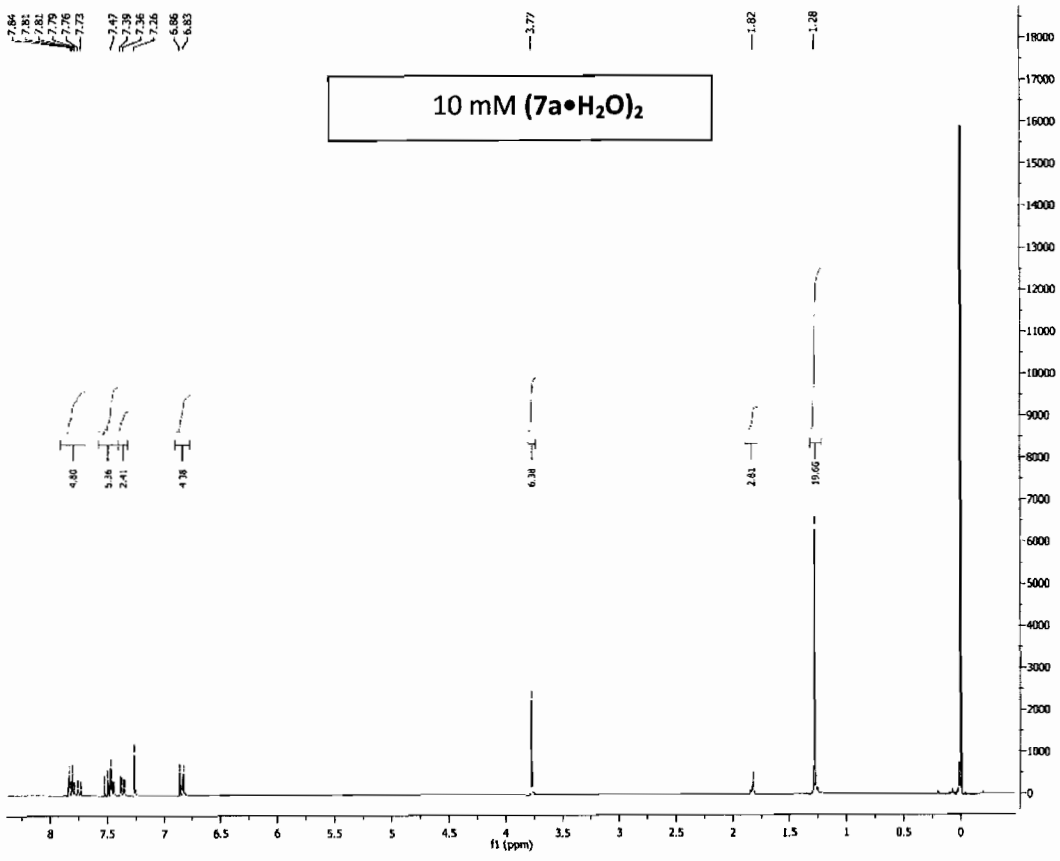
10 mM (7a•H2O)2
7.84
7.81
7.81
7.79
7.76
7.73
7.47
7.39
7.36
7.26
6.86
6.83
3.77
1.82
1.28
4.80
5.36
2.41
4.38
6.38
2.81
19.66
f1 (ppm)

[1•H_2O]•[7a•H_2O]. 1•H_2O (3.650 mg, 0.00488 mmol) and **7a•H_2O** (3.740 mg, 0.00480 mmol) were dissolved in seperate portions of $CDCl_3$ with 1 % TMS (1 mL) passed through basic alumina and dried with 3 Å molecular sieves. Aliquots (400 μL) from each solution were transfered to an NMR tube via syringe and thoroughly mixed. ^1H NMR spectra were recorded on a Varian 300 MHz spectrometer. Proton signals were referenced to the 1 % TMS included in the $CDCl_3$. ^1H NMR (300 MHz, $CDCl_3$): δ 7.81-7.73 (m, 10H), 7.52-7.44 (m, 12H), 7.38-7.33 (m, 8H), 7.18 (d, J = 9 Hz, 4H), 6.85 (d, J = 9 Hz, 6H), 7.18 (d, J = 6 Hz, 3H) 2.29 (s, 6H), 1.26 (s, 18H).

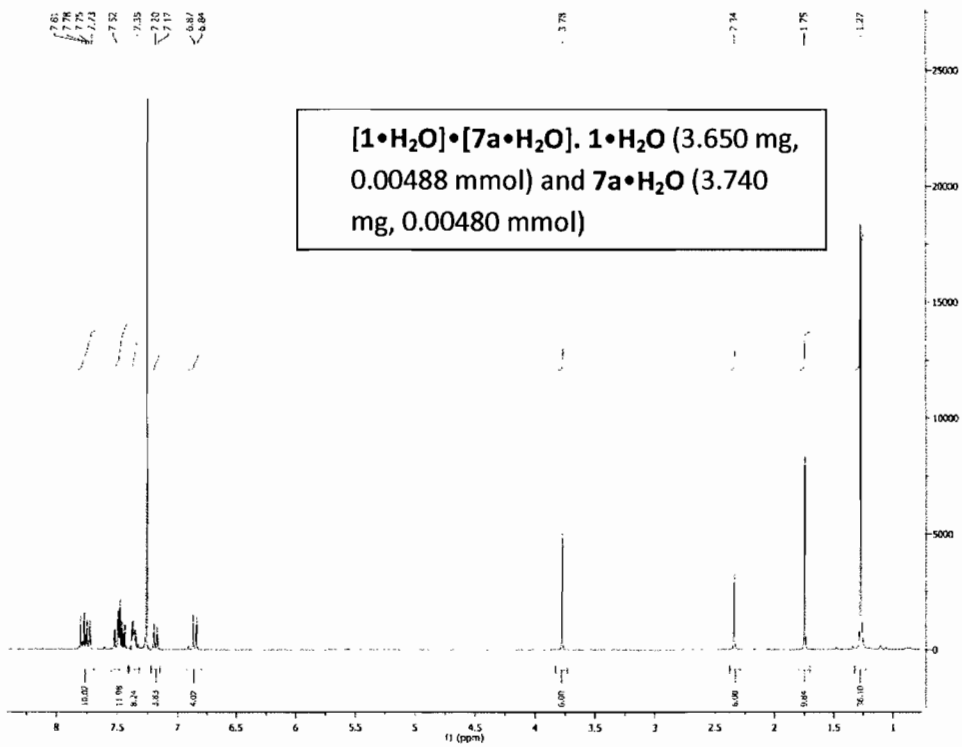

[H1$^+$•Cl$^-$]•[H7a$^+$•Cl$^-$]. The stock solutions from the preparation of **[1•H_2O]•[7a•H_2O]** (above) were combined and protonated with HCl gas (see below, **General salt preparation**). ^{1}H NMR spectra were recorded on a Varian 300 MHz spectrometer. Proton signals were referenced to the 1 % TMS included in the $CDCl_3$. ^{1}H NMR (300 MHz, $CDCl_3$): δ 9.49 (s, 2H), 9.44 (s, 2H), 8.30 (b, 2H), 8.18 (d, J = 9 Hz, 4H), 8.12 (d, J = 9 Hz, 4H), 7.71 (d, J = 6 Hz, 4H) 7.46 (m, 12H), 7.17 (d, J = 6 Hz, 4 H), 6.85 (d, J = 6 Hz, 4H), 3.73 (s, 6H), 2.27 (s, 6H), 1.25 (s, 36H).

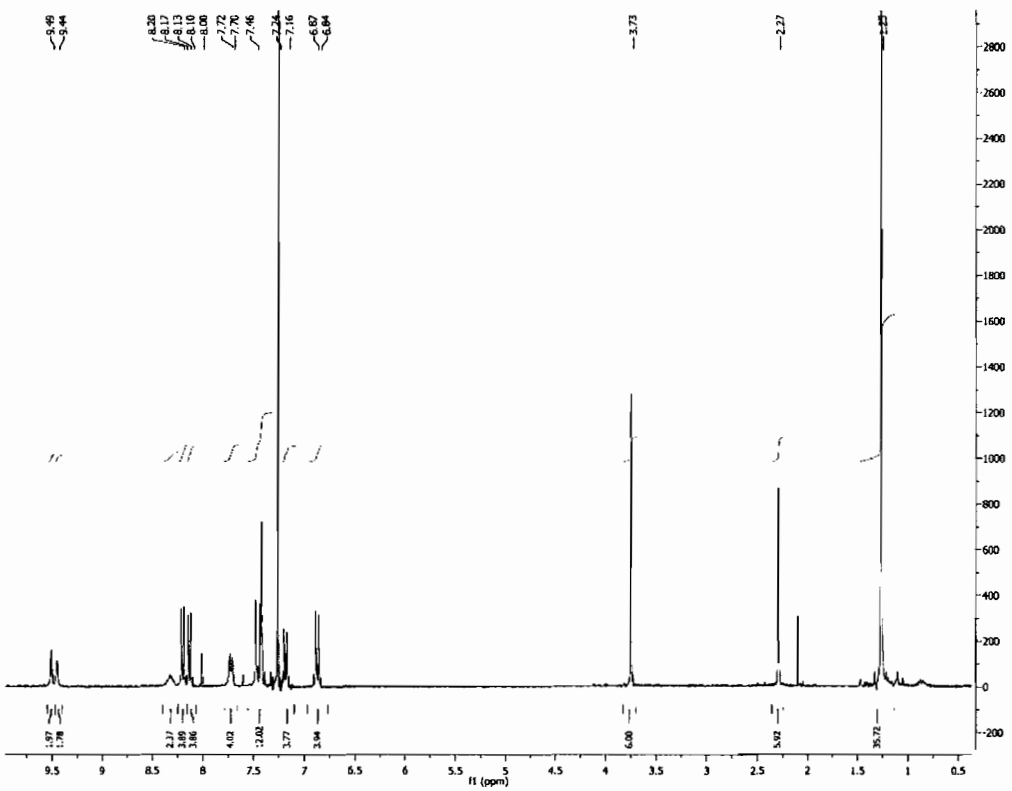

General salt preparation. A 10 mM stock solution of sulfonamide receptor dissolved in $CDCl_3$ with 1 % TMS that has been passed through basic alumina and stored over 3 Å molecular seives was prepared. With a 9 inch pipette and 10 ml pipet bulb HCl gas is passed through the sulfonamide solution 20 times. The resulting yellow solution is diluted to the original volume and an appropriate aliqout is removed for study.

$(H1^+•Cl^-)_2$. 10 mM stock solutions of $(H1^+•Cl^-)_2$ were prepared according to the **General salt preparation** (above). ^{1}H NMR (300 MHz, $CDCl_3$): δ 9.51 (b, 2H), 8.40 (b, 1H), 8.13 (d, J = 6 Hz, 4H), 8.00-7.75 (b, 4H), 7.48-7.41 (m, 6H), 7.18 (d, J = 6 Hz, 3H) 2.29 (s, 6H), 1.26 (s, 18H).

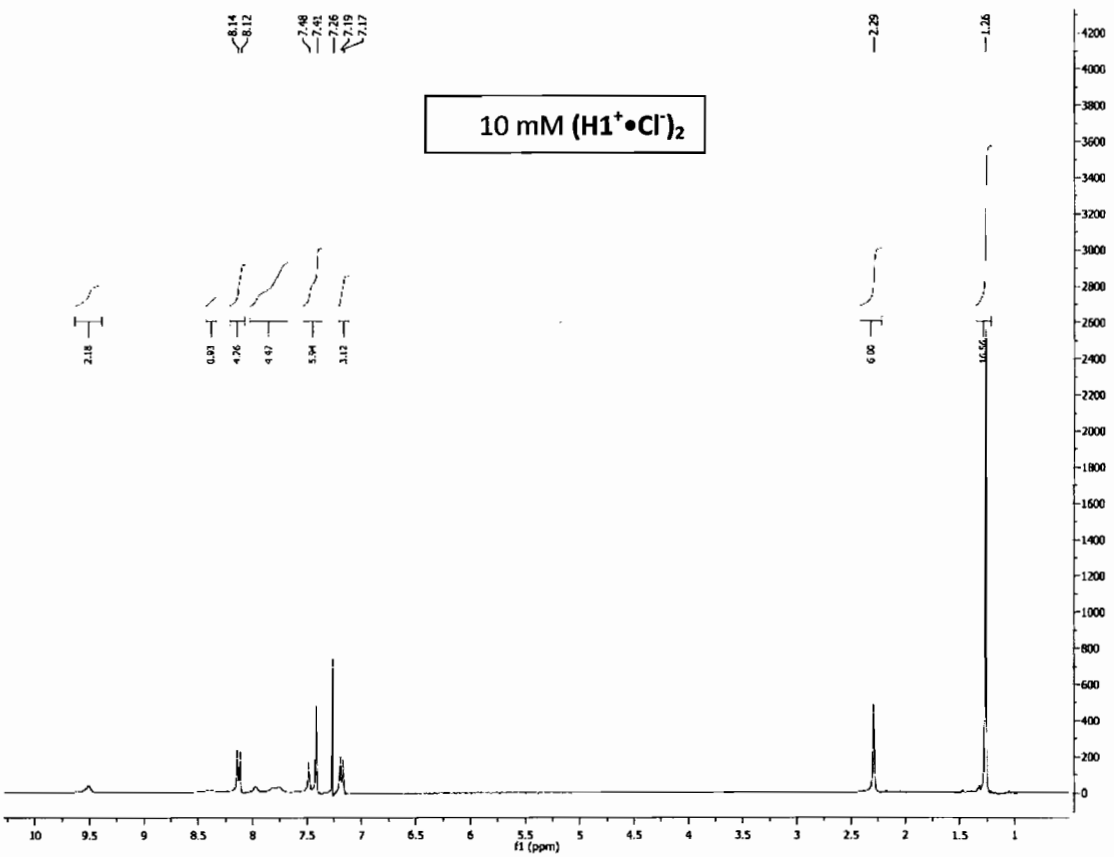

(H7a$^+$•Cl$^-$)$_2$. 10 mM stock solutions of (**H7a**$^+$•Cl$^-$)$_2$ were prepared according to the **General salt preparation** (above).^{1}H NMR (300 MHz, $CDCl_3$): δ 9.36 (b, 2H), 8.31 (t, 1H), 8.17 (d, J = 9 Hz, 4H), 7.72 (d, J = 9 Hz, 4H), 7.40 (m, 6H), 6.86 (d, J = 9 Hz, 4H) 3.75 (s, 6H), 1.26 (s, 18H).

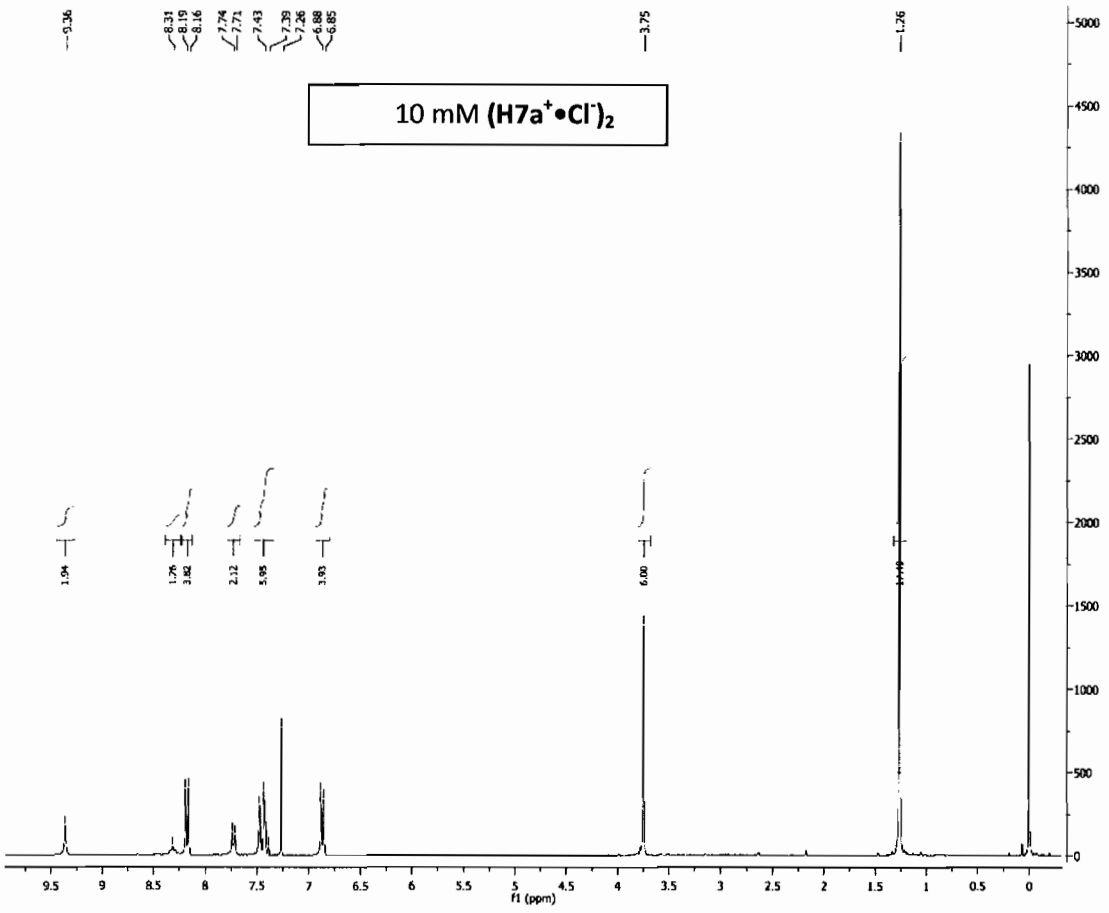

Dilution experiment: $(\mathbf{1 \cdot H_2O})_2$ (88.260 mg, 0.180 mmol) was dissolved in $CDCl_3$ (600 µl) saturated with H_2O. $CDCl_3$ saturated with H_2O was prepared by mixing equal parts (v/v) $CDCl_3$ and H_2O for 30 minutes followed by separation of the two layers. Aliquots of $CDCl_3$ saturated with H_2O were added to the initial solution of receptor (197 mM) until the end point of the titration is reached (minimal change in chemical shift observed per per aliquot of $CDCl_3$). All additions were performed through septa with a Hamilton gas tight microsyringe at room temperature. ^1H NMR spectra were recorded after each addition on a Varian 300 MHz spectrometer. Proton signals were referenced to the residual $CHCl_3$ signal. The dimerization constant K_{dim} was calculated by plotting the change in the shift of the sulfonamide proton versus the total concentration and the resulting data was fit to a 1:1 dimerization with the non-linear regression curve fitting software WinEQNMR.

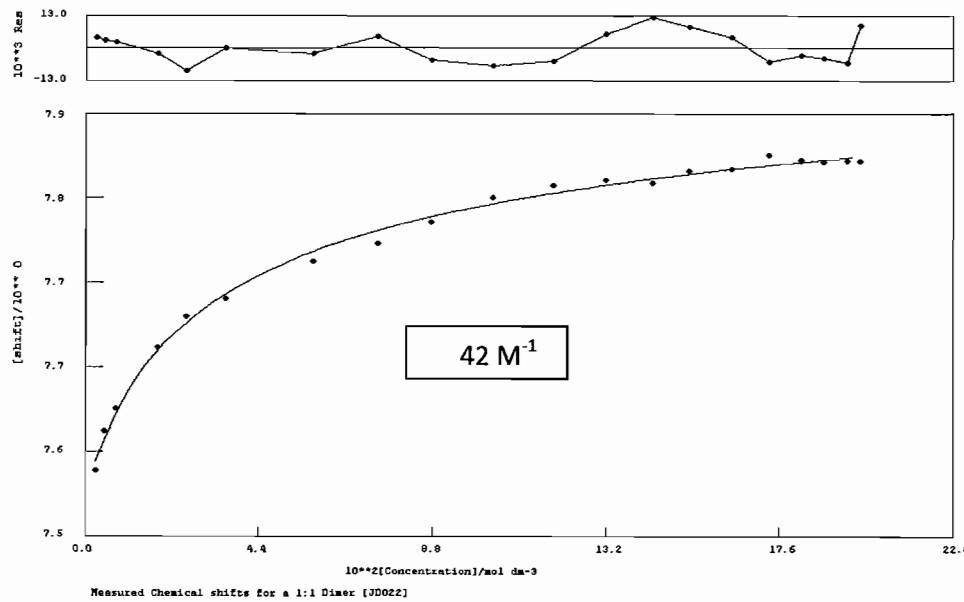

vol removed prior to addition	file	vol added (ml)	Vol prior to addition	Total vol in NMR tube after	[R]	NH peak
0	JD022_0	0	0	0.6	1.967E-01	7.855
0	JD022_1	0.01	0.6	0.61	1.934E-01	7.855
0	JD022_2	0.02	0.61	0.63	1.873E-01	7.854
0	JD022_3	0.02	0.63	0.65	1.815E-01	7.856
0	JD022_4	0.03	0.65	0.68	1.735E-01	7.86
0	JD022_5	0.04	0.68	0.72	1.639E-01	7.847
0	JD022_6	0.05	0.72	0.77	1.532E-01	7.845
0	JD022_7	0.05	0.77	0.82	1.439E-01	7.834
0	JD022_8	0.075	0.82	0.895	1.318E-01	7.837
0	JD022_9	0.1	0.895	0.995	1.186E-01	7.832
0	JD022_10	0.15	0.995	1.145	1.031E-01	7.82
0	JD022_11	0.2	1.145	1.345	8.773E-02	7.797
0	JD022_12	0.25	1.345	1.595	7.398E-02	7.777
0	JD022_13	0.45	1.595	2.045	5.770E-02	7.761
1.25	JD022_14	0.5	0.795	1.295	3.542E-02	7.725
0	JD022_15	0.5	1.295	1.795	2.556E-02	7.708
0	JD022_16	0.7	1.795	2.495	1.839E-02	7.679
1.75	JD022_17	1	0.745	1.745	7.850E-03	7.621
0	JD022_18	1	1.745	2.745	4.990E-03	7.599
1	JD022_19	1.3	1.745	3.045	2.860E-03	7.562

NOESY1D experiment. (1•H_2O)$_2$ (88.260 mg, 0.180 mmol) was dissolved in $CDCl_3$ (600 µl) saturated with H_2O. $CDCl_3$ saturated with H_2O was prepared by mixing equal parts (v/v) $CDCl_3$ and H_2O for 30 minutes followed by separation of the two layers. ^1H NMR spectra were recorded on a Varian 500 MHz spectrometer. Proton signals were referenced to the residual $CHCl_3$ signal. NOE between the water and sulfonamide protons were observed by irradiating either the guest water protons (3.042 ppm) or the hydrogen bonding sulfonamide protons (7.570 ppm) and observing signal enhancement from the other protons.

OBG-5mm

Pulse Sequence: NOESY1D
Solvent: CDCl3
Temp. 25.0 C / 298.1 K
User: 1-15-87
INOVA-500 "icarus"

Relax. delay 1.000 sec
Pulse 99.0 degrees
Mixing 0.500 sec
Acq. time 2.341 sec
Width 6999.7 Hz
61 repetitions
OBSERVE H1, 500.1042443 MHz
DATA PROCESSING
Line broadening 1.5 Hz
FT size 131072
Total time 37 min, 7 sec

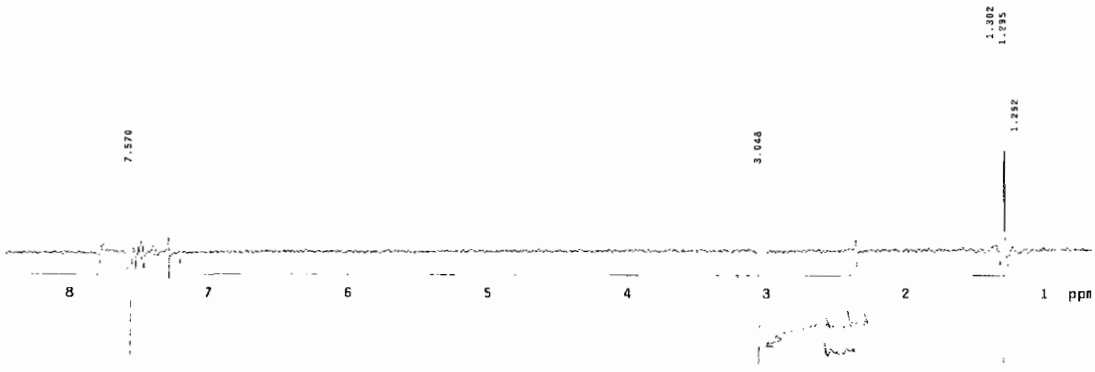

OBG-5mm

Pulse Sequence: NOESY1D
Solvent: CDCl3
Temp. 25.0 C / 298.1 K
User: 1-15-87
INOVA-500 "icarus"

Relax. delay 2.000 sec
Pulse 99.0 degrees
Mixing 0.500 sec
Acq. time 2.341 sec
Width 6999.7 Hz
64 repetitions
OBSERVE H1, 500.1012313 MHz
DATA PROCESSING
Line broadening 1.5 Hz
FT size 131072
Total time 38 min, 23 sec

Crystal growth conditions. Sulfonamide receptors were dissolved in a 10x75 mm test tube with EtOAc to a concentration > 10 mM (for halide salts HX gas was passed through the EtOAc solution of receptor). Alternatively, 1 drop of concentrated HX is added and the resulting yellow solution is thoroughly mixed). Hexanes cooled to 0°C were layered on top of receptor solutions and set aside. After 3 days colorless (neutral receptor complex) or yellow (protonated receptor complex) single crystals were harvested for X-ray diffraction studies. Refer to cif files for exact structural details.

REFERENCES

CHAPTER I

(1) P. Gamez, T. J. Mooibroek, S. J. Teat and J. Reedijk, *Acc. Chem. Res.,* 2007, **40**, 435-444.

(2) B. L. Schottel, H. T. Chifotides and K. R. Dunbar, *Chem. Soc. Rev.*, 2008, **37**, 68-83.

(3) B. P. Hay and V. S. Bryantsev, *Chem. Commun.*, 2008, *in press*.

(4) C. L. Jackson and W. F. Boos, *Am. Chem. J.*, 1898, **20**, 444-455.

(5) C. L. Jackson and F. H. Gazzolo, *Am. Chem. J.*, 1900, **23**, 376-396.

(6) J. Meisenheimer, *Justus Liebigs Ann. Chem.*, 1902, **323**, 205-226.

(7) E. Buncel, A. R. Norris and K. E. Russell, *Quart. Rev. Chem. Soc.*, 1968, **22**, 123-146.

(8) R. S. Mulliken, *J. Am. Chem. Soc.*, 1952, **74**, 811-824.

(9) G. A. Artamkina, M. P. Egorov and I. P. Beletskaya, *Chem. Rev.*, 1982, **82**, 427-459.

(10) C. F. Bernasconi, *Acc. Chem. Res.*, 1978, **11**, 147-152.

(11) C. F. Bernasconi, *Chimia*, 1980, **34**, 1-11.

(12) M. J. Strauss, *Chem. Rev.*, 1970, **70**, 667-712.

(13) M. J. Strauss, *Acc. Chem. Res.*, 1974, **7**, 181-188.

(14) F. Terrier, *Chem. Rev.*, 1982, **82**, 77-152.

(15) S. Chowdhury, E. P. Grimsrud, T. Heinis and P. Kebarle, *J. Am. Chem. Soc.*, 1986, **108**, 3630-3635.

(16) S. Chowdhury, T. Heinis and P. Kebarle, *J. Am. Chem. Soc.*, 1986, **108**, 4662-4663.

(17) S. Chowdhury and P. Kebarle, *J. Am. Chem. Soc.*, 1986, **108**, 5453-5459.

(18) S. Chowdhury, H. Kishi, G. W. Dillow and P. Kebarle, *Can. J. Chem.*, 1989, **67**, 603-610.

(19) S. Chowdhury, G. Nicol and P. Kebarle, *Chem. Phys. Lett.*, 1986, **127**, 130-132.

(20) E. P. Grimsrud, S. Chowdhury and P. Kebarle, *Int. J. Mass Spectrom. and Ion Processes*, 1986, **68**, 57-70.

(21) T. Heinis, S. Chowdhury, S. L. Scott and P. Kebarle, *J. Am. Chem. Soc.*, 1988, **110**, 400-407.

(22) K. Hirao and P. Kebarle, *Can. J. Chem.*, 1989, **67**, 1261-1267.

(23) K. Hiraoka, S. Mizuse and S. Yamabe, *J. Phys. Chem.*, 1987, **91**, 5294-5297.

(24) K. Hiraoka, S. Mizuse and S. Yamabe, *J. Chem. Phys.*, 1987, **86**, 4102-4105.

(25) P. Kebarle and S. Chowdhury, *Chem. Rev.*, 1987, **87**, 513-534.

(26) G. J. C. Paul and P. Kebarle, *J. Am. Chem. Soc.*, 1991, **113**, 1148-1154.

(27) B. Chiavarino, M. E. Crestoni, S. Fornarini, F. Lanucara, J. Lemaire and P. Maitre, *Angew. Chem. Int. Ed.*, 2007, **46**, 1995-1998.

(28) H. Sun and S. G. DiMagno, *Angew. Chem. Int. Ed.*, 2006, **45**, 2720-2725.

(29) I. Alkorta, I. Rozas and J. Elguero, *J. Am. Chem. Soc.*, 2002, **124**, 8593-8598.

(30) M. Mascal, A. Armstrong and M. D. Bartberger, *J. Am. Chem. Soc.*, 2002, **124**, 6274-6276.

(31) D. Quinonero, C. Garau, C. Rotger, A. Frontera, P. Ballester, A. Costa and P. M. Deya, *Angew. Chem. Int. Ed.*, 2002, **41**, 3389-3392.

(32) C. F. Carolina, A.; Quinoner, D.; Ballester, P.; Costa, A.; Deya, P. M., *Chem. Phys. Chem.*, 2003, **4**, 1344-1348.

(33) A. Clements and M. Lewis, *J. Phys. Chem. A*, 2006, **110**, 12705-12710.

(34) D. Escudero, A. Frontera, D. Quinonero and P. M. Deya, *Chem. Phys. Lett.*, 2008, **455**, 325-330.

(35) C. Estarellas, D. Quinonero, A. Frontera, P. Ballester, J. Morey, A. Costa and P. M. Deya, *J. Phys. Chem. A*, 2008, **112**, 1622-1626.

(36) A. Frontera, F. Saczewski, M. Gdaniec, E. Dziemidowicz-Borys, A. Kurland, P. M. Deya, D. Quinonero and C. Garau, *Chem. Eur. J.*, 2005, **11**, 6560-6567.

(37) C. Garau, A. Frontera, P. Ballester, D. Quinonero, A. Costa and P. M. Deya, *Eur. J. Org. Chem.*, 2004, 179-183.

(38) C. Garau, A. Frontera, D. Quinonero, P. Ballester, A. Costa and P. M. Deya, *Chem. Phys. Lett.*, 2004, **399**, 220-225.

(39) C. Garau, A. Frontera, D. Quinonero, P. Ballester, A. Costa and P. M. Deya, *J. Phys. Chem. A*, 2004, **108**, 9423-9427.

(40) C. Garau, A. Frontera, D. Quinonero, P. Ballester, A. Costa and P. M. Deya, *Chem. Phys. Lett.*, 2004, **392**, 85-89.

(41) C. Garau, D. Quinonero, A. Frontera, P. Ballester, A. Costa and P. M. Deya, *Org. Lett.*, 2003, **5**, 2227-2229.

(42) C. Garau, D. Quinonero, A. Frontera, P. Ballester, A. Costa and P. M. Deya, *J. Phys. Chem. A*, 2005, **109**, 9341-9345.

(43) C. Garau, D. Quinonero, A. Frontera, A. Costa, P. Ballester and P. M. Deya, *Chem. Phys. Lett.*, 2003, **370**, 7-13.

(44) A. Garcia-Raso, F. M. Alberti, J. J. Fiol, A. Tasada, M. Barcelo-Oliver, E. Molins, D. Escudero, A. Frontera, D. Quinonero and P. M. Deya, *Eur. J. Org. Chem.*, 2007, 5821-5825.

(45) A. Garcia-Raso, F. M. Alberti, J. J. Fiol, A. Tasada, M. Barcelo-Oliver, E. Molins, D. Escudero, A. Frontera, D. Quinonero and P. M. Deya, *Inorg. Chem.*, 2007, **46**, 10724-10735.

(46) J. M. Hermida-Ramon and C. M. Estevez, *Chem. Eur. J.*, 2007, **13**, 4743-4749.

(47) M. Mascal, *Angew. Chem. Int. Ed.*, 2006, **45**, 2890-2893.

(48) D. Quinonero, A. Frontera and M. Deya Pere, *Chem. Phys. Chem*, 2008, **9**, 397-399.

(49) D. Quinonero, A. Frontera, C. Garau, P. Ballester, A. Costa and P. M. Deya, *Chem. Phys. Chem.*, 2006, **7**, 2487-2491.

(50) D. Quinonero, C. Garau, A. Frontera, P. Ballester, A. Costa and P. M. Deya, *Chem. Phys. Lett.*, 2002, **359**, 486-492.

(51) H. Schneider, K. M. Vogelhuber, F. Schinle and J. M. Weber, *J. Am. Chem. Soc.*, 2007, **129**, 13022-13026.

(52) D. Escudero, A. Frontera, D. Quinonero, A. Costa, P. Ballester and P. M. Deya, *J. Chem. Theory Comput.*, 2007, **3**, 2098-2107.

(53) C. Garau, D. Quinonero, A. Frontera, D. Escudero, P. Ballester, A. Costa and P. M. Deya, *Chem. Phys. Lett.*, 2007, **438**, 104-108.

(54) M. R. Jackson, R. Beahm, S. Duvvuru, C. Narasimhan, J. Wu, H.-N. Wang, V. M. Philip, R. J. Hinde and E. E. Howell, *J. Phys. Chem. B*, 2007, **111**, 8242-8249.

(55) D. Kim, P. Tarakeshwar and K. S. Kim, *J. Phys. Chem. A*, 2004, **108**, 1250-1258.

(56) D. Quinonero, A. Frontera, D. Escudero, P. Ballester, A. Costa and P. M. Deya, *Chem. Phys. Chem.*, 2007, **8**, 1182-1187.

(57) D. Quinonero, C. Garau, A. Frontera, P. Ballester, A. Costa and P. M. Deya, *J. Phys. Chem. A*, 2005, **109**, 4632-4637.

(58) B. L. Schottel, H. T. Chifotides, M. Shatruk, A. Chouai, L. M. Perez, J. Bacsa and K. R. Dunbar, *J. Am. Chem. Soc.*, 2006, **128**, 5895-5912.

(59) M. Zaccheddu, C. Filippi and F. Buda, *J. Phys. Chem. A*, 2008, **112**, 1627-1632.

(60) O. B. Berryman, F. Hof, M. J. Hynes and D. W. Johnson, *Chem. Commun.*, 2006, 506-508.

(61) O. B. Berryman, V. S. Bryantsev, D. P. Stay, D. W. Johnson and B. P. Hay, *J. Am. Chem. Soc.*, 2007, **129**, 48-58.

(62) R. Ahuja and A. G. Samuelson, *Cryst. Eng. Comm.*, 2003, **5**, 395-399.

(63) C. A. Black, L. R. Hanton and M. D. Spicer, *Chem. Commun.*, 2007, 3171-3173.

(64) C. A. Black, L. R. Hanton and M. D. Spicer, *Inorg. Chem.*, 2007, **46**, 3669-3679.

(65) C. S. Campos-Fernandez, B. L. Schottel, H. T. Chifotides, J. K. Bera, J. Bacsa, J. M. Koomen, D. H. Russell and K. R. Dunbar, *J. Am. Chem. Soc.*, 2005, **127**, 12909-12923.

(66) H. Casellas, C. Massera, F. Buda, P. Gamez and J. Reedijk, *New J. Chem.*, 2006, **30**, 1561-1566.

(67) P. de Hoog, P. Gamez, I. Mutikainen, U. Turpeinen and J. Reedijk, *Angew. Chem. Int. Ed.*, 2004, **43**, 5815-5817.

(68) S. Demeshko, S. Dechert and F. Meyer, *J. Am. Chem. Soc.*, 2004, **126**, 4508-4509.

(69) R. M. Fairchild and K. T. Holman, *J. Am. Chem. Soc.*, 2005, **127**, 16364-16365.

(70) I. Y. A. Gural'skiy, P. V. Solntsev, H. Krautscheid and K. V. Domasevitch, *Chem. Commun.*, 2006, 4808-4810.

(71) P. U. Maheswari, B. Modec, A. Pevec, B. Kozlevcar, C. Massera, P. Gamez and J. Reedijk, *Inorg. chem.*, 2006, **45**, 6637-6645.

(72) B. L. Schottel, J. Bacsa and K. R. Dunbar, *Chem. Commun.*, 2005, 46-47.

(73) X.-P. Zhou, X. Zhang, S.-H. Lin and D. Li, *Cryst. Growth Des.*, 2007, **7**, 485-487.

(74) M. Albrecht, C. Wessel, M. de Groot, K. Rissanen and A. Luechow, *J. Am. Chem. Soc.*, 2008, **130**, 4600-4601.

(75) P. S. Lakshminarayanan, I. Ravikumar, E. Suresh and P. Ghosh, *Inorg. Chem.*, 2007, **46**, 4769-4771.

(76) T. Dorn, C. Janiak and K. Abu-Shandi, *Cryst. Eng. Comm.*, 2005, **7**, 633-641.

(77) M. Mascal, I. Yakovlev, E. B. Nikitin and J. C. Fettinger, *Angew. Chem. Int. Ed.*, 2007, **46**, 8782-8784.

(78) T. J. Mooibroek, C. A. Black, P. Gamez and J. Reedijk, *Cryst. Growth Des.*, 2008, **8**, 1082-1093.

(79) B. Han, J. Lu and J. K. Kochi, *Cryst. Growth Des.*, 2008, **8**, 1327-1334.

(80) Y. S. Rosokha, S. V. Lindeman, S. V. Rosokha and J. K. Kochi, *Angew. Chem. Int. Ed.*, 2004, **43**, 4650-4652.

(81) H. J. Schneider, *Angew. Chem. Int. Ed.*, 1991, **1411**, 1417-1436.

(82) G. Bruno, G. Cafeo, F. H. Kohnke and F. Nicolo, *Tetrahedron*, 2007, **63**, 10003-10010.

(83) G. Gil-Ramirez, E. C. Escudero-Adan, J. Benet-Buchholz, P. Ballester, *Angew. Chem. Int. Ed.* 2008, *in press*.

(84) H. Maeda, T. Morimoto, A. Osuka and H. Furuta, *Chem. Asian J.*, 2006, **1**, 832-844.

(85) H. Maeda, A. Osuka and H. Furuta, *J. Inclusion Phenom. Macrocyclic Chem.*, 2004, **49**, 33-36.

CHAPTER II

(1) P. D. Beer and P. A. Gale, *Angew. Chem. Int. Ed.,* 2001, **40**, 486.

(2) A. P. Bisson, V. M. Lynch, M.-K. C. Monahan, and E. V. Anslyn, *Angew. Chem. Int. Ed.,* 1997, **36**, 2340.

(3) J. L. Sessler, S. Camiolo, and P. A. Gale, *Coord. Chem. Rev.*, 2003, **240**, 17.

(4) A. Bianchi, K. Bowman-James, E. Garcia-Espana, and Editors, 'Supramolecular Chemistry of Anions', Wiley-VCH, New York, 1997.

(5) D. Quinonero, C. Garau, C. Rotger, A. Frontera, P. Ballester, A. Costa, and P. M. Deya, *Angew. Chem. Int. Ed.,* 2002, **41**, 3389.

(6) A. Frontera, F. Saczewski, M. Gdaniec, E. Dziemidowicz-Borys, A. Kurland, P. M. Deya, D. Quinonero, and C. Garau, *Chem. Eur. J.*, 2005, **11**, 6560.

(7) M. Mascal, A. Armstrong, and M. D. Bartberger, *J. Am. Chem. Soc.*, 2002, **124**, 6274.

(8) D. Kim, P. Tarakeshwar, and K. S. Kim, *J. Phys. Chem. A*, 2004, **108**, 1250.

(9) C. Garau, A. Frontera, D. Quinonero, P. Ballester, A. Costa, and P. M. Deya, *J. Phys. Chem. A*, 2004, **108**, 9423.

(10) P. de Hoog, P. Gamez, W. L. Driessen, and J. Reedijk, *Tetrahedron Lett.*, 2002, **43**, 6783.

(11) P. de Hoog, P. Gamez, I. Mutikainen, U. Turpeinen, and J. Reedijk, *Angew. Chem. Int. Ed.,* 2004, **43**, 5815.

(12) S. Demeshko, S. Dechert, and F. Meyer, *J. Am. Chem. Soc.*, 2004, **126**, 4508.

(13) Y. S. Rosokha, S. V. Lindeman, S. V. Rosokha, and J. K. Kochi, *Angew. Chem. Int. Ed.,* 2004, **43**, 4650.

(14) J. Pang, Y. Tao, S. Freiberg, X.-P. Yang, M. D'Iorio, and S. Wang, *J. Mater. Chem.*, 2002, **12**, 206.

(15) C. Garau, A. Frontera, D. Quinonero, P. Ballester, A. Costa, and P. M. Deya, *Chem. Phys. Chem.*, 2003, **4**, 1344.

(16) J. C. Ma and D. A. Dougherty, *Chem. Rev.*, 1997, **97**, 1303.

(17) A hydrogen bonding interaction is included in our first receptor design to enhance the association of the receptor for anions. ^{1}H NMR and UV-Vis spectroscopic studies of simple electron deficient aromatics such as hexafluorobenzene, 1,3,5-trifluorobenzene, 1,3,5-tribromobenzene and 1,3,5-trichlorobenzene showed no measurable binding with the halides. This suggested that a single anion-π interaction using a halogenated aromatic would not be strong enough to drive binding in solution.

(18) T. Sakamoto, Y. Kondo, S. Iwashita, T. Nagano, and H. Yamanaka, *Chem. Pharm. Bull.*, 1988, **36**, 1305.

(19) N. Shimizu, T. Kitamura, K. Watanabe, T. Yamaguchi, H. Shigyo, and T. Ohta, *Tet. Lett.*, 1993, **34**, 3421.

(20) M. G. Banwell, B. D. Kelly, O. J. Kokas, and D. W. Lupton, *Org. Lett.*, 2003, **5**, 2497.

(21) The X-ray crystal structure of **1** is in agreement with recent theoretical studies regarding the attractive interaction between the lone pair of a heteroatom and an electron-deficient aromatic ring.

(22) I. Alkorta, I. Rozas, and J. Elguero, *J. Org. Chem.*, 1997, **62**, 4687.

(23) CAChe, version 5.0, Fujitsu America, Beaverton, USA, **2002**.

(24) M. J. Hynes, *J. Chem. Soc., Dalton Trans.*, 1993, 311.

(25) The dimerization constants for receptors **1** and **2** were measured by ^{1}H NMR titrations (see method described in: A. P. Bisson; C. A. Hunter; J. C. Morales; K. Young. *Chem. Eur. J.* **1998** *4*, 845). Receptor **1** exhibits weak dimerization ($K_a \sim 2\ M^{-1}$) in $CDCl_3$, whereas receptor **2** shows no measurable dimerization. Attempts to correct anion binding constants for the dimerization of receptor **1** failed to produce an acceptable fit to the data. Presumably, the weak dimerization in receptor **1** plays a negligible role in the binding of anions (see ESI).

(26) O. B. Berryman, D. W. Johnson, **2005**, *unpublished results*.

(27) D. Quinonero, C. Garau, A. Frontera, P. Ballester, A. Costa, and P. M. Deya, *Chem. Phys. Lett.*, 2002, **359**, 486.

(28) M. H. Abraham, P. L. Grellier, D. V. Prior, P. P. Duce, J. J. Morris, and P. J. Taylor, *J. Chem. Soc., Perkin Trans. 2*, 1989, 699.

(29) Reference 28 presents a scale of hydrogen bond acidities based on logK values. While the sulfonamide functionality is not specifically addressed, data for other acidic functionalities are presented with the equation log K = $L_b pK_a + D_b$ relating pK_a and hydrogen bonding K_a, where L_b and D_b are constants specific for a given family of molecules. Estimates using the upper limit of these constants result in predicted K_a values for receptor **2** sufficient to be detected by ^{1}H NMR spectroscopy.

CHAPTER III

(1) (a) *Supramolecular Chemistry of Anions*; Bianchi, A., Bowman-James, K., García-España, E., Eds.; Wiley-VHC, New York, 1997; (b) Schmidtchen, F. P.; Berger, M. *Chem. Rev.* **1997**, *97*, 1609; (c) Gale, P. A. *Coord. Chem. Rev.* **2000**, *199*, 181; (d) Gale, P. A. *Coord. Chem. Rev.* **2001**, *213*, 79; (d) Beer, P. D.; Gale, P. A. *Angew. Chem. Int. Ed.* **2001**, *40*, 486; (e) Fitzmaurice, R. J.; Kyne, G. M.; Douheret, D.; Kilburn, J. D. *J. Chem. Soc., Perkin Trans. 1* **2002**, 841; (f) Martínez-Máñez, R.; Sacenón, F. *Chem. Rev.* **2003**, *103*, 4419; (g) Suksai, C.; Tuntulani, T. *Chem. Soc. Rev.* **2003**, *32*, 192; (h) Choi, K.; Hamilton, A. D. *Coord. Chem. Rev.* **2003**, *240*, 101; (i) Lambert, T. N.; Smith, B. D. *Coord. Chem. Rev.* **2003**, *240*, 129; (j) Davis, A. P.; Joos, J.-B. *Coord. Chem. Rev.* **2003**, *240*, 143; (k) Gale, P. A. *Coord. Chem. Rev.* **2003**, *240*, 191; (l) *Fundamentals and Applications of Anion Separations*; Moyer, B. A., Singh, R. P., Eds.; Kluwer Academic/Plenum, New York, 2004: (m) Chupakhin, O. N.; Itsikson, N. A.; Morzherin, Y. Y.; Charushin, V. N. *Heterocycles* **2005**, *66*, 689; (n) Kubik, S.; Reyheller, C.; Stüwe, S. *J. Incl. Phenom. Macro. Chem.* **2005**, *52*, 137; (o) Schmidtchen, F. P. *Top. Curr. Chem.* **2005**, *255*, 1.

(2) Mascal, M.; Armstrong, A.; Bartberger, M. D. *J. Am. Chem. Soc.* **2002**, *124*, 6274.

(3) Quinoñero, D.; Garau, C.; Rotger, C.; Frontera, A.; Ballester, P.; Costa, A.; Deyà, P. M. *Angew. Chem. Int. Ed.* **2002**, *41*, 3389.

(4) Quinoñero, D.; Garau, C.; Frontera, A.; Ballester, P.; Costa, A.; Deyà, P. M. *Chem. Phys. Lett.* **2002**, *359*, 486.

(5) Alkorta, I.; Rozas, I.; Elguero, J. *J. Am. Chem. Soc.* **2002**, *124*, 8593.

(6) Kim, D.; Tarakeshwar, P.; Kim. K. S. *J. Phys. Chem. A.* **2004**, *108*, 1250.

(7) Garau, C.; Frontera, A.; Quinoñero, D.; Ballester, P.; Costa, A.; Deyà, P. M. *J. Phys. Chem. A* **2004**, *108*, 9423.

(8) Garau, C.; Frontera, A.; Quinoñero, D.; Ballester, P.; Costa, A.; Deyà, P. M. *Chem. Phys. Lett.* **2004**, *392*, 85.

(9) Garau, C.; Frontera, A.; Ballester, P.; Quinoñero, D.; Costa, A.; Deyà, P. M. *Eur. J. Org. Chem.* **2005**, 179.

(10) Quinoñero, D.; Garau, C.; Frontera, A.; Ballester, P.; Costa, A.; Deyà, P. M. *J. Phys. Chem. A* **2005**, *109*, 4632.

(11) Garau, C.; Quinoñero, D.; Frontera, A.; Ballester, P.; Costa, A.; Deyà, P. M. *J. Phys. Chem. A* **2005**, *109*, 9341.

(12) Frontera, A.; Saczewski, F.; Gdaniec, M.; Dziemidowicz-Borys, E.; Kurland, A.; Deyà, P. M.; Quinoñero, D.; Garau, C. *Chem. Eur. J.* **2005**, *11*, 6560.

(13) Related charge-insulator complexes—in which an aromatic ring is sandwiched between an anion and a metal cation—lie outside the scope of the present study. For theoretical studies see: (a) Garau, C.; Quinoñero, D.; Frontera, A.; Ballester, P.; Costa, A.; Deyà, P. M. *New J. Chem.* **2003**, *2*, 211. (b) Garau, C. Frontera, A.; Quinoñero, D.; Ballester, P.; Costa, A.; Deyà, P. M. *Chem. Phys. Lett.* **2003**, *382*, 534. (c) Alkorta, I.; Elguero, J. *J. Phys. Chem. A* **2003**, *107*, 9428. For representative solid-state examples see: (d) Fairchild, R. M.; Holman, K. T. *J. Am. Chem. Soc.* **2005**, *127*, 16364. (e) Staffilani, M.; Hancock, K. S. B.; Steed, J, W.; Holman, K. T.; Atwood, J. L.; Juneja, R. K.; Burkhalter, R. S. *J. Am. Chem. Soc.* **1997**, *119*, 6324. (f) Holman, K. T.; Halihan, M. M.; Mitchell, A. R.; Burkhalter, R. S.; Steed, J. W.; Jurisson, S. S.; Atwood, J. L. *J. Am. Chem. Soc.* **1996**, 118, 9567.

(14) Rosokha, Y. S.; Lindeman, S. V.; Rosokha, S. V.; Kochi, J. K. *Angew. Chem. Intl. Ed.* **2004**, *43*, 4650.

(15) Demeshko, S.; Dechert, S.; Meyer, F. *J. Am. Chem. Soc.* **2004**, *126*, 4508.

(16) Single crystal X-ray structures also provide examples of anions interacting with charged π systems in which electron-deficient aromatic rings are coordinated to metal cations: (a) de Hoog, P.; Gamez, P. Mutikainen, I.; Turpeinen, U.; Reedijk, J. *Angew. Chem. Int. Ed.* **2004**, *43*, 5815; (b) Schottel, B. L.; Bacsa, J.; Dunbar, K. R. *Chem. Commun.* **2005**, 46; (c) Shottel, B. L.; Chifotides, T. H.; Shatruk, M. Chouai, A.; Pérez, L. M.; Gacsa, J.; Dunbar, K. R. *J. Am. Chem. Soc.* **2006**, *128*, 5895.

(17) NMR studies of *N*-confused porphyrins demonstrate an enhanced association with anions when C_6F_5 substituents are present: (a) Maeda, H.; Osuka, A.; Furuta, H. *J. Inclusion Phenom. Macrocyclic Chem.* **2004**, *49*, 33; (b) Maeda, H.; Furuta, H. *J. Porphyrins Phthalocyanines* **2004**, *8*, 67. For an example of an aryl sulfonate interacting with a neutral arene: (c) Schneider, H. J.; Werner, F.; Blatter, T. *J. Phys. Org. Chem.* **1993**, *6*, 590.

(18) Berryman, O. B.; Hof, F.; Hynes, M. J.; Johnson, D. W. *Chem. Commun.* **2006**, 506.

(19) Hoffman, R. W.; Hettche, F. *New. J. Chem.* **2003**, *27*, 172.

(20) Sheldrick, G. M. *SADABS: Area Detector Absorption Correction*, University of Göttingen: Göttingen, Germany, 2001.

(21) Sheldrick, G. M. *SHELXTL: Program Library for Structure Solution and Molecular Graphics*, 5.10; Bruker AXS: Madison, WI, 2000.

(22) *NWChem, A Computational Chemistry Package for Parallel Computers, Version 4.6* (2004), Straatsma, T. P. et al. *Computer Phys. Comm.* **2000**, *128*, 260-283.

(23) Möller, C.; Plesset, M. S. *Phys. Rev.* **1934**, *46*, 618.

(24) (a) Dunning, T. H., Jr. *J. Chem. Phys.* **1989**, *90*, 1007. (b) Kendall, R. A.; Dunning, T. H., Jr.; Harrison, R. J. *J. Chem. Phys.* **1992**, *96*, 6796.

(25) (a) *NBO, Version 5.0*, Glendening, E. D.; Badenhoop, J. K.; Reed, A. E.; Carpenter, J. E.; Bohmann, J. A.; Morales, C. M.; Weinhold, F. Theoretical Chemistry Institute, University of Wisconsin, Madison, WI, 2001; http://www.chem.wisc.edu/~nbo5. (b) A.E. Reed, A. E.; Curtiss, L. A.; Weinhold, F. *Chem. Rev.* **1988**, *88*, 899. (c) Weinhold, F.; Landis, C. *Valency and Bonding*; Cambridge University Press: Cambridge UK, 2005.

(26) (a) *Cambridge Structural Database, Version 5.27*, November 2005, Cambridge Crystallographic Data Centre, 12 Union Road, Cambridge, CB2 1EZ, UK; (a) Allen, F. H.; Kennard, O.; Taylor, R. *Acc. Chem. Res.* **1983**, *16* 146; (b) Allen, F. H.; Davies, J. E.; Galloy, J. J.; Johnson, O.; Kennard, O.; Macrae, C. F.; Mitchell, E. M.; Smith, J. M.; Watson, D. G. *J. Chem. Inf. Comput. Sci.* **1991**, *31*, 187. (c) Allen, F. H.; Kennard, O. *Chemical Design Automation News* **1993**, *8*, 31.

(27) A previous histogram for electronegative atoms interacting with perfluoroarenes reported hits for compounds exhibiting a contact between the interacting heteroatom and an arene carbon if the distance was ≤ the sum of van der Waals radii.[3] In fact, the actual criterion used in those studies was the sum of van der Waals radii + 1.0 Å, which is the default option provided in the Quest Version 5 database searching program: C. Garau personal communication, February, 2006.

(28) Bryantsev, V. S.; Hay, B. P. *J. Am. Chem. Soc.* **2005**, *127*, 8282.

(29) Bryantsev, V. S.; Hay, B. P. *Org. Lett.* **2005**, *7*, 5031.

(30) Such complexes were first reported in: (a) Jackson, C. J.; Gazzolo F. H. *J. Am. Chem. Soc.* **1900**, *23*, 376. A structure was later isolated and characterized in: (b) Meisenheimer, J. *Justus Liebigs Ann. Chem.* **1902**, *323*, 205.

(31) (a) Strauss, M. J. *Chem. Rev.* **1970**, *70*, 667; (b) Strauss, M. J. *Acc. Chem. Res.* **1974**, *7*, 181; (c) Bernasconi, C. F. *Acc. Chem. Res.* **1978**, *11*, 147.

(32) Besler, B. H.; Merz, K. M.; Kollman, P. A. *J. Comput. Chem.* **1990**, *11*, 431.

(33) Wiberg, K. B.; Rablen, P. R. *J. Comp. Chem.* **1993**, *14*, 1504.

(34) Table 1 of ref. 2 refers to a stable "attack" complex formed by Cl^- and trifluorotriazine. This is the only reported instance where a donor π-acceptor complex was calculated for Cl^-, Br^- or I^-.

(35) Ahuja, R.; Samuelson, A. G. *Crys. Eng. Commun.* **2003**, *5*, 395.

(36) We do not observe a preference for the anion to be located over the *para*-position. Possible explanations include (i) electrostatic attraction between the anion and metal cation and (ii) the electropositive metal center inductively stabilizes anion binding at the *ortho*-positions more than at the *para*-position.

(37) The C–H groups in Cu(II)-coordinated pyridine are more acidic than those in benzene. Thus, the strength for one of these interactions should exceed –8.6 kcal mol^{-1}.[28,29] With three electron donating amine substituents, the melamine π system should form weaker complexes than triazine. Thus, the strength of this anion-π interaction should be less than –8.4 kcal mol^{-1} (Table 3.2).

CHAPTER IV

(1) O. B. Berryman, V. S. Bryantsev, D. P. Stay, D. W. Johnson, B. P. Hay, *J. Am. Chem. Soc.* **2006**, *129*, 48.

(2) B. P. Hay, V. S. Bryantsev, *Chem. Commun.* **2008**, *in press*.

(3) For recent overviews see: (a) P. Gamez, T. J. Mooibroek, S. J. Teat, and J. Reedijk, *Acc. Chem. Res.*, **2007**, *40*, 435; (b) B. L. Schottel, H. T. Chifotides, and K. R. Dunbar, *Chem. Soc. Rev.*, **2008**, *37*, 68.

(4) A. Bianchi, K. Bowman-James, E. Garcia-Espana, Editors, Supramolecular Chemistry of Anions, Wiley-VCH, New York, **1997**.

(5) J. L. Sessler, P. A. Gale, W.-S. Cho, Anion Receptor Chemistry, The Royal Society of Chemistry, Cambridge, UK, **2006**.

(6) J. L. Sessler, D. E. Gross, W.-S. Cho, V. M. Lynch, F. P. Schmidtchen, G. W. Bates, M. E. Light, P. A. Gale, *J. Am. Chem. Soc.* **2006**, *128*, 12281.

(7) Y. S. L. Rosokha, S. V.; Rosokha, S. V.; Kochi, J. K., *Angew. Chem.* **2004**, *116*, 4750; *Angew. Chem. Int. Ed.* **2004**, *43*, 4650.

(8) O. B. Berryman, F. Hof, M. J. Hynes, D. W. Johnson, *Chem. Commun.* **2006**, 506.

(9) R. M. Fairchild, K. T. Holman, *J. Am. Chem. Soc.* **2005**, *127*, 16364.

(10) H. Maeda, A. Osuka, H. Furuta, *J. Incl. Phenom. Macrocycl. Chem.* **2004**, *49*, 33.

(11) H. J. Schneider, F. Werner, T. Blatter, *J. Phys. Org. Chem.* **1993**, *6*, 590.

(12) ^{1}H NMR spectroscopy has been used previously to demonstrate the importance of complementary C-H•••X– hydrogen bonding modes in receptors that bind anions using traditional H-bonds (a-e) or electrostatic attractions (f,g): a) C. -H. Lee, H.-K. Na, D.-W. Yoon, D.-H. Won, W.-S. Cho, V. M. Lynch, S. V. Shevchuk, J. L. Sessler, *J. Am. Chem. Soc.* **2003**, *125*, 7301; b) J. Y. Kwon, Y. J. Jang, S. K. Kim, K.-H. Lee, J. S. Kim, J. Yoon, *J. Org. Chem.* **2004**, *69*, 5155; c) Q.-Y. Chen, C.-F. Chen, *Tetrahedron Lett.* **2004**, *45*, 6493; d) S. Ghosh, A. R. Choudhury, T. N. G. Row, U. Maitra, *Org. Lett.* **2005**, *7*, 1441; e) C. Fujimoto, Y. Kusunose, H. Maeda, *J. Org. Chem.* **2006**, *71*, 2389; f) K. J. Wallace, W. J. Belcher, D. R. Turner, K. F. Syed, J. W. Steed, *J. Am. Chem. Soc.* **2003**, *125*, 9699; g) I. E. D. Vega, P. A. Gale, M. E. Light, S. J. Loeb, *Chem. Commun.* **2005**, 4913.

(13) G. Hennrich, E. V. Anslyn, *Chem. Eur. J.* **2002**, *8*, 2218.

(14) J. C. Lee, Y. Choi, *Synth. Commun.* **1998**, *28*, 2021.

(15) Crystal data for **1**: $C_{36}H_{30}N_6O_{18}$, M = 834.66, triclinic, P-1, a = 5.6949(12) Å, b = 19.833(4) Å, c = 33.883(7) Å, α = 84.106(4)°, β = 85.278(5)°, γ = 81.873(5)°, V = 3759.6(14) Å^3, Z = 4, μ(Mo-Kα) = 0.121 mm^{-1}. Final residuals (1321 parameters) $R1$ = 0.0566 for 16401 reflections with $I > 2\sigma(I)$, and $R1$ = 0.1090, $wR2$ = 0.1446, GooF = 1.007 for all 23621 data. CCDC # 661394.

(16) Crystal data for **2**: $(C_{36}H_{30}N_6O_{18})(C_2H_6OS)_3$, M = 1069.04, monoclinic, $P2(1)/n$, a = 28.272(12) Å, b = 5.075(2) Å, c = 37.126(15) Å, β = 110.669(7)°, V = 4984(4) Å^3, Z = 4, μ(Mo-Kα) = 0.091 mm^{-1}. Final residuals (544 parameters) $R1$ = 0.0857 for 8731 reflections with $I > 2\sigma(I)$, and $R1$ = 0.1736, $wR2$ = 0.2640, GooF = 0.946 for all 33339 data. CCDC # 661395.

(17) UV-Vis titrations for receptors **1** and **2** with $NHep_4^+I^-$ at 21 °C were performed to corroborate the ^{1}H NMR titrations herein. Regrettably, the charge transfer band that grows in throughout the titration appears as a shoulder on the residual $NHep_4^+I^-$ band that increases throughout the titration. Thus UV-vis spectroscopy is impracticle for binding constant determination in this system. Nevertheless, binding isotherms were obtained and can be fit to 1:1 binding models with the program DynaFit (P. Kuzmic, *Anal. Biochem.* **1996**, *237*, 260.) resulting in association constants of 4.5 M^{-1} for receptor **1** and 6.0 M^{-1} for receptor **2**. Receptors containing aromatic rings that are more electron-deficient and should exhibit charge transfer bands with anions that are further downfield are being synthesized to address this problem and will be reported in due course.

(18) K. Hirose, *J. Incl. Phenom. Macrocycl. Chem.* **2001**, *39*, 193.

(19) Titrations of receptors **1** and **2** (~5 mM) with tetra-*n*-butylammonium bromide ($NBu_4^+Br^-$) were performed at room temperature resulting in lower association constants (averaging 4-6 M^{-1}). These data indicate that counter cation and/or temperature plays a role in the anion binding ability of this system. Nevertheless, titrations of receptor **1** at these concentrations (~5 mM) with $NBu_4^+Br^-$ better illustrate the dramatic chemical shift changes for this receptor.

(20) Analogous titrations of **1** (2 mM) at 27 °C with $NHep_4^+$halides also exhibit striking peak movement (up to 0.632 ppm for $NHep_4^+Cl^-$, 0.500 ppm for $NHep_4^+Br^-$ and 0.390 ppm for $NHep_4^+I^-$) throughout the experiment (Table 4.1 and Appendix C).

(21) DFT calculations were performed with the NWCHEM program (a) using the B3LYP functional (b-e) with the DZVP basis set and DGauss A1 coulomb fitting (f) (Optimized geometries and absolute energies for all structures are provided as Supporting Information). (a) Bylaska et al. NWChem, A Computational Chemistry Package for Parallel Computers, Version 5.0, 2006, Pacific Northwest National Laboratory, Richland, Washington 99352-0999, USA; for a full author list see supporting information. (b) Becke, A. D. *Phys. Rev. A* **1988**, *38*, 3098. (c) Becke, A. D. In The Challenge of d and f Electrons: Theory and Computation; Salahub, D. R.; Zerner, M. C., Eds.; ACS Symposium Series, No. 394, American Chemical Society: Washington D. C., **1989**; p166. (d) Becke, A. D. Int. J. Quantum Chem. Symp. **1989**, *23*, 599. (e) Perdew, J. P. *Phys. Rev. B* **1986**, *33*, 8822. (f) N. Godbout, D. R. Salahub, J. Andzelm, E. Wimmer, *Can. J. Chem.* **1992**, *70*, 560.

(22) (a) V. S. Bryantsev, B. P. Hay, *J. Am. Chem. Soc.* **2005**, *127*, 8282. (b) V. S. Bryantsev, B. P. Hay, *Org. Lett.* **2005**, *7*, 5031.

(23) An alternate conformation, 6.0 kcal/mol higher in energy, was located for **1**•Br^-, where the Br^- forms a weak σ complex (3.432 Å) with one arene and bifurcated aryl H-bonds (2.832 Å, 3.043 Å, 2.909 Å and 3.021 Å) with the other two (see Appendix C). It is possible that the H-bond complex and/or the weak σ structure is responsible for the pale yellow or colors observed in solution when receptors **1** and **3** are mixed with Br^- or I^-.

(24) As a control, no color is observed when $NHep_4^+I^-$ is dissolved in C_6D_6 and heated to 27 °C

(25) $NHep_4^+I^-$ stock solutions were kept in a sonicator at 27 °C to insure salt solubility

CHAPTER V

(1) P. A. Kollman and L. C. Allen, *Chem. Rev.*, 1972, **72**, 283-303.

(2) G. C. Pimentel and A. L. McClellan, *The Hydrogen Bond*, **1960**.

(3) G. C. Pimentel and A. L. McClellan, *Ann. Rev. Phys. Chem.*, 1971, **22**, 347-385.

(4) W. H. Rodebush, *Chem. Rev.*, 1936, **19**, 59-65.

(5) P. A. Kollman, *J. Am. Chem. Soc.*, 1972, **94**, 1837-1842.

(6) E. N. Lassettre, *Chem. Rev.*, 1937, **20**, 259-303.

(7) A. S. N. Murthy and C. N. R. Rao, *J. Mol. Struct.*, 1970, **6**, 253-282.

(8) D. Ajami and J. Rebek, Jr., *J. Am. Chem. Soc.*, 2006, **128**, 15038-15039.

(9) N. Branda, R. M. Grotzfeld, C. Valdes and J. Rebek, Jr., *J. Am. Chem. Soc.*, 1995, **117**, 85-88.

(10) S. M. Butterfield and J. Rebek, Jr., *Chem. Commun.*, 2007, 1605-1607.

(11) R. J. Hooley, P. Restorp, T. Iwasawa and J. Rebek, Jr., *J. Am. Chem. Soc.*, 2007, **129**, 15639-15643.

(12) T. Iwasawa, R. J. Hooley and J. Rebek, Jr., *Science*, 2007, **317**, 493-496.

(13) L. R. MacGillivray and J. L. Atwood, *Nature*, 1997, **389**, 469-472.

(14) A. W. Frank and D. J. Daigle, *Phosphorus, Sulfur Relat. Elem.*, 1981, **10**, 255-259.

(15) R. Huang and B. J. Frost, *Inorg. Chem.*, 2007, **46**, 10962-10964.

CHAPTER VI

(1) Ahn, C. M.; Shin, W.-S.; Woo, H. B.; Lee, S.; Lee, H.-W. *Bioorg. Med. Chem. Lett.* **2004**, *14*, 3893-3896.

(2) Baxter, P. N. W.; Dali-Youcef, R. *J. Org. Chem.* **2005**, *70*, 4935-4953.

(3) Holmes, B. T.; Deb, P.; Pennington, W. T.; Hanks, T. W. *J. Polym. Res.* **2006**, *2006*, 133-144.

(4) Rajadurai, C.; Ivanova, A.; Enkelmann, V.; Baumgarten, M. *J. Org. Chem.* **2003**, *68*, 9907-9915.

(5) Yamaguchi, Y.; Kobayashi, S.; Wakamiya, T.; Matsubara, Y.; Yoshida, Z.-I. *Angew. Chem. Int. Ed.* **2005**, *44*, 7040-7044.

(6) Phelps, D.; Crihfield, A.; Hartwell, J.; Hanks, T. W.; Pennington, W. T.; Bailey, R. D. *Mol. Cryst. Liq. Cryst.* **2000**, *354*, 1111.

(7) Chen, J.; Korner, S.; Craig Stephen, L.; Rudkevich Dmitry, M.; Rebek, J., Jr. *Nature* **2002**, *415*, 385-386.

(8) Dalgarno, S. J.; Tucker, S. A.; Bassil, D. B.; Atwood, J. L. *Science* **2005**, *309*, 2037-2039.

(9) Hof, F.; Craig, S. L.; Nuckolls, C.; Rebek, J., Jr. *Angew. Chem. Int. Ed.* **2002**, *41*, 1488-1508.

(10) Pluth, M. D.; Bergman, R. G.; Raymond, K. N. *Science* **2007**, *316*, 85-88.

(11) Yoshizawa, M.; Tamura, M.; Fujita, M. *Science* **2006**, *312*, 1472.

(12) Rhee, Y. M.; Sorin, E. J.; Jayachandran, G.; Lindahl, E.; Pande, V. S. *Proc. Natl. Acad. Sci. U. S. A.* **2004**, *101*, 6456-6461.

(13) Dym, O.; Mevarech, M.; Sussman, J. L. *Science* **1995**, *267*, 1344-1346.

(14) Richard, S. B.; Madern, D.; Garcin, E.; Zaccai, G. *Biochemistry* **2000**, *39*, 992-1000.

(15) Sessler, J. L.; Gale, P. A.; Cho, W.-S. *Anion Receptor Chemistry*, Royal Society of Chemistry, Cambridge, **2006**.

(16) Liu, K.; Cruzan, J. D.; Saykally, R. J. *Science* **1996**, *271*, 929-933.

(17) Friedman, J.; Meharenna, Y. T.; Wilks, A.; Poulos, T. L. *J. Biol. Chem.* **2007**, *282*, 1066-1071.

(18) Nagano, S.; Poulos, T. L. *J. Biol. Chem.* **2005**, *280*, 31659-31663.

(19) MacBeth, C. E.; Golombek, A. P.; Young, V. G., Jr.; Yang, C.; Kuczera, K.; Hendrich, M. P.; Borovik, A. S. *Science* **2000**, *289*, 938-941.

(20) Hof, F.; Trembleau, L.; Ullrich, E. C.; Rebek, J., Jr. *Angew. Chem. Int. Ed.* **2003**, *42*, 3150-3153.

(21) MacGillivray, L. R.; Atwood, J. L. *Nature* **1997**, *389*, 469-472.

(22) Yamanaka, M.; Shivanyuk, A.; Rebek, J., Jr. *J, Am. Chem. Soc.* **2004**, *126*, 2939-2943.

(23) Atwood, J. L.; Barbour, L. J.; Jerga, A. *Chem. Commun.* **2001**, 2376-2377.

(24) Biros, S. M.; Rebek, J., Jr. *Chem. Soc. Rev.* **2007**, *36*, 93-104.

(25) An understanding of the coordination preferences of anions is emerging, but the directionality is still less defined than for their cationic counterparts. For a detailed discussion, see: Kang, S. O.; Hossain, M. A.; Bowman-James, K. *Coord. Chem. Rev.* **2006**, *250*, 3038.

(26) Sanchez-Quesada, J.; Seel, C.; Prados, P.; de Mendoza, J.; Dalcol, I.; Giralt, E. *J. Am. Chem. Soc.* **1996**, *118*, 277-278.

(27) Vilar, R. *Angew. Chem. Int. Ed.* **2003**, *42*, 1460-1477.

(28) Coles, S. J.; Frey, J. G.; Gale, P. A.; Hursthouse, M. B.; Light, M. E.; Navakhun, K.; Thomas, G. L. *Chem. Commun.* **2003**, 568-569.

(29) Gale, P. A.; Navakhun, K.; Camiolo, S.; Light, M. E.; Hursthouse, M. B. *J. Am. Chem. Soc.* **2002**, *124*, 11228-11229.

(30) Nielsen, K. A.; Cho, W.-S.; Sarova, G. H.; Petersen, B. M.; Bond, A. D.; Becher, J.; Jensen, F.; Guldi, D. M.; Sessler, J. L.; Jeppesen, J. O. *Angew. Chem. Int. Ed.* **2006**, *45*, 6848-6853.

(31) For an example of water and halides occupying the same binding sites in a protein, see: Fiedler, T. J.; Davey, C. A.; Fenna, R. E. *J. Biol. Chem.* **2000**, *275*, 11964.

(32) Wan, W. B.; Haley, M. M. *J. Or. Chem.* **2001**, *66*, 3893-3901.

(33) Crystal data for (**1**•H_2O)$_2$: ($C_{43}H_{45}N_3O_5S_2$)$_2$, M_r = 1495.88 , 0.31 x 0.18 x 0.15 mm, triclinic, *P*-1, a = 10.0377(17) Å, b = 12.755(2) Å, c = 17.357(3) Å, α = 111.270(3)°, β = 96.113(3)°, γ = 102.966(3)°, V = 1974.4(6) Å^3, Z = 1 (i.e., one dimer per unit cell), ρ_{calcd} = 1.258 g mL^{-1}, μ = 0.183 mm^{-1}, $2\theta_{max}$ = 54.00°, T = 173(2) K, $R1$ = 0.0470 for 6966 reflections (662 parameters) with $I > 2\sigma(I)$, and $R1$ = 0.0580, $wR2$ = 0.1222, and GOF = 1.028 for all 8480 data, max/min residual electron density +0.502/-0.682 e Å^{-3}.

(34) Crystal data for (**2**•H_2O)$_2$: ($C_{41}H_{39}N_5O_9S_2$)$_2$, M_r = 1619.78 , 0.30 x 0.20 x 0.01 mm, triclinic, *P*-1, a = 10.1068(15) Å, b = 12/5999(19) Å, c = 17.186(3) Å, α = 110.709(3)°, β = 97.006(3)°, γ = 100.306(3)°, V = 1972.9(5) Å^3, Z = 1, ρ_{calcd} = 1.363 g mL^{-1}, μ = 0.198 mm^{-1}, $2\theta_{max}$ = 54.00°, T = 173(2) K, $R1$ = 0.0642 for 4980 reflections (674 parameters) with $I > 2\sigma(I)$, and $R1$ = 0.1233, $wR2$ = 0.1462, and GOF = 1.034 for all 8413 data, max/min residual electron density +0.312/-0.432 e Å^{-3}.

(35) The "staggered" conformation for sulfonamides refers to the conformation in which the lone pair of the nitrogen atom bisects the O-S-O angle (the lone pair is *anti*-periplanar to the S-C bond), see: Hirsch, A. K. H.; Lauw, S.; Gersbach, P.; Schweizer, W. B.; Rohdich, F.; Eisenreich, W.; Bacher, A.; Diederich, F. *Chem. Med. Chem.* **2007**, *2*, 806.

(36) Hynes, M. J. *J. Chem. Soc. Dalton Transactions* **1993**, 311-312.

(37) Other potential guest molecules that did not co-crystallize with sulfonamide receptors include: hydrogen sulfide, methanol, ethanol, isopropanol, acetone, acetonitrile, dimethylsulfoxide, tetrahydrofuran, tetra-*n*-butylammonium halides and HSO_4^-.

(38) Crystal data for (**H1**$^+$•Br^-)$_2$: ($C_{43}H_{44}BrN_3O_4S_2$)$_2$, M_r = 1621.68, 0.21 x 0.07 x 0.02 mm, triclinic, *P*-1, a = 9.632(16) Å, b = 13.33(2) Å, c = 17.47(3) Å, α = 108.39(4)°, β = 94.56(5)°, γ = 106.51(4)°, V = 2005(6) Å^3, Z = 1, ρ_{calcd} = 1.343 g mL^{-1}, μ = 1.175 mm^{-1}, $2\theta_{max}$ = 54.00°, T = 173(2) K, $R1$ = 0.0598 for 5748 reflections (599 parameters) with $I > 2\sigma(I)$, and $R1$ = 0.1021, $wR2$ = 0.1527, and GOF = 1.035 for all 8622 data, max/min residual electron density +0.680/-0.371 e Å^{-3}.

(39) Crystal data for $(\mathbf{H2}^{+}\bullet Cl^{-})_2$: $(C_{41}H_{38}ClN_5O_8S_2)_2$, M_r = 1656.66, 0.30 x 0.25 x 0.02 mm, triclinic, *P*-1, a = 9.8907(13) Å, b = 12.9533(17) Å, c = 17.012(2) Å, α = 107.831(2)°, β = 95.845(2)°, γ = 103.618(2)°, V = 1980.5(4) Å^3, Z = 1, ρ_{calcd} = 1.389 g mL^{-1}, μ = 0.262 mm^{-1}, $2\theta_{max}$ = 54.00°, T = 173(2) K, $R1$ = 0.0572 for 6572 reflections (594 parameters) with $I > 2\sigma(I)$, and $R1$ = 0.0744, $wR2$ = 0.1594, and GOF = 1.045 for all 8472 data, max/min residual electron density +0.564/-0.290 e Å^{-3}.

(40) The UV-Vis spectrum of $\mathbf{H1}^{+}\bullet BF_4^{-}$ is consistent with the yellow color of the protonated receptor in organic solutions. Upon protonation receptor **1** exhibits a new absorption peak with a λ_{max} at 400 nm. The unique absorption characteristics of receptor $\mathbf{H1}^{+}$ were used to study the host/guest interactions of this molecule in solution. Specifically, tetra-n-butylammonium halides were titrated into CH_2Cl_2 solutions of $\mathbf{H1}^{+}\bullet BF_4^{-}$ while maintaining constant receptor concentrations. Evident changes in the UV-Vis spectra were observed upon addition of halide anions. In all cases the absorption bands at 240, 290 and 330 nm were shown to increase in intensity throughout the titration while the intensity of the absorption band at 400 nm decreased, exemplifying isosbestic behavior. Unfortunately, at low concentrations equilibrium conditions were not observed precluding the determination of binding constants by UV-Vis spectrophotometric titrations. ^{1}H NMR spectroscopic titrations in $CDCl_3$ were employed to examine the anion binding capability of receptor $\mathbf{H1}^{+}$ for tetra-*n*-butylammonium halides. The binding isotherms obtained from titrations of $\mathbf{H1}^{+}\bullet BF_4^{-}$ with halides exhibit a steep linear increase up to one equivalent of halide, with chloride affecting the steepest binding isotherm and iodide the shallowest. The second portion of the equilibrium exhibits a much smaller influence on the overall chemical shift of the complex. The second portion of the binding isotherm has made it difficult to determine association constants. Host guest equilibria will be reported in due course.

(41) Subsequent iterations of this experiment resulted in the formation of precipitate suggesting that the first trial was supersaturated. The relatively low solubility of this complex in organic solvents has hindered further determination of association constants.

(42) Crystal data for $(\mathbf{H1}^{+}Cl^{-})\bullet(\mathbf{1}\bullet H_2O)$: $(C_{43}H_{43}N_3O_4S_2)_2\bullet H_2O\bullet HCl$, M_r = 1514.32, 0.20 x 0.08 x 0.02 mm, triclinic, *P*-1, a = 9.9702(13) Å, b = 12.8868(17) Å, c = 17.363(2) Å, α = 111.314(2)°, β = 95.475(3)°, γ = 103.737(2)°, V = 1977.7(4) Å^3, Z = 1, ρ_{calcd} = 1.271 g mL^{-1}, μ = 0.215 mm^{-1}, $2\theta_{max}$ = 54.00°, T = 173(2) K, $R1$ = 0.0671 for 5583 reflections (559 parameters) with $I > 2\sigma(I)$, and $R1$ = 0.1074, $wR2$ = 0.1673, and GOF = 1.027 for all 8485 data, max/min residual electron density +0.842/-0.723 e Å^{-3}.